R-08-87

Background complementary hydrogeochemical studies

SDM-Site Forsmark

Birgitta E Kalinowski (editor)
Svensk Kärnbränslehantering AB

August 2008

Svensk Kärnbränslehantering AB
Swedish Nuclear Fuel
and Waste Management Co
Box 250, SE-101 24 Stockholm
Tel +46 8 459 84 00

ISSN 1402-3091
SKB Rapport R-08-87

Background complementary hydrogeochemical studies

SDM-Site Forsmark

Birgitta E Kalinowski (editor)
Svensk Kärnbränslehantering AB

August 2008

Preface

The overall objectives of the hydrogeochemical description for Forsmark are to establish a detailed understanding of the hydrogeochemical conditions at the site and to develop models that fulfil the needs identified by the safety assessment groups during the site investigation phase. Issues of concern to safety assessment are radionuclide transport and technical barrier behaviour, both of which are dependent on the chemistry of groundwater and pore water and their evolution with time.

The work has involved the development of descriptive and mathematical models for groundwaters in relation to rock domains, fracture domains and deformation zones. Past climate changes are one of the major driving forces for hydrogeochemical changes and therefore of fundamental importance for understanding the palaeohydrogeological, palaeohydrogeochemical and present evolution of groundwater in the crystalline bedrock of the Fennoscandian Shield.

Understanding current undisturbed hydrochemical conditions at the proposed repository site is important when predicting future changes in groundwater chemistry. The causes of copper corrosion and/or bentonite degradation are of particular interest as they may jeopardise the long-term integrity of the planned SKB repository system. Thus, the following variables are considered for the hydrogeochemical site descriptive modelling: pH, Eh, sulphur species, iron, manganese, uranium, carbonate, phosphate, nitrogen species, total dissolved solids (TDS), isotopes, colloids, fulvic and humic acids and microorganisms. In addition, dissolved gases (e.g. carbon dioxide, methane and hydrogen) are of interest because of their likely participation in microbial reactions.

In this series of reports, the final hydrogeochemical evaluation work of the site investigation at the Forsmark site, is presented. The work was conducted by SKB's hydrogeochemical project group, ChemNet, which consists of independent consultants and university researchers with expertise in geochemistry, hydrochemistry, hydrogeochemistry, microbiology, geomicrobiology, analytical chemistry etc. The resulting site descriptive model version, mainly based on 2.2 data and complementary 2.3 data, was carried out during September 2006 to December 2007. Several groups within ChemNet were involved and the evaluation was conducted independently using different approaches ranging from expert knowledge to geochemical and mathematical modelling including transport modelling. During regular ChemNet meetings the results have been presented and discussed.

The original works by the ChemNet modellers are presented in five level III reports containing complementary information for the bedrock hydrogeochemistry Forsmark Site Descriptive Model (SDM-Site Forsmark, R-08-47) level II report.

There is also one additional level III report: Fracture mineralogy of the Forsmark area by Sandström et al. R-08-102.

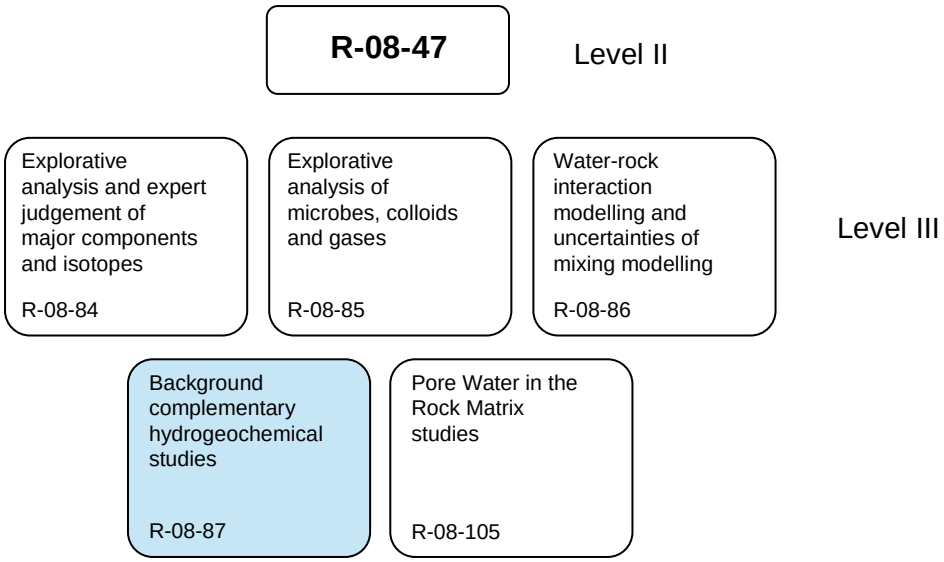

The ChemNet members contributing to this report are (in alphabetic order):

David Arcos, Amphos, Barcelona, Spain (section 2)
Lara Duro, Amphos, Barcelona, Spain (section 2)
Mel Gascoyne, GGP Inc. Pinawa, Canada (section 3)
Ioana Gurban, 3D-Terra, Montreal, Canada (section 1 and 3)
Jorge Molinero, Amphos, Barcelona, Spain (section 2)
Ann-Chatrin Nilsson, Geosigma AB, Uppsala, Sweden (section 4)

This report is a compilation of five different projects that have been finished independently of each other.

Section #1: M3 modelling and 2D visualisation of the hydrochemical parameters by Ioana Gurban.

The focus of this part is on updating the hydrochemical model, to make uncertainty tests and to present the final models that can be integrated better with the hydrodynamic models. M3 modelling helps to summarise and understand the measured data, by using the major elements and the isotopes $\delta^{18}O$ and $\delta^{2}H$ as variables.

The visualisation of the mixing proportions along the boreholes helps to understand the distribution of the data in the domain and to check and compare the results of different models; and therefore to choose the model which best describes the measured data.

Section #2: Coupled hydrogeological and solute transport, visualisation and supportive detailed reaction modelling by Jorge Molinero, David Arcos, Lara Duro.

Reactive mixing and reactive solute transport models are used as quantitative tools in order to evaluate how much disturbance can be allowed for a given groundwater sample at repository depth and still meet the SKB suitability criteria. Spatial analysis and 3D visualisation of available representative samples in Forsmark was performed. The computed M3 mixing fractions show a spatial distribution qualitatively correlated with key hydrochemical signatures, such as strontium (for Deep Saline), magnesium (for Littorina), $\delta^{18}O$ and $\delta^{2}H$ (for Glacial) and tritium (for Modified meteoric).

Section #3: Application of the Drilling Impact Study (DIS) to Forsmark groundwaters by Mel Gascoyne, Ioana Gurban.

In the Drilling Impact Study (DIS) project a tracer is used as an indicator of contamination to attempt to correct the groundwater composition for dilution or contamination by surface waters. By calculating the drilling water volume lost in the fractures during drilling, it is possible to determine how much water should be pumped out from the section before sampling.

Section #4: Analytical uncertainties. Ann-Chatrin Nilsson.

There is high confidence in the set of major constituents for each sample. Independent methods were used to check the consistency of the major ions and to confirm the concentrations of chloride, sulphate, bromide and iron.The bromide analyses were found to be more uncertain than most other major ions.

Section 1

Forsmark Site: M3 modelling and 2D visualisation of the hydrochemical parameters in Forsmark groundwater

Ioana Gurban,
3D Terra

Contents

1 Introduction

This report presents the results of the mixing modelling and 2D visualisation of Forsmark 2.2 and 2.3 groundwater data. The focus is on updating the hydrochemical model, to make uncertainty tests and to present the final models that can be integrated better with the hydrodynamic models. The need for additional uncertainty tests was identified during the Forsmark 1.2, 2.1 and 2.2 modelling stages. Issues such as the use of different end-members were addressed. The model presented in this report contains all available data from the Forsmark 2.3 data freeze. The code M3 was updated to a new version including hyperspace option calculations. The new M3 code was tested and compared with the old version, in 2D and in hyperspace.

Some issues, such as the use of tritium as a variable and the use of the meteoric (corresponding to the precipitation in 1960 with 168TU) end-member, were already addressed in the Laxemar 2.1 exercise /SKB 2006a/. The alternative models and the experience gained from Laxemar 2.1 helped to clarify previously unsolved issues such as: which variables to use for the modelling, the use of altered meteoric end-member representing the upper bedrock, the use of only groundwater data and better understanding of the end-members deep saline (brine) and glacial. These issues were integrated and a new bedrock model was built for Forsmark 2.1 /SKB 2006b/. This model was updated with more data from the Forsmark 2.2 and 2.3 data freezes and with a better understand of the conceptual model, especially in terms of the end-members used for the modelling. Since the data freeze 2.3 includes also the data from 2.2, in this paper only the results of the Forsmark 2.3 modelling and visualisation are presented.

2 M3 modelling

2.1 Data selection

The M3 method consists of 4 steps: a standard principal component analysis (PCA), selection of reference waters, calculations of mixing proportions, and, finally, mass balance calculations (for more details see /Laaksoharju 1999, Laaksoharju et al. 1999, Gómez et al. 2006/).

The Forsmark data was analysed in the different stages (Forsmark 1.1, 1.2 and 2.1) with different versions of the M3 code. The old M3 2D version /Laaksoharju 1999/ was updated and hyperspace calculations are now possible. The new M3 version /Gómez et al. 2006/ of M3 makes possible the calculations in 2PC or n-PC (n principal components, where n is the number of end-members of the model). Several tests were made with the new version of M3 in the Forsmark 2.1 stages. This helped to verify that the new M3 2D works exactly like the old M3 code, and then to compare and judge the benefits or limitations by using 2D or n-PC calculations. In general, in the 2D calculations more data can be included. When using the n-PC calculations, less data are included but the predictions of the conservative elements fit better with the measured values. Therefore, in this report, only the M3 n-PC version is used. Several versions of M3 were tested during the previous exercises and the final version is used here (M3 beta9).

For Forsmark version 1.1 /Laaksoharju et al. 2004/, 2 models were built at a regional scale and at a local scale. One hundred and eighteen samples from Forsmark met the M3 criteria (complete dataset for major elements and isotopes, no gaps in data) and were used in the M3 modelling. These samples were from boreholes (core and percussion), soil pipes, lake water and stream water.

For Forsmark version 1.2 /SKB 2005/, two models were built: at a regional scale and at a local scale. Three hundred and sixty-seven samples from Forsmark 1.2 met the M3 criteria (data for major elements and isotopes) and were used in the M3 modelling. These samples were from boreholes (core and percussion), soil pipes (shallow and near-surface groundwater), lake water, sea water, running water and precipitation. From the 367 samples available, 182 were considered representative from a hydrochemical point of view and 185 non-representative.

The Forsmark 2.1 modelling employed only groundwater data, from percussion and core boreholes, (145 groundwater samples of which 35 were considered representative).

For Forsmark 2.2 a bedrock model was built at local scale. 259 samples from Forsmark 2.2 met the M3 criteria (data for major elements and isotopes) and were used in the M3 modelling. These samples were from core boreholes and percussion boreholes. Since the intention is to build a bedrock model, the soil pipes (shallow and near-surface groundwater), lake water, sea water, running water and precipitation samples were not used. From the 259 samples available, 49 were considered representative from a hydrochemical point of view and 210 non-representative.

The present Forsmark 2.3 modelling also employs only groundwater data, from percussion and core boreholes, (290 groundwater samples from which 64 are considered representative). All the data used in the M3 modelling are presented in SKB database SIMON. Since the Forsmark 2.2 data is included in the Forsmark 2.3 data, only the results from Forsmark 2.3 are presented. The modelling of Forsmark 2.3 shows the same trends and results as 2.2, but more data and more representative data are available. For example, KFM10A was not included in the Forsmark 2.2 data freeze; also more samples at depth in different boreholes are available in Forsmark 2.3 (KFM01A, KFM01D, KFM03A, KFM06A, KFM08A).

2.2 End-members

The end-members are the most extreme waters present in the hydrogeochemical system studied (here Forsmark 2.2 and 2.3). The end-members can be samples from the site or modelled extreme waters, defined by expert judgement after a hydrogeochemical evaluation of the site. The following reference waters were used in the M3 modelling (for analytical data see Table 2-1).

- **Deep Saline end-member:** Brine type of reference water**,** Represents the deep brine type (Cl = 47,000 mg/l) of water sampled from borehole KLX02: 1,631–1 681 m /Laaksoharju et al. 1995/. An old age for the Deep Saline is suggested by the measured ^{36}Cl values indicating a minimum residence time of 1.5 Ma for the Cl component /Laaksoharju and Wallin 1997/. This sample from Laxemar was used as the end-member for Forsmark, but with low sulphate: 10 mg/l instead of 906. This is explained by /Gimeno et al. 2008/ (sections 2.1.1, 2.1.5 and 2.1.6).
- **Saline end-member:** The most saline water sampled at Forsmark has Cl = 14,800 mg/l in KFM07A, the representative sample is 8,879 at 759.72 m depth. This sample would not be saline enough to compare the sites Forsmark and Laxemar. Statistical calculations made by /Gomez et al. 2006/ show that the best choice for the saline end-member is that with the Cl around 50,000 mg/l. However, a local model for Forsmark was built by employing sample 8,879 as saline reference water (Model 3).
- **Glacial end-member:** Represents a possible melt-water composition from the last glaciation > 13,000BP. Modern sampled glacial melt water from Norway was used for the major elements and the $\delta^{18}O$ isotope value (−21**‰** SMOW) was based on measured values of $\delta^{18}O$ in calcite surface deposits /Tullborg and Larson 1984/. The $\delta^{2}H$ value (−158‰ SMOW) is a modelled value based on the global relationship ($\delta^{2}H = 8 \times \delta^{18}O + 10$) for the meteoric water line.
- **Old Meteoric-Glacial end-member:** In order to better predict the $\delta^{18}O$ values, a mixture of Old Meteoric-Glacial type of water was used as end-member. This water has $\delta^{2}H = –118‰$ and $\delta^{18}O = –16‰$. This is explained by /Gimeno et al. 2008/ (sections 2.1.2, 2.1.5 and 2.1.6).
- **Littorina Water end-member:** Represents modelled Littorina water (see Table 2-1). The Littorina composition is more extreme (more marine) than the Baltic sea composition. Therefore Littorina water is used in the calculations.
- **Altered meteoric end-member:** Corresponds to an upper bedrock water composition, obtained by the infiltration of meteoric water (the origin can be rain or snow) in the bedrock. The composition of the sample HFM16 (12281) was used as end-member.

Table 2-1. Groundwater analytical or modelled data (Littorina and old meteoric-glacial) used as end-members in the M3 modelling for Forsmark 2.3.

End Member	ID Code	Cl (mg/l)	Na (mg/l)	K (mg/l)	Ca (mg/l)	Mg (mg/l)	HCO3 (mg/l)	SO4 (mg/l)	d2H ‰	d18O ‰
Deep saline	Laxemar SGKLX02	47200	8200	45.5	19300	2.12	14.1	10	-44.9	-8.9
Saline	KFM07A (8879)	14800	2850	13.7	5840	19.9	6.19	99.30	-86.7	-13.1
Glacial		0.5	0.17	0.4	0.18	0.1	0.12	0.5	-158	-21
Old meteoric-glacial		0.5	0.17	0.4	0.18	0.1	0.12	0.5	-118	-16
Littorina Sea		6500	3674	134	151	448	92.5	890	-37.8	-4.7
Altered meteoric	HFM16 (12281)	204	276.0	7.16	45.8	10.6	466.00	95.10	-81.1	-11.1

Several tests were made with different saline, glacial and meteoric compositions. The feasibility study for the end-members was tested by /Gimeno et al. 2008/, where the choice of the end-members is explained in detail. The final end-members used are the Deep Saline, Glacial, Littorina, and Altered Meteoric. These waters can explain most of the samples from Forsmark and Laxemar.

2.3 Models

The M3 code is applied to the Forsmark 2.3 groundwater data, using as variables the major elements and δ^2H and $\delta^{18}O$, and as end-members, Littorina, Altered meteoric (which is sample 12281 from HFM16), Deep Saline (formerly Brine), Saline, Old meteoric –glacial (KFM07A, sample 8879) and Glacial.

Several models were studied for Forsmark 2.3: with different end-members and different variables. In this report are presented the three most representative models. All these three models employ as variables the major elements, δ^2H and $\delta^{18}O$. The end-members used in these three models are as following:

1. Model 1 (Figure 2-1) employs the Littorina, Altered meteoric, Glacial and Deep saline end-members for the M3 modelling.
2. Model 2 (Figure 2-2) employs the Littorina, Altered meteoric, Old Meteoric-Glacial and Deep Saline end-members for the M3 modelling.
3. Model 3 (Figure 2-3) employs the Littorina, Altered meteoric, Glacial and Saline end-members for the M3 modelling.

The PCA applied on Forsmark 2.3 data is illustrated in Figures 2-1, 2-2 and 2-3. A total of 290 groundwater samples from Forsmark 2.3 were used for this plot. The PCA in Figure 2-1 shows upper bedrock samples affected by meteoric alteration, a marine trend showing Baltic Sea water influence and, for some samples, a possible Littorina sea water influence. A glacial and a deep groundwater trend are also shown.

Model 1:

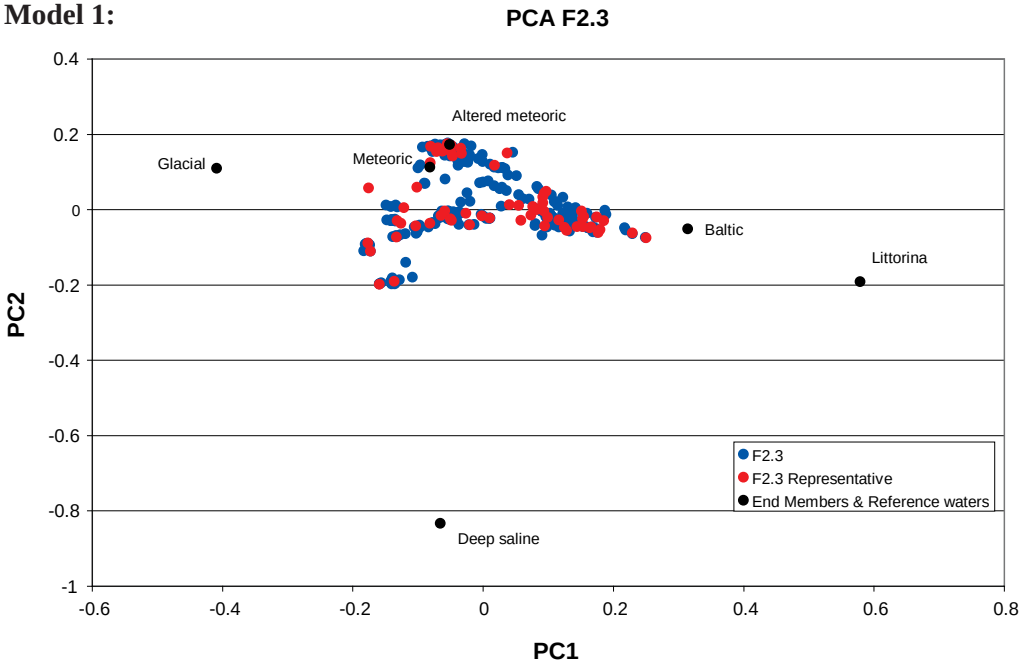

Figure 2-1. *Results of principal component analysis and the identification of the reference waters for Forsmark 2.3 data set. The first principal component accounted for 0.47 of the variance, the first and second principal components, 0.85, and the first, second and third principal components, 0.93. The coverage is 98.6% in n-PC and 95.6% in 2D. All the major elements, $\delta^{18}O$ and $\delta^{2}H$ are used as variables. The Littorina, Deep Saline, Glacial and Altered Meteoric reference waters are used as end-members for the modelling. The total data available for Forsmark 2.3 are 290 samples of which 64 are considered representative (in red on the figure).*

Model 2:

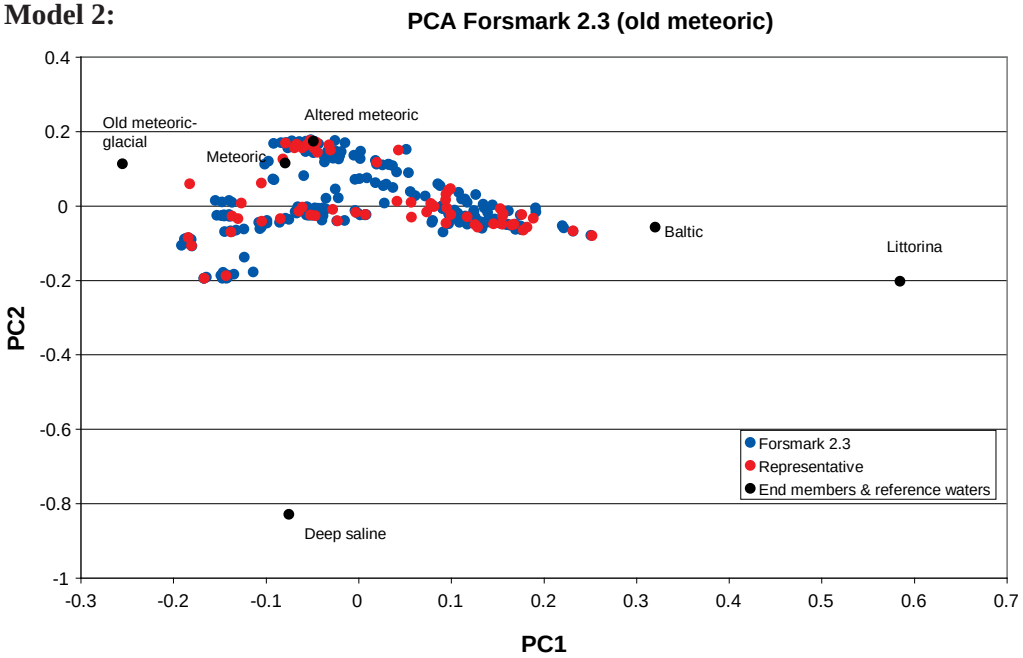

Figure 2-2. *Results of principal component analysis and identification of the reference waters for Forsmark 2.3 data set. The first principal component accounted for 0.48 of the variance, the first and second principal components 0.85, the first, second and third principal component: 0.93. The coverage is 98.6% in n-PC (as for the previous model) and 93% in 2D. All the major elements, $\delta^{18}O$ and $\delta^{2}H$ are used as variables. The Littorina, Deep Saline, Old Meteoric-Glacial and Altered Meteoric reference waters are used as end-members for the modelling. The total data available for Forsmark 2.3 are 290 samples of which 64 are considered representative (in red on the figure). The "Old Meteoric-Glacial" end-member ($\delta^{2}H$ = –118 and $\delta^{18}O$= –16) replaces the Glacial ($\delta^{2}H$ = –158 and $\delta^{18}O$= –21).*

Model 3:

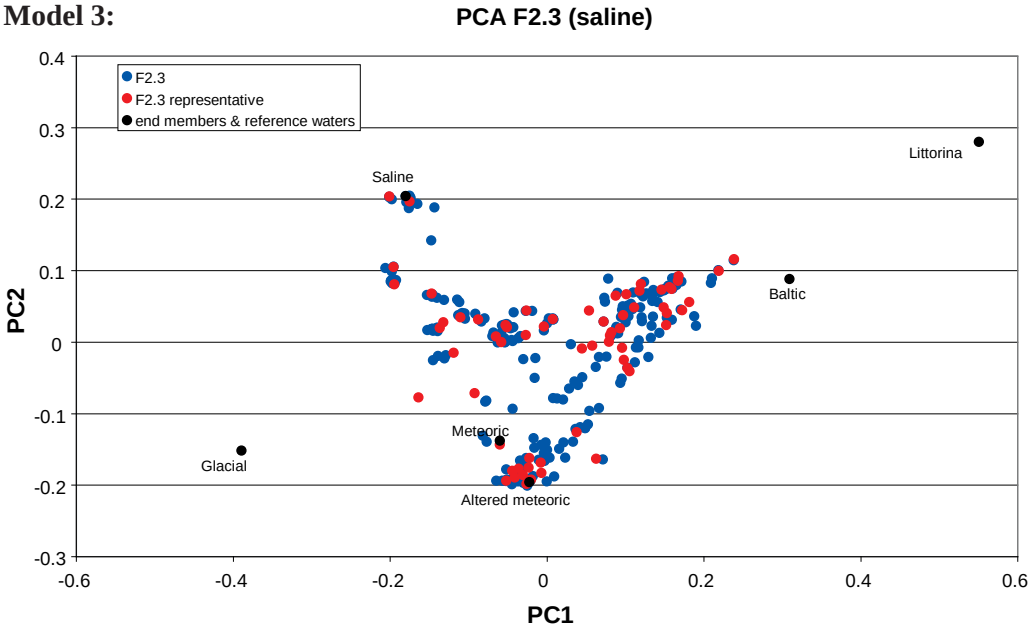

Figure 2-3. *Results of the principal component analysis and the identification of the reference waters for the Forsmark 2.3 data set. The first principal component accounted for 0.49 of the variance, the first and second principal components, 0.87, and the first, second and third principal components 0.93.The coverage is 96.6% in n-PC and 92.2% in 2D. All the major elements,$\delta^{18}O$ and $\delta^{2}H$ are used as variables. The Littorina, Deep Saline, Glacial and Altered Meteoric reference waters are used as end-members for the modelling. The total data available for Forsmark 2.3 are 290 samples of which 64 are considered representative (in red on the figure). The Saline end-member represents the sample 8879 from KFM07A (depth 759.m), and is the most saline sample from Forsmark.*

From all the three models, the PCA analysis employing all groundwater samples with major species (Na, K, Ca, Mg, SO_4^{2-}, HCO_3^-, Cl) and isotopes the δ^2H and $\delta^{18}O$ and with the end-members: Littorina, Deep Saline, Glacial, Altered Meteoric, give the most suitable characterization of the Forsmark 2.3 dataset because:

a) more robust calculations and almost all the samples are included in the PCA (98.6% coverage); it should be mentioned that the M3 2D version gave lower coverage (95.6% with old glacial end-member and 93% with the old meteoric- glacial end-member).

b) the use of an altered meteoric end-member, chosen from the upper bedrock samples solves the dilemma of the use of the Tritium. If a meteoric water was used as end-member, than the tritium should be used as a variable. The previous exercises showed that the tritium is not a reliable parameter.

c) the use of only conservative variables does not give a unique solution, therefore the benefit of using also non-conservative elements is shown

d) calculates mixing proportions including the same end-members used by the hydrogeologists

e) the data are selected based on the sampling date; the new entries in SICADA are difficult to identify.

3 2D visualisation of the Cl, $\delta^{18}O$, TDS and mixing proportions of the K-series boreholes

Figures 3-1 to 3-7 show the Cl, $\delta^{18}O$, TDS and mixing proportions calculated along the K-series boreholes with the M3 code. The three models (1, 2 and 3), with glacial, old meteoric-glacial and saline reference waters, are presented. Only the representative samples are shown.

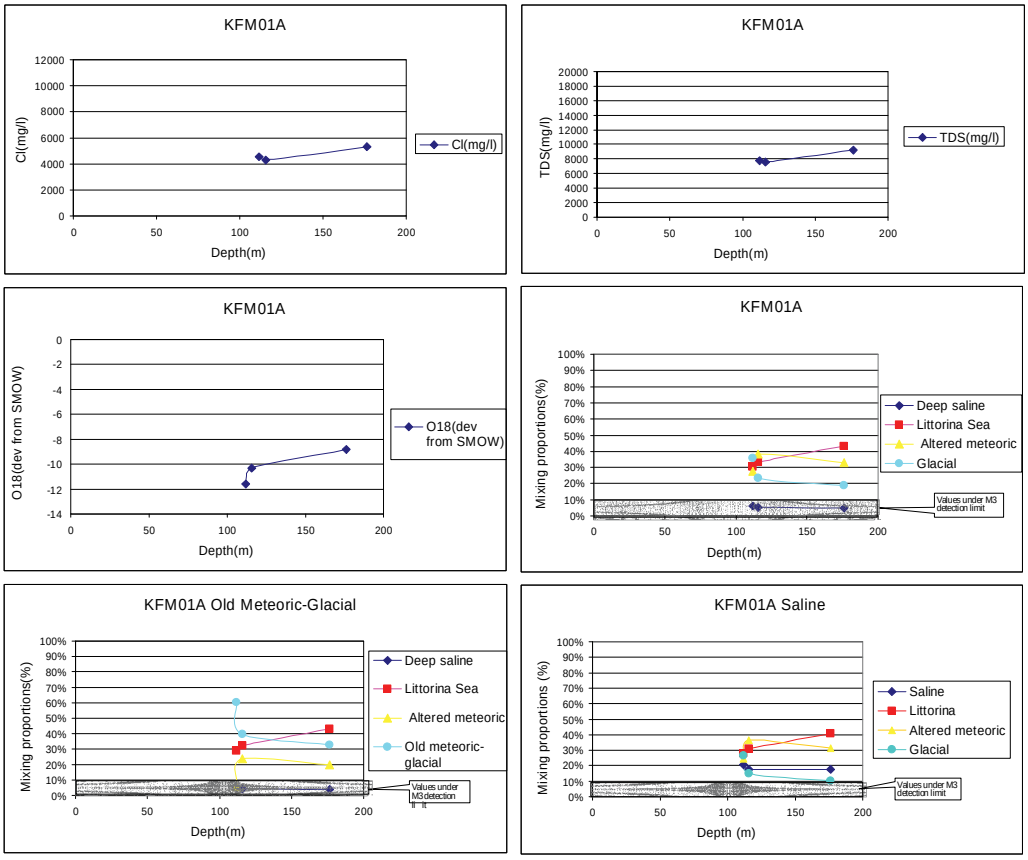

Figure 3-1. *Cl, TDS, $\delta^{18}O$, and mixing proportions (for the 3 models) along KFM01A.*

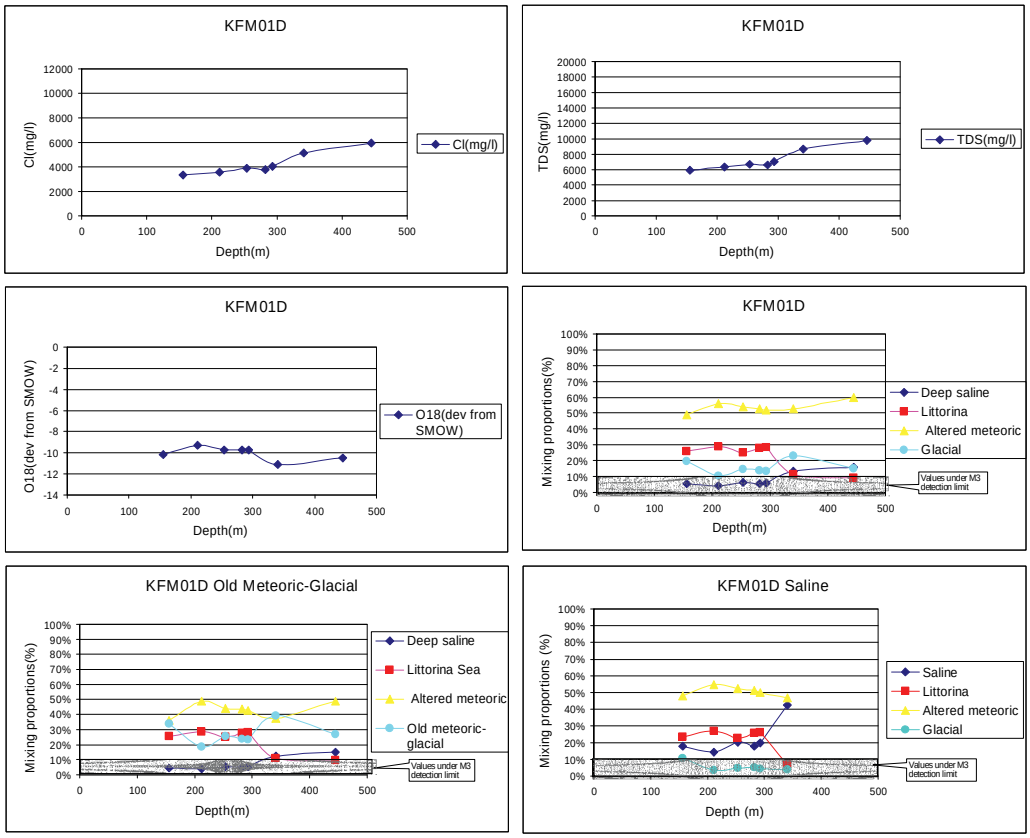

Figure 3-2. *Cl, TDS, $\delta^{18}O$, and mixing proportions (for the 3 models) along KFM01D.*

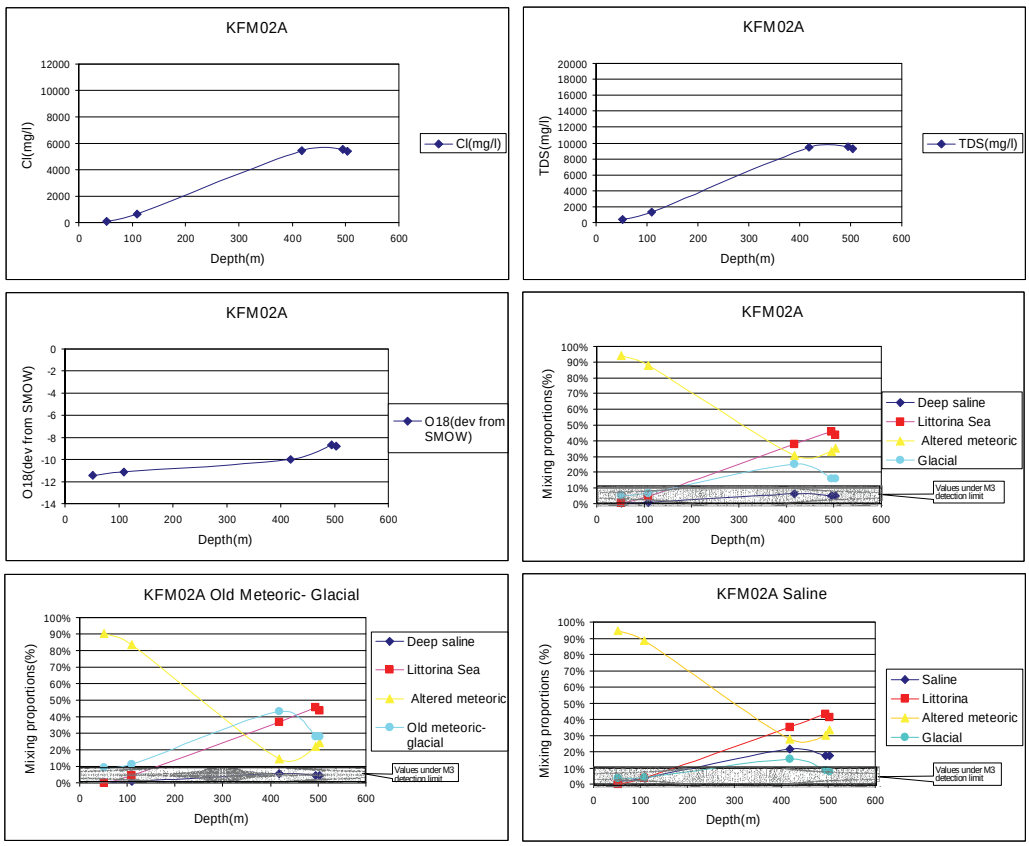

Figure 3-3. *Cl, TDS, $\delta^{18}O$, and mixing proportions (for the 3 models) along KFM02A.*

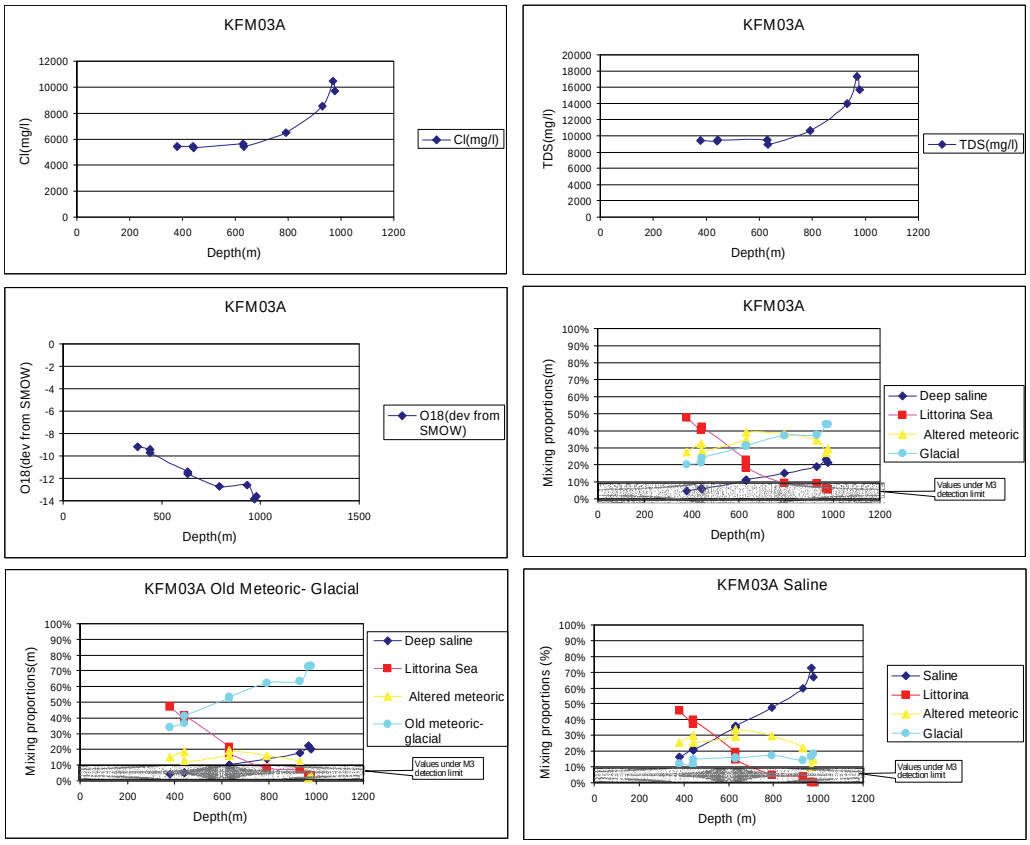

Figure 3-4. *Cl, TDS, $\delta^{18}O$, and mixing proportions (for the 3 models) along KFM03A.*

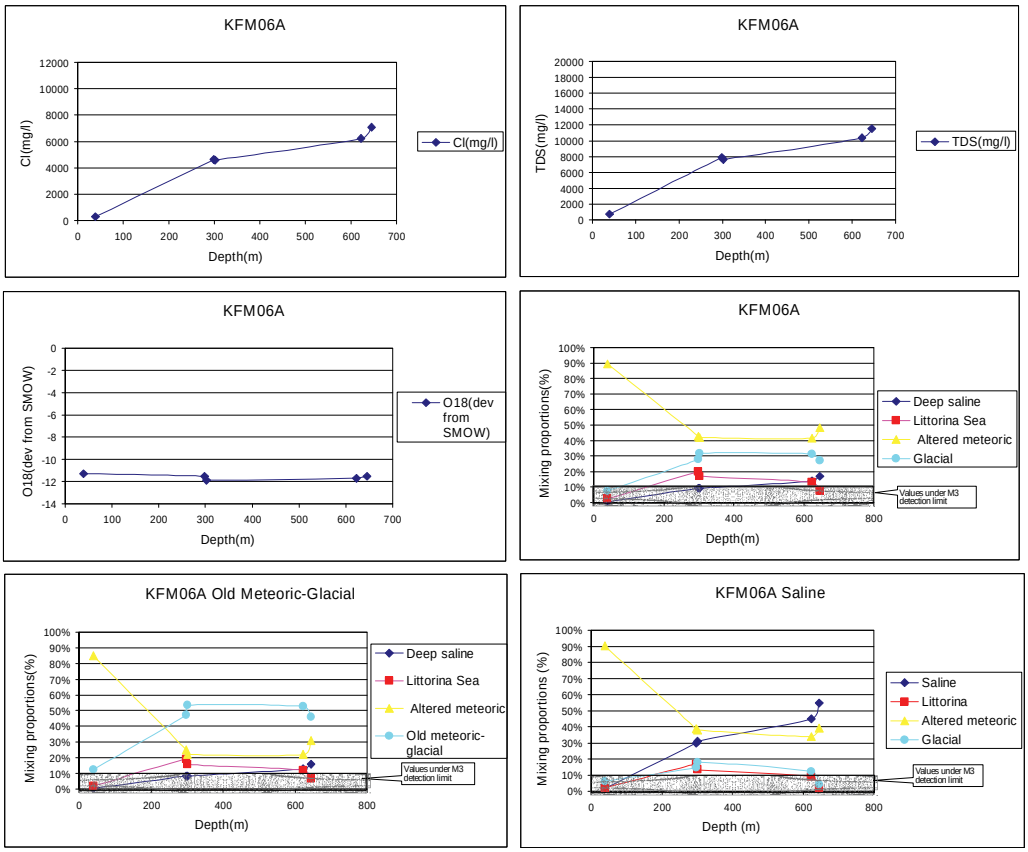

Figure 3-5. *Cl, TDS, $\delta^{18}O$, and mixing proportions (for the 3 models) along KFM06A.*

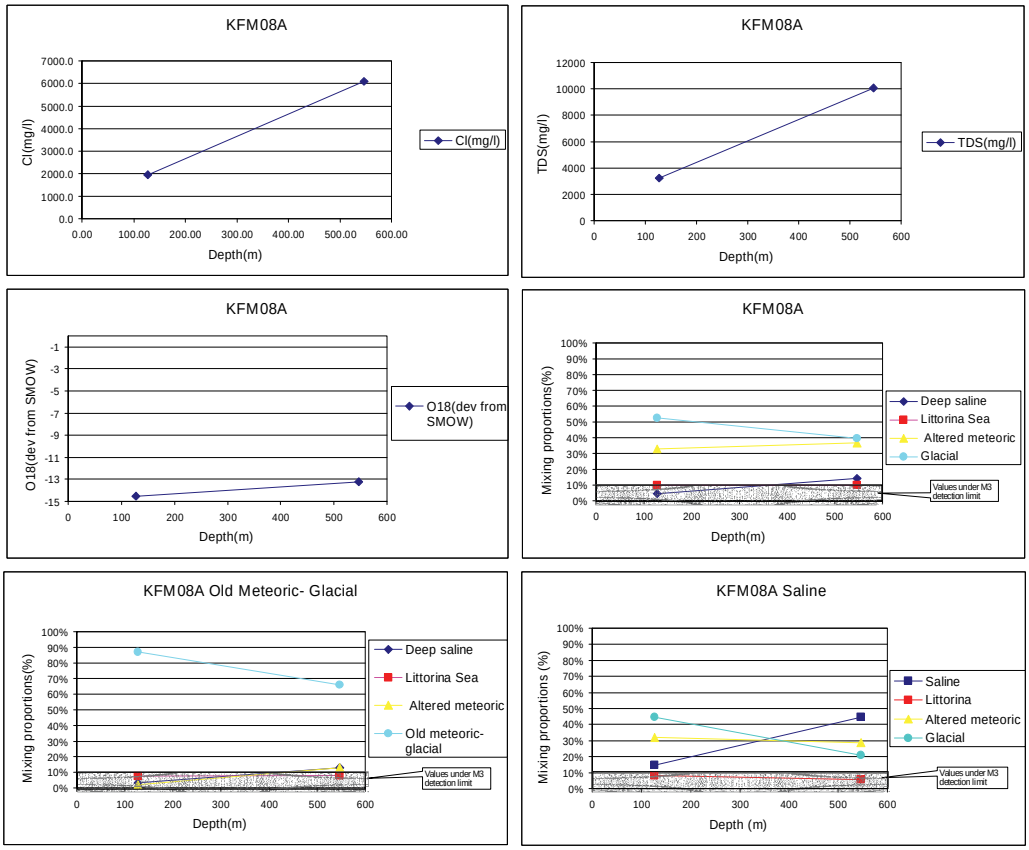

Figure 3-6. *Cl, TDS, $\delta^{18}O$, and mixing proportions (for the 3 models) along KFM08A.*

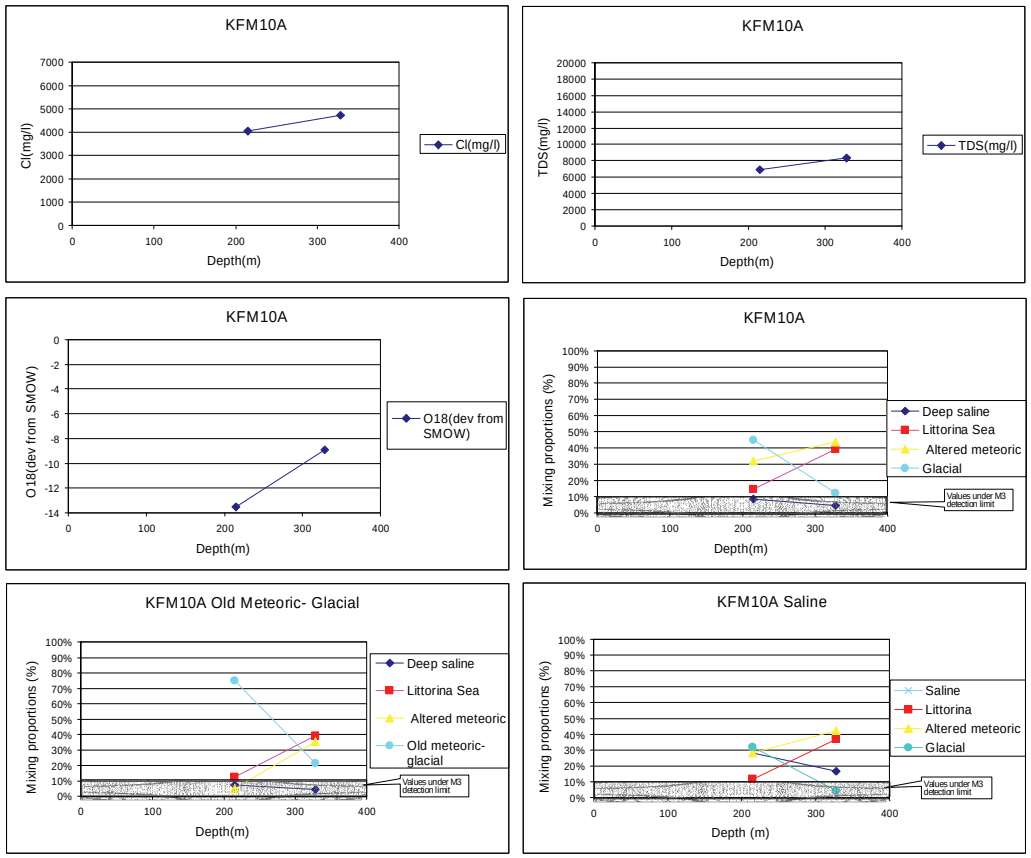

Figure 3-7. *Cl, TDS, $\delta^{18}O$, and mixing proportions (for the 3 models) along KFM10A.*

By employing the Old Meteoric-Glacial reference water, more glacial water is predicted at depth and less-altered meteoric water, which is in better agreement with the conceptual model made by “expert judgement”.

The M3 modelling gives mixing proportions along the boreholes, which, together with the Cl, $\delta^{18}O$ and TDS, can help the hydrogeologists for groundwater modelling calibration. The inclusions of samples from greater depth obtained from Forsmark 2.3 data freeze bring more understanding to the bedrock model. The Forsmark 2.3 model is very similar to 1.2, 2.1 and 2.2, but samples from depth give the opportunity to characterize also a deeper part of the bedrock. This can help to give more mixing proportions to the hydrogeologists for modelling calibration and verification.

Figure 3-8 shows the PCA for Forsmark 2.3 data set where the boreholes with time series are indicated. The red points show the first sample in the serie for a given section in a borehole and the green point the last sample of the serie. In the Forsmark 2.3 dataset there are 23 sections in core-drilled boreholes with 3 or more time series.

The average of the mean groundwater variability at Forsmark during groundwater sampling (first/last sample) is about 5%. The maximum variability is for the section –115.79 in KFM01A and is about 25%.

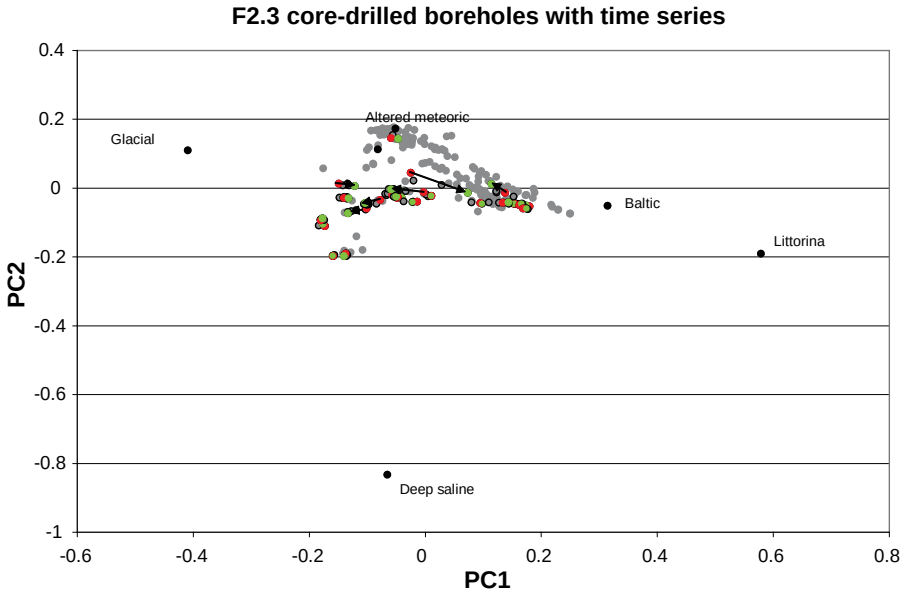

Figure 3-8. *The Forsmark 2.3 data PCA. In grey are indicated all the Forsmark samples. The core-drilled boreholes with time series are shown as grey dots with black circles. The red dots represent the first sample in the time series and the green dots represent the last sample in the time series. The arrows show the variability of the samples with time series in the PCA. This analyse indicates that the samples are quite stable. Only one section presents a higher variability (KFM01A, section secmid –115.79 m).*

4 Uncertainity analyses and verification using the conservative elements $\delta^{18}O$ and Cl

The model used in mass balance modelling should describe as well as possible the measured data. The conservative variables Cl and $\delta^{18}O$ were used to check the accuracy of the model. These parameters are considered to be fully conservative and should not be affected by reactions; therefore the values predicted by the models should be as close as possible to the measured data. In this respect, the best model is the one which predicts the best conservative parameters, which should not be changed by the calculations. Figures 4-1 and 4-2 show the calculated values of Cl and $\delta^{18}O$ plotted against the measured values. Three models are presented: one uses Glacial as an end-member, another uses the old Meteoric-Glacial as an end-member and the third uses the saline end-member, as described in Models 1, 2 and 3. The perfect fit line (in black) in shown in both figures.

A vertical shift in all three graphs is seen at around 5,000 to 6,000 Cl. This can be explained by the existence of one mixing trend, up to 6,000 mg/ l Cl, composed by altered meteoric, glacial (or old meteoric-glacial) and Littorina waters. At concentrations higher than 6,000 mg/l Cl, another trend is observed. This trend shows a mixture of altered meteoric, glacial (or old meteoric-glacial) and Littorina, plus the saline water.

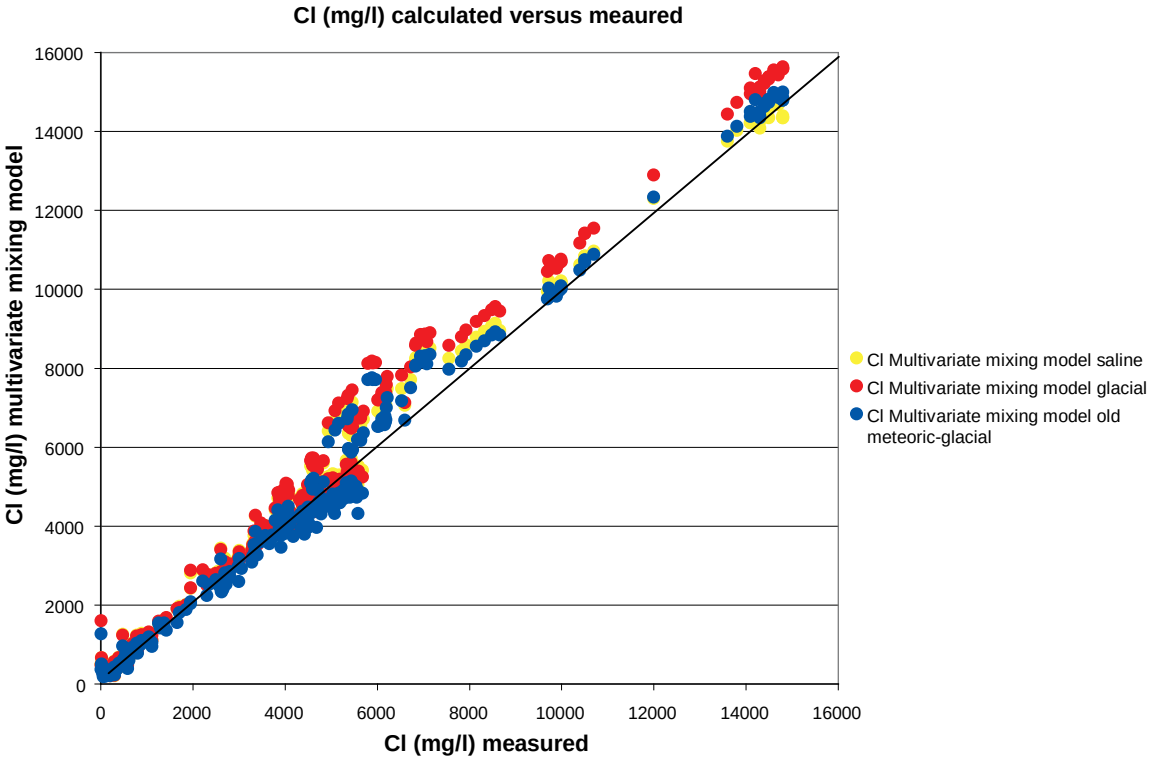

Figure 4-1. *Cl (mg/l) measured versus multivariate mixing model. The Cl is one of the variables used in the M3 calculations. The model uses all the variables (major elements and $\delta^{2}H$ and $\delta^{18}O$) and predicts the new values of all the parameters used. The deviation for each parameter from the measured value to the calculated value represents the effects of mixing and/or reactions. As the Cl is a conservative parameter, the calculated values should not differ from the measured values. In black the perfect fit line.*

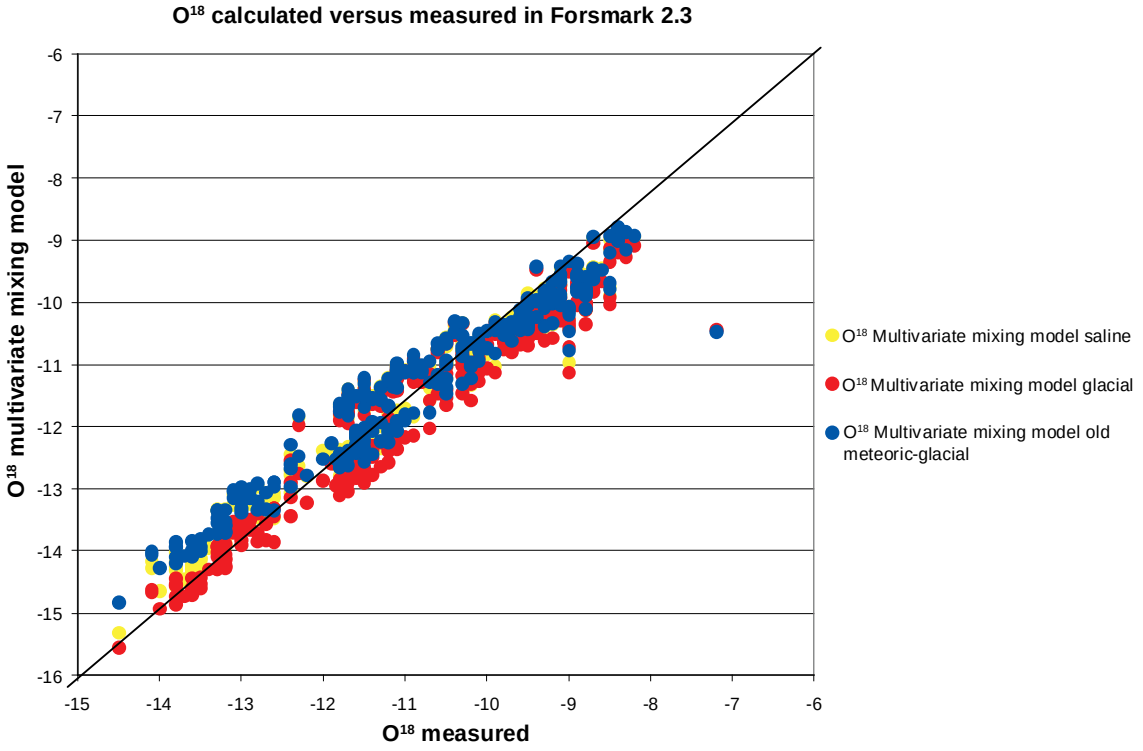

Figure 4-2. *$\delta^{18}O$ measured versus multivariate mixing model. The $\delta^{18}O$ is one of the variables used in the M3 calculations. The model uses all the variables (major elements and $\delta^{2}H$ and $\delta^{18}O$) and predicts the new values of all the parameters used. The deviation for each parameter from the measured value to the calculated value represents the effects of mixing and/or reactions. As the $\delta^{18}O$ is a conservative parameter, the calculated values should not differ from the measured values. In black the perfect fit line.*

The measured values, when compared with the predictions given by the different models, should show that the best model is the one with the smallest error. All three models predict the Cl and $\delta^{18}O$ fairly well, when compared with the ideal fit line.

In order to quantify the accuracy of the model, the RMSE (root mean square error) was calculated for the 3 different models. The best model is the one with the smallest error, as per the following calculations:

1. Calculate the difference between data and model = the "error" on the model with respect to the data: y_data - y_model
2. Compute the signed variance of the errors: sigma (error) and the mean error to get rid of biases
3. Get the RMSE = SQRT (sigma (error) + (mean_error)^2)

The model with the smallest RMSE-ul gives the best predictions.

The best model is the model that describes the best the Cl and $\delta^{18}O$. The Figures 3-8 and 4-1 show that all the models are good. Therefore, all the models can be used, but the best is to use the one that fits the conceptual model best and the hydrochemical understanding (as described also by /Gimeno et al. 2008/).

Table 4-1. RMSE for the Cl and $\delta^{18}O$ predicted with the 3 different models.

	Cl model1 glacial	Cl model2 old meteoric-glacial	Cl model3 saline	O18 model1 glacial	O18 model2 old meteoric-glacial	O18 model3 saline
variance	335246	248342	176720	0.20	0.16	0.13
mean error^2	259512	12629	128262	0.61	0.25	0.29
RMSE	771	511	552	0.90	0.64	0.64

5 Analytical uncertainty handled by M3

At every phase of the hydrogeochemical investigation programme – drilling, sampling, analysis, evaluation, modelling – uncertainties are introduced. These have to be accounted for, addressed fully, and clearly documented to provide confidence in the end result, whether it will be the site descriptive model or repository safety analysis and design /Smellie et al. 2002/. Handling the uncertainties involved in constructing, a site descriptive model has been documented in detail by /Andersson et al. 2001/. The uncertainties can be conceptual uncertainties, data uncertainty, spatial variability of data, chosen scale, degree of confidence in the selected model, and error, precision, accuracy and bias in the predictions.

For example, the analytical error of the samples may be ± 10%. This possible error was tested with the M3 code. In Figure 5-1 is shown the location of a given sample in the PCA (for exemplification sample 4538 from KFM01A) and the location of two synthetic samples made by adding/removing 10% from the initial composition.

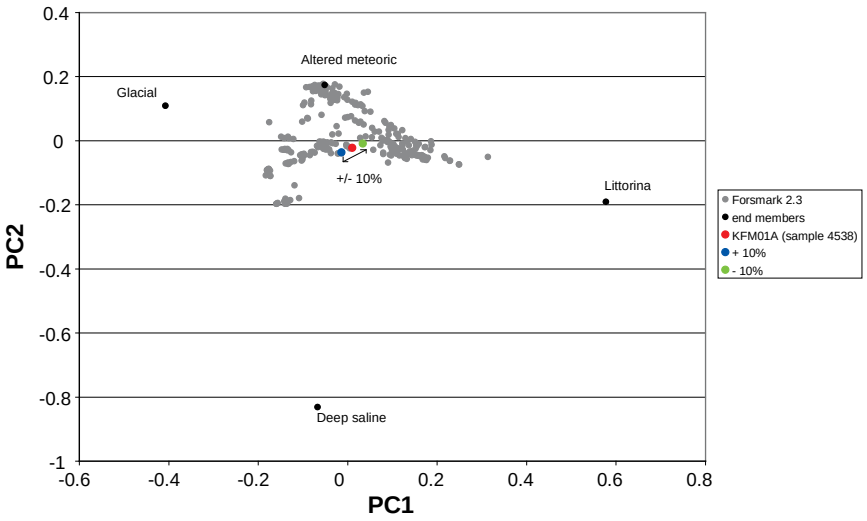

Figure 5-1. *Analytical uncertainty evaluation for Forsmark 2.3.The red dot represents the sample 4538. The green and blue dots represent compositions of +/– 10% from the original composition.*

6 Visualisation of the mixing proportions versus depth

In general, by employing the Old Meteoric-Glacial, more glacial water is predicted at depth and less altered meteoric, which is in better agreement with the conceptual model. By using the Glacial end-member, more altered meteoric water is predicted at greater depths (Figures 6-1 to 6-3). The choice of the end-members should be made according to the conceptual model. This is shown also in the Figures 3-1 to 3-7, where the mixing proportions of different waters are visualised along the boreholes. The Littorina and Deep Saline are not affected by the use of a different glacial end-member.

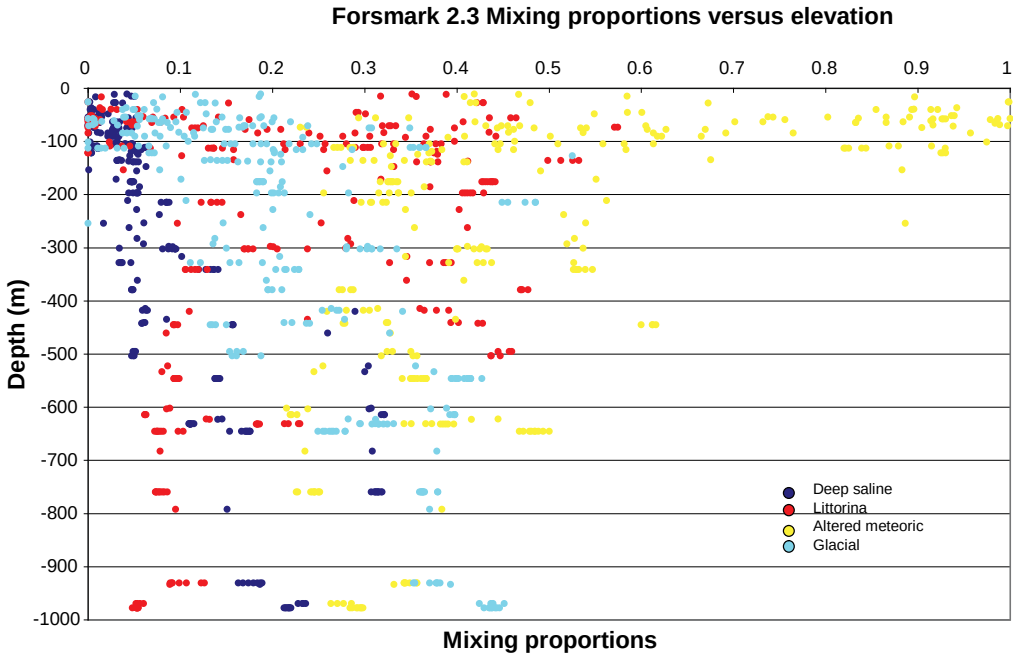

Figure 6-1. *Mixing proportions of Deep Saline, Littorina, Altered meteoric and Glacial end-members versus depth in Forsmark 2.3.*

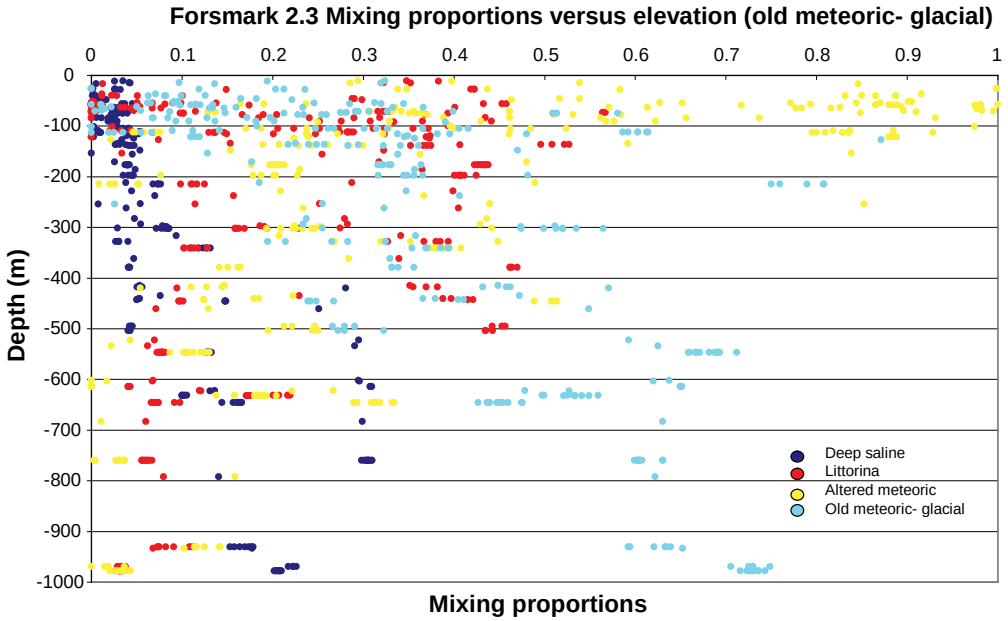

Figure 6-2. *Mixing proportions of Deep Saline, Littorina, Altered meteoric and Old Meteoric-Glacial end-members versus depth in Forsmark 2.3.*

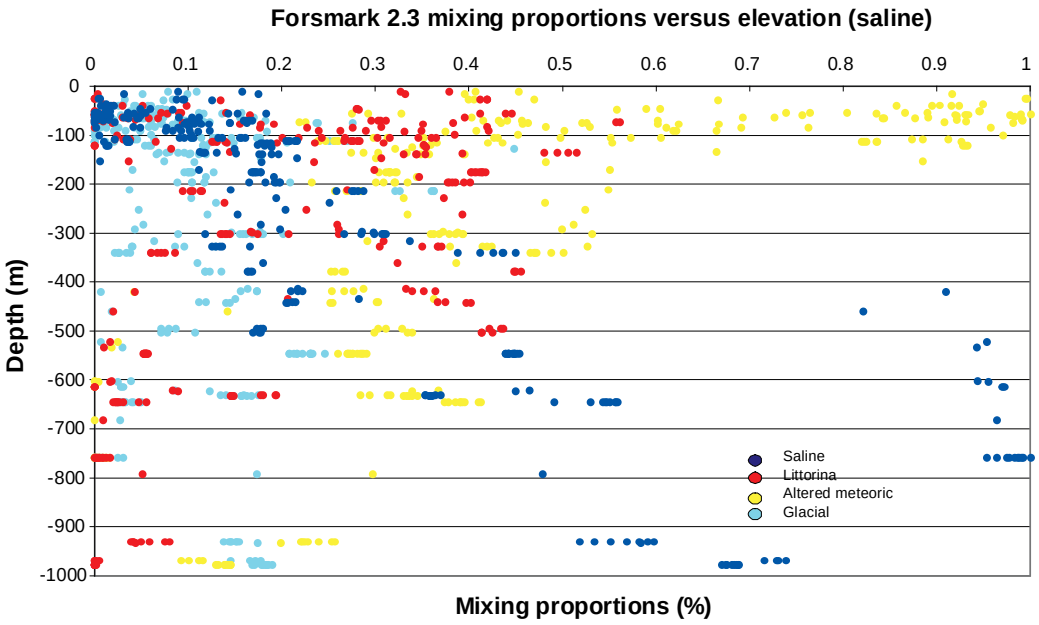

Figure 6-3. *Mixing proportions of Saline, Littorina, Altered meteoric and Glacial end-members versus depth in Forsmark 2.3.*

7 Extended data

New data became available on December 30, 2007, after the completion of the Forsmark 2.3 final report. The new data, called extended data, are mainly from new boreholes like KFM08D, KFM11A and KFM12A. Among these samples, only 53 met the M3 criteria (complete dataset for major elements and isotopes, no gaps in data) and were used in the new M3 modelling. These samples were from boreholes core and percussion. 13 of these samples were qualified as representative. The aim of the new modelling was to see if the new samples would change in anyway the overall interpretation of the Forsmark 2.3 model.

Figure 7-1 shows the new PCA made for the Forsmark 2.3 dataset plus the extended data.

The PCA in Figure 6-3 shows that the Forsmark 2.3 and extended data have the same distribution and almost the same variance and coverage as the Forsmark 2.3 data set alone. Only one sample from KFM12A (sample number 12788) has more glacial signature ($\delta^{18}O$= –15.6).

The mixing proportions calculated with Forsmark 2.3 dataset plus the extended data do not differ from the mixing proportions calculated with the Forsmark 2.3 data set alone (the difference is less than 1%). This means that the extended data do not affect the results of the modelling of the Forsmark 2.3 dataset.

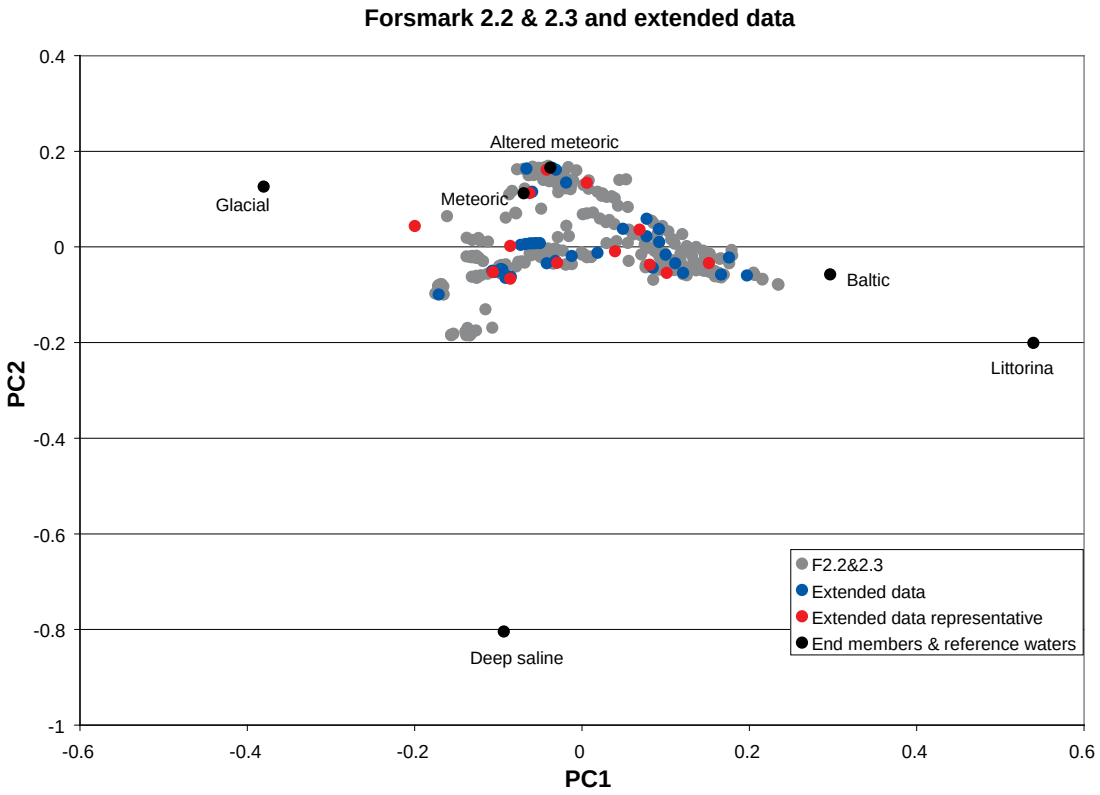

Figure 7-1. *Results of principal component analysis and identification of the reference waters for Forsmark 2.3 data set and extended data. The first principal component accounted for 0.47 of the variance, the first and second principal components 0.84, the first, second and third principal component: 0.93. The coverage is 98.9% in n-PC and 95.7% in 2D. These results are very similar to the values given by the models where only Forsmark 2.3 data set was emplyed. All the major elements, $\delta^{18}O$ and $\delta^{2}H$ are used as variables. The Littorina, Deep Saline, Glacial and Altered Meteoric reference waters are used as end-members for the modelling. The total data available for Forsmark 2.3 (in grey in the figure) are 290 samples of which 64 are considered representative. The extended data are presented in blue and the representative extended data in red.*

8 Concluding remarks

This work represents the stage 2.3 of the hydrochemical evaluation and modelling of the Forsmark data. This comprises M3 modelling and 2D visualisation of the data along the boreholes. The following conclusions can be drawn:

- M3 modelling helped to summarise and understand the data, by using as variables the major elements and the isotopes $\delta^{18}O$ and D.
- Previous alternative models and the experience from Forsmark 1.2, 2.1 and 2.2, helped to clarify different previously unsolved issues such as: the use of variables, tests with different end-members, the use of only groundwater data in order to build a bedrock hydrochemical model.
- The visualisation of the mixing proportions along the boreholes helps to understand the distribution of the data in the domain and to check and compare the results of different models; and therefore to chose the model which best describes the measured data.
- The different M3 modelling tests resulted in the following conclusions: a) When calculating mixing proportions only samples from the boreholes will be used, b) the altered meteoric end-member which best describes the more shallow groundwater compositions is defined by a representative upper bedrock sample; the Littorina end-member employed the existing modelled compositions; the Deep saline and glacial end-members compositions were tested by means of a feasibility study and employed in the modelling.

- Three models were presented. All the models are good and can be used, but the best is to use the one that fits the conceptual model best and the hydrogeochemical understanding.
- The use of Littorina, Glacial, Deep Saline and Altered Meteoric end-members makes possible the comparison of different sites such as Laxemar and Forsmark.
- All the data used in the M3 modelling and the results of the modelling and visualisation along the boreholes are presented in SKB database SIMON.
- The extended data do not affect the results of the modelling of the Forsmark 2.3 dataset (the difference between the mixing proportions calculated with both models is less than 1%).

9 References

Andersson J, Christiansson R, Munier R, 2001. Djupförvarsteknik: Hantering av osäkerheter vid platsbeskrivande modeller. Tech. Doc. (TD-01-40), SKB, Stockholm, Sweden.

Gimeno M J, Auqué L F, Gómez J B, Acero P, 2008. Water-rock interaction modelling and uncertqinties of mixing modelling. SDM-Site Forsmark. SKB R-08-86, Svensk Kärnbränslehantering AB.

Gómez J, Laaksoharju M, Skårman E, Gurban I, 2006. M3 version 3.0: Concepts, methods, and mathematical formulation. SKB TR-06-27, Svensk Kärnbränslehantering AB.

Laaksoharju M, Smellie J, Nilsson A-C, Skårman C, 1995. Groundwater sampling and chemical characterisation of the Laxemar deep borehole KLX02. SKB TR 95-05, Svensk Kärnbränslehantering AB.

Laaksoharju M, Wallin B (eds), 1997. Evolution of the groundwater chemistry at the Äspö Hard Rock Laboratory. Proceedings of the second Äspö International Geochemistry Workshop, June 6–7, 1995. SKB International Co-operation Report ISRN SKB-ICR-91/04-SE. ISSN 1104-3210 Stockholm, Sweden.

Laaksoharju M, 1999. Groundwater Characterisation and Modelling: Problems, Facts and Possibilities. Dissertation TRITA-AMI-PHD 1031, ISSN 1400-1284, ISRN KTH/AMI/ PHD 1031-SE; ISBN 91-7170-. Royal Institute of Technology, Stockholm, Sweden. Also as SKB TR-99-42, Svensk Kärnbränslehantering AB.

Laaksoharju M, Skårman C, Skårman E, 1999. Multivariate Mixing and Mass-balance (M3) calculations, a new tool for decoding hydrogeochemical information. Applied Geochemistry Vol. 14, #7, 1999, Elsevier Science Ltd., pp 861–871.

Laaksoharju M, Gimeno M, Auqué L, Gómez J, Smellie J, Tullborg E-L, Gurban I, 2004. Hydrogeochemical evaluation of the Forsmark site, model version 1.1. SKB R-04-05, Svensk Kärnbränslehantering AB.

SKB, 2005. Hydrogeochemical evaluation. Preliminary site description Forsmark area – version 1.2. SKB R-05-17, Svensk Kärnbränslehantering AB.

SKB, 2006a. Hydrogeochemical evaluation. Preliminary site description Laxemar subarea – version 2.1. SKB R-06-70, Svensk Kärnbränslehantering AB.

SKB, 2006b. Hydrogeochemical evaluation of the Forsmark site, modelling stage 2.1 – issue report. SKB R-06-69, Svensk Kärnbränslehantering AB.

Smellie J, Laaksoharju M, Tullborg E-L, 2002. Hydrochemical site descriptive model – a strategy for the model development during site investigation. SKB R-02-49, Svensk Kärnbränslehantering AB.

Tullborg E-L, Larson S Å, 1984. δ18O and δ13C for limestones, calcite fissure infillings and calcite precipitates from Sweden. Geologiska föreningens i Stockholm förhandlingar 106(2).

Section 2

Coupled hydrogeological and solute transport, visualisation and supportive detailed reaction modelling

Jorge Molinero, David Arcos and Lara Duro
Amphos

Executive summary and main conclusions of the work

This report constitutes the contribution of AMPHOS XXI Consulting (Formerly Enviros-Spain) to the version 2.3 of the Hydrochemical Analysis of Forsmark site. According to the "Activity Plan for Hydrochemical Site Characterization Models 2.2 and 2.3 for Forsmark" /Laaksoharju 2007/, the AMPHOS Team is responsible for the Governing Activities 5 and 9, and should participate actively in activities 4,6,7,10,11,12 and 13.

Chapter 2 summarises the main findings achieved by **spatial analysis of hydrochemical information** using 3D visualisation techniques with the available Forsmark 2.3 hydrochemical database. A major improvement compared with previous versions is that the current visualisation tool can handle the Fracture Domain geometries of the site, which is useful for integration of hydrochemical data with current geological-hydrogeological conceptual models. It is seen that computed M3 mixing fractions show a spatial distribution qualitatively correlated with key hydrochemical signatures, such as strontium (for Deep Saline), magnesium (for Littorina), 18-O and 2-H (for Glacial) and tritium (for Modified meteoric). It is worth noting that the most saline waters with the highest Deep Saline signatures are located at deformation zones adjacent to the strongly foliated rocks, which constitute fracture domains FFM04 and FFM05, out of the target area. Maximum glacial signatures are also located outside the target area. In general terms, it is seen that hydrochemical spatial distribution is consistent with the current hydrogeological conceptual model, where the "shallow bedrock aquifer" would be responsible for the observed preservation of Littorina signatures down to a depth of 150–200 m.

The SurfaceNet group has also been working with hydrochemical information and some areas with deep/old water signatures have been detected. **Chapter 3** contains a brief summary of the analysis of **consistency between SurfaceNet and ChemNet interpretation** of such waters. It is seen that SurfaceNet and ChemNet hydrochemical interpretations are consistent in that shallow groundwater near Eckarfjärden contains hydrochemical signatures that can be older/deeper than expected. Particularly, ChemNet observations point towards glacial signatures at that location. On the other hand, the old/deep signatures found by SurfaceNet in the near-surface waters at northwest and east locations of Forsmark are interpreted as clear Littorina signatures in the ChemNet analysis.

It is well known that site characterization activities can potentially induce groundwater contamination which could **compromise the SKB "suitability criteria" for groundwaters at repository depth**. Reactive mixing and reactive solute transport models have been used as quantitative tools in order to evaluate how much disturbance can be allowed for a given groundwater sample at repository depth and still meet the SKB suitability criteria. All these modelling exercises are reported in **Chapter 4**. After this work it is concluded that suitability criteria related to TDS and pH would always be fulfilled even for complete disturbance of the repository depth sample. Ca+Mg criteria could be surpassed in case of producing dilutions higher than 90 percent of the native groundwater sample. It is seen that cation exchange processes have an effect in this case by lowering the Ca+Mg concentrations in the groundwater, compared with a pure conservative mixing. The oxygen consumption capacity of the granite bedrock has been also evaluated by using reactive transport modelling. A hypothetic contamination event by atmospheric oxygen at repository depth would be consumed in a relatively short period of time (about 1 year) if the maximum amounts of reported pyrite are included in the reactive transport model. However, model results have been proved to be sensitive with respect to uncertain parameters such as the exact mineralogical composition and the specific reactive surface area of such minerals. An interesting conclusion is that, in the base case considered in the model, the oxygen intrusion in a borehole would just affect a very short distance into the bedrock (about 1 cm).

An important product generated by the ChemNet group is hydrochemical mixing modelling. Mixing model results are delivered to other disciplines and constitute a relevant piece of information for the establishment of the overall conceptual model of the site. Magnesium is a very interesting solute because it is present in sea waters at much larger amounts than in the rest of the reference waters and, therefore, could constitute an indicator for relict Littorina sea water.

Littorina mixing fractions and magnesium concentrations have been used for testing and calibration of hydrogeological models in the past HydroNet activities. However, it is well known that dissolved magnesium is a reactive species that can be involved in a number of hydrogeochemical processes, one of the most relevant being cation exchange. **Chapter 5** shows a cautionary exercise which aims at **evaluating the magnitude of the error** that could be committed when **magnesium is used as a conservative tracer for Littorina water**. Computed results show that conservative mixing models would underestimate the actual Littorina signature due to the unaccounted effect of cation exchange processes. Then, the calibration of hydrogeological models against either measured magnesium concentrations or M3 computed Littorina mixing fractions, would probably lead to overestimation of the flushing rates in the hydrogeological models, because larger groundwater recharge flows could be required in order to compute smaller amounts of relict Littorina water in the bedrock. Therefore, even it could be a qualitative indicator for Littorina Sea water signature, magnesium should not be used as a quantitative tracer for such an end-member.

Chloride and bromide mass ratios constitute a powerful tool to detect waters with different origin. In fact, such a tool is particularly suitable for tracing the marine origin of waters. **A Chloride/Bromide analysis using the Forsmark database has been done and the main results are shown in Chapter 6**. It can be stated that groundwater samples available at Forsmark can be explained as a result of mixing/evolution between a marine end-member (Littorina), a dilute end-member (Meteoric and/or Glacial) and a Brackish end-member. Two important conclusions have been made based on this analysis: (1) The Brackish end-member shows a non-marine signature, and it is very different than the deep saline waters sampled at both Laxemar and Olkiluoto sites; (2) Quantitative estimations of Littorina signatures by simple binary mixings shows that the M3 methodology could produce large quantitative errors, most probably due to propagating numerical errors.

A relevant issue in the hydrochemical understanding of the Forsmark site is related to the **processes that modify meteoric water composition in the shallow zone of the system**, where Quaternary sediments are present. One of the main uncertainties is related to the process or processes that control the redox in this shallow system as well as the cation exchange related to sheet silicates present in the sediments from this zone. Detailed hydrochemical modelling of the near-surface zone is shown in **Chapter 7**. Two distinctive evolutions can be identified regarding the chemical evolution of near-surface waters from the Forsmark, one involving only surface waters interacting with solid materials from sediments and soils and the other involving the mixing with relict high salinity waters. The evolution of dilute waters is mainly related to the oxidation of organic matter and an additional calcium source that has been exemplified in the calculations by the dissolution of trace amounts of gypsum that could be present in the unsaturated zone. Other reactions taken into account in the model are equilibrium with calcite and a cation exchanger. The evolution of the more saline waters in the near-surface system is mainly related to the mixing with ancient Littorina Sea water trapped in the system and the equilibrium with a cation exchanger associated with the clay fraction of the materials considered. It is also reported that the redox of the near-surface system appears to be controlled by Fe(II)/Fe(III) pair, but shifting to the S(-II)/S(VI) pair. The scarcity of Eh data does not allow a more conclusive statement on the specific processes responsible for controlling the redox of the shallow groundwater system.

A major additional issue at the Forsmark site is that **measured uranium concentrations appeared to be higher than expected** according to the measured redox potential. However, one of the main conclusions from the work reported in **Chapter 8** is that the concentrations of uranium in the Forsmark groundwaters are not, in general, so anomalously high. The apparently high solubilities under reducing conditions are a consequence of the speciation of uranium in solution, which is mainly in the form of U(VI) tricarbonato species. Most measured data can be explained by the reprecipitation of the uranium released from a primary pitchblende-like source in the form of amorphous UO_2 solid phase, whose solubility is very close to the one of $UO_2 \cdot 2H_2O(s)$ in the thermodynamic database used by SKB. According to the available representative groundwater samples from cored boreholes, only three locations (at specific sections

of borehole KFM02, 03 and 08) seem to present a relatively higher uranium concentration than that corresponding to the solubility of a U(IV) solid oxide. No indications of different chemistry of these groundwater samples seem to explain those apparent discrepancies, thus the reasons must be sought for in different processes accounting for the enhanced solubilisation of uranium in these particular (3) borehole sections. Some of the processes that could account for the enhanced solubilisation of uranium in these few samples presenting anomalous values are: (1) influence of in situ bacterial activity, (2) influence of dissolved organic carbon and, (3) influence of drilling fluid presenting uranium complexing agents such as those resulting from the solubilisation of Fe(III) hydroxides. It is worth noting that such possible enhancing solubility processes can not be conclusively proved with the available information.

Contents

1 Introduction and scope of the work

The general aim of the ChemNet work in Forsmark is to describe the representative volume in the framework of the Complete Site Investigation strategy. Accordingly, datafreeze 2.2 contains all the data necessary for such a description (see comment item #1) This report constitutes the contribution of the AMPHOS team to the model stages 2.2–2.3 of the Hydrochemical Analysis of the Forsmark site.

It was determined in previous modelling stages that a crucial tool for hydrochemical analysis and, especially, for integration with other disciplines, was the spatial analysis and 3D visualisation of available data. Chapter 2 summarises the main findings achieved by using advanced 3D visualisation techniques with the available Forsmark 2.2 hydrochemical database. A major improvement compared with previous versions is that the current visualisation tool can handle the Fracture Domain geometries of the site, which is useful for integration of hydrochemical data with current geological-hydrogeological conceptual models. On the other hand, the SurfaceNet group has also been working with hydrochemical information and some areas with deep/old water signatures have been detected. Chapter 3 shows the analysis of consistency between SurfaceNet and ChemNet interpretation of such waters.

It is well known that site characterization activities can potentially induce groundwater contamination at repository depth which could compromise the SKB “suitability criteria” for groundwaters at repository depth. Reactive mixing and reactive solute transport models have been used as quantitative tools in order to evaluate how much disturbance can be allowed for a given groundwater sample at repository depth and still meet the SKB suitability criteria. All these modelling exercises are reported in Chapter 4.

An important product generated by the ChemNet group is hydrochemical mixing modelling. Mixing model results are delivered to other disciplines and constitute a relevant piece of information for the establishment of the overall conceptual model of the site. Magnesium is a very interesting solute because it is present in sea waters at much larger amounts than in the rest of the reference waters and, therefore, could constitute an indicator for relict Littorina sea water. Littorina mixing fractions and magnesium concentrations are commonly used for testing and calibration of hydrogeological models within the HydroNet activities. However, it is well known that dissolved magnesium is a reactive species that can be involved in a number of hydrogeochemical processes, one of the most relevant being cation exchange. Chapter 5 shows a cautionary exercise which aims at evaluating the magnitude of the error that could be committed when magnesium is used as a conservative tracer for Littorina water. This chapter has been already discussed and delivered to the HydroNet group.

Another relevant issue in the hydrochemical understanding of the Forsmark site is related to the processes that modify meteoric water composition in the shallow zone of the system, where Quaternary sediments are present. One of the main uncertainties is related to the process or processes that control the redox in this shallow system as well as the cation exchange related to sheet silicates present in the sediments from this zone. Detailed hydrochemical modelling of the near-surface zone is shown in Chapter 6 of this report.

A major additional issue at the Forsmark site is that measured uranium concentrations appears to be higher than expected according to the measured redox potential. One of the issues of concern within this stage of the modelling is trying to understand the reason for such high concentrations. Our contribution to this issue is reported in Chapter 7.

The main conclusions that can be extracted from all the work performed are finally summarised in Chapter 8.

2 3D visualisation of measured and modelled data

Figure 2-1 shows a general location view of the Forsmark area, including the main surface features (lakes and coastline), the ID of key boreholes and the location of the deformation zone A2. The same figure also shows the spatial distribution of the borehole sections with available chemical samples of relatively different quality for hydrochemical modelling purposes (categories 1 to 5).

Figure 2-2 show measured chloride concentrations using the same view of the Forsmark area that is shown in Figure 2-1.

Figure 2-3 shows the mixing proportions of Deep Saline water as computed by the M3 model. It can be seen that the Deep Saline signature computed by the M3 model is reflecting a similar qualitative pattern as the chloride concentrations (also in strontium measurements, not shown here). The most saline waters with the highest Deep signatures are located at the deepest samples available in boreholes KFM07A and KFM09A. It is worth noting that these two samples have been collected at deformation zones adjacent to strongly foliated rocks, which constitute fracture domains FFM04 and FFM05 (see Figure 2-4 and Figure 2-5), along the margins of the target area (according to the current Fracture Domain Concept; /Olofsson et al. 2007/). On the other hand, the deepest sample at KFM03A also shows high Deep Saline signature (around 50%) and correspond to a depth of around 960 m (right and bottom in Figure 2-1), outside the candidate area in Forsmark but corresponding to the conductive bedrock over (hanging wall) Fracture Zone A2.

Figure 2-6 shows the FFM01 fracture domain and the available representative samples. There are relatively few samples at this “target” fracture domain, due to the fact that this fracture domain (FFM01) is characterized by very tight rock with low fracture frequency, mainly sealed or not open. Then, the resulting rock mass at FFM01 fracture domain shows very low permeability for sampling purposes, resulting in the lack of hydrochemical information, with the exception of the new data gathered by the matrix fluid research program.

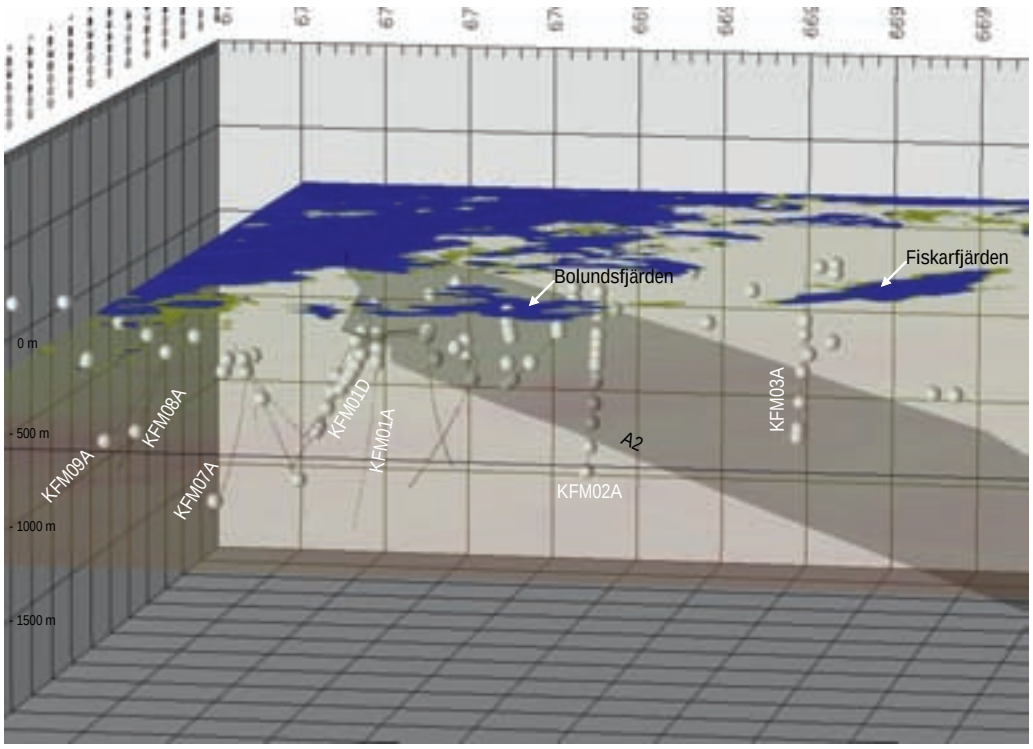

Figure 2-1. *General location view of the Forsmark area and the spatial distribution of the borehole sections with available chemical samples used for hydrochemical modelling purposes (categories 1 to 5).*

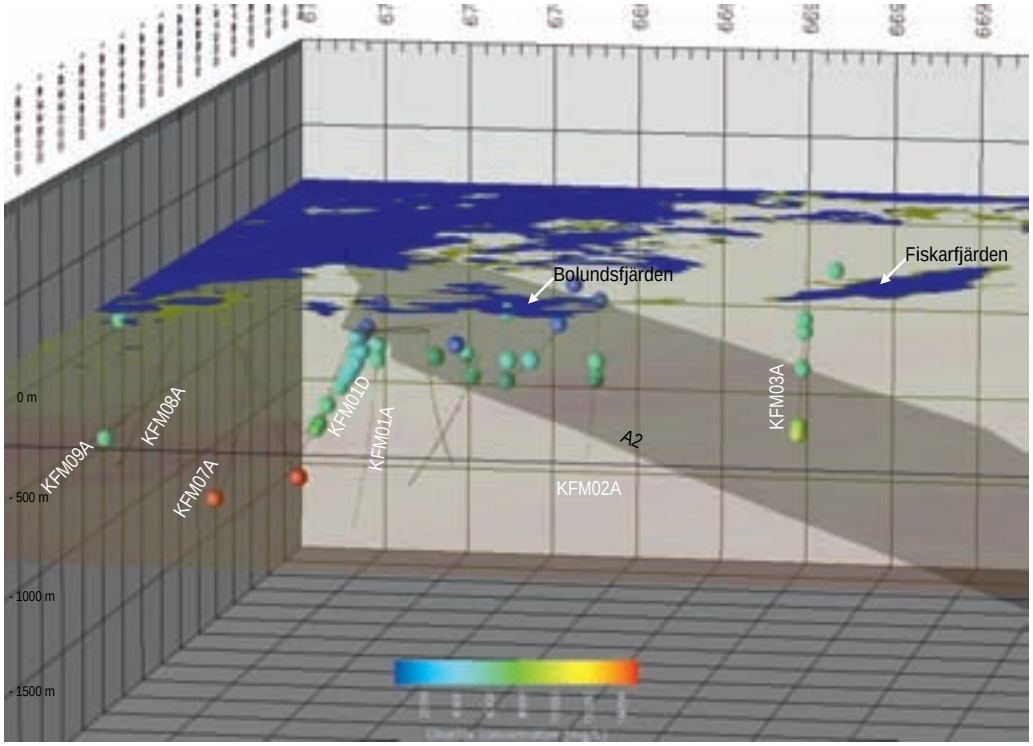

Figure 2-2. *Visualisation of chloride concentrations.*

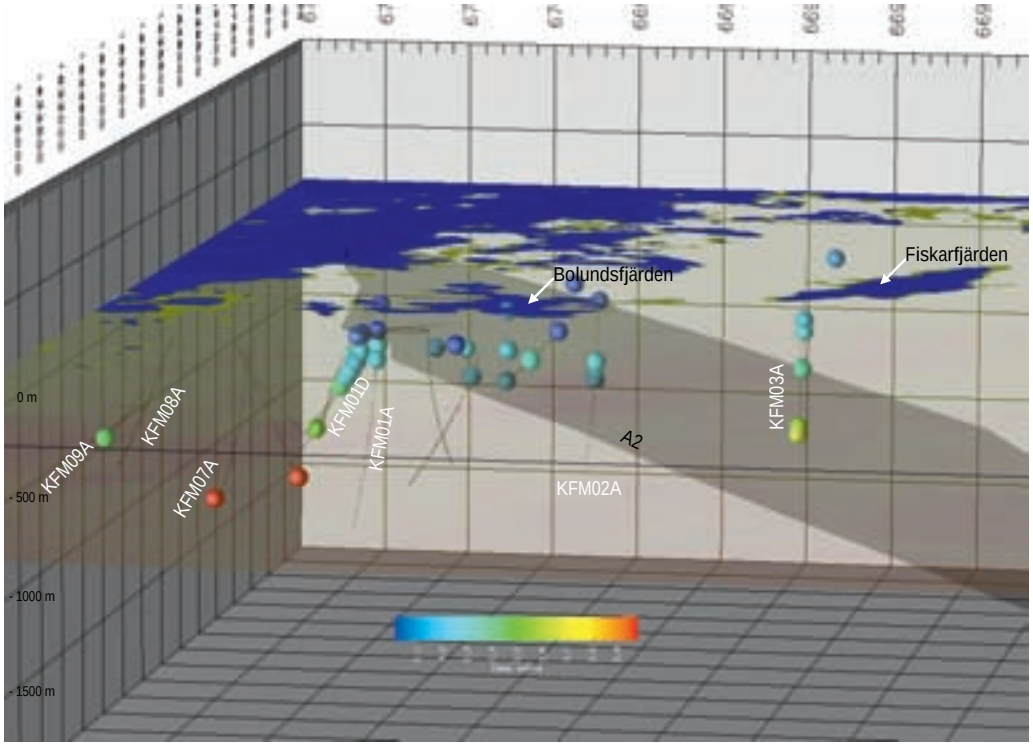

Figure 2-3. *Computed M3 mixing proportions of Deep Saline end-member.*

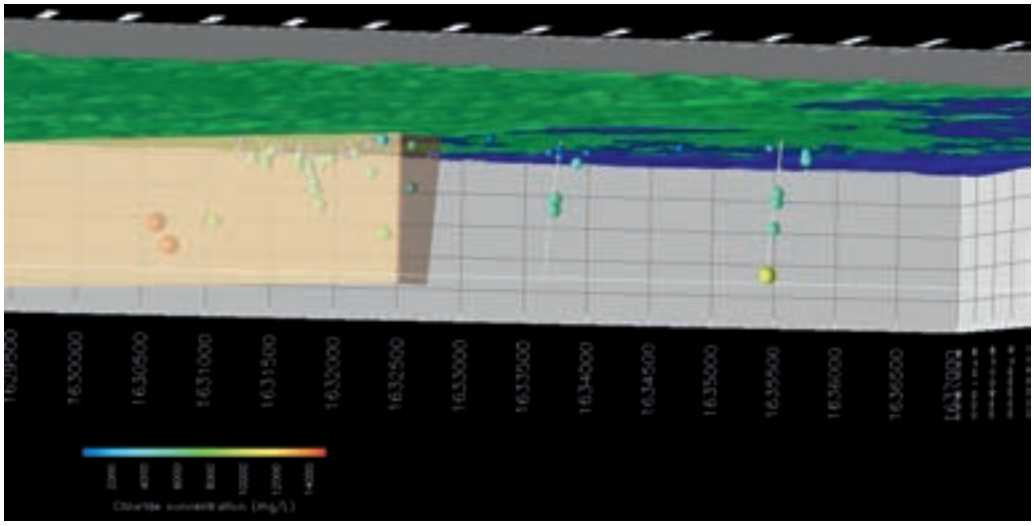

Figure 2-4. *Fracture Domain FFM04 and chloride concentrations. It must be noticed that a different point of view is used. Symbol size is proportional to chloride concentration.*

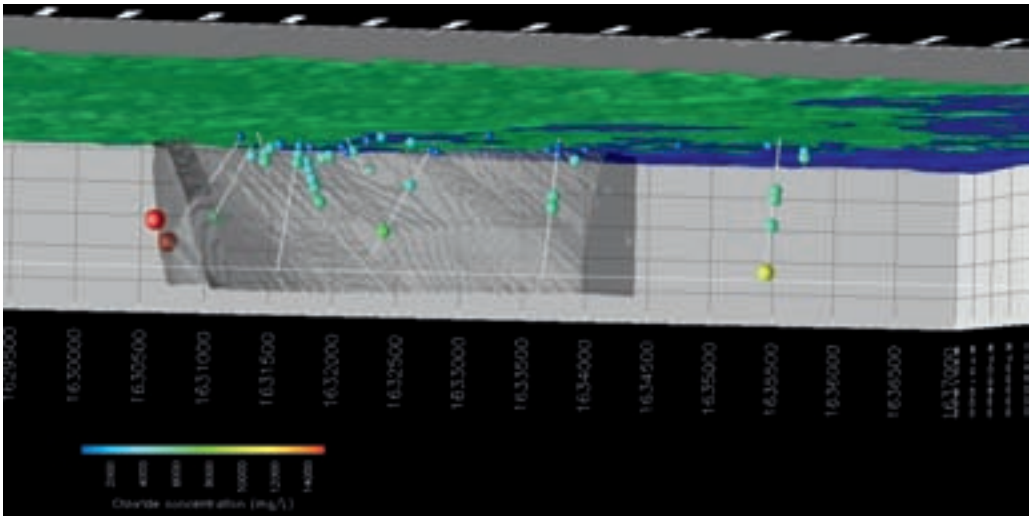

Figure 2-5. *Fracture Domain FFM05 and chloride concentrations. It must be noticed that a different point of view is used. Symbol size is proportional to chloride concentration.*

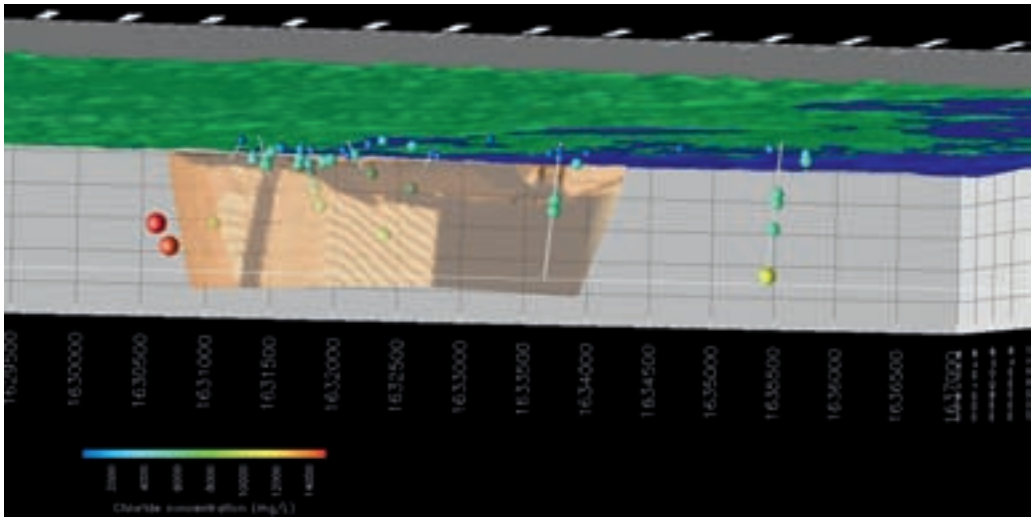

Figure 2-6. *Fracture Domain FFM01 and chloride concentrations. It must be noticed that a different point of view is used. Symbol size is proportional to chloride concentration.*

Figure 2-7 and Figure 2-8 show deuterium and oxygen-18 deviation, respectively (only representative samples), in a SE-NW view of the Forsmark area. As expected, both hydrochemical parameters are correlated with the Glacial mixing proportions computed by the M3 model (Figure 2-9).

It can be seen that the highest Glacial signature (>40%) is found in the deepest available sample, collected at borehole KFM03A (960 m) outside the target area. Deep groundwater at fracture domains FFM04 and FFM05 also show noticeable Glacial signatures (>30%).

According to the 2.2 hydrochemical database, the percussion borehole HFM12 shows a clear indication of glacial water close to the ground surface, probably associated with the Eckarfjärden Deformation Zone. It can be seen in Figure 2-7 and Figure 2-8 the low values of both O-18 and Deuterium near Eckarfjärden lake, and the correspondence with the relatively high (31%) glacial water signature computed by M3 (Figure 2-9). This signature is consistent with an independent hydrochemical study by SurfaceNet /Tröjbom and Söderbäck 2006, Tröjbom et al. 2007/, which identify the Eckarfjärden area as a potential discharge zone with deep groundwater signatures. Additional information about the consistency between ChemNet and SurfaceNet hydrochemical interpretation is described in the next section of this report.

Figure 2-10 and Figure 2-11 show magnesium and sulphate concentration, respectively (only representative samples), in a SE-NW view of the Forsmark area. It can be seen that both hydrochemical parameters are also highly correlated and provide almost the same qualitative picture than that given by Littorina mixing proportions computed by the M3 model (Figure 2-12).

As it can be seen in Figure 2-12, groundwater with Littorina sea water signature has been detected at depths between 100 and 600 m mainly in fracture domain FFM02 and FFM03. Zones deeper than 600 m contain groundwater without marine signatures.

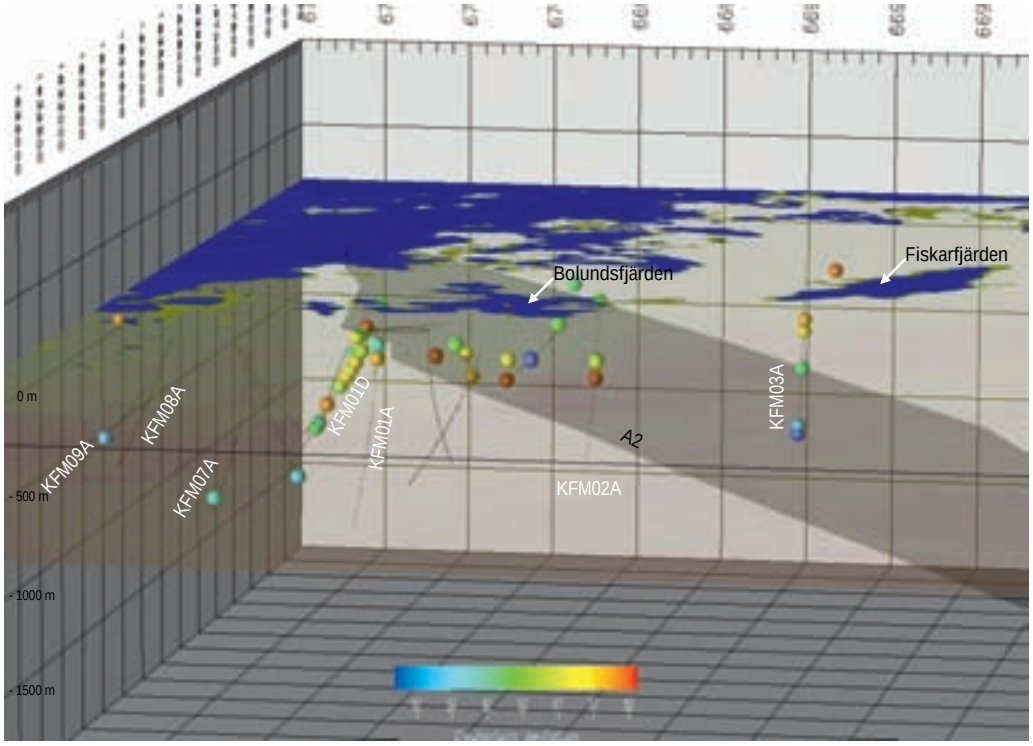

Figure 2-7. *Measured deuterium deviations.*

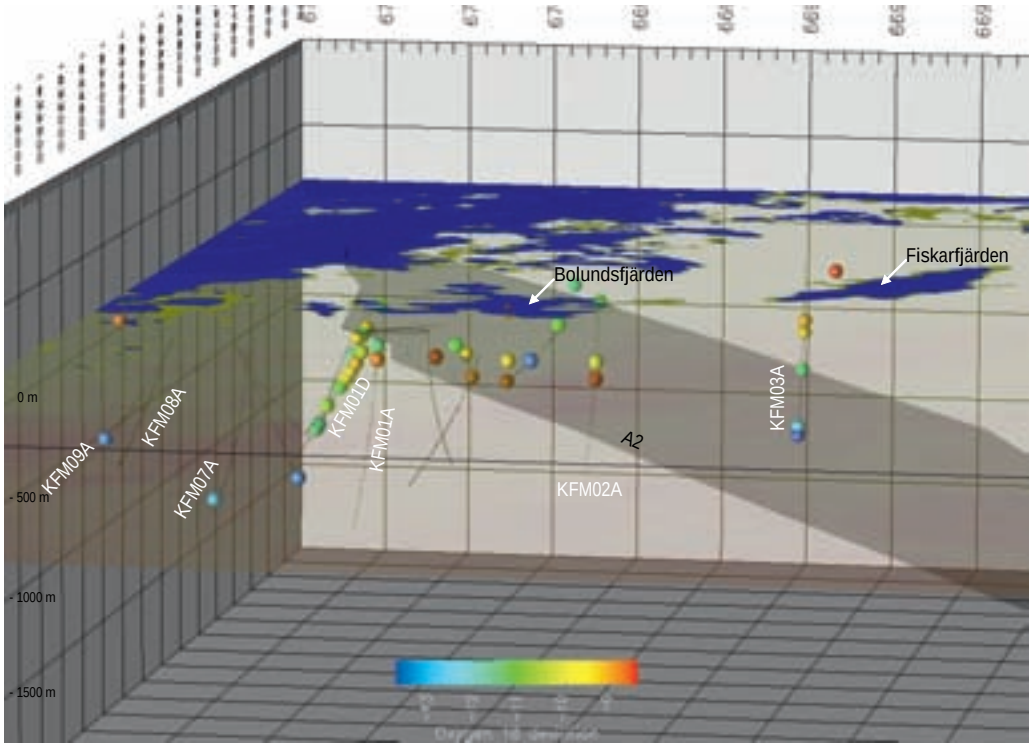

Figure 2-8. *Measured oxygen-18 deviations.*

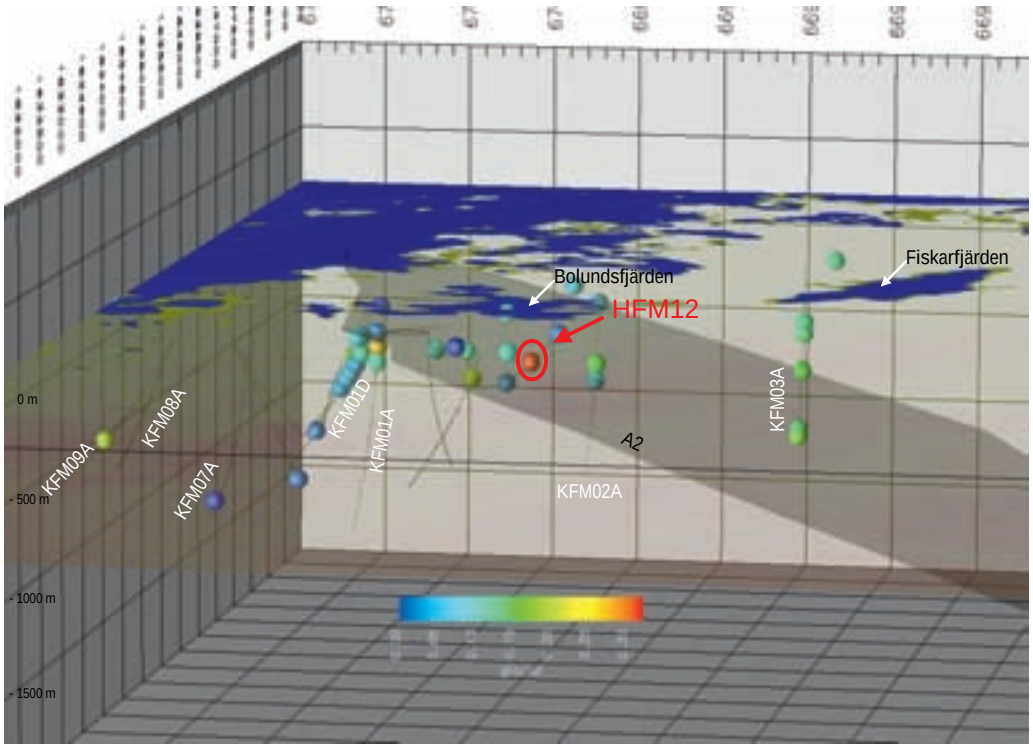

Figure 2-9. *Computed M3 mixing proportions of Glacial end-member.*

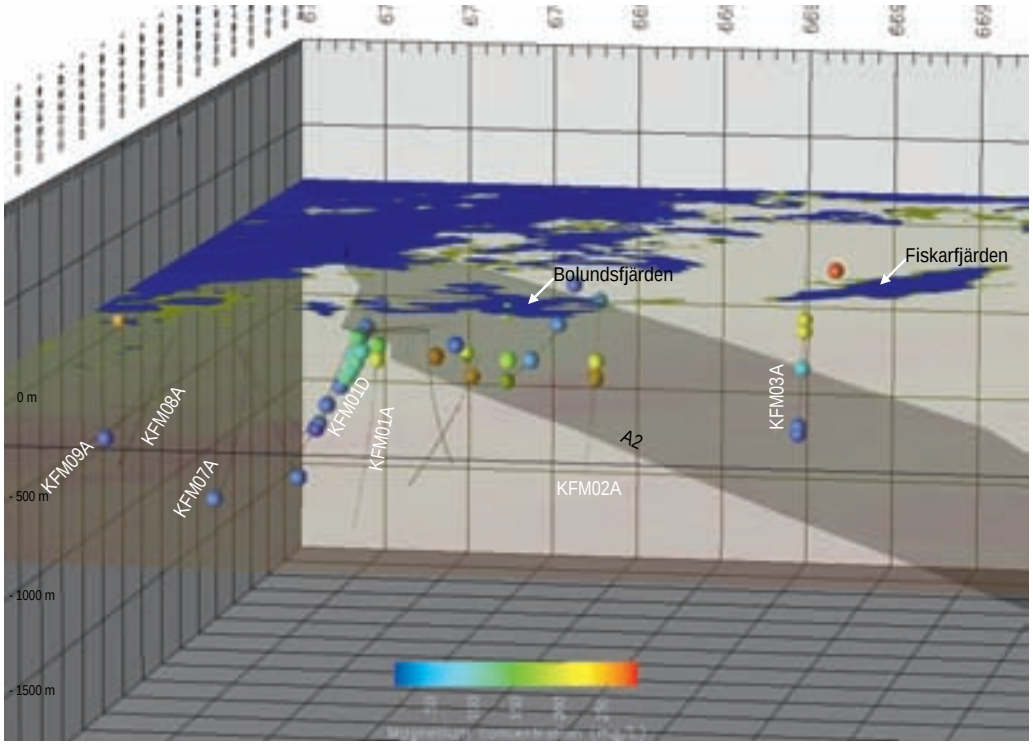

Figure 2-10. *Measured magnesium concentration.*

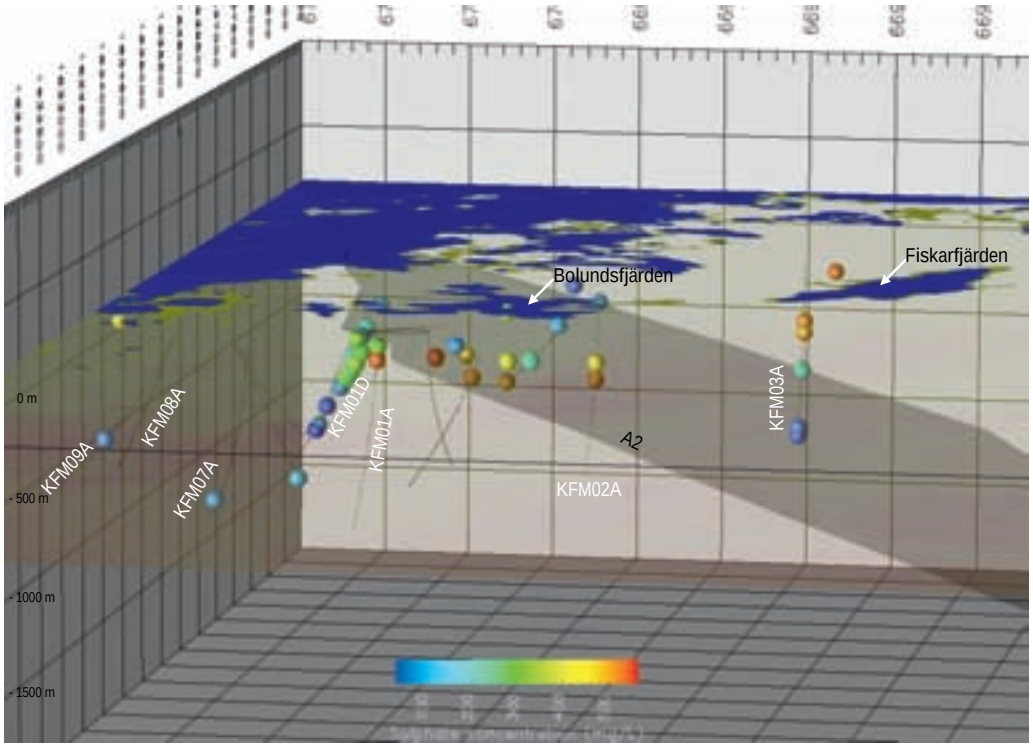

Figure 2-11. *Measured sulphate concentration.*

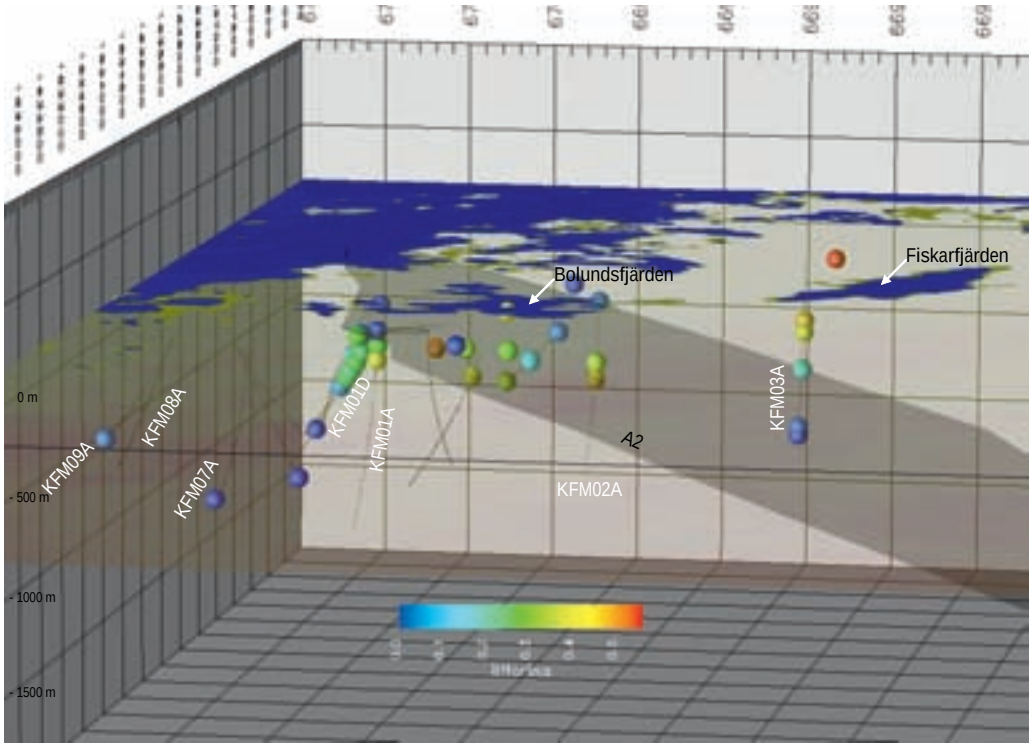

Figure 2-12. *Computed M3 mixing proportions of Littorina end-member.*

Figure 2-13 shows measured tritium activities. It is worth noting that modern dilute groundwater with tritium values higher than 4 TU is restricted to the first 100–200 m, mainly in fracture domain FFM02. This modern dilute water constitutes a very active hydrogeological system developed through the subhorizontal open and highly conductive fractures in the shallow bedrock /Follin et al. 2007/.

Figure 2-14 shows the mixing proportions of the Modified meteoric end-member as computed by the M3 model. It can be seen that such a meteoric end-member is highly correlated with measured tritium activities shown in Figure 2-13.

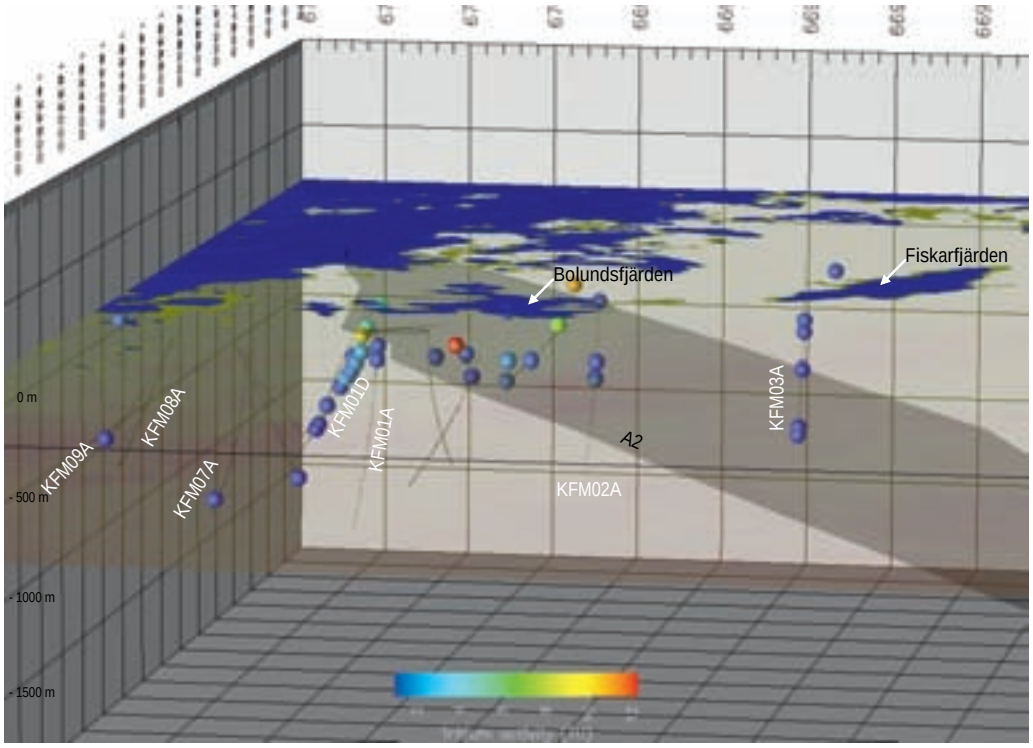

Figure 2-13. *Measured tritium activities.*

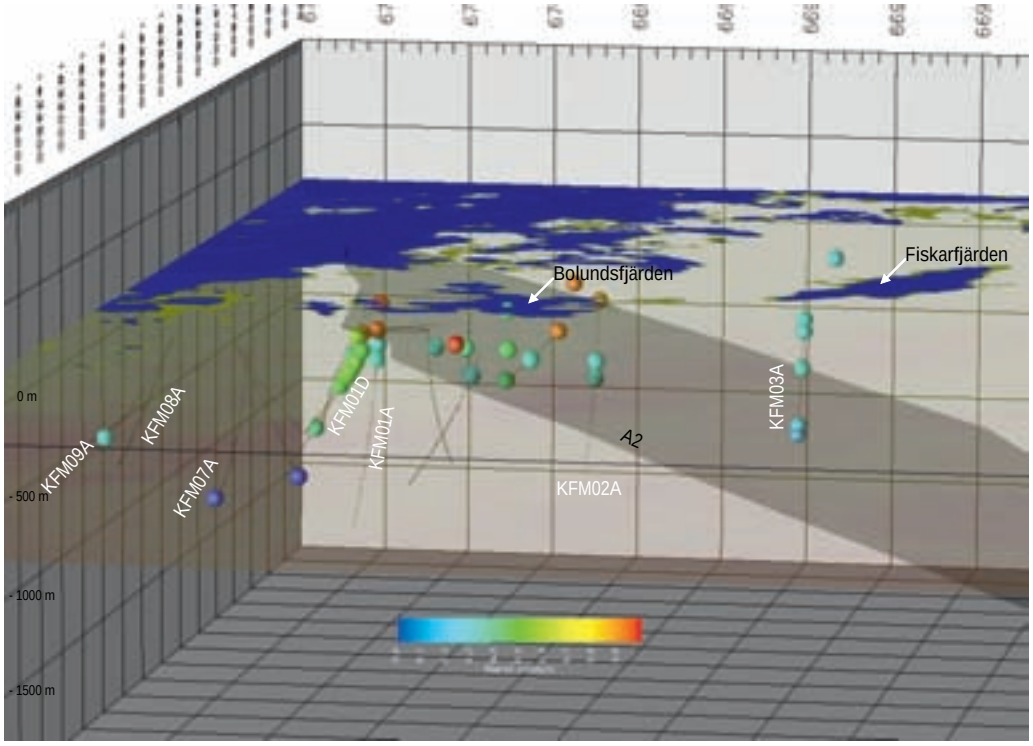

Figure 2-14. *Computed M3 mixing proportions of Modified meteoric end-member.*

3 Consistency between ChemNet and SurfaceNet discharge points

Possible hydrochemical indications of deep/old groundwater in near-surface locations at Forsmark have been investigated by both ChemNet and SurfaceNet working groups.

SurfaceNet work was reported by /Tröjbom et al. 2007/. The purpose of their study was to explore how the superficial observations in soil pipes, streams and lakes relate to the chemical composition of the deeper groundwaters of the bedrock, searching for superficial indications of discharging deep ground water. Such an objective was faced by means of Principal Component Analysis of chemical available samples. Near-surface groundwater samples were thus grouped into categories, beginning with Group A, those samples that have a likely deep chemical signature.

According to /Tröjbom et al. 2007/, near-surface chemical data show different areas with probable deep discharge signatures: (1) a volume in the north-western part that reach relatively shallow levels (dominated by KFM06A and KFM07A), and (2) a deeper volume located in the eastern part (dominated by KFM03A). Also (3) the percussion boreholes HFM11and HFM12 belong to this group.

On the other hand, 3D spatial analysis of hydrochemical information has been performed within the activities of the ChemNet Group, as was explained in the previous section of this report. It is worth noting that during the phase Forsmark 1.2 it was already detected that there are two main exceptions of low stable isotope values (potentially indicative of glacial signatures) in relatively shallow groundwater samples. They correspond to water samples collected in percussion boreholes (HFM11 and HFM12), located very close to Eckarfjärden Lake and Deformation Zone. 1 shows $\delta^{18}O$ measurements again, but highlighting those values lower than –12 per mil. The aforementioned shallow samples with potential glacial signatures have been marked with a red circle in 1.

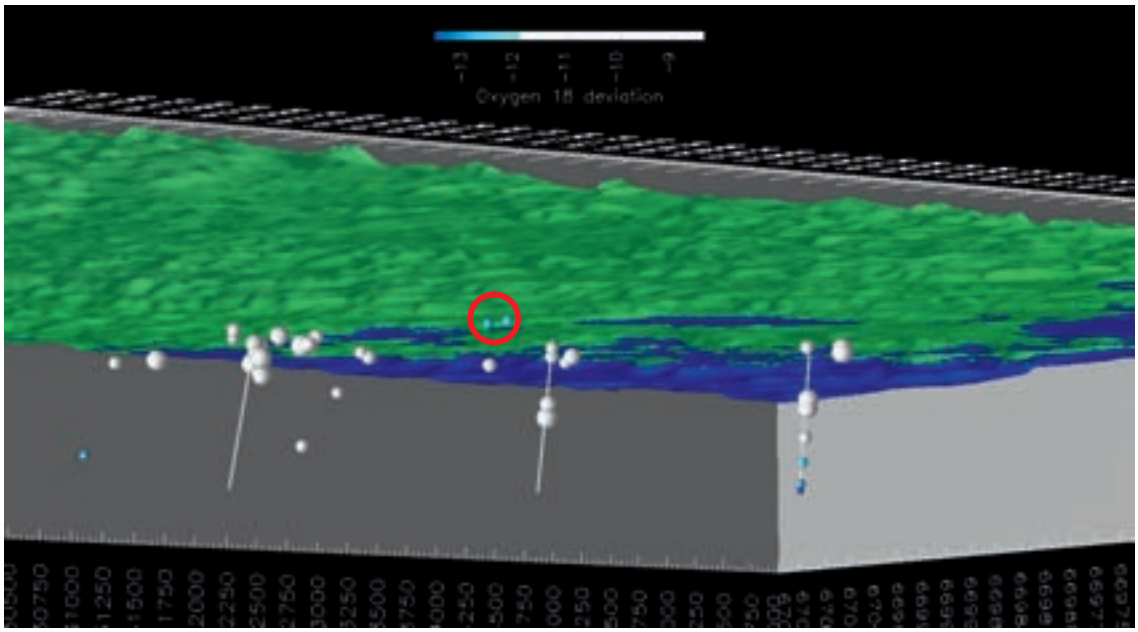

Figure 3-1. *Spatial distribution of the $\delta^{18}O$ deviations in the bedrock groundwater samples available in Forsmark. Values lower than –12‰ have been highlighted. Two shallow samples with potential glacial signatures have been marked in a red circle.*

The conclusions of SurfaceNet and ChemNet are consistent in that shallow groundwater near Eckarfjärden contains hydrochemical signatures that can be older/deeper than expected. In particular, ChemNet observations point towards glacial signatures at that location.

The old/deep signatures found by SurfaceNet in the near-surface waters at northwest and east locations are interpreted as Littorina signatures in the ChemNet analysis, which is in agreement with the SurfaceNet interpretation.

4 Coupled modelling: analysis of SKB suitability criteria

4.1 Introduction

Groundwater at repository depth must fulfill a number of hydrochemical suitability criteria defined by SKB. Such suitability criteria are prescribed as follows /SKB 2006/:

	Eh (mV)	pH (units)	TDS (g/L)	DOC (mg/L)	Colloids (mg/L)	Ca+Mg (mg/L)
Criterion	< 0	6–10	< 100	< 20	< 0.5	> 40

A sound analysis about different scenarios and the associated impact on the suitability criteria belongs to safety assessment activities and, therefore is beyond the scope of the present work. However, it is well known that site characterization activities (mainly drilling activities) introduce perturbations in the system that can impact the actual hydrochemistry of the groundwater samples collected in the site. This is why it is believed to be appropriate to perform scoping calculations in order to evaluate how much disturbance can be allowed for a given groundwater sample at repository depth and still meet the SKB suitability criteria. (see item 6) Two main approaches have been selected to face these scoping calculations: (1) simple mixing and reaction modelling and (2) coupled reactive transport modelling.

4.2 Mixing and reaction modelling: evaluation of the cation exchange processes

Two extreme possibilities can be expected when dealing with hydrochemical disturbances produced by the site characterization activities: (1) Dilution of the native groundwater due to the mixing with fresh groundwater of meteoric origin used as drilling fluid, and (2) Contamination of the native groundwater due to mixing with more saline groundwater existing within the radius of influence produced by the pumping during sampling activities. The occurrence of one or another possibility will depend on several hydrogeologic factors such as the initial salinity field, the spatial distribution of hydraulic conductivity – fracture networks in the surroundings of the borehole, etc… Both situations (i.e. dilution and concentration) can be observed in the chemical time series available during sampling activities at the Forsmark site. The two possibilities have been considered here in the current scoping calculations.

The representative sample number 12354 of the Forsmark database has been selected as “native groundwater at repository depth” for this particular exercise (see item 7). This sample has been collected at borehole KFM01A and corresponds to an average elevation of –445 m.a.s.l. The first scoping exercise was the simulation of the reactive mixing processes between the “native Forsmark groundwater” and the “modified meteoric” end-member as defined in the Forsmark 2.2 ChemNet “datafreeze”. Such a diluted end-member corresponds to a representative sample (number 8335) collected at percussion borehole HFM09, which has been judged as representative of dilute groundwater from the first 100 m of the rock domain, and can be also considered

representative of the typical drilling fluid used in the site. Then, a mixing and reaction model between “native” and “modified meteoric” samples has been made, in order to simulate the dilution process. Numerical calculations have been performed with the PHREEQC software package /Parkhurst and Appelo 1999/.

Figure 4-1 shows the computed behaviour of major solutes in a conservative dilution process. It can be seen that a linear dilution trend is computed with both end-members. Figure 4-2 shows the evolution of calcite saturation index along the simulated dilution process. It can be seen that native end-member is close to equilibrium with respect to calcite, whilst dilute meteoric water is slightly under-saturated. However, all the mixing fractions between both end-members result in slightly saturated waters.

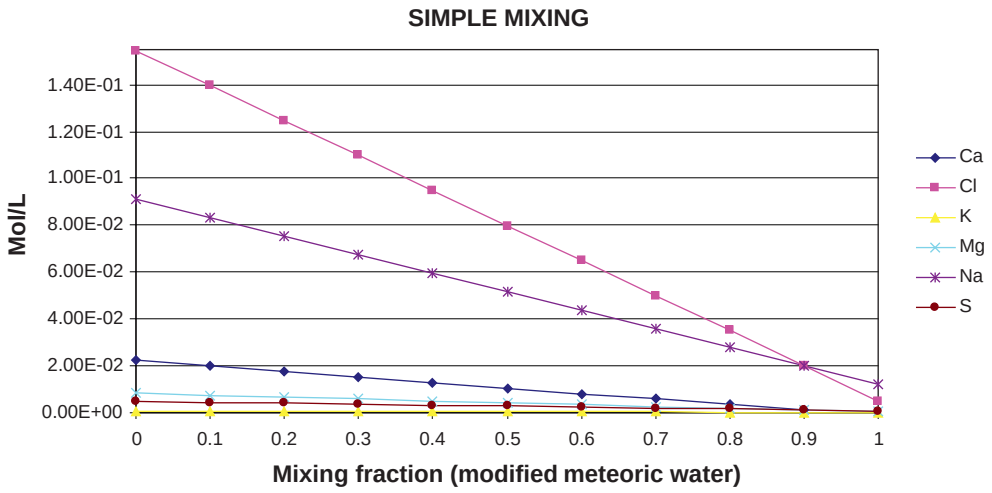

Figure 4-1. *Concentration of major solutes in the mixing process between meteoric and native groundwater (repository depth) at Forsmark.*

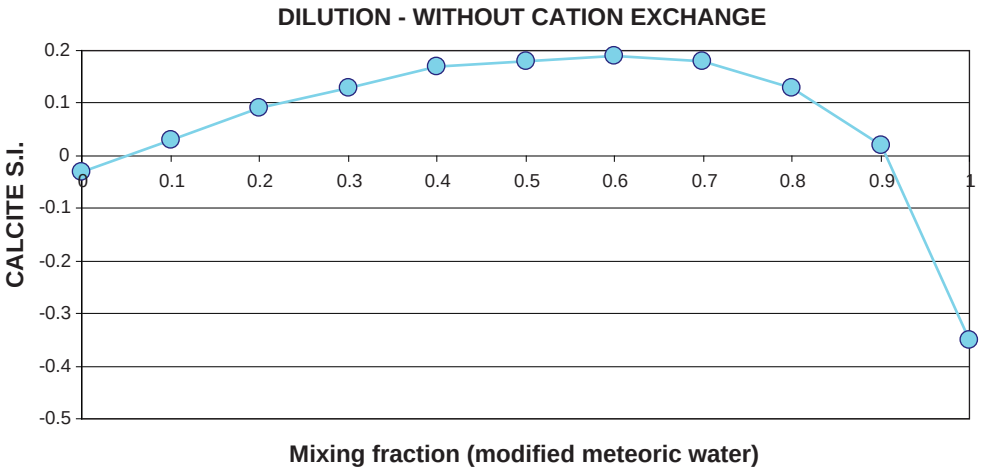

Figure 4-2. *Computed saturation index of calcite in the mixing process between modified meteoric and native groundwater (repository depth) at Forsmark.*

Precipitation of calcite during the dilution keeps the computed pH in the near-neutral range, as it is shown in Figure 4-3. Black solid lines show the limits of the SKB suitability criteria. Then, it can be stated that the pH suitability criteria defined by SKB is not at risk even in the case of an extreme contamination by drilling fluids during site characterization activities.

Figure 4-4 shows the behaviour of Ca+Mg during the conservative dilution process of Forsmark native groundwater by mixing with meteoric water. It can be seen that the computed Ca+Mg concentration is always higher than the limit established by the SKB suitability criteria. In fact, even the Ca+Mg concentration of the "modified meteoric" end member is higher than the abovementioned limit, so there is no possibility of surpassing such a limit with the current conservative mixing model.

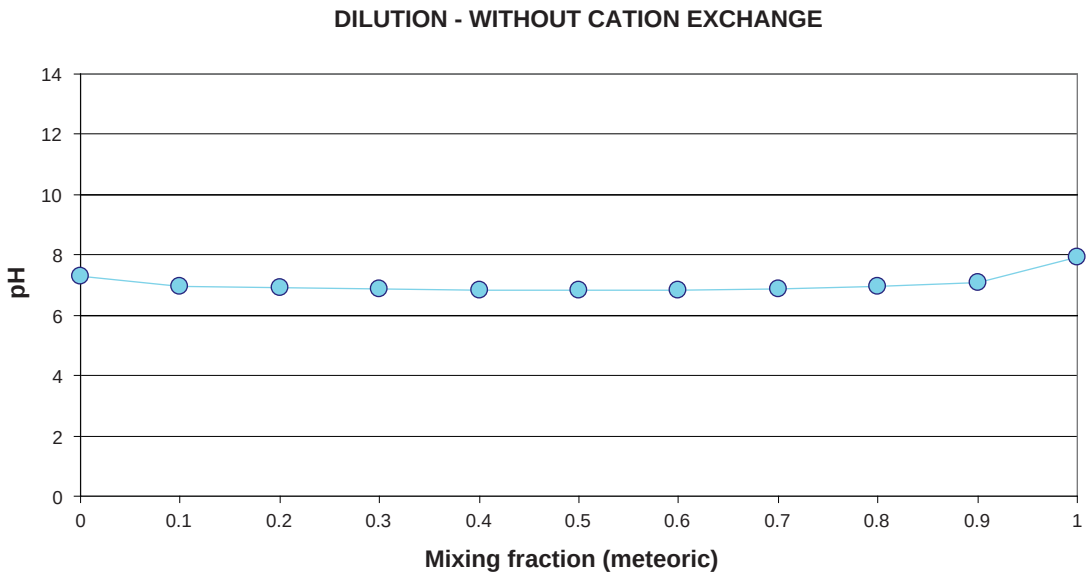

Figure 4-3. *Computed pH in the mixing process between meteoric and native groundwater (repository depth) at Forsmark. It can be seen that pH is always in the near-neutral pH range and thus safely within the SKB suitability criteria range (black solid lines 6-10).*

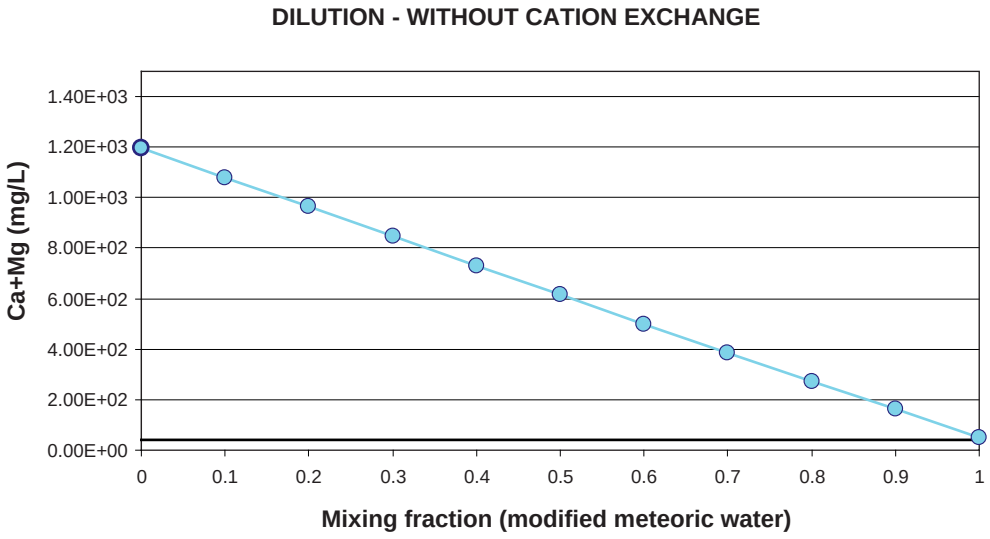

Figure 4-4. *Computed Ca+Mg in the mixing process between meteoric and native groundwater (repository depth) at Forsmark. It can be seen that Ca+Mg concentrations are always safely above the SKB suitability criteria (black solid line).*

The performed dilution model shown in the abovementioned figures does not take into account the cation exchange processes that may take place in the mixing process. However, Site Characterization activities have provided evidence on the existence of clay minerals able to trigger exchange processes both in fracture zones and host rock at the Forsmark site. Figure 4-5 shows Cation Exchange Capacity values measured on different cores taken from boreholes in Forsmark (Personal communication E Gustafsson).

This CEC value has then been used in the abovementioned mixing (dilution) model in order to take into account the cation exchange model. Cation exchange has been simulated involving Ca^{2+}, Na^{+}, K^{+} and Mg^{2+} dissolved species, according to the parameters listed in Table 4-1.

The dilution model is highly sensitive to the occurrence of cation exchange processes. Figure 4-6 shows the comparison between computed Ca^{2+} and Na^{+} behaviour in the mixing processes both considering or not the occurrence of cation exchange processes.

It can be seen that cation exchange processes produce an uptake of Ca^{2+} from the groundwater to the exchanger and a release of Na+ from the exchanger to the groundwater. Therefore, Ca^{2+} concentrations in groundwater are lower when cation exchange is considered in the model. This may have an impact in the evaluation of SKB suitability criteria, since it is prescribed that Ca+Mg must be higher than 40 mg/L. Figure 4-7 shows computed concentrations of Ca+Mg in the dilution of Forsmark native groundwater, when cation exchange processes are considered in the mixing model. It can be seen (Figure 4-7) that in this case the resulting mixing water may fulfill SKB suitability criteria also for a 100% of dilution with modified meteoric water and even considering the cation exchange process.

Table 4-1. Values of cation exchange parameters used in the dilution mixing model with cation exchange.

Species	Moles	Equivalents	Equivalent fraction	Log gamma
CaX2	4.751	9.502	6.645E-01	–0.421
NaX	2.670	2.670	1.867E-01	–0.110
MgX2	1.013	2.027	1.417E-01	–0.402
KX	1.019E-01	1.019E-01	7.122E-03	–0.121

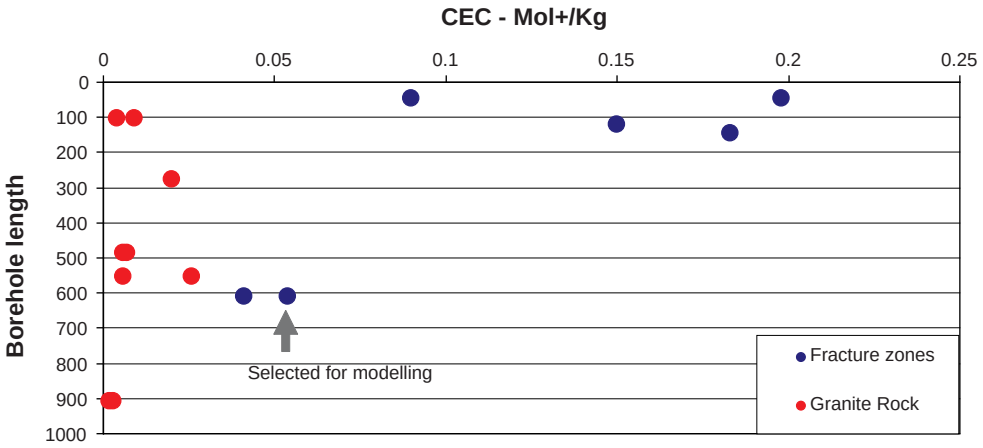

Figure 4-5. *CEC values measured at cores from Forsmark boreholes. Blue symbols represent fracture zones and red symbols represent rock matrix. Values from fracture zones at repository depth have been selected as representative for this scoping calculation exercise.*

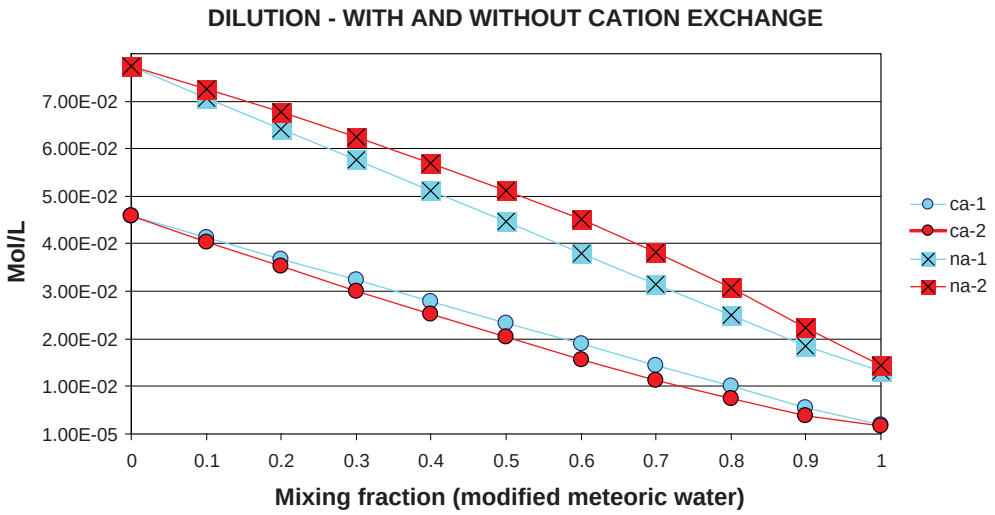

Figure 4-6. *Computed results of Ca^{2+} (circles) and Na^{+} (squares) without considering (blue) and considering (red) cation exchange process in the mixing model. Using "Modified meteoric" end-member.*

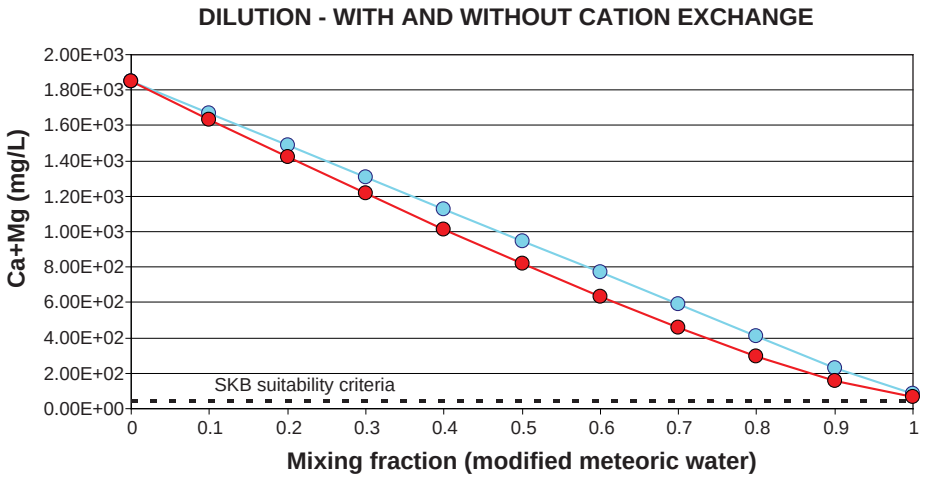

Figure 4-7. *Computed results of Ca+Mg concentrations without considering (blue) and considering (red) the cation exchange process. The dashed black line represents the SKB suitability criteria (>40 mg/L).*

It is worth noting that the previous results correspond to the case where the fresh water end-member corresponds to the "Modified meteoric end-member". Modified meteoric has been defined from a groundwater sample (#8335) that is actually highly concentrated in comparison with other dilute near-surface groundwater. In fact the Dilute Groundwater end-member itself fulfils the SKB Ca+Mg criteria. Then, this case corresponds to a very optimistic case in the current evaluation of the disturbance that can be allowed for a given groundwater sample as a result of the site characterization activities.

A new mixing model has been constructed in order to evaluate a more "aggressive" fresh water end-member. In this case, the "classical" meteoric water has been used, which correspond to extremely diluted water (typical rain water). Figure 4-8 shows the comparison between computed Ca^{2+} and Na^{+} behaviour in the mixing processes both considering or not the occurrence of cation exchange processes in the new mixing model.

In this case, the resulting mixing water shows lower contents of both Ca^{2+} and Mg^{2+} than in the previous case. Figure 4-9 shows computed concentrations of Ca+Mg in the dilution process considering the Meteoric end-member. It can be seen (Figure 4-9) that, even in this "aggressive" case, the SKB suitability criteria are fulfilled almost during the whole dilution process, except for dilution (contamination) factors higher than 90%.

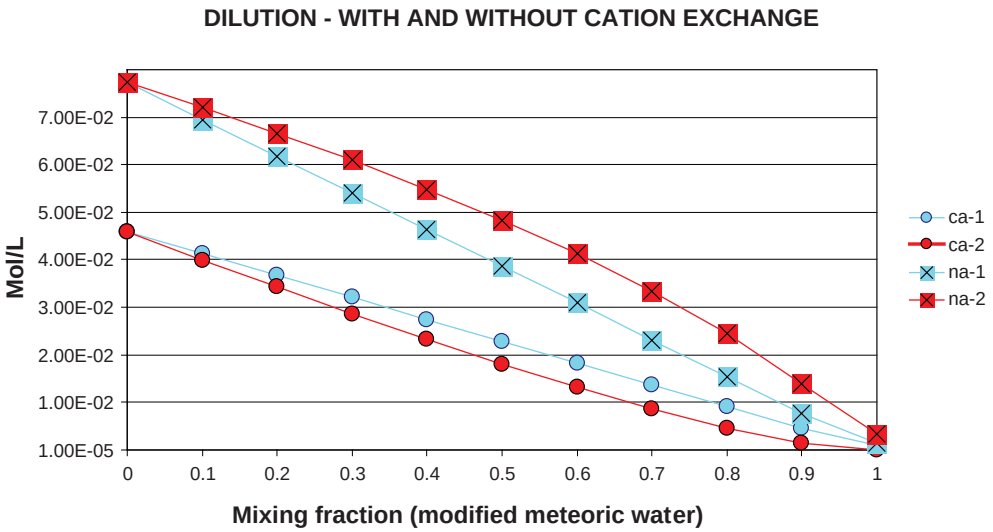

Figure 4-8. *Computed results of Ca^{2+} (circles) and Na^{+} (squares) without considering (blue) and considering (red) cation exchange process in the mixing model using the Meteoric end-member.*

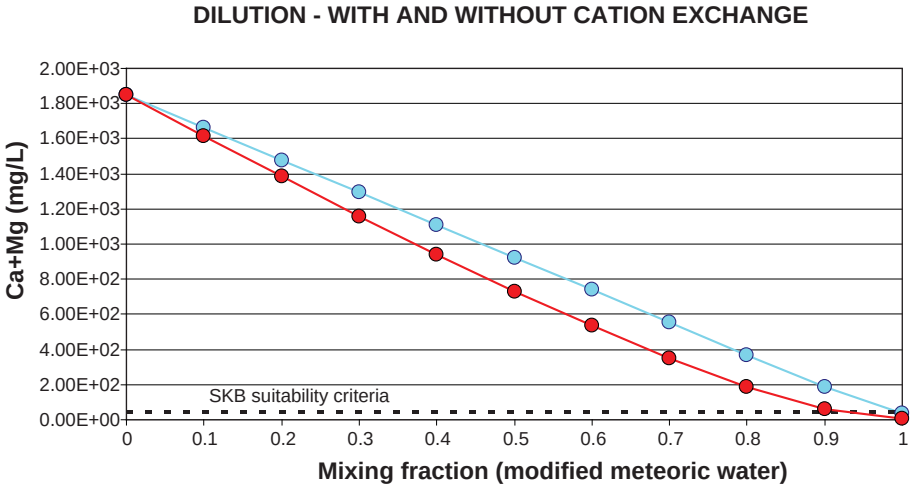

Figure 4-9. *Computed results of Ca+Mg concentrations without considering (blue) and considering (red) cation exchange process. The dashed black line represents the SKB suitability criteria (>40 mg/L). Using meteoric end-member.*

It is worth noting that computed results could be sensitive to the cation exchange parameters used in the model. As pointed out previously, Forsmark CEC values have been taken into account for the modelling. As a matter of fact, the selected CEC value corresponds to a measurement made in a fracture zone at repository depth. Host rock measurements indicate smaller Cation Exchange Capacities, but other fracture zones (shallower than repository depth) exhibit much higher CEC values. In addition, cation exchange constants (selectivity coefficients) were unknown at the time of preparing this report, and the values listed in Table 4-1 correspond to the default values available in the PHREEQC database (data from /Dzombak and Morel 1990/).

Forsmark site-specific selectivity coefficients have been estimated, in an attempt to reduce the uncertainties in the previous reactive mixing modelling. A representative water sample is available in the borehole KFM05A at a depth of 100.0–121.6 m. The sampling point corresponds to the “interface” between rock unit RU1 and the deformation zone ZFMA2 (Figure 4-10).This water sample is assumed to represent the hydrochemical conditions of the A2 fracture zone at shallow depths. Even though the water sample has been judged as representative it should be seen that the drilling water residue is still 5.25%, so its composition should be taken with caution.

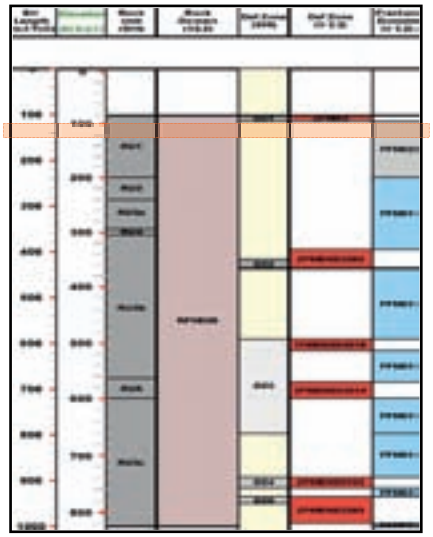

Dissolved species	Concentration (mg/L)
Na	1710
K	46.90
Ca	862
Mg	197
HCO^{3-}	127
Cl	4370
$SO4^{2-}$	486
S	160
Br	13.5
Si	5.78
Li	0.056
Sr	4.89
TOC	2.6
cond. (lab) pH (lab)	1320 µS/cm 7.18

Figure 4-10. *Location (horizontal orange bar) and composition of the groundwater sample used for the estimation of Forsmark cation exchange coefficients.*

CEC analytical data are available for the KFM01B borehole, at a depth of 47.40 m (with a grain size smaller than 0.125 mm). According to the available geological model, this sample corresponds to the ZFMA2 domain (Figure 4-11).

Assuming that both sets of analytical data (in the solid and liquid phases) are representative of the A2 shallow conditions and that the hydrochemical system is in equilibrium, the selectivity coefficients can be directly computed by the Mass Action Law. A density of 2.7 g/cm^3 was considered for the solid phase, and a porosity value of 0.1 has been assumed for the fracture zone. The computed selectivity coefficients are referred to the Ca^{2+} (master species) and have been calculated according to the Gaines-Thomas convention (Table 4-2).

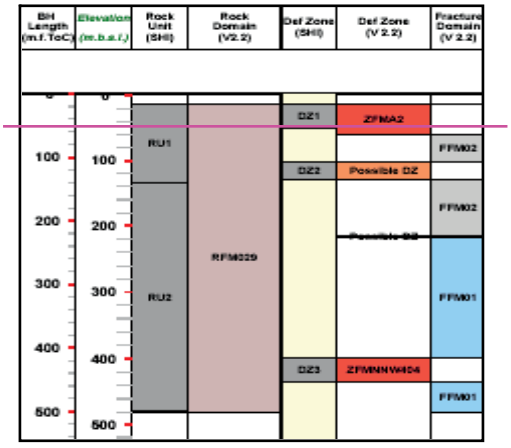

Species	(cmol/kg)
NaX	0.97
KX	0.73
CaX2	7.12
MgX2	2.64
CsX	6.7·10–5
RbX	5.11·10–3
SrX2	–
CEC	19.8

Figure 4-11. *Location (horizontal pink line) of the sample and measured concentration of the exchanger used for the estimation of Forsmark cation exchange coefficients.*

Table 4-2. Cation exchange reactions and the computed selectivity coefficients according to the Gaines-Thomas convention.

Species	Reaction	Log KMe/Ca
NaX	$Na^+ + ½\ CaX_2 = ½\ Ca^{2+} + NaX$	–1.706
MgX2	$Mg^{2+} + CaX_2 = Ca^{2+} + MgX_2$	–0.007
KX	$K^+ + ½\ CaX_2 = ½\ Ca^{2+} + KX$	–0.036

The reactive mixing calculations have been repeated again in order to evaluate the sensitivity of the model results with respect to the cation exchange selectivity coefficients. A new run (Run2) using the site-specific selectivity coefficients evaluated previously (Table 4-2) has been made. All the parameters are set identical to the previous run. Figure 4-12 shows the computed results of dissolved Ca^{2+} and Na^+ with the new run (Run 2), and the comparison with the previous results (Run 1).

It can be seen in Figure 4-12 that computed results of dissolved Ca^{2+} and Na^+ are very similar in Run 1 and Run 2, meaning that the reactive mixing model lacks sensitivity with respect to the values of the selectivity coefficients.

Figure 4-13 shows the Ca+Mg evolution of the new computed results (and the comparison with the previous results). It can be seen that the selectivity coefficient values used in the models have very little influence on the computed results of the evolution of Ca+Mg.

Another parameter considered in the SKB suitability specifications is TDS that should not be higher than 100 g/L. As commented previously, the occurrence of saline groundwater due to the pumping performed during sampling could result in an increase of TDS of the water sample collected at repository depth, due to a possible upconning effect. It is worth noting that the current Deep Saline end-member available at Forsmark corresponds to the most saline water sampled at the site, which has around 80 g/L of TDS. Then, taking into account this end member, there is no possibility to surpass the SKB limit of 100 g/L, as shown in Figure 4-14.

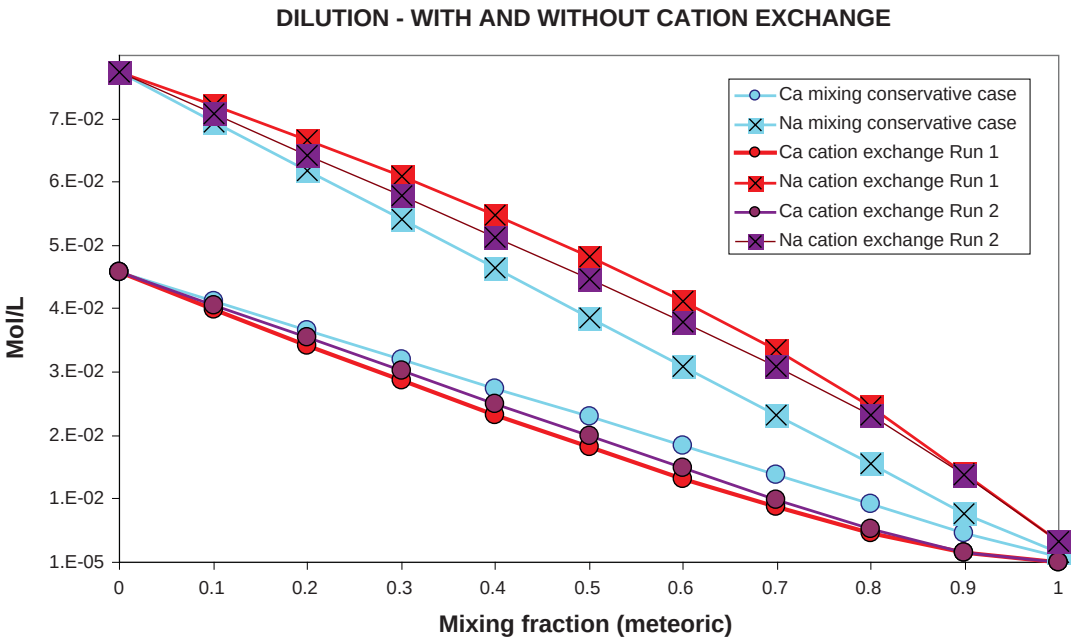

Figure 4-12. *Computed results of Ca+Mg concentrations in the conservative model, Run 1 and Run2.*

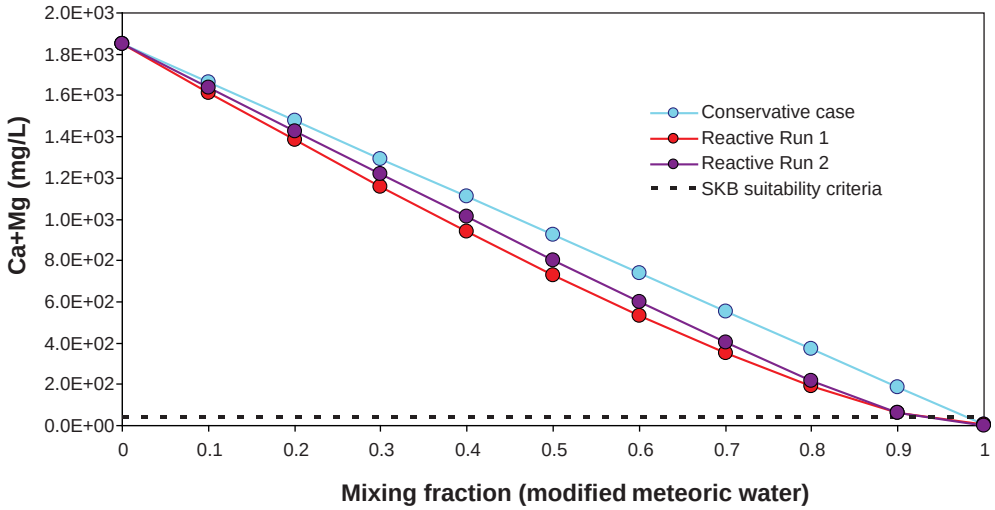

Figure 4-13. *Computed results of Ca+Mg concentrations in the conservative case, the reactive mixing #1 and the reactive mixing #2. Dashed black line represent the SKB suitability criteria (>40 mg/L). Using meteoric end-member.*

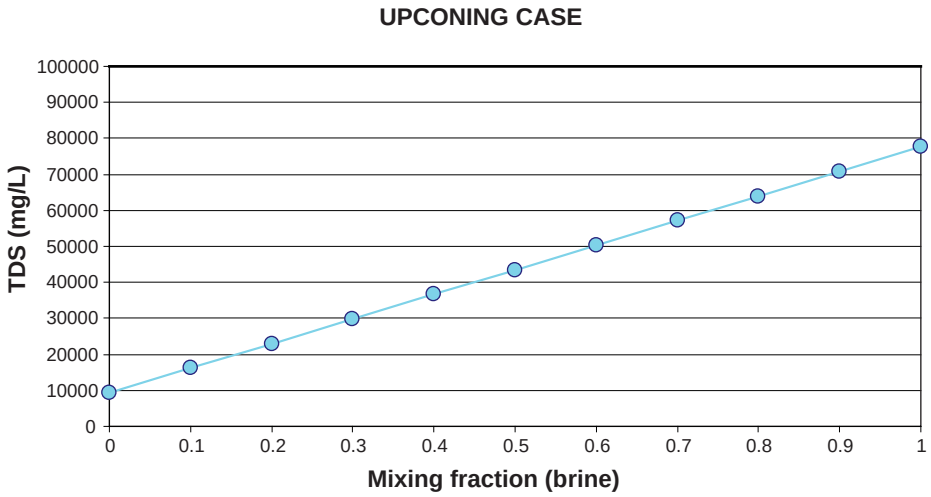

Figure 4-14. *Computed TDS according to the mixing model between "native groundwater", at repository depth, and "Deep Saline" end-member (Forsmark conceptual model 2.2). Solid black line represents SKB suitability criteria (< 100 g/L).*

4.3 Reactive transport modelling: evaluation of oxygen reduction capacity

Redox conditions in deep hard rock environments are usually stable with redox potentials between –0.1 and –0.4 V /Haveman et al. 1998/. However, the actual redox conditions at repository depth could be altered by the presence of atmospheric O_2 due to contamination introduced by site characterization activities. Even trace amounts of O_2 could result in an oxidizing redox potential /King et al. 2001/. For instance, an O_2 concentration of just 8 ppb, which is equivalent to 0.1% of the O_2 concentration corresponding to a groundwater at equilibrium with atmospheric conditions, would lead to positive redox potentials (at pH 7 and 25°C).

One of the hydrochemical suitability criteria defined by SKB deals with the redox conditions of the repository, which must be negative (less than 0). Therefore, evaluating the buffer capacity of the Forsmark bedrock for consumption of dissolved O_2 that may reach repository depth during the repository operational stage is of interest.

Here we show the main results obtained in a modelling exercise aimed at evaluating the oxygen reduction capacity of the Forsmark bedrock, at repository depth. The simulated case corresponds to a site characterization borehole section, at repository depth, that eventually has suffered a leakage which results in an alteration of the native groundwater, by equilibrium with atmospheric oxygen. In such an extreme case, the oxygen will diffuse into the granite rock and, at the same time, will interact geochemically with Fe^{2+}-containing minerals present in the granite. In theory, the Fe^{2+} in those minerals could be oxidised to Fe^{3+} by the reduction of O_2. The main objective is to evaluate the response time of the Forsmark granite to consume the dissolved oxygen in the borehole section.

Geometrically, the borehole is assumed to have a radius of 3.8 cm and 1 m of surrounding granite has been considered for the water rock interaction model. It is assumed that the water in the granite is virtually stagnant and diffusion into the rock mass is the only transport mechanism in the model. The effective diffusion coefficient in the intact rock is set to 10^{-12} m^2/s, and the total porosity of the rock is 0.24%, according to the mean value reported by /Drake et al. 2006/.

The representative sample number 12354 of the Forsmark database has been selected as “native groundwater at repository depth” for this particular exercise. This sample has been collected at borehole KFM01 and corresponds to an average elevation of –445 m.a.s.l.

According to /Drake et al. 2006/ the candidate area at the Forsmark site is dominated by a granitic to granodioritic rock (rock code 101057) that occupies about 84% of the candidate site volume. One of the most interesting minerals from the point of view of oxygen reduction capacity is pyrite. The pyrite content was not distinguished from other opaque minerals in the characterization performed by /Drake et al. 2006/. The amount of opaque minerals in the dominating granite (rock code 101057) is 0.3% ± 0.2, thus providing a theoretical maximum pyrite content of the rock. However, a maximum pyrite content based on the S content in the rock has been calculated to be about 0.4 %. The other two main Fe^{2+}-containing minerals in Forsmark are biotite and chlorite. It can be expected that both minerals will also contribute to the oxygen reduction capacity of the rock. Table 4-3 shows the measured amounts of minerals in the Forsmark rock unit 101057.

Table 4-3. Mineralogical composition (vol %) of the granitic to granodioritic rock unit (101057) in Forsmark after /Drake et al. 2006/).

Mineral	Range	Mean	Std	
Quartz	27.8–45.8	35.6	4.2	N=46
K-feldspar	0.2–36.0	22.5	8.6	
Plagioclase	24.0–63.8	35.6	8.5	
Biotite	0.8–8.2	5.1	1.6	
Chlorite	0–1.2	0.2	0.3	N=23
Epidote	0.1–3.2	0.6	0.7	
Titanite	0–1.0	0.2	0.2	
Allanite	0–0.6	0.2	0.2	
Opaque	0–0.8	0.3	0.2	

According to the data summarised above, 3 main minerals are considered as the main contributors to the oxygen reduction capacity in Forsmark. These three minerals have been included in the reactive transport model, assuming the following abundance (Table 4-4).

In addition to the 3 minerals mentioned above, 50 homogeneous (aqueous) hydrochemical processes have been included in the reactive transport model (Table 4-5).

Three different runs of the reactive transport model have been performed. Run #1 corresponds to a conservative scenario where only diffusion of the oxygen into the granite takes place. This run will serve as a reference against which to compare the effect of the oxygen reduction capacity of the minerals, under realistic conditions of repository depth. Run #2 corresponds to the reactive transport base run. It makes use of all the parameters and conditions described above. Finally, Run #3 corresponds to a complementary run, in order to evaluate the sensitivity of the model with respect to the specific reactive surface of the minerals. According to our experience, it is expected that this parameter would constitute the main source of uncertainty in the model. Then, Run #3 shares all the characteristics of Run #2 but the reactive specific surface of the minerals whose values have been set equal to 1 order of magnitude shorter than those listed in Table 4-4.

Figure 4-15 shows the computed time evolution of oxygen consumption at the borehole, for the 3 simulated cases. It can be seen that in the base reactive case (Run 2) dissolved oxygen in borehole water would be almost depleted in 200 days, whilst more than 10,000 days would be required in order to deplete the same amount of oxygen just by conservative diffusion (Run 1). It is worth noting that, as expected, the specific surface area of the minerals is a sensitive parameter for this kind of model. Decreasing the reactive surface area by 1 order of magnitude leads to an increase of about 5 times in the time needed to consume the initial oxygen (Run 3).

Table 4-4. Reactive minerals, relative abundance, specific reactive surface and dissolution kinetic laws assumed in the numerical model.

Reactive Mineral	Abundance (vol.)	Sp. Surface	Kinetic rate
Biotite	5%	12 dm^2/dm^3	/Malmström and Banwart 1997/
Chlorite	0.2%	12 dm^2/dm^3	/Gustafsson and Puigdomenech 2003/
Pyrite	0.1%	27 dm^2/dm^3	/Williamson and Rimstidt 1994/

Table 4-5. Geochemical and microbial components and processes considered in the hydrobiogeochemical model. Stoichiometric coefficients and equilibrium constant are taken from EQ3/6, /Wolery 1992/.

Components	Ca^{2+}, Cl^-, Fe^{2+}, H_2O, H^+, HCO_3^-, K^+, Mg^{2+}, Na^+, $O_{2(aq)}$, $SiO_{2(aq)}$, SO_4^{2-}, CH_4, DOC
Aqueous complexes	$Ca(H_3SiO_4)_{2(aq)}$, $CaCl^+$, $CaCl_{2(aq)}$, $CaCO_{3(aq)}$, $CaH_2SiO_{4(aq)}$, $CaH_3SiO_4^+$, $CaHCO_3^+$, $CaOH^+$, $CaSO_{4(aq)}$, $CO_{2(aq)}$, CO_3^{-2}, $Fe(OH)_{2(aq)}$, $Fe(OH)_2^+$, $Fe(OH)_{3(aq)}$, $Fe(OH)_4^-$, Fe^{+3}, $FeCl^+$, $FeCl_{2(aq)}$, $FeCl_4^{-2}$, $FeCO_{3(aq)}$, $FeCO^{3+}$, $FeHCO_3^+$, $FeOH^{+2}$, $FeSO_{4(aq)}$, $H_{2(aq)}$, $H_2SiO_4^{-2}$, $H_4(H_2SiO_4)_4^{-4}$, $H_6(H_2SiO_4)_4^{-2}$, $HCl_{(aq)}$, HS^-, $HSiO_3^-$, HSO_4^-, $KCl_{(aq)}$, $KHSO_{4(aq)}$, $KOH_{(aq)}$, KSO_4^-, $Mg(H_3SiO_4)_{2(aq)}$, $MgCl^+$, $MgCO_{3(aq)}$, $MgH_2SiO_{4(aq)}$, $MgH_3SiO_4^+$, $MgHCO_3^+$, $MgSO_{4(aq)}$, $NaCl_{(aq)}$, $NaCO_3^-$, $NaHCO_{3(aq)}$, $NaHSiO_{3(aq)}$, $NaOH_{(aq)}$, $NaSO_4^-$, OH^-
Minerals	Biotite, Chlorite, Pyrite

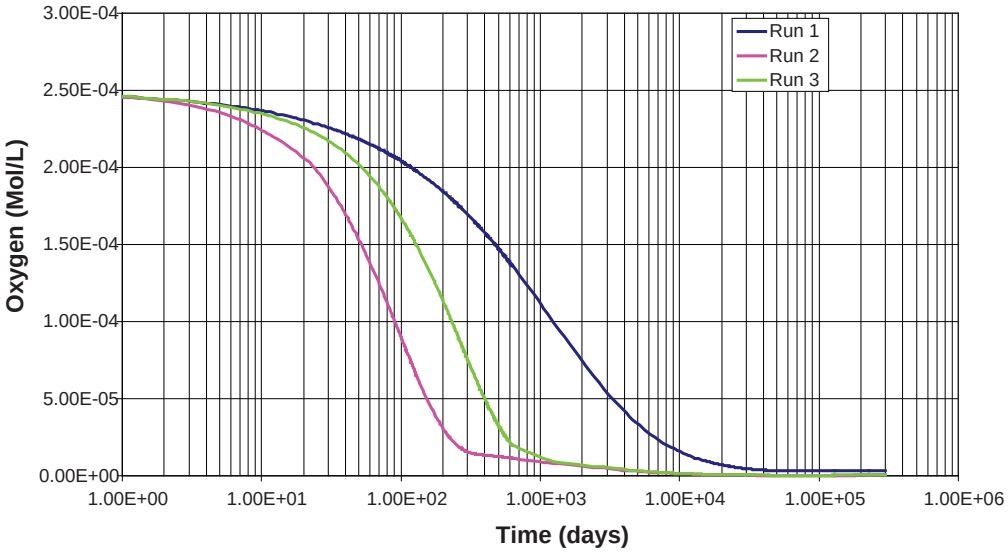

Figure 4-15. *A comparison of computed results of time evolution of oxygen depletion in the borehole, in the 3 simulated scenarios.*

As expected, the numerical model predicts that pyrite is the most effective mineral contributing to oxygen consumption, since its reaction rate is orders of magnitude faster than the rates of chlorite and biotite. Small amounts of pyrite present in granite would be able to consume oxygen as it diffuses from the borehole to the granite bedrock. Figure 4-16 shows the computed amounts of dissolved pyrite in the borehole surroundings. It can be seen that most of pyrite dissolves in the first 100 days, and consequently most of dissolved oxygen is consumed in the same time. It can be also seen that no pyrite is dissolved after 2 years because all the oxygen has been virtually depleted from the system at that time. From Figure 4-16 it can be also derived that the expected oxygen penetration length into the granite would be of about 1 cm.

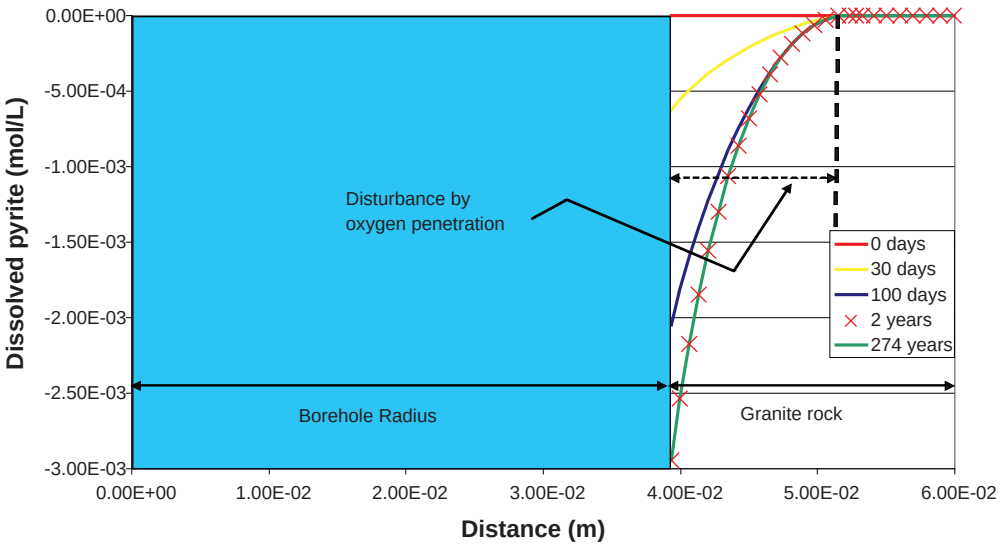

Figure 4-16. *Computed dissolved pyrite in the borehole surroundings at several times. Reactive base case (Run 2).*

5 The use of Magnesium as a tracer for Littorina water

5.1 Motivation

Mixing models are widely used in the context of the site characterization activities that are being conducted in Sweden. Mixing models have been proved in the past as very useful hydrochemical tools for understanding the complex palaeo-hydrogeological framework of the Fennoscandian Shield. The M3 model /Laaksoharju et al. 1999/ is a sophisticated mixing approach that makes use of multivariate statistical techniques (Principal Component Analysis) in order to elucidate the mixing proportions of available groundwater samples. M3 results point towards a conceptual palaeo-hydrogeological model involving 4 main end-members: (1) Deep Saline; (2) Glacial; (3) Littorina Sea and (4) Modified meteoric (dilute granite groundwater). Even with some limitations and uncertainties, available groundwater samples (both at Laxemar and Forsmark) can be largely explained as a result of mixing between the abovementioned end-members.

A major practical application of the M3 model is that its results can be used to constrain and calibrate the hydrogeological numerical models that are being performed in the framework of the site characterization programs at Laxemar and Forsmark. These hydrogeological models are being used to simulate the evolution of the groundwater system since the last glacial maximum. The main approach to calibrate past model versions has been to compare hydrogeological calculations against M3 model results. However, this approach has been questioned recently. Quoting one of the conclusions written by /Hartley et al. 2007/: *"It is considered that it was more useful to compare the predictions with the observation for the concentrations of major ions and isotope ratios than with the inferred M3 mixing fractions, because the errors in the latter can be very large"*.

Here we agree with such a conclusion. It is always conceptually better to compare the hydrogeological model results with actual measurements than with other model results. However this is only true for conservative species not for the reactive ones. Chloride, Bromide, 18-O and 2-H are the main conservative species available for its use in hydrogeological models. Unfortunately, the palaeo-hydrogeological history of the two sites is too complex to be clearly explained by the use of only these four conservative tracers (which at the same time are clearly correlated by pair combinations between them). Then, the rest of the species that are dissolved in groundwater are needed to get a real understanding of the hydrogeology. Magnesium is one of the most interesting because it is present in sea waters at much larger amounts than in the rest of reference waters. Then, it is tempting to use dissolved magnesium as a quantitative tracer of Littorina signature could appear. This becomes even more tempting when one looks at the correlation between computed M3 Littorina mixing fractions and measured magnesium concentrations (Figure 5-1).

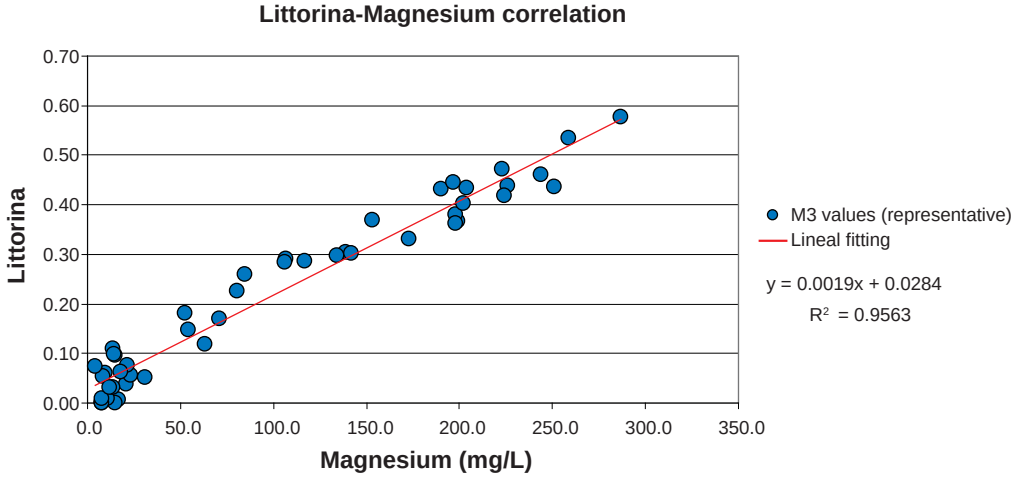

Figure 5-1. *Correlation between Littorina mixing fractions and dissolved magnesium in groundwater samples from Forsmark.*

However, it is well known that dissolved magnesium is a reactive species that can be involved in a number of hydrogeochemical processes, one of the most relevant being cation exchange. The work summarised here aims at evaluating the magnitude of the error that could be committed when magnesium is used as a conservative tracer for Littorina water. For that purpose, a few reactive mixing models accounting for cation exchange processes have been performed.

5.2 Reactive mixing model set-up

Three reactive mixing models simulating cation exchange processes have been performed. All the models have been solved by means of PHREEQCI v. 2.13.2 /USGS 2007/, based on PHREEQC v.2 /Parkhurst and Appelo 1999/.

The key parameters affecting cation exchange processes are: (1) the total CEC of the bedrock and, (2) the values of exchange constants (selectivity coefficients) for the cation exchange reactions. Site characterization activities have provided evidence on the existence of clay minerals able to initiate exchange processes both in fracture zones and host rock, at least at the Forsmark site. The available CEC values measured on different cores taken from boreholes at the Forsmark site (Personal communication E Gustafsson) were shown in Figure 4-5.

Figure 4-5 shows that cation exchange capacity is larger in the fracture zones than in the granite rock. The cation exchange capacity is especially large within the fractures zones located in the first 150 m of the bedrock (see Figure 4-5), where the more active hydrogeological system is dominated by flowing fresh groundwater which has favored silicate weathering, producing clay minerals. However, it can also be seen in Figure 4-5 that cation exchange capacity at greater depths is not negligible. A value of 0.05 moles/kg has been selected for the current modelling exercise, which corresponds to the measured value in fracture zones at repository depth in Forsmark.

There is no site-specific information available about selectivity coefficients neither at the Forsmark nor at the Laxemar sites. For this reason, the default values set at the PHREEQC database have been used for the current modelling. They correspond to the values extracted from /Dzombak and Morel 1990/. The three performed models account for the cation exchange of Ca^{2+}, Na^{+}, Mg^{2+} and K^{+}.

Reactive Mixing Model #1. It simulates the dilution of Littorina water by Modified Meteoric water. End-member compositions correspond to the “official” definitions provided by ChemNet Forsmark datafreeze v2.2 (see Table 5-1). The exchanger (solid phase) was initially equilibrated with the Littorina water. Next, mixing steps of 10% were simulated in a chained run (90% Littorina – 10% DGW; 80% Littorina – 20% Modified meteoric, and so on). A conservative mixing run was also computed in order to have a reference against which to compare the reactive mixing results.

Table 5-1. Chemical compositions of the end-member waters as delivered in the Forsmark 2.2 datafreeze.

End-member	Cl (mg/L)	Na (mg/L)	K (mg/L)	Ca (mg/L)	Mg (mg/L)	HCO_3 (mg/L)	SO_4 (mg/L)	δ^2H‰	$\delta^{18}O$‰
Deep saline	47,200	8,200	45.5	19,300	2.12	14.1	10	–44.9	–8.9
Glacial	0.5	0.17	0.4	0.18	0.1	0.12	0.5	–158.0	–21
Littorina sea	6,500	3674	134	151	448	92.5	890	–37.8	–4.7
Modified meteoric	181	274	5.60	41.1	7.5	466	85.1	–80.6	–11.10

Reactive Mixing Model #2. This is a very similar model to run #1 but Modified meteoric was substituted by the Glacial end-member. Then, it corresponds to a situation when Littorina is diluted by Glacial water. The objective of this model is to evaluate if there are major differences when Littorina water is mixed with two different dilute waters.

Reactive Mixing Model #3. According to the current palaeo-hydrogeological conceptual model, Littorina water was first mixed with glacial water due to density turnover produced by the fact that Littorina water (saline and denser) was on top of the previously injected glacial water (dilute and less dense). Afterwards, as a consequence of the uplift due to isostatic rebound, the land rose above the sea level and topographically driven infiltration of fresh water began. Then, recent fresh water of meteoric origin flushed out the previous mixing of Glacial and Littorina water and, consequently, ternary mixtures of the 3 end-members are plausible. Initial "native" water consisting of 50% Littorina and 50% Glacial was equilibrated with the exchanger in order to simulate this scenario. The dilution of this initial water was then simulated by mixing with Modified meteoric water by 10% intervals, as done in the previous models.

5.3 Computed results

Figure 5-2 shows the computed behaviour of dissolved cations considered in the mixing model #1 during the dilution of Littorina water by Modified meteoric. Figure 5-3 shows a comparative view of the behaviour of the four selected cations in the exchanger (solid phase). It can be seen (Figure 5-3) that the model computes the uptake (from the solution to the exchanger) of calcium and magnesium and the release (from the exchanger to the solution) of sodium and potassium, until a 70% of mixing is reached, whereas this trend is reversed at increasing percentage of mixing.

Since there is a selective uptake of magnesium by the exchanger during the first half of the dilution, the groundwater solution is relatively decreased in magnesium. This can be seen by comparing the computed results of the reactive and conservative mixings (Figure 5-4).

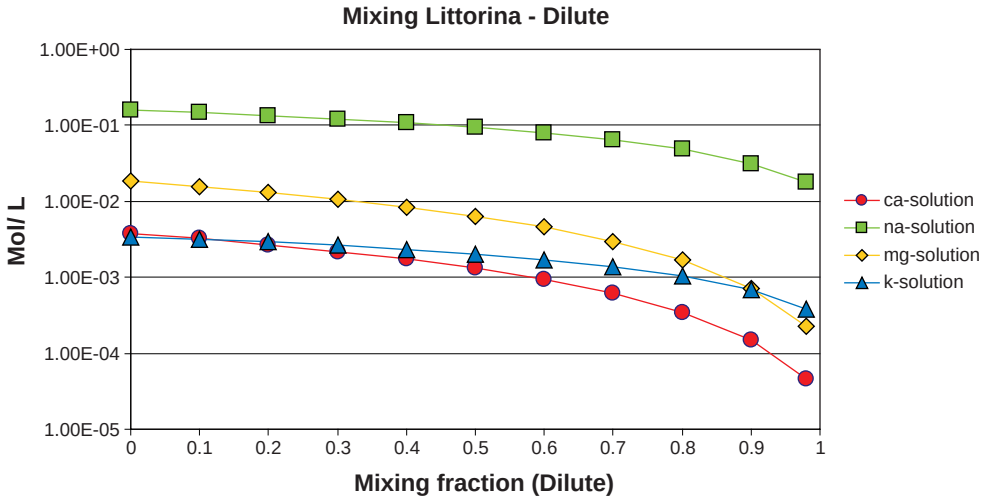

Figure 5-2. *Computed dissolved concentrations of the four cations for the reactive mixing model simulating the dilution process of Littorina water by mixing with Modified meteoric water.*

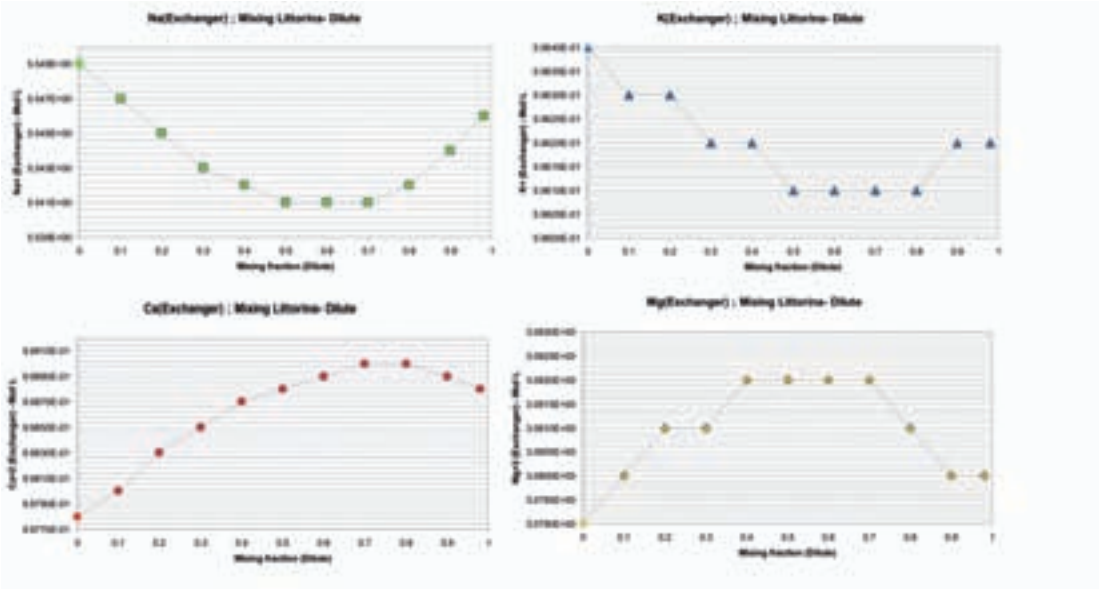

Figure 5-3. *Evolution trend of cations in the exchanger (solid phase) along the mixing (dilution) process. Sodium (upper-left); Potassium (upper-right); Calcium (lower-left); Magnesium (lower-right).*

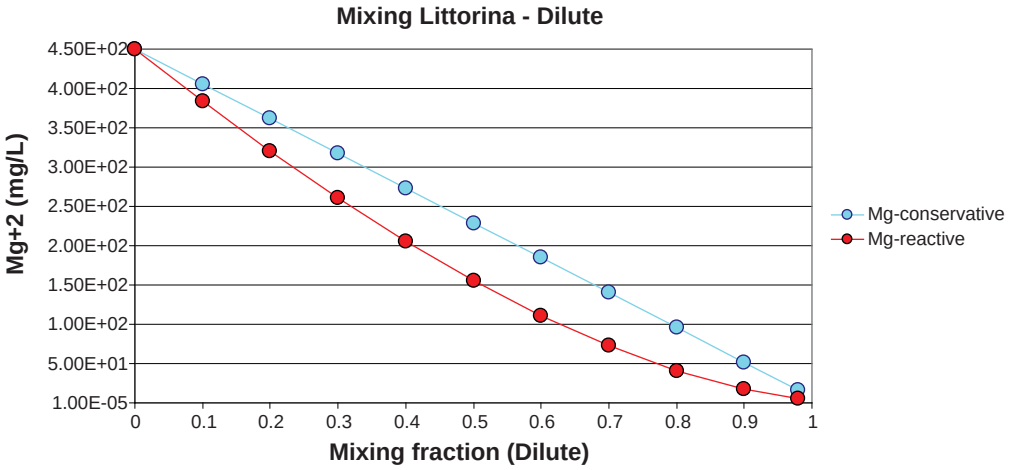

Figure 5-4. *Computed dissolved concentrations of magnesium both for conservative (blue) and reactive (red) mixing models simulating the dilution process of Littorina water by mixing with Modified meteoric water. It is worth noting that the reactive mixing model computes less magnesium in solution than pure conservative mixing.*

Figure 5-5 shows computed magnesium concentrations both for the reactive and conservative mixings of model # 2 (i.e. the dilution of Littorina by Glacial water instead of that by Modified meteoric). It can be seen that computed results are almost identical to those computed for the model # 1. It is worth noting that both cases are actually a very similar mixing of marine type water by fresh dilute water.

Figure 5-6 shows computed magnesium concentrations both for the reactive and conservative mixings of model # 3 (i.e. the dilution of a previous mixing of 50-50 Littorina and Glacial water by Modified meteoric water).

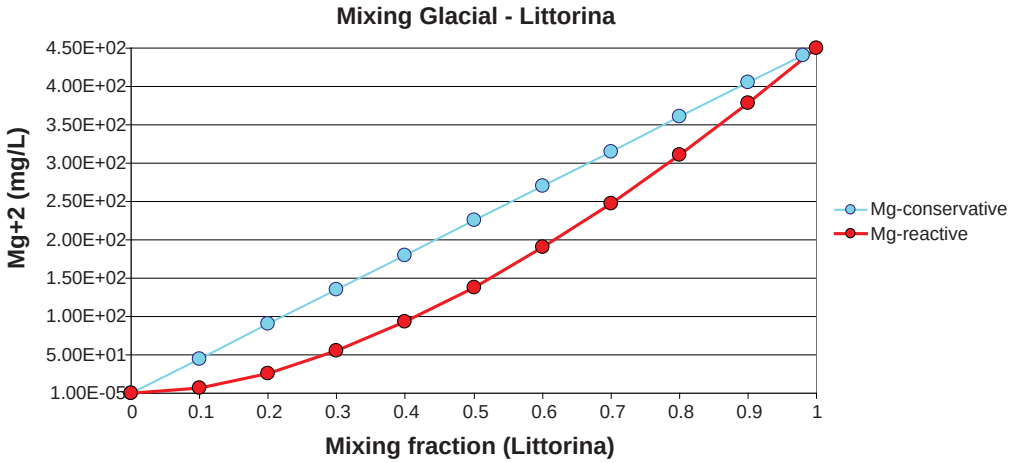

Figure 5-5. *Computed dissolved concentrations of magnesium both for conservative (blue) and reactive (red) mixing models simulating the dilution process of Littorina water by mixing with Glacial water. It is worth noting that the computed results are almost the same than those obtained by the dilution with Modified meteoric water.*

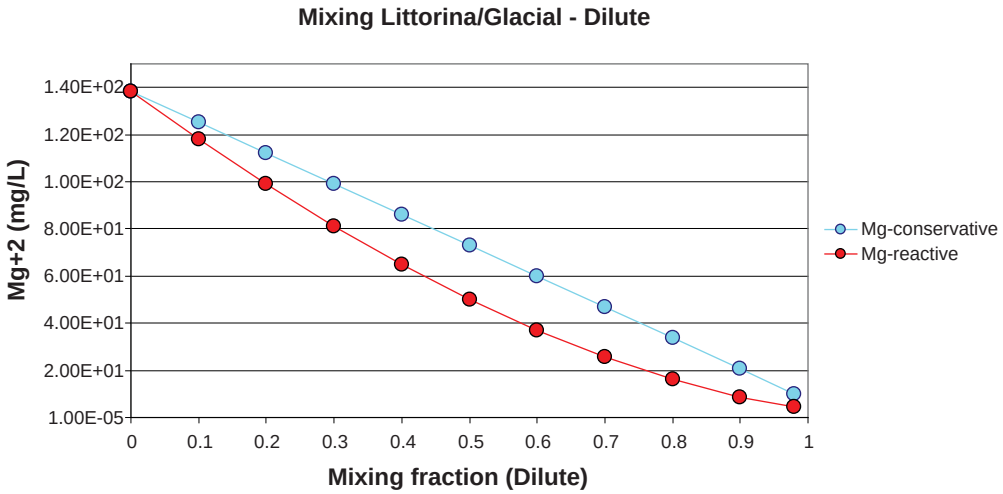

Figure 5-6. *Computed dissolved concentrations of magnesium both for conservative (blue) and reactive (red) mixing models simulating the dilution process of a previous mixing of Littorina and Glacial waters by Modified meteoric water.*

5.4 Discussion

The main conclusion of this work is that dissolved magnesium is clearly affected by cation exchange processes. Therefore, even though it could be a qualitative indicator for Littorina Sea water signature, it should not be used as a quantitative tracer for such an end-member.

The magnitude of the error can be evaluated by a simple example. A likely scenario, according to the current conceptual model, would be to have the occurrence of a mixing between Modified meteoric which is flushing a previous mixing of Littorina and Glacial water and is the simulated example in the reactive mixing model number 3. Let's consider a groundwater sample with a measured magnesium concentration of 73 mg/L. This would correspond to about 33% of Modified meteoric according to the reactive mixing model #3 (see Figure 5-6). This water sample would then represent about 66% of the previous Littorina-Glacial mixing and, therefore, it contains also about 33% of "pure" Littorina signature. However, a simple conservative mixing model (neglecting cation exchange) between the 3 end-members would only give 25% of Littorina signature for the same sample (see Figure 5-6). The difference with the M3 results

would be still larger. Such a sample would be classified by the current M3 model as having a signature of about 17% of Littorina water (see Figure 4-5 and use the fitting equation). This means that both a conservative mixing approach and the M3 model would underestimate the actual Littorina signature due to the unaccounted effect of cation exchange processes. The underestimation can be as large as almost a factor of 2 in the case of the M3 model and by a factor of more than 1.3 in the simple ternary (using three end-members) conservative mixing.

Since M3 and conservative mixing lead to underestimation of the Littorina signature, the calibration of hydrogeological models against either measured magnesium concentrations or M3 computed Littorina mixing fractions, would probably lead to overestimation of the flushing rates in such hydrogeological models (larger groundwater recharge flows, in order to compute smaller amounts of relict Littorina water in the bedrock).

Finally, it is worth calling attention to the fact that reactive mixing models performed here are also uncertain mainly due to the absence of site specific parameters for the cation exchange processes, except for the CEC values which correspond to measured values at Forsmark. It is worth noting that measured CEC values are noticeably larger at shallower depths, probably reflecting a larger amount of clay minerals as a result of silicates weathering processes. Then, the impact of the cation exchange processes on the magnesium concentrations would be even more dramatic for those waters mixed shallower than repository depth. It should also be noted that an additional uncertainty is related to the fact that there are other geochemical processes that could also influence the cation exchange behaviour and these have been neglected in the current modelling. The reactive mixing models presented here are a conceptual simplification to the real coupled reactive transport phenomena that actually takes place in the bedrock. The work presented here should be taken as a cautionary exercise aiming to show the high degree of uncertainty that actually exists in the current estimations of the amounts of Littorina relict water in the groundwater of the Forsmark site.

6 Testing the palaeohydrogeochemical conceptual model at Forsmark by using Chloride-Bromide mass ratios

6.1 Motivation

The study of the Bromide – Chloride relationship (called Br/Cl from now) is a well known hydrochemical tool useful to determine the origin of the salinity dissolved in groundwater (/Drever 1982, Nordstrom et al. 1989, Louvat et al. 1999, Stober and Bucher 1999, Casanova et al. 2001, Rao et al. 2005, Freeman 2007/ among many others). Br/Cl is especially useful for tracing marine signatures, due to the fact that such an ionic ratio has a relatively constant value around 0.0033. Then, assuming a conservative behaviour for both anions the dilution of any original marine water will affect both components in the same amount, so the ratio will remain constant thus allowing the detection of the marine signature even in diluted samples. Recent papers, such as /Davis et al. 2004/ summarised several applications on the use of Br/Cl to infer the geochemical provenance of different groundwater.

On the other hand, mixing models are also broadly used in hydrogeological and hydrochemical studies. Computed proportions of end-member waters provide a powerful tool for palaeohydrogeological site understanding but also for calibration of numerical models of groundwater flow and solute transport. SKB is using mixing modelling, among other approaches, for site understanding at Forsmark. SKB's mixing models are based on the M3 methodology /Laaksoharju et al. 1999/ that has been applied in several places, but especially at the Äspö site.

This report contains the study of the bromide and chloride contents in the available groundwater samples at Forsmark. The current conceptual model for the Holocene palaeohydrogeochemistry at the Forsmark site is tested based on the information given by these two tracers. The conclusions of the interpretation based on the bromide and chloride mass ratios are compared with the hydrochemical facies defined by the major solutes and with the computed results of the M3 mixing model.

6.2 Bromide and chloride signatures in Forsmark groundwaters

Figure 6-1 shows the Br/Cl values measured in the groundwater samples collected at Forsmark, plotted against the chloride concentration. Available Baltic Sea water samples (also taken from the Forsmark database) are included in the plot. It can be seen that Baltic Sea water samples plots consistently around the expected value for marine water, with a mobile average Br/Cl value of about 0.0032. It can be also seen that there is a certain scattering in the marine Br/Cl values, ranging between 0.002 and 0.005. This fluctuation could reflect the analytical uncertainty in the Br- measurements and/or can be due to other reasons, such as Br- sorption on organic ligands (humics, fulvics, etc) presents in the sea.

Figure 6-1 shows that there are a number of groundwater samples in Forsmark that show a clear marine signature (marked as blue rectangle in Figure 6-1). These samples have a Br/Cl value similar to the measured value in the current Baltic Sea. It should be assumed that those groundwaters with marine signature represent “ancient” marine samples, because there is not a driving force which could explain nowadays major intrusions of Baltic Sea water into the bedrock at inland positions in Forsmark. The most suitable explanation would be the density driven infiltration of the Littorina sea water that was located over previously infiltrated glacial melt water of lower density. It is estimated that maximum Littorina water infiltration happened about 6,000 years ago. Then, according to this conceptual hypothesis, the groundwater samples inside the blue rectangle in Figure 6-1 could be interpreted as having a Littorina signature. An additional support to this conclusion is that there are a number of groundwater samples with clear marine signature and, in addition, with higher chloride contents than the current Baltic Sea, which is consistent with the Littorina hypothesis (the estimated chloride content of the Littorina water is 6,500 mg/L).

Figure 6-1 also shows a set of groundwater samples that do not have marine signature, showing higher values of Br/Cl. Usually, they correspond to samples containing more than 4,500 mg/L of chloride that follow a trend of progressive increase of Br/Cl, to finally reach a relatively constant value of about 0.01 for chloride contents higher than 9,000 mg/L (see Figure 6-1).

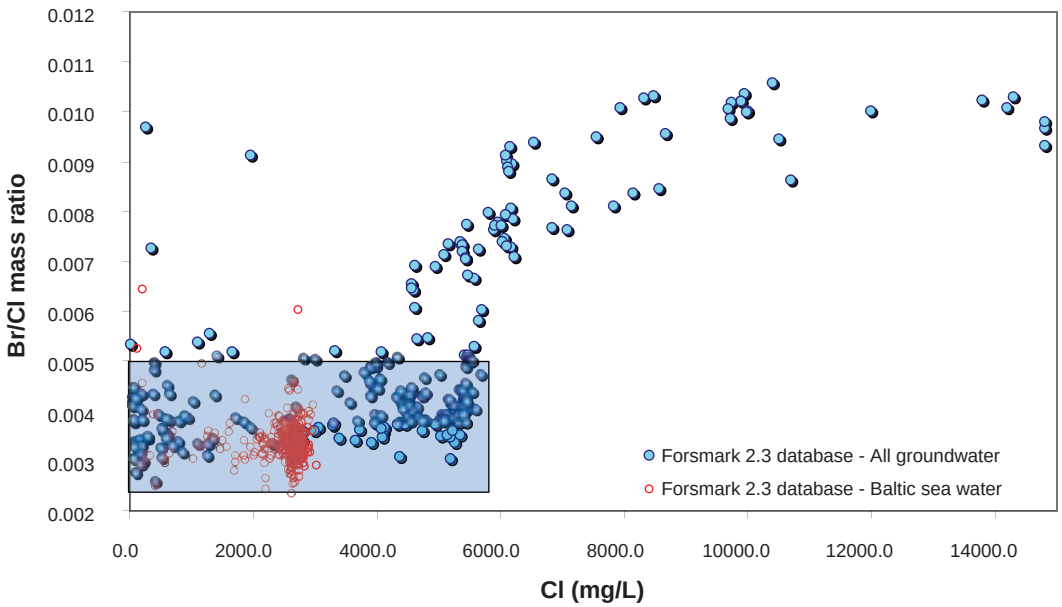

Figure 6-1. *Br/Cl relationship plotted against chloride values. Blue dots represent groundwater samples and open red circles represent Baltic Sea water samples.*

It is worth mentioning that bromide data can be affected by analytical uncertainty, especially the more diluted samples, where the concentrations could be very low. According to the P-reports of the hydrochemical characterization activities at Forsmark, bromide has been analysed both by ICP techniques (with reported detection limit of 0.001 mg/L) and by IC techniques (with reported detection limit of 0.2 mg/L). Since most of the samples have been probably analysed by IC the analytical error can be large for the highly diluted waters. This fact becomes evident looking at the Br/Cl ratios of surface and near surface water (not shown in this report), which have a very large scatter in the values. However, such a randomly behaviour of Br/Cl is not seen in the case of the groundwater samples. Figure 6-2 shows the same groundwater data than Figure 6-1 but including some theoretical binary mixing lines. It is interesting to point out that, in principle, all the groundwater samples should plot at or above the theoretical dilution line of the Littorina (sea) water. It can be seen (Figure 6-2) that very few groundwater samples plot below such line, and the maximum deviation in the most diluted samples, is of about 0.0015. According to this, it is thought that the analytical uncertainty related with the Cl- and Br- measurements do not constitute a problem that could compromise the conclusions of this report.

According to Figure 6-2, it can be stated that Br/Cl data could be, in general, well explained by different combinations of conservative binary mixing models. According to the current palaeohydrogeological conceptual model of the site, the following sequence of events could be invoked to explain the available data:

1) Infiltration of both old meteoric and glacial-melt groundwaters which produces dilution of Brackish Non-Marine Groundwater in the granitic bedrock.
2) Infiltration of Littorina water by density driven flow (with a maximum intensity about 6,000 year ago) and the mixing with fresher water located in the near surface bedrock.
3) The subsequent mixing of the diluted Littorina water with the previous mixing of old meteoric/glacial and brackish non-marine groundwaters in deeper parts of the bedrock.
4) The infiltration of recent meteoric waters during the last 500 years (aprox.) after the Forsmark site emergence to sub-aerial conditions, with the consequent dilution of the shallower part of the current hydrogeologic system.

Figure 6-3 summarises the 4 main palaeohydrogeological events and its hypothetical influence in the Br/Cl values. The arrows in Figure 6-3 are inspired in the theoretical binary mixing models shown in Figure 6-2.

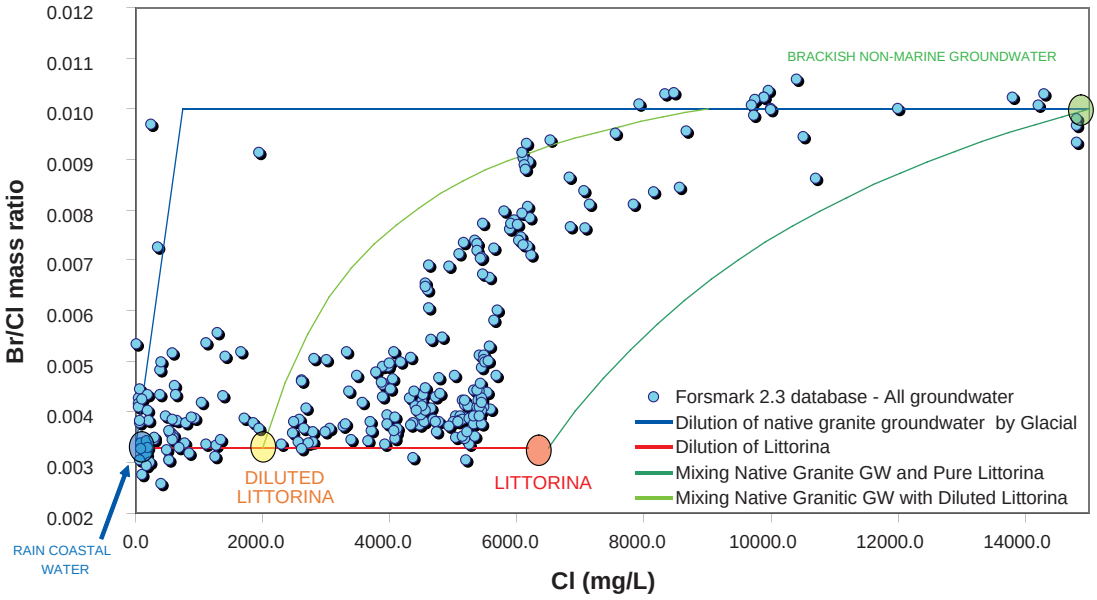

Figure 6-2. *Br/Cl relationship plotted against chloride values. Blue dots represent groundwater samples. Theoretical mixing lines between four end-members have been computed and plotted in the graph.*

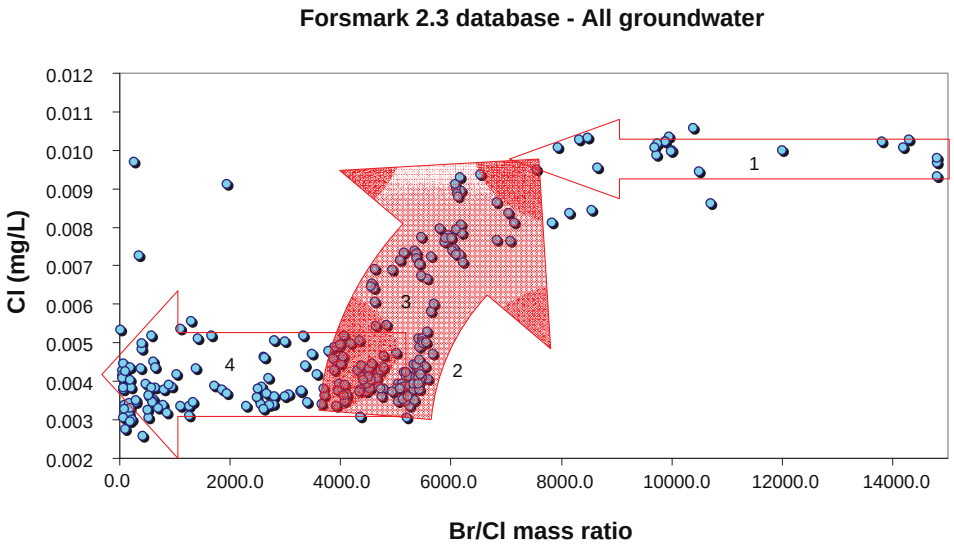

Figure 6-3. *Br/Cl relationship plotted against chloride values. The effect of the main paleohydro-geological events are sketched in the graph. (1) Dilution of Brackish Non-Marine Groundwater by the infiltration of fresh water (probably from both old meteoric and glacial origin), (2) infiltration of Littorina water and the mixing with fresh water in the near surface bedrock, (3) mixing of the diluted Littorina water with the previous mixing of old meteoric/glacial and brackish non-marine groundwaters and, (4) infiltration of recent meteoric waters during the last 500 years.*

Figure 6-1, Figure 6-2 and Figure 6-3 were produced using all the available groundwater samples in the Forsmark 2.3 database. In order to avoid the possible influence of major contamination events in the samples, a plot only using higher quality samples (samples from category 1 to 4) is shown in . It is worth noting that it also includes: (1) the most saline deep waters available in other Fennoscandian sites (Laxemar and Olkiluoto), (2) the expected pure Littorina end-member and, (3) the Br/Cl values measured in fluid inclusions in the granite rocks from Stripa /Nordstrom et al. 1989/.

According to Br/Cl data, the non-marine groundwater samples of Forsmark can not be explained by invoking any kind of conservative mixing with a saline end-member similar to the one measured at the deepest locations of the Olkiluoto and Laxemar sites. It can be stated that Br/Cl data indicate that there are a number of groundwater samples at Forsmark, with no marine signature, that tend to an end-member water highly consistent with the typical values of Br/Cl measured at the fluid inclusions of the granite rock of Stripa site. There are other leaching experiments performed in granite (and other igneous rocks) that also produced waters with similar Br/Cl values of about 0.01 /Stober and Bucher 1999/. /Nordstrom et al. 1989/ proposed a water rock interaction origin of the salinity in the groundwaters, mainly based on the analysis of Br/Cl ratio measured in the fluid inclusions. In Figure 6-4 the Br/Cl relationships plotted against chloride values.

Further support to this hypothesis was found by Sr isotopes measured in fluid inclusions and deep groundwaters (N. Waber, personal communication). Indeed, it is worth emphasizing the differences between Stripa and Forsmark sites (hydrogeological, geochemical, geological, etc), but Br/Cl information at Forsmark allows to propose the water rock interaction processes as a likely hypothesis (at least not to be ruled out) for the origin of the salinity in the brackish non-marine groundwaters. Such “Brackhish Non-Marine” water is proposed as a new end-member apparently more suitable than “Deep Saline” for hydrochemical description of the site.

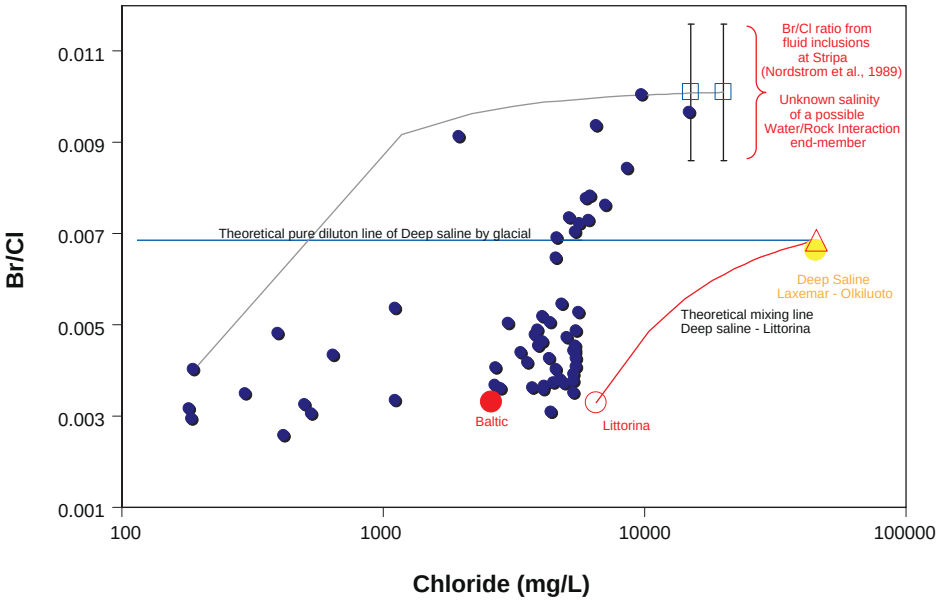

Figure 6-4. *Br/Cl relationship plotted against chloride values, including the deep saline waters of Olkiluoto and Laxemar. The assumed Littorina end-member and the measured values of the fluid inclusions found in granitic rocks from Stripa are also included. The blue dots are groundwaters at the Forsmark site.*

According to the type of plot shown in Figure 6-5, 3 main groups of groundwater samples can be distinguished.

Group 1. Contains diluted groundwater samples with chloride contents lower (or close to) 1,000 mg/L and marine signature. Most probably these samples correspond to recently-infiltrated meteoric waters mixed up with older marine waters.

Group 2. They correspond to the samples with strongest marine signatures, most probably reflecting the highest Littorina influence. They have salinity contents between the current Baltic Sea and the pure Littorina end-member.

Group 3: They correspond to water samples in the theoretical evolution/mixing line between the marine and the brackish non-marine end members. Most probably these samples are reflecting the mixing between old diluted waters (old meteoric and/or glacial) and Littorina sea water.

6.3 Consistency between Br/Cl analysis and other hydrochemical information

Even that the 3 groups explained above (and plotted in Figure 6-5) have been proposed only based on Br- and Cl- values, the differences between the groups of samples can also be detected in the rest of the major chemical components. Figure 6-6 shows a Piper diagram using the same water samples plotted in Figure 6-5 (category 1 to 4). The 3 different groups have been plotted with different symbols in Figure 6-6. Water samples from Group 1 show an evolution line from calcium-sodium bicarbonate water to sodium chloride waters. Water samples from Group 2 correspond to a predominant sodium and potassium chloride hydrochemical facies. Water samples from Group 3 are also chloride waters but show, in general, a different hydrochemical facies, richest in calcium.

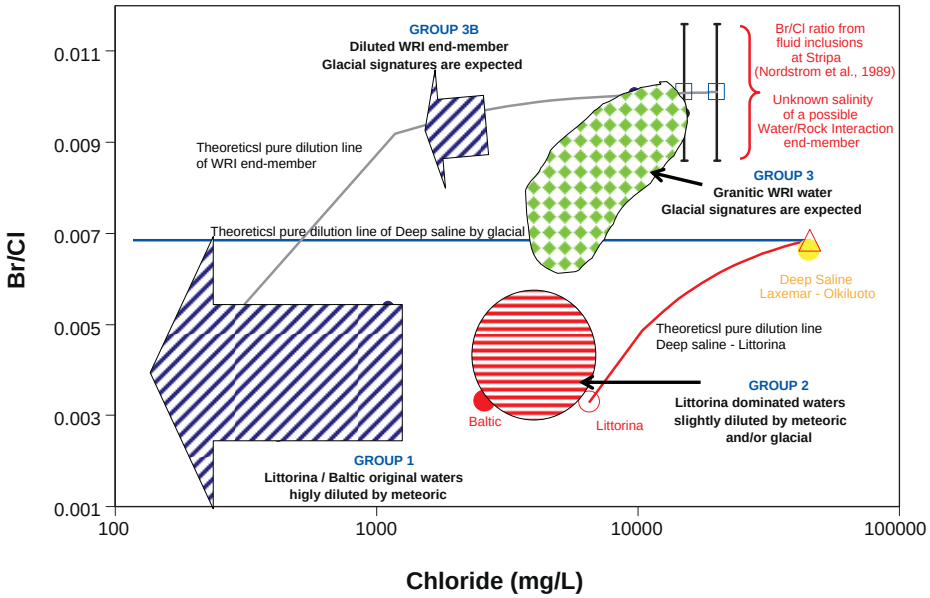

Figure 6-5. *The 3 different groups that can be separated according to the Br/Cl relationship plotted against chloride values.*

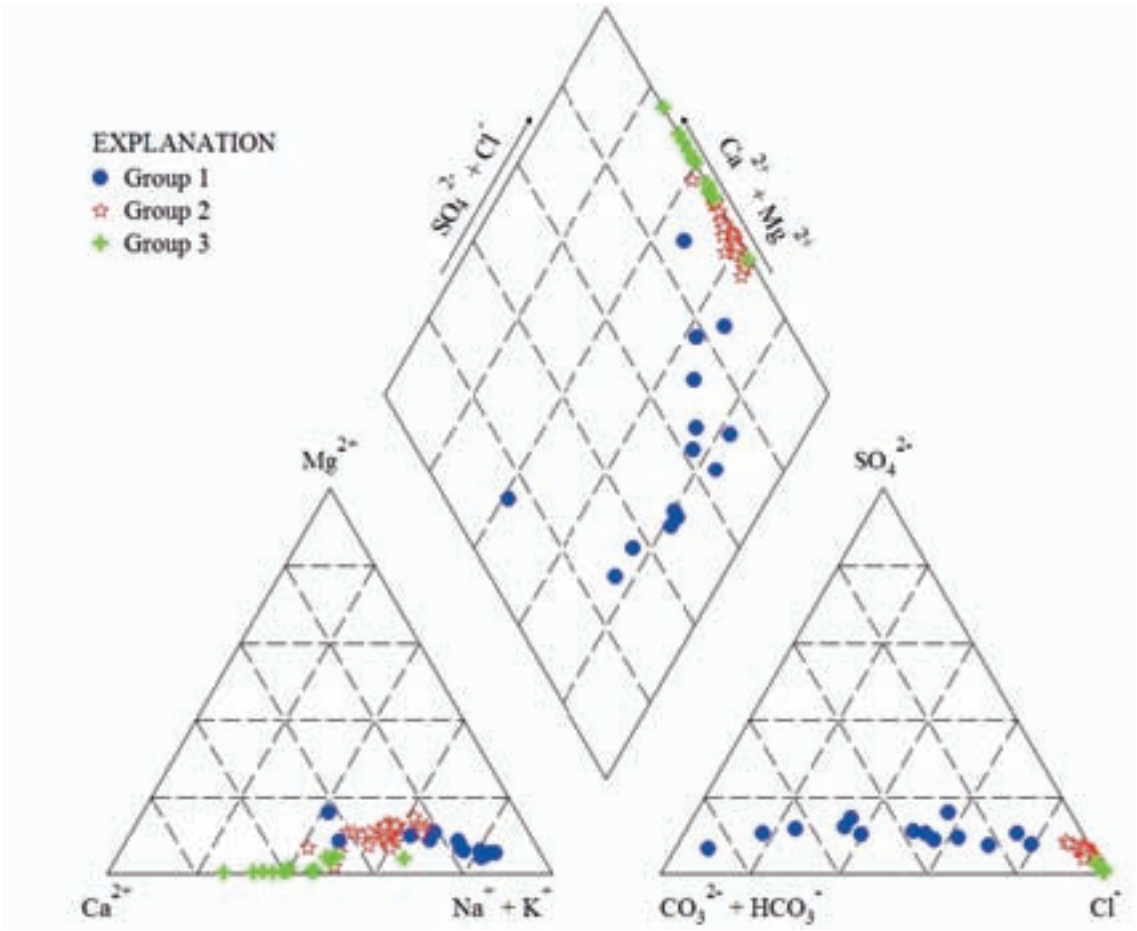

Figure 6-6. *Piper diagram showing the 3 different groups of groundwater samples that were separated according to the Br/Cl relationships. It is worth noting that such groups can also be detected by the major chemical solutes measured in the groundwater samples.*

6.4 Consistency between Br/Cl analysis and M3 model

The current palaeohydrogeochemical conceptual model of the Forsmark site is strongly based on the computed results of the M3 mixing model. The work reported here did also make use of such a paleohydrogeochemical conceptual model as the main hypothesis to explain the measured trends of Cl/Br. Then, the 3 main groundwater groups that have been proposed based on Br/Cl should be consistent with the mixing proportions computed by the M3 model. In order to perform such a consistency testing exercise, M3 computed results have been used, as reported by Gurban. (Section 1 in this report).

Figure 6-7 and Figure 6-8 show the comparison between the 3 groundwater groups derived from Br/Cl analysis and the mixing proportions of the 4 end-members computed with the M3 model.

Looking at Figure 6-7 and Figure 6-8 it can be stated that the groundwater groups detected by Br/Cl analysis show a high qualitative consistency with the computed results of the M3 mixing model. Group 1 correspond to the groundwater samples dominated by the “Altered Meteoric” end member, group 2 correspond to the groundwater samples with the highest proportions of “Littorina”, and group 3 correspond to the samples with, in general, higher proportions of “Glacial” and “Deep Saline” end-members.

Although the qualitative consistency can be judged as high, there are some exceptions in the expected trends. For example, there are two groundwater samples in Group 2 that show relatively low Littorina contents (less that 15%; see Figure 6-7), which was unexpected. Coincidently, these 2 samples are the same samples showing highest Deep Saline signatures within Group 2 (see Figure 6-8). In fact, all the groundwater samples of Group 2 have Deep Saline mixing proportions signatures of about 5%, which is below the accuracy limit of the M3 method, evaluated as 10% /Gómez et al. 2008/. Then, all the groundwater samples of Group 2 could actually be Deep Saline free, according to M3 accuracy, which would be consistent with the conclusions of the Br/Cl analysis. However, this “artificial/numerical background of Deep Saline” in the M3 results could generate quantitative propagating errors that could be relevant. According to the current conceptual model used in the M3 approach, the only sources of salinity are Deep Saline and Littorina end-members. As it has been shown, most ground-water

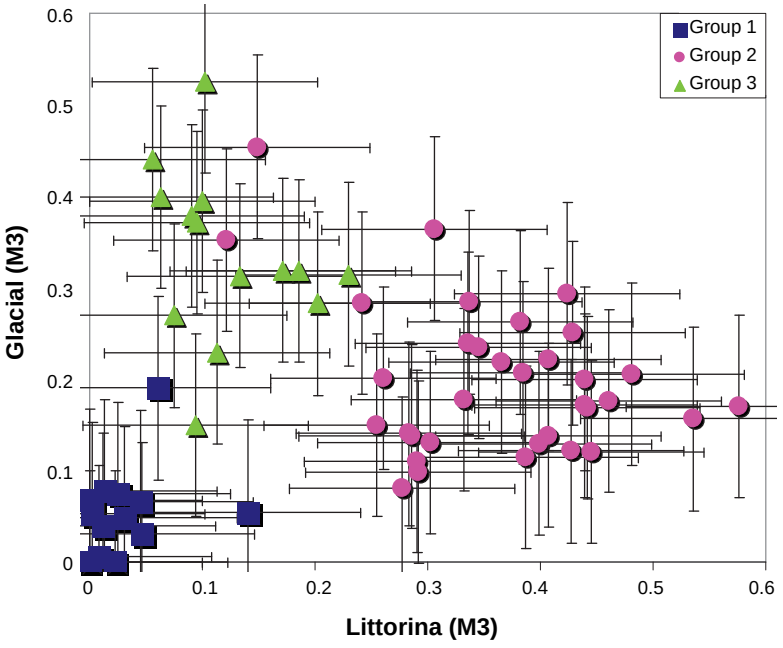

Figure 6-7. *M3 computed proportions of Glacial and Littorina end-members in the 3 groundwater groups proposed by Br/Cl analysis.*

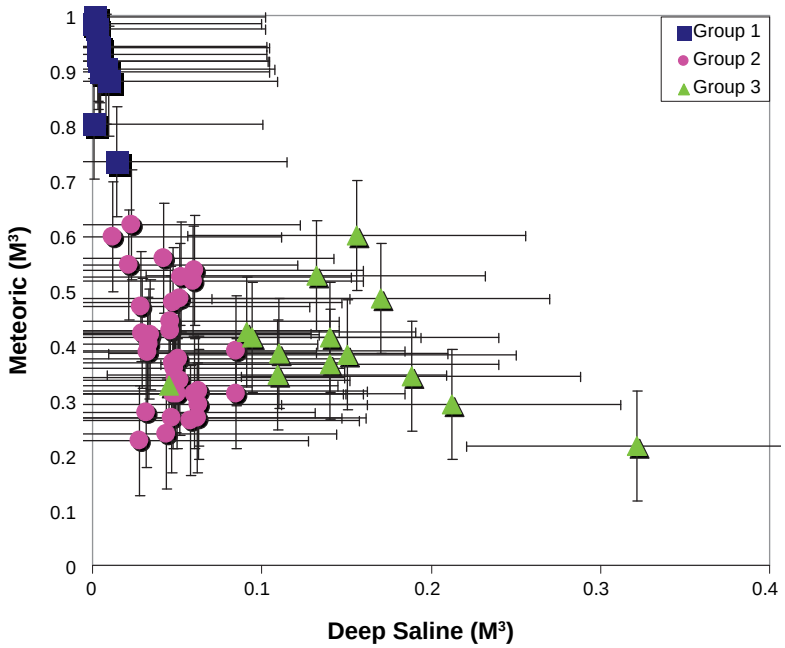

Figure 6-8. *M3 computed proportions of Meteoric and Deep saline end-members in the 3 groundwater groups proposed by Br/Cl analysis.*

samples in Group 2 have about 5% of Deep Saline signature, and almost 10% is computed in one particular sample. It is worth noting that 10% of Deep Saline means a chloride content of 4,550 mg/L, which is 70% of the chloride content of pure Littorina. Since the final chloride mass balance should be kept constant in each water sample, the M3 model should necessarily underestimate the quantitative amount of actual Littorina signatures in the groundwater samples having a numerical noise of Deep Saline signature. The next section of this report is devoted to analyse the magnitude of the possible underestimation of Littorina water in Forsmark.

6.5 Br/Cl analysis and Littorina signature

The estimation of Littorina signature in the groundwater is of capital importance for the site characterization studies. On one hand, it is fundamental for the hydrochemical and paleohydrogeological conceptual model of the sites. On the other hand, the infiltration of the Littorina pulse into the bedrock (with its maximum intensity about 6,000 year ago) constitutes a natural large-scale, and long-term tracer test that give a unique opportunity for calibration and validation of hydrogeological numerical models.

As shown in Figure 6-1, current Baltic Sea water show a variation range on Br/Cl ratios, but a clear average value of 0.0032 which is coincident with the typical marine value. Looking at the groundwater database, one can see that there are 9 groundwater samples with Br/Cl values between 0.0029 and 0.0036. A working hypothesis is adopted so that such a Br/Cl range is narrow enough as to assume that these 9 groundwater samples represent the pure dilution of Littorina water. Figure 6-9 shows the plot of Br/Cl versus Cl values of the 9 selected samples, the whole Baltic Sea database, and the theoretical dilution line of the Littorina end-member. It is firmly thought that the adopted working hypothesis is highly reasonable.

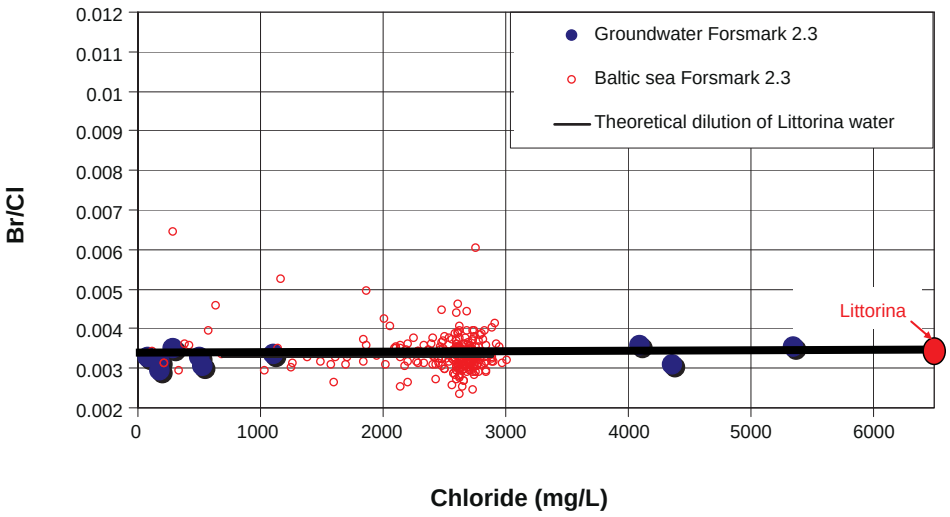

Figure 6-9. *Br/Cl ratio of the theoretical Littorina dilution line, the Baltic Sea water samples and 9 groundwater samples of the Forsmark site. A working hypothesis is adopted so that such 9 samples correspond to diluted Littorina water.*

Then, excluding any other salinity source for the 9 groundwater samples shown in Figure 6-9, it is possible to calculate a simple binary mixing model using chloride as a conservative tracer, between the Littorina end-member and a dilute end-member (whatever it might be glacial or meteoric). In fact both extreme waters are much more dilute than Littorina as to safely assume a dilute end-member with no chloride. The binary mixing model can be formulated as:

$$Cm = CLx + Cd(1–x)$$

where C denotes chloride concentration, sub-indexes m, L and d denote “mixture”, “Littorina” and “diluted”, respectively, and x is the mixing fraction of the Littorina end-member. Neglecting the chloride concentration of the dilute end-member (which is hundreds to thousands of times lower that the Littorina value), the mixing proportion of Littorina in the mixture can be safely approximated as:

$$x \approx Cm/CL$$

Figure 6-10 shows the Littorina mixing proportions computed by the pure dilution mixing model, plotted against the Littorina proportions computed with the M3 model. It can be seen that there is a high qualitative agreement between computed results of M3 and the binary mixing (high correlation factor). However, Littorina mixing fractions computed with the binary mixing model are systematically higher than those computed with M3. The underestimation of Littorina mixing fraction can be as large as a factor of 2 in those samples closer to the Littorina end-member.

The sample with higher Littorina signature in Figure 6-10 corresponds to sample number 12247, collected at borehole HFM33 at an average elevation of –50 m. The single dilution model computes 82.3% of Littorina signature in this sample whereas the M3 model computes 44%. This difference is because the M3 model also computes a 5.2% of Deep Saline end-member in the same sample, which is obviously not real but just numerical noise. However, such “numerical” Deep Saline signature amounts for 2,366 mg/L of chloride, which at the same time could be translated as 36.4% of the Littorina chloride content that is “lost” in the M3 model, due to the propagation of the numerical noise in Deep Saline end-member. Adding the M3 “actual” Littorina fraction and the M3 “lost” Littorina fraction amounts for 80.4%, which compares very well with the 82.3% Littorina fraction computed by the pure dilution model.

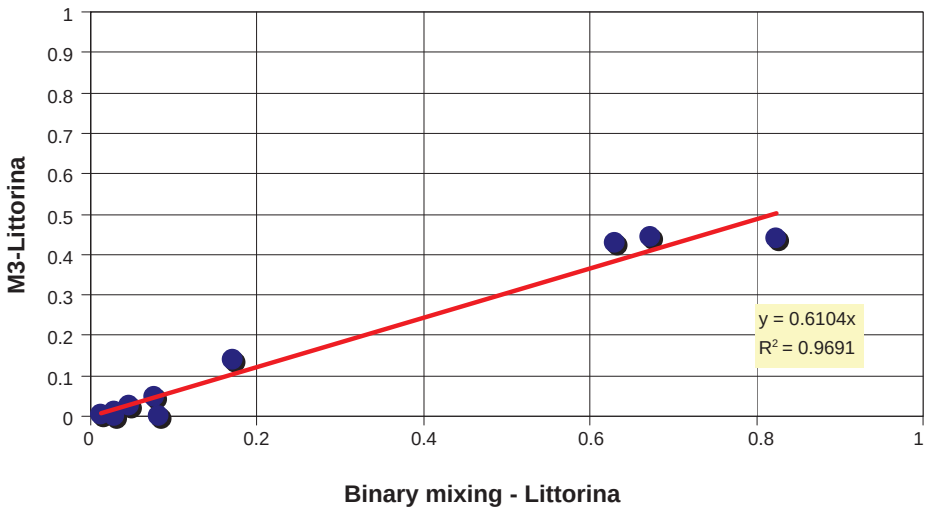

Figure 6-10. *Comparison between M3-derived Littorina proportions and computed results with the single binary mixture model (Littorina dilution) in the 9 selected groundwater samples.*

6.6 Remarks

Marine signature can be detected in groundwater samples by means of the bromide and chloride mass ratios. According to this study, a number of groundwater samples of Forsmark do not have a marine origin and can not be explained neither by mixing with deep brines similar to those detected in Laxemar or Olkiluoto. Some process and/or a new end-member, able to produce the observed enrichment in the bromide-chloride ratios, must exist. The bromide-chloride ratio of the non-marine waters is highly consistent with the ratios measured in the granite fluid inclusions at Stripa site. According to all this, a possible Brackish Non-Marine end member is proposed for the Forsmark site. The most likely hypothesis seems to be that such end-member results from water rock interaction processes in the bedrock. It is thought that this issue deserves further investigation in the future.

The analysis of bromide-chloride ratio has allowed the definition of 3 different groundwater types:

(1) Diluted groundwater with marine signature, showing a clear evolution path in their hydrochemical facies from calcium bicarbonate to sodium chloride. These water samples coincide with the highest meteoric signatures computed with the M3 model.

(2) Clearly marine-influenced groundwater, with salinity values between the current Baltic Sea and the past Littorina Sea and sodium-chloride hydrochemical facies. These water samples coincide with the highest Littorina signatures computed with the M3 model.

(3) Non-marine groundwater of variable salinity, showing a hydrochemical tendency towards calcium chloride facies, consistent with a mixing/evolution path between diluted marine and a Brackish Non-Marine end member. In general, these water samples coincide with the maximum signatures of both glacial and deep saline signatures computed with the M3 model.

Although the Br/Cl results show good qualitative agreement with the mixing proportions computed by the M3 model, a quantitative exercise shows that the current M3 model could be underestimating the amount of Littorina signature in Forsmark. Such an underestimation can be as large as a factor of 2 in those samples with stronger Littorina signatures.

7 Buffer capacity of near-surface groundwater at Forsmark

The chemical composition of near-surface waters is the result of several processes affecting surface waters as they infiltrate through the near-surface sediments and rocks. The main processes controlling the chemical modifications of such surface waters are related to the mixing with other near-surface waters, the interaction with the minerals present in the sediments and filling the fractures in the granites or the reactions with soils.

The aim of this work is to build up a geochemical conceptual model supported by numerical simulations that can explain how surface waters in the Forsmark area evolve from present-day near-surface waters due to the effect of the above mentioned processes. To fulfil this objective first we have analysed the existing chemical data for surface and near-surface waters from Forsmark. Thus, the main geochemical processes controlling the chemical composition of these waters can be identified and a conceptual model for the system evolution can be determined. In order to validate this conceptual model, some numerical simulations have been conducted with the geochemical code PHREEQC v2.0 /Parkhurst and Appelo 1999/.

7.1 Identification of geochemical processes

Near-surface waters in Forsmark have been mainly sampled from SFM soil pipes and PFM boreholes. The analysis of the chemical data from these samples allowed identifying two different groups of waters, GROUP-1 corresponding to very diluted waters (with chloride and sodium concentrations close to that of surface waters) and GROUP-2 following a mixing trend between surface waters and seawater (Figure 7-1).

The chemical evolution of GROUP-2 waters can be interpreted as the mixing of surface waters with present-day seawater or water from old Littorina Sea trapped in the sediments. If mixing with present-day seawater, one can expect that these samples are located near the coast or close to lakes clearly connected with the Baltic Sea. However, once plotted the location of the samples in the map of the Forsmark area (Figure 7-2) it can be seen that, although some of the GROUP-2 samples are located near the coast or close to lakes clearly connected with the Baltic Sea, some other samples are located inland. The explanation for these samples can be related to the fact that ancient seawater trapped in these zones mixes with surface water as it infiltrates into the system.

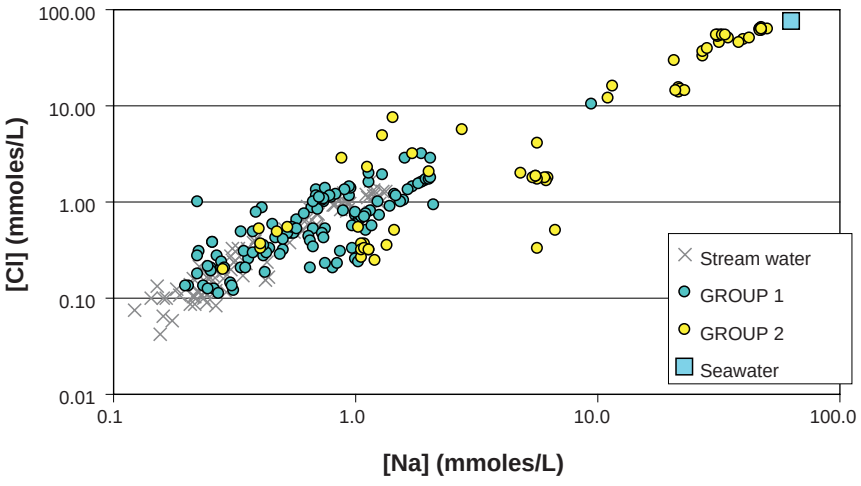

Figure 7-1. *Cl-Na graph showing the two near-surface groups of waters.*

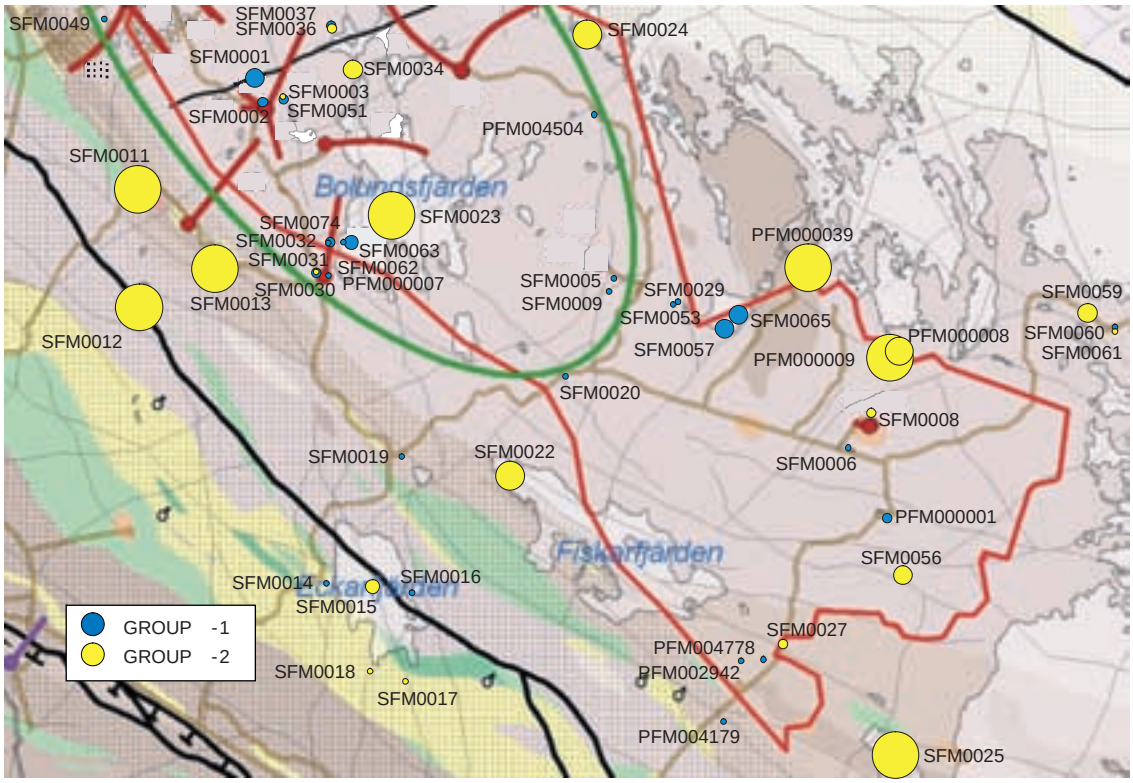

Figure 7-2. *Map of the Forsmark area with the location of near-surface water samples.*

Although, based on the chloride composition of near-surface waters, it can be stated that all the samples follow a single mixing trend between surface waters and seawater, the calcium and carbonate concentrations of these waters show a very different behaviour for the two groups (Figure 7-3). GROUP-1 follows a trend of increasing both calcium and carbonate concentration, whereas GROUP-2 follows a trend of increasing calcium concentration but decreasing the carbonate concentration.

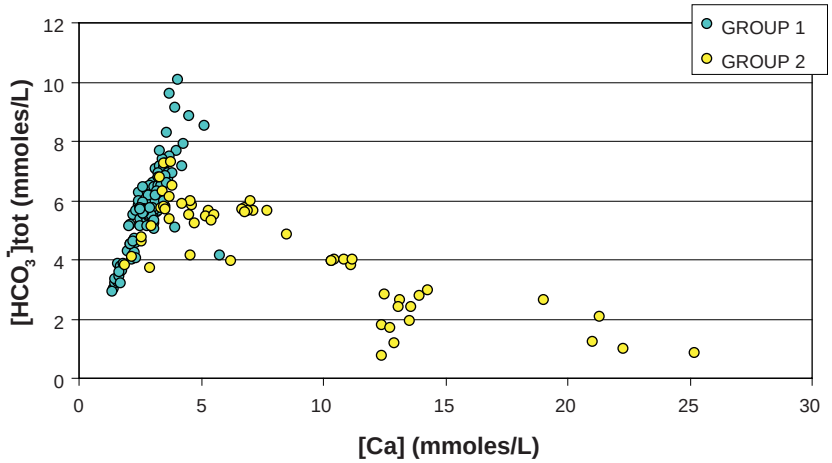

Figure 7-3. *Ca-HCO_3^- graph showing the different evolution of the two groups of near-surface waters identified in Forsmark.*

The increase in both carbonate and calcium concentrations in GROUP-1 samples could be related to the dissolution of calcite. Analysis of chemical data of the waters from GROUP-1 indicates that most of them are already in equilibrium with calcite. This makes it difficult for these waters to evolve to higher concentrations of both carbonate and calcium unless there is an additional process scavenging calcium from the water and thus allowing the dissolution of additional calcite. A careful examination of some of these samples (Figure 7-4) indicates that the increase in calcium concentration is half that corresponding to the dissolution of calcite (dashed line in Figure 7-4), if all the inorganic carbon is assumed to come from the dissolution of this mineral. There are several processes that could explain this behaviour:

1. Dissolution of dolomite instead of calcite.
2. A sink for calcium as calcite dissolves (i.e. cation exchange in clay minerals).
3. An additional source for inorganic carbon (i.e. organic matter degradation).
4. Different sources for inorganic carbon and calcium.

In the first case, if dolomite dissolution occurs, a similar increase of magnesium concentration as for calcium must be expected. However, as shown in Figure 7-5, a minor increase of magnesium concentration is observed, and the [Ca]:[Mg] ratio is close to 10. Therefore, the dissolution of dolomite instead of calcite can be disregarded or there is a sink for both magnesium and calcium, as indicated in the second hypothesis listed above.

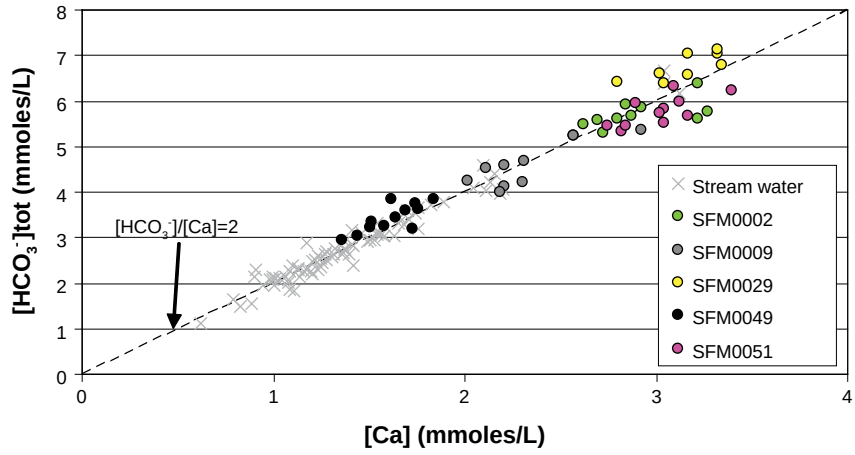

Figure 7-4. *Ca-HCO_3^- graph showing the evolution of GROUP-1 waters.*

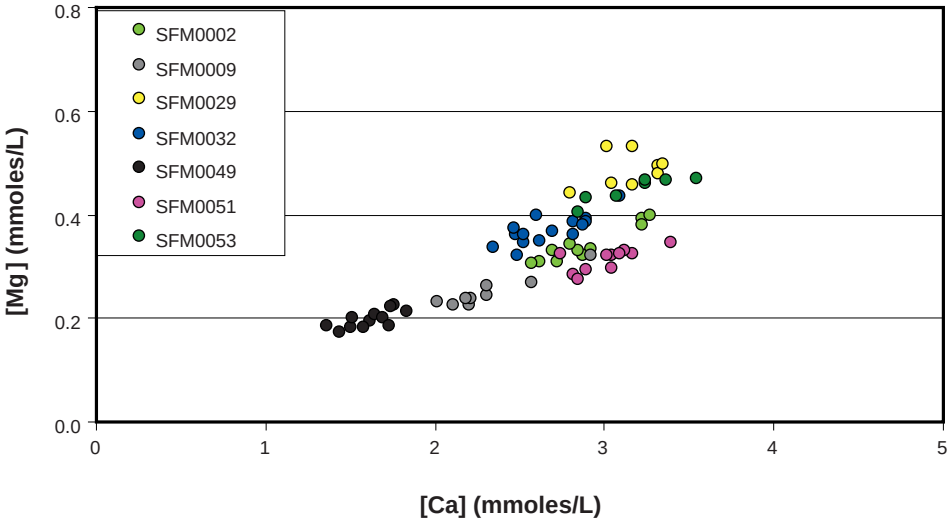

Figure 7-5. *Ca-Mg graph showing the evolution of GROUP-1 waters.*

Examination of the second hypothesis indicates that an equivalent concentration of other cations (i.e. sodium or potassium) should account for the difference between the increase in carbonate concentration and the increase in calcium. Considering that the increase in carbonate concentration is about 4 mmol/L (from 3 to 7 mmol/L) and the increase in calcium concentration is approximately 2 mmol/L (from 1.5 to 3.5 mmol/L), then the concentration increase of other cations must compensate the deficit of 2 mmol/L of calcium. Considering an increase in the magnesium concentration of 0.3 mmol/L (from 0.2 to 0.5 mmol/L), as shown in Figure 7-5, there are still 1.7 mmol/L to be compensated, which in the case of monovalent cations is equivalent to 3.4 mmol/L. However, the difference in concentration of monovalent cations (sodium plus potassium) is less than 2 mmol/L, and therefore the consideration of a lower increase of calcium concentration due to cation exchange reactions should be also disregarded.

The third and fourth of the hypotheses listed above suggest an additional source for carbonate or completely different sources for both calcium and carbonate. In the case of calcium, other sources that can be reliable are cation exchange reactions and/or the dissolution of gypsum, whereas for inorganic carbon, a reliable additional source could be the oxidation of organic matter according to the following generic reaction: (see item 12).

$$CH_2O + O_2 \rightarrow HCO_3^- + H^+$$

Organic matter is present in the sediments and soils from Forsmark, whereas the presence of trace amounts of gypsum could be possible especially in the unsaturated zone associated to dry and/or windy periods when it can eventually precipitate.

The redox of the near-surface system is somewhat controversial. Some samples seem to indicate that equilibrium with Fe(III) hydroxides is buffering the redox (Figure 7-6), as is also the case for surface waters. However, some samples lie in the sulphate/sulphide pair redox area as is the case for deep groundwaters. In any case, the presence of Fe(III) hydroxides in the system seems to indicate that the Fe(II)/Fe(III) is the most likely pair controlling the redox in the near-surface system.

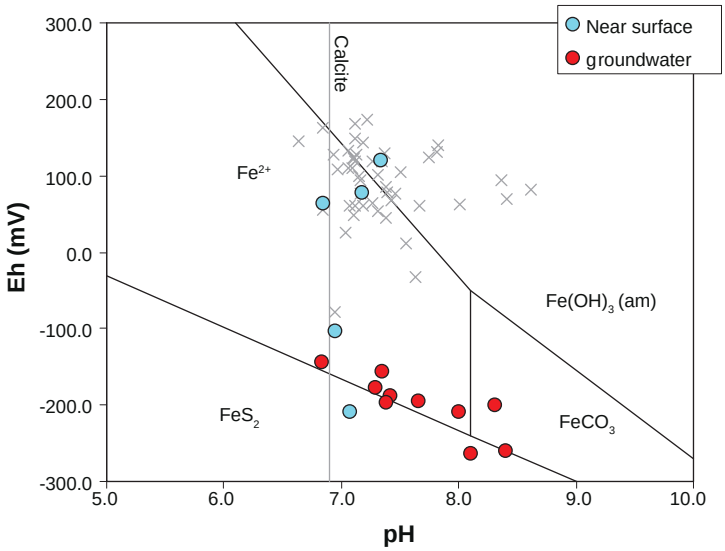

Figure 7-6. *Eh-pH diagram showing the iron system and the measured values for groundwaters in Forsmark /see Gimeno et al. 2008/. Grey crosses correspond to the surface waters.*

GROUP-2 waters should be affected by similar processes in addition to mixing with a saline water, although the relative importance of the processes could be modified due to substantial changes in the chemical composition of the water due to the mixing process. As an example, the calcium concentration of the Littorina Sea is below 4 mmol/L, although as seen in Figure 7-3, the maximum concentration of near-surface groundwater is slightly above 25 mmol/L. This could be related to exchange reactions in the clay fraction of sediments and soils of the Forsmark area, where the cation occupancy of such exchange sites in equilibrium with evolved surface waters enhance the Na–Ca exchange due to mixing with Littorina Sea or present-day seawater, with a much higher Na/Ca ratio. This process will result in a substantial increase in calcium concentration, indicating that in addition to mixing the cation exchange process is the main mechanism controlling the chemical composition of groundwater in those zones where mixing occurs.

7.2 Evaluation of geochemical processes through numerical simulations

First of all, it is essential to understand that most of the geochemical changes in near-surface groundwaters occur in highly diluted waters and, therefore, there is a large uncertainty associated to the geochemical process under consideration. This is true for most sampled waters, except for those samples that are clearly affected by a mixing process with higher salinity water (GROUP-2). Therefore, the simulations of the geochemical processes identified in the previous section could affect slightly some chemical parameters, whereas some other parameters, especially pH and Eh could be strongly affected when considering such processes. This will help to identify which of the processes under consideration is reliable, despite the fact that most of the samples from GROUP-1 only reflect small changes in their chemical composition, including pH.

In this context, the simulations conducted to evaluate the different processes to explain the observed evolution for GROUP-1 waters, indicate that when considering an additional source for inorganic carbon, as organic carbon oxidation, together with calcite equilibrium, leads to a decrease in pH, which has not been observed in near-surface water samples. Additionally, the amount of calcite dissolved is very small and it can not account for the maximum calcium concentration observed. Therefore, an additional source for calcium has to be considered.

In addition to oxidation of organic matter, the dissolution of small amounts of gypsum and the equilibrium with calcite are considered as a source for calcium and as a buffer for the pH evolution, respectively, a substantial improvement is achieved in the simulation of the geochemical trends observed. The reproducibility of the observed chemical evolution is improved when minor changes due to cation exchange reactions are considered. The simulation results indicate that the calcium and carbonate concentrations are properly reproduced when accounting for gypsum dissolution and organic matter oxidation as the main sources for Ca and HCO_3^-, respectively (Figure 7-7).

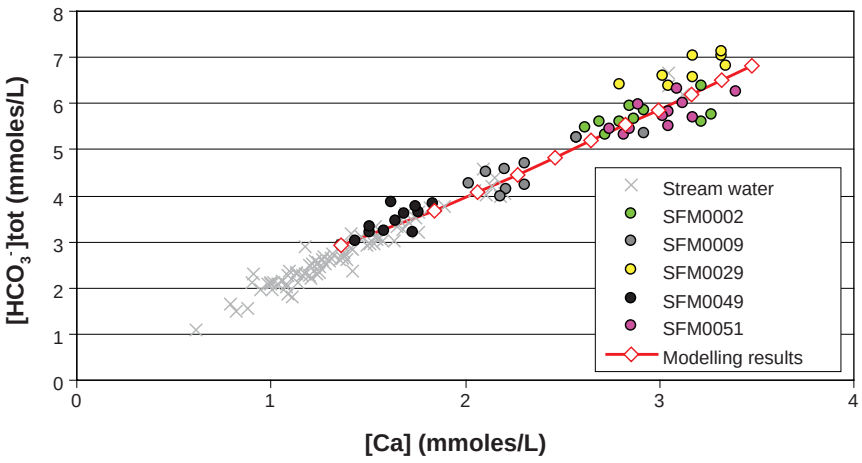

Figure 7-7. *Total inorganic carbon concentration vs. calcium concentration in selected near-surface waters corresponding to GROUP-1 and comparison with modelling results.*

The consideration of gypsum dissolution as the source for calcium is sustained when looking at the predicted evolution of the sulphate concentration and compared with measured values (Figure 7-8). In this case the predicted sulphate evolution reproduces fairly well the measured values when considering the dissolution of small (trace) amounts of gypsum. Moreover, the consideration of the equilibrium with calcite, results in a pH evolution that fits the measured values of the GROUP-1 near-surface waters (Figure 7-9).

Finally, the evolution of the rest of major cations (Figure 7-10) is properly reproduced when considering cation exchange reactions.

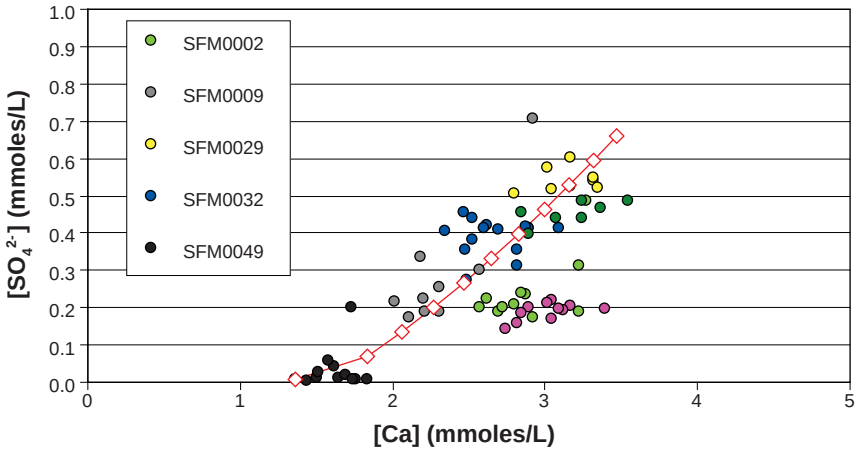

Figure 7-8. *Sulphate concentration vs. calcium concentration in selected near-surface waters corresponding to GROUP-1 and comparison with modelling results.*

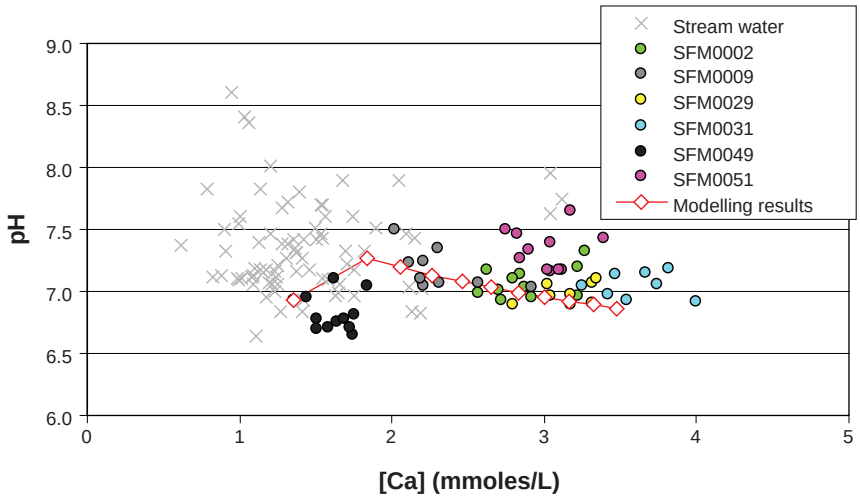

Figure 7-9. *pH vs. calcium concentration in selected near-surface waters corresponding to GROUP-1 and comparison with modelling results. (#14 again)*

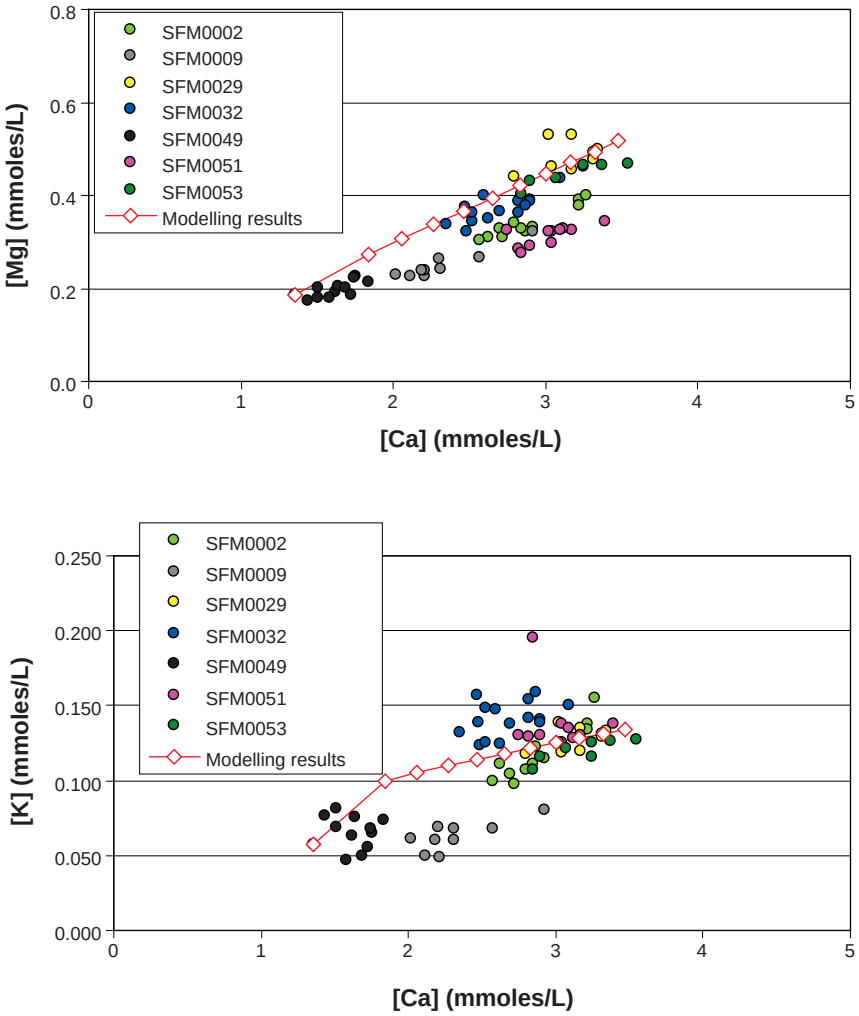

Figure 7-10. *Magnesium and potassium concentrations vs. calcium concentration in selected near-surface waters corresponding to GROUP-1 and comparison with modelling results.*

In summary, although at a first glance it seems that the chemical evolution of dilute near-surface waters is controlled by the dissolution of calcite, a careful examination of the analytical data and the performed numerical simulations indicate that the main processes controlling the chemical evolution of GROUP-1 waters is the oxidation of organic matter and the dissolution of small amounts of gypsum. The origin of gypsum could be linked to the evaporational processes associated with the unsaturated zone, leading to precipitation of such soluble phases. Moreover, there are other minor processes, subordinated to the previous ones, that control some of the other chemical parameters of the system, as the equilibrium with calcite and with the cation exchange capacity of a given clay mineral fraction. In addition, the consideration of different amounts of gypsum dissolved can explain the variability observed in the behaviour of diluted near-surface waters, leading to minor changes in cation concentrations and accounting for the scattering of the measured sulphate concentrations and pH.

The consideration of such a set of processes affecting the composition of surface waters as they penetrate into the subsurface system could have implications on the consideration of a given surface water end-member in the mixing process to explain the present-day groundwaters found at depth in Forsmark. Therefore, an evolved diluted near-surface water (“modified meteoric” in the new mixing model version) would be a better end-member for mixing calculations.

The evolution of GROUP-2 near-surface waters, although it concern to a limited number of samples, results in an increase of calcium concentration and a decrease of the carbonate concentration. This effect can be properly reproduced when considering the mixing with a water composition corresponding to the Littorina Sea and the equilibration of the resulting water with a cation exchanger and calcite. Thus, the resulting water after mixing has a large sodium concentration that enhances the Na by Ca exchange and leads to the subsequent calcite precipitation. This calcite precipitation results in a decrease of carbonate concentration (Figure 7-11) as well as to a decrease in pH associated with the precipitation of calcite (Figure 7-12).

The evolution of other major cations is controlled by the mixing process, in the case of sodium, or by the cation exchange process, in the case of magnesium and potassium. The modelling results fit quite well the both Mg and K concentrations measured in those near-surface waters clearly affected by the mixing process (Figure 7-13).

In summary, the evolution observed for a limited number of samples from the near-surface system in Forsmark indicates that they are controlled by the mixing with higher salinity water, whose resulting composition is modified due to the cation exchange process and the pH is buffered by the equilibrium with calcite.

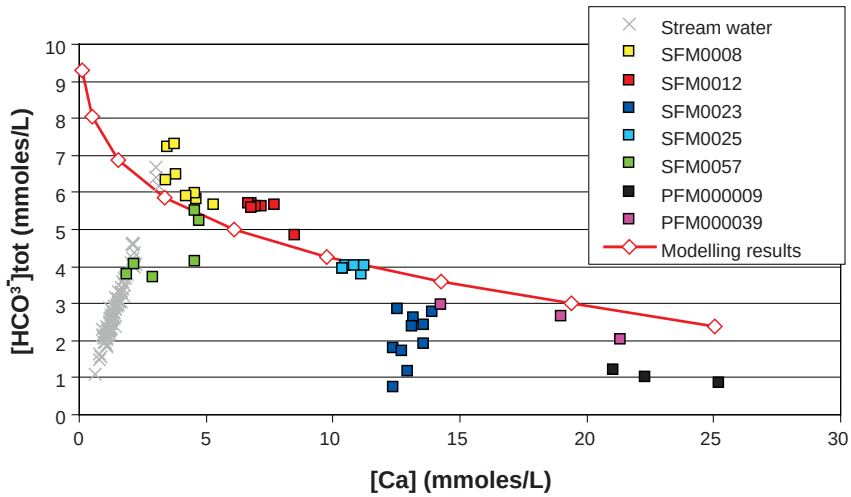

Figure 7-11. *Total inorganic carbon concentration vs. calcium concentration in selected near-surface waters corresponding to GROUP-2 and comparison with modelling results.*

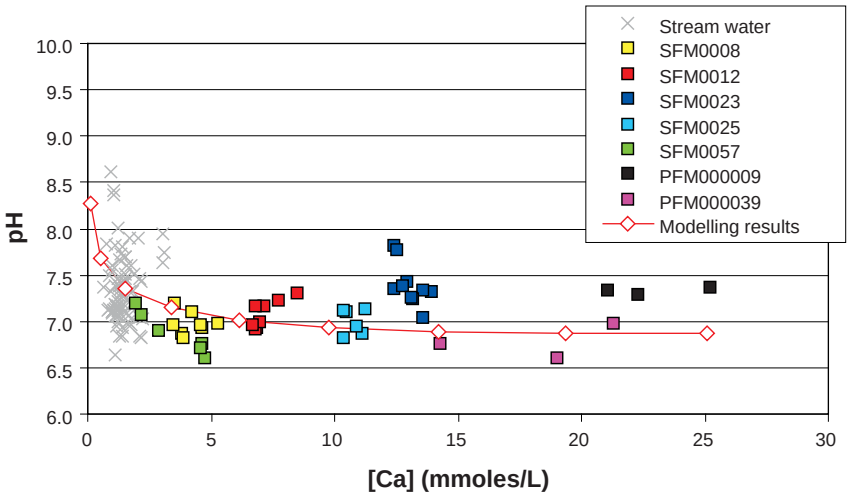

Figure 7-12. *pH vs. calcium concentration in selected near-surface waters corresponding to GROUP-2 and comparison with modelling results.*

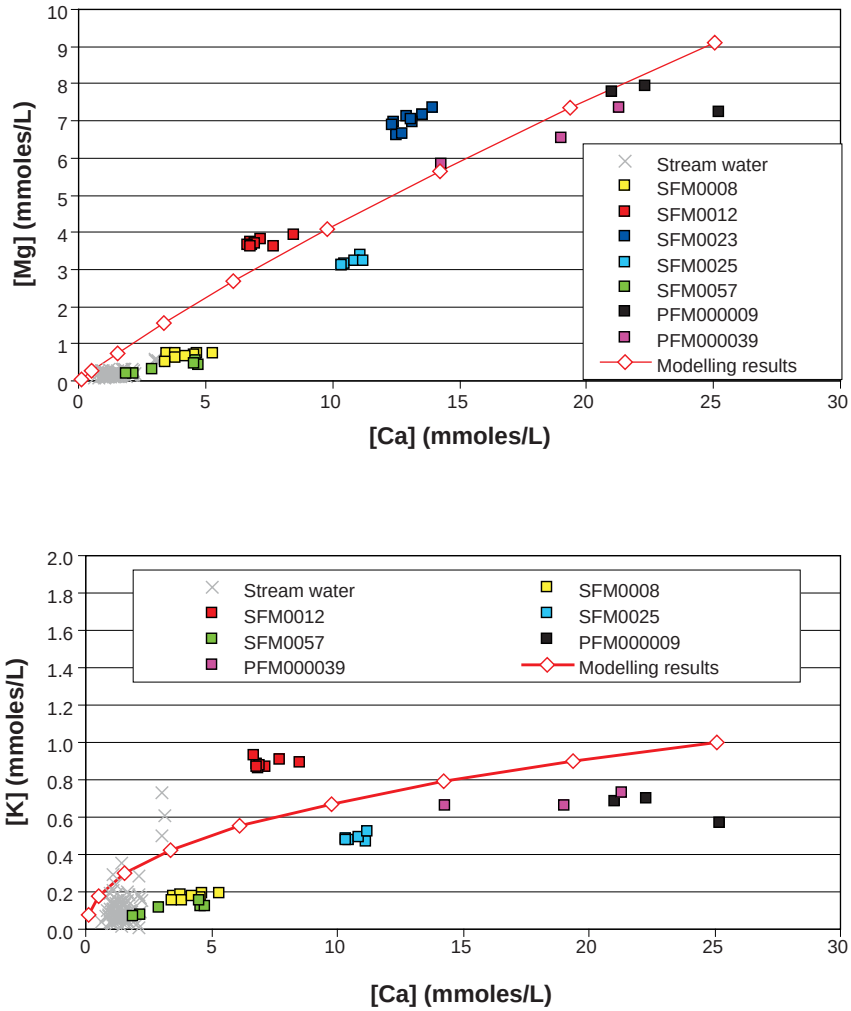

Figure 7-13. *Magnesium and potassium concentrations vs. calcium concentration in selected near-surface waters corresponding to GROUP-2 and comparison with modelling results.*

8 Uranium concentrations in groundwater

The concentrations of uranium analysed in samples from cored boreholes (KFM) at Forsmark span over 3 orders of magnitude, between $1 \cdot 10^{-10}$ mol/L to $5 \cdot 10^{-7}$ mol/L. The source of uranium in the area is not very clear, although in the characterization of fresh pegmatite and granite samples, concentrations above 60 ppm have been reported. The uranium content in fracture fillings from Forsmark is usually low, between 0.46 and 70 ppm, although in two fracture fillings intersected in borehole KFM03A elevated concentrations have been measured (2,310 and 2,200 ppm) by /Sandström and Tullborg 2006/ and /Drake et al. 2006/. A positive correlation between the uranium content in fracture fillings and that in groundwater is observed /Drake et al. 2006/ (Figure 8-1), pointing to a control of uranium concentration in groundwaters due to precipitation-dissolution of uranium minerals in fractures. A mineralogical study of the fracture filling from borehole KFM03A, (the borehole with the highest uranium content), revealed the presence of uranium oxides (likely altered pitchblende). Therefore, the precipitation-dissolution of these uranium oxides is likely to exert an effective control on the uranium concentration in groundwaters.

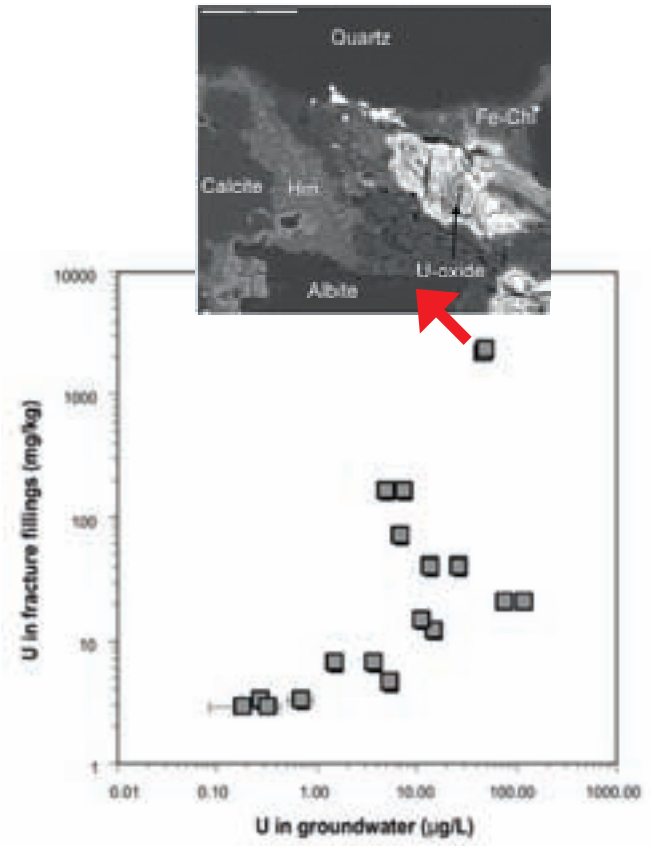

Figure 8-1. *Uranium content in fracture fillings (ppm) versus uranium in water (ppb) samples /from Drake et al. 2006/. The picture above shows a backscattered electron image from borehole KFM03A 643.80–644.17 m with altered U-oxide (pitchblende) together with chlorite (Fe-Chl), hematite (Hm) and calcite. The scale in the picture is indicated by the white bar, equivalent to 50 µm /from Sandström and Tullborg 2006/).*

The main objective of this work is to assess which is the main process(es) responsible for the measured uranium concentrations in the Forsmark groundwaters. To this aim, the data from the Forsmark 2.2 datafreeze corresponding to the samples from KFM01A to KFM09A with uranium determinations have been selected. A very schematic cross section of the area showing the location of the samples is shown in Figure 8-2.

The composition of the samples is rather similar in terms of major cations and anions.
The major composition of the groundwater samples is shown in Table 8-1.

8.1 Redox potential

In order to test the possibility of the observed uranium oxides exerting a control on the aqueous uranium concentrations, the redox potential is needed. The redox potential is not always available for the samples. In agreement with previous assessments reported by /Gimeno et al. 2006/, we have calculated the redox potential that the groundwater samples would present if controlled by the FeS(ppt)/SO_4^{2-} redox couple. The agreement between the calculated and the measured redox values, in case they were reported, is shown in Figure 8-3. The equilibrium constants used for the FeS(ppt) solubility and for the sulphate to sulphide reduction are:

$FeS(ppt) + H^+ = Fe^{2+} + HS^-$, with logK = –3.9

$SO_4^{2-} + 9H^+ + 8e^- = HS^- + 4\ H_2O$, with logK = 33.65

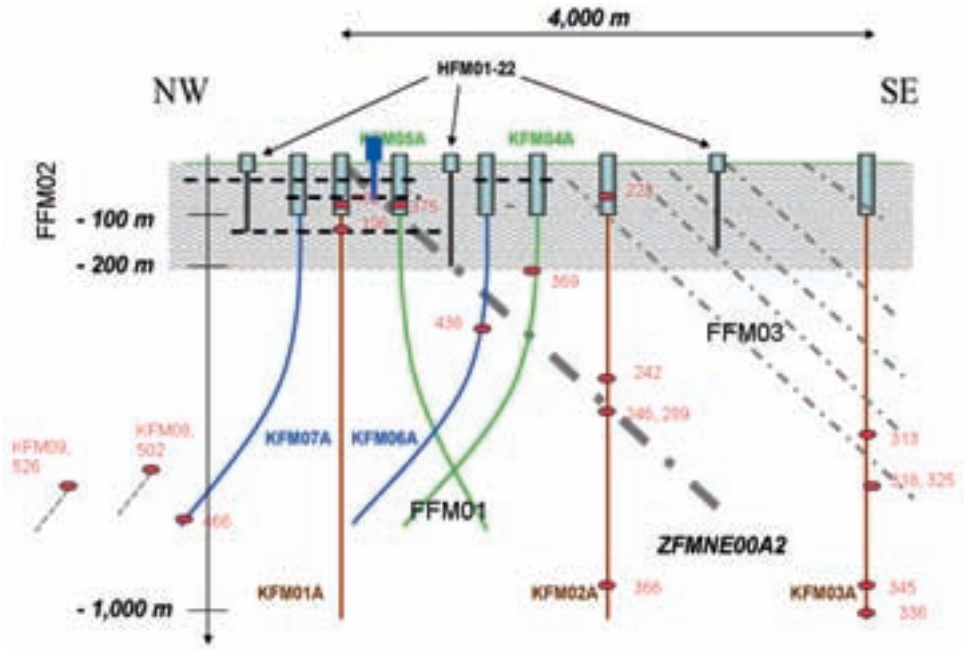

Figure 8-2. *Cross section of the area showing the location of the samples (not to scale).*

Table 8-1. Major composition of the groundwater samples. Concentrations in mol/L. Eh in mV. (see item 15)

ID sample	183	196	205	212	289	223	242	246
Borehole	KFM01A	KFM01A	KFM01D	KFM01D	KFM02A	KFM02A	KFM02A	KFM02A
pH for modelling	7.65	7.41	8.10	8.40	6.83	7.52	7.37	7.19
Eh for modelling	–195	–188	–263	–260	–143			
Na	0.08	0.09	0.07	0.08	0.09	0.02	0.08	0.09
K	6.6E–04	7.5E–04	2.4E–04	2.0E–04	8.8E–04	2.5E–04	5.5E–04	9.3E–04
Ca	3.6E–02	3.9E–02	6.8E–02	7.6E–02	3.9E–02	5.8E–03	4.8E–02	3.7E–02
Mg	5.9E–03	8.5E–03	5.7E–04	6.3E–04	9.4E–03	1.3E–03	8.3E–03	1.0E–02
Cl	0.13	0.15	0.15	0.16	0.15	0.02	0.15	0.16
SO_4	3.3E–03	5.7E–03	8.2E–04	4.0E–04	5.2E–03	9.3E–04	4.5E–03	5.3E–03
HCO_3	1.0E–03	1.6E–03	3.5E–04	3.3E–04	2.1E–03	5.8E–03	1.5E–03	2.1E–03
U	6.3E–09	6.3E–08	8.2E–09	3.4E–09	3.7E–07	2.27E–08	5.84E–08	5.13E–07

The agreement between both Eh series is better than when considering that the couple Fe(II)/$Fe(OH)_3$(s) is exerting the redox control (compare Figure 8-3 with Figure 8-4). This is in agreement with the discussion in chapter 6 of this report, where it is concluded that the redox state of the superficial waters is controlled by the Fe(II)/Fe(III) system, but the deep groundwater system is more likely to be controlled by the sulphate/sulphide redox couple.

We will therefore assume that the redox potential of the groundwater samples is fairly well represented by that obtained from a sulphide-sulphate controlling couple. In this way, we can estimate the missing redox potentials of those samples presenting uranium data but not redox data. It is important to point out that we have considered the formation of FeS(ppt) instead of that of pyrite due to the fact that the dynamics of the redox system will probably favour the formation of the amorphous phase over that of pyrite, given that the formation of pyrite will require a further sulphidation of the secondary readily precipitating FeS(ppt) (see also discussion in /Gimeno et al. 2008/).

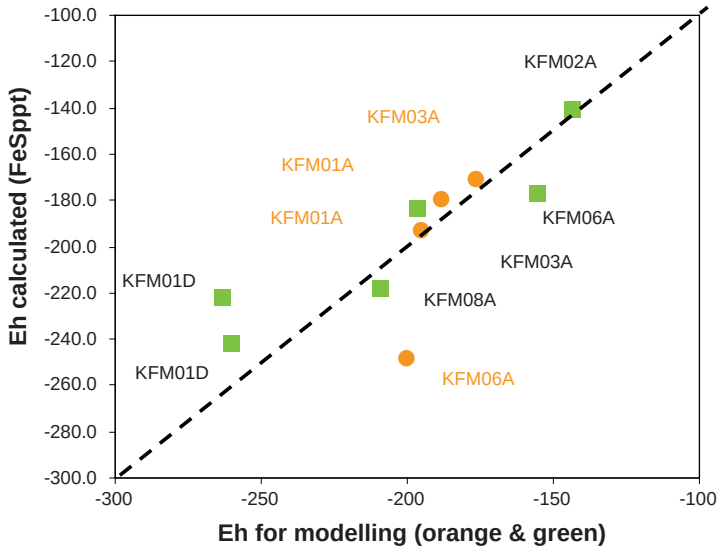

Figure 8-3. *Comparison between Eh for modelling reported in Forsmark v.2.2 SICADA datafreeze and Eh calculated by assuming equilibrium between FeS(ppt) and aqueous sulphate. Colour code corresponds to the accepted representative samples.*

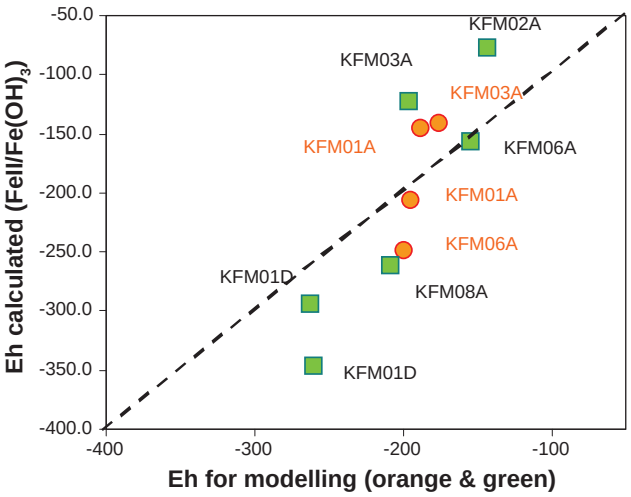

Figure 8-4. *Comparison between Eh for modelling reported in Forsmark v.2.2 SICADA datafreeze and Eh calculated by assuming equilibrium between Fe(II) and $Fe(OH)_3$(s). Colour code corresponds to the accepted representative samples.*

The pH/pe (pe = Eh/59.16) data of the samples selected are shown in Figure 8-5.

The pH values of the samples plotted in Figure 8-5 range from 6.3 in the deepest sample of KFM03A to 8.2 in sample KFM09, while the value of the redox potential (in pe units) ranges from –2 to –4 (–120 to –240 mV approximately).

The control of the redox state of the system is extremely important and it is worth mentioning that in many natural systems investigated, the redox potential is mainly exerted by the very dynamic Fe(II)/Fe(III) system (see Figure 8-6).

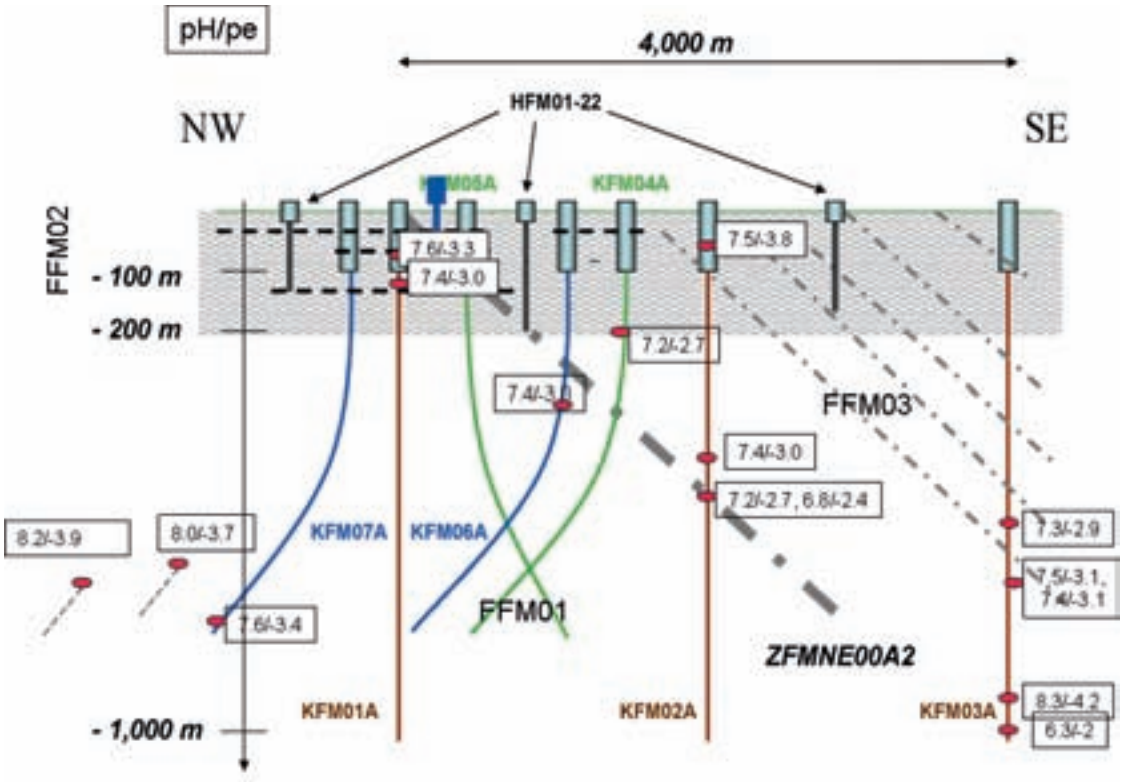

Figure 8-5. *pH/pe values of the groundwater samples studied in this work. Missing redox potentials have been calculated by assuming equilibrium FeS(ppt)/Fe(II), as explained in the text.*

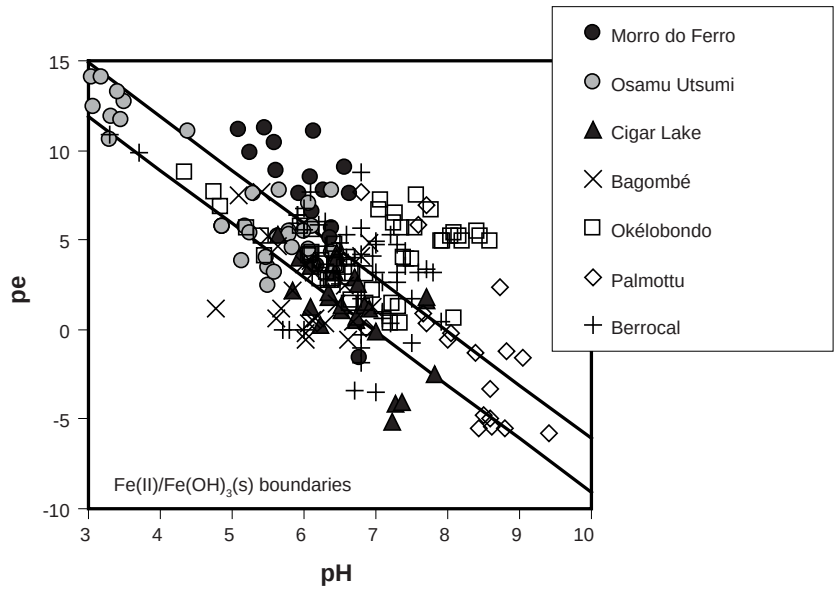

Figure 8-6. *Eh (in terms of pe) and pH data of 7 different sites showing the boundaries between Fe(II) and $Fe(OH)_3$(s). The two different lines stand for the different crystallinity of $Fe(OH)_3$(s) solid phases. For additional details the reader is referred to /Stumm and Morgan 1996/.*

Many of the studies conducted on natural analogues (see /Hofmann 1999/ and /Bruno et al. 2001/ for further details) have observed, directly or indirectly, the association of uranium with iron(III) oxy-hydroxides. This association has been in many cases proposed as one of the major reasons for the retention of uranium under oxidising and mildly reducing conditions, where Fe(III) hydroxides readily precipitate when oxidising or dissolve under reduction to form aqueous Fe(II). Fe(III) hydroxides surfaces present a high affinity to retain U(VI) and further evolve to the formation of more intimately linked type of uranium-iron interaction /Payne 1999, Bruno et al. 2001/. In sites such as Poços de Caldas, Oklo and el Berrocal, the concentrations of uranium in groundwaters were explained in some cases by assuming co-precipitation of uranium with Fe(III) oxyhydroxides. This interaction was strong under oxidising conditions due to the precipitation of Fe(III) solids and a release of uranium was observed when moving towards more reducing conditions due to the reductive dissolution of the Fe(III) solids. Nevertheless, this does not seem to be the case in most of the Forsmark groundwater samples studied here if, according to the previous calculations, we assume that it is the sulphide-sulphate system that controls the redox state.

8.2 Uranium calculations

The calculated Eh values (given by equilibrium of FeS with the analysed sulphate concentrations) and the measured pH values can be superimposed on a Pourbaix diagram of the uranium system (see Figure 8-7) from where a relatively good correspondence of the experimental data with the $UO_2 \cdot 2H_2O$(s)/U(VI)-carbonate species boundary is anticipated.

It is important to highlight that, under the conditions of the groundwater samples, the main uranium aqueous species is the hexavalent uranium tricarbonate and not the tetravalent uranium hydroxide $U(OH)_4$(aq). The solubility of amorphous UO_2 under reducing conditions and in the absence of important carbonate concentrations where the major species is $U(OH)_4$(aq), is on the order of $10^{-8.5}$ mol/L. Nevertheless, in all the groundwater samples studied here, this is not the case and, therefore, concentrations of uranium above this value can be explained. Another interesting point related to the predominance of highly charged U(VI) species is that the influence of ionic strength will be important, in contrast with the systems where the uncharged species dominate.

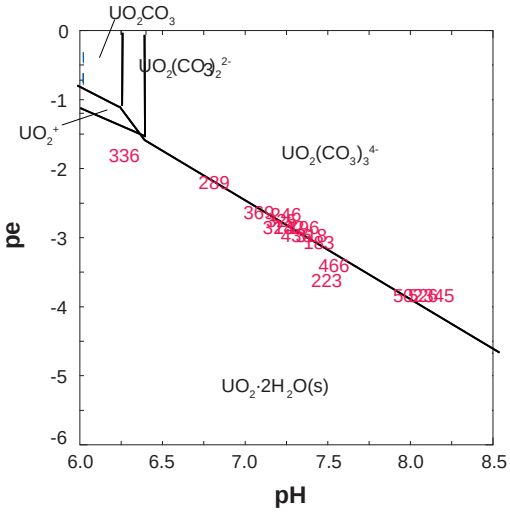

Figure 8-7. *Experimental pH data and Eh data calculated by assuming equilibrium FeS(ppt)/Fe(II) superimposed on a Pourbaix diagram for the uranium system. The diagram has been calculated using the database developed for the SKB solubility assessment within SR-Can /Duro et al. 2006/ and 2mM carbonates, 20 mM Ca, 10^{-7} M U and I = 0.2M.*

The calculated uranium concentration in equilibrium with $UO_2 \cdot 2H_2O(s)$ for each groundwater sample in comparison with the measured value is shown in Table 8-2. In the same table, the saturation index of the groundwater sample with respect to this solid is shown. In general we can see that the calculations agree with the data (within ± 0.6 log units) except for some samples (in bold in the Table 8-2), for which the calculations underestimate the actual measurements. This would mean that the measured concentrations in these 3 locations are above the ones expected from a solubility control exerted by $UO_2 \cdot 2H_2O(s)$ under the conditions assumed in the calculations.

The location of the samples in the same cross section shown in the previous figures will give some light to the interpretation of these results. In Figure 8-6 we have represented the concentrations of uranium measured for all the samples under study and we have highlighted those samples presenting a super-saturation above 0.7 with regard to the amorphous tetravalent uranium oxide considered in the calculations.

For most of the samples, the assumption of a concentration control exerted by $UO_2 \cdot 2H_2O$ is able to reproduce the results except for samples from KFM02A at 420 m depth, samples from KFM03A at ca 600 m depth and sample KFM08A at 687 m depth (marked in yellow in the previous figure). There are no apparent reasons for these discrepancies, given that the general geochemistry of these groundwater samples does not present significant differences with the rest of the samples. The fracture mineralogy is not available for all the areas but what seems interesting is that the high concentration of uranium in sample KFM03A seems to be related to the high content of uranium in the solid, as previously presented in Figure 8-1.

Table 8-2. Groundwater samples with the measured pH, the Eh calculated by assuming redox control exerted by FeS-S(VI), measured uranium concentrations (in mole/L), calculated uranium concentrations (in mole/L) in equilibrium with $UO_2 \cdot 2H_2O$, Saturation Index of $UO_2 \cdot 2H_2O$. For explanations see the text.

ID sample	IDCODE	pH for modelling	Eh for modelling	U meas	U calc	SI
183	KFM01A	7.65	–195.0	6.34E–09	1.59E–08	–0.4
196	KFM01A	7.41	–188.0	6.26E–08	1.51E–08	0.6
205	KFM01D	8.10	–263.0	8.15E–09	3.12E–09	0.4
212	KFM01D	8.40	–260.0	3.36E–09	3.27E–09	0.0
289	**KFM02A**	**6.83**	**–143.0**	**3.72E–07**	**4.15E–08**	**1.0**
223	KFM02A	7.52	–223.7	2.27E–08	3.26E–08	–0.2
242	KFM02A	7.37	–176.8	5.84E–08	3.43E–08	0.2
246	**KFM02A**	**7.19**	**–162.0**	**5.13E–07**	**7.90E–08**	**0.8**
313	KFM03A	7.29	–176.0	9.29E–09	2.76E–08	–0.5
325	**KFM03A**	**7.38**	**–196.0**	**1.94E–07**	**3.79E–09**	**1.7**
318	**KFM03A**	**7.49**	**–184.5**	**1.90E–07**	**5.96E–09**	**1.5**
336	KFM03A	6.27	–116.7	1.16E–09	1.67E–08	–1.2
345	KFM03A	8.26	–246.4	1.87E–09	3.03E–09	–0.2
369	KFM04A	7.16	–160.2	2.61E–07	8.01E–08	0.5
436	KFM06A	7.35	–155.0	4.02E–08	2.55E–08	0.2
466	KFM07A	7.60	–197.9	1.42E–09	3.47E–09	–0.4
502	**KFM08A**	**8.00**	**–209.0**	**2.67E–08**	**3.61E–09**	**0.9**
526	KFM09A	8.16	–233.1	2.25E–10	2.96E–09	–1.1

Different possibilities can be proposed for the explanation of the anomalous uranium concentrations in the samples. One of them is an enhanced mobilisation of uranium due to processes mediated by microbial activity. If this were the case we would expect some influence of the dissolved organic carbon, although according to the data available no discrepant DOC values are measured in these samples with regard to the others (see Figure 8-9).

Another possible explanation that has been proposed is that the contamination by drilling water could have caused an over-solubilisation of the uranium solid phases or that it could have perturbed the original uranium content in the groundwater sample (see /Buckau 2006/). Although no definite conclusions can be extracted from this hypothesis, what seems clear is that some correlation can be found between the percentage of drilling water contamination in the sample and the supersaturation of the groundwater with respect to uranium oxide (see Figure 8-10).

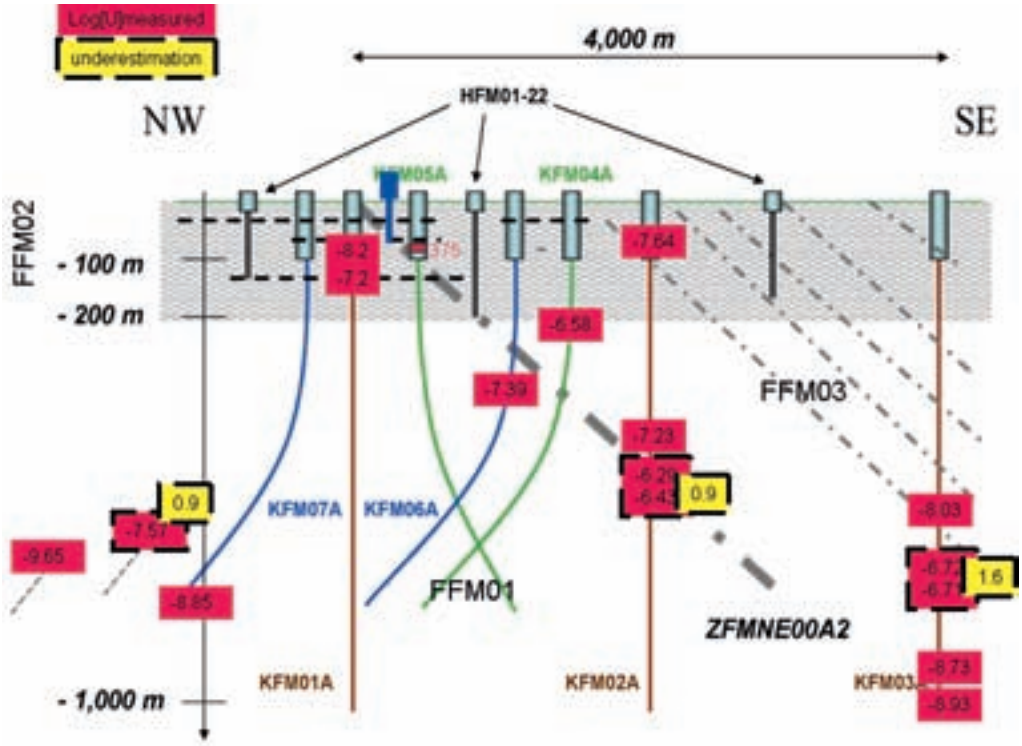

Figure 8-8. *Cross section of the area showing the experimental uranium concentrations analysed (in log units in red) and those samples for which the calculated concentration in equilibrium with $UO_2 \cdot 2H_2O$ underestimate the actual values (yellow labels showing the average extent of the underestimation).*

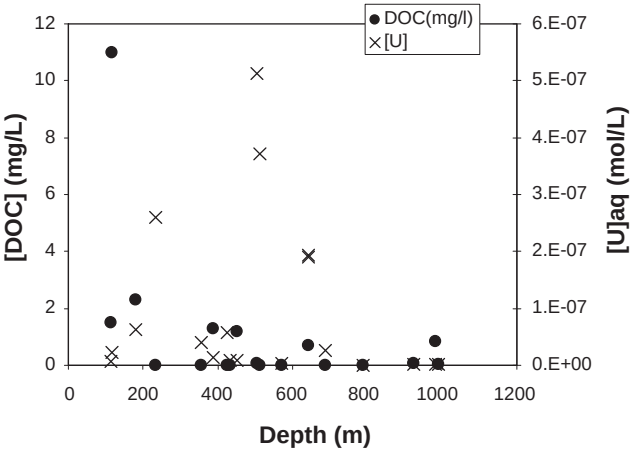

Figure 8-9. *Evolution of dissolved organic carbon and the concentration of uranium in groundwater with depth.*

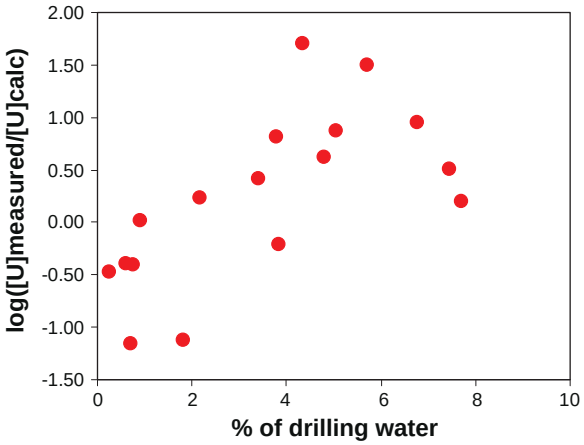

Figure 8-10. *Influence of the % of drilling water in the sample with the excess of uranium dissolved with respect to $UO_2 \cdot 2H_2O$ solubility.*

Although this is a possibility, what is not clear is the type of ligand that the drilling water may contain that can enhance the mobility of uranium. Drilling waters used in the area correspond to waters collected in the shallower 100 meters. Depending on the composition of the drilling waters they could contain some type of uranium complexing agents. One type of complexing agents can be those related to the presence of bacterial activity in the upper 100 meters of Forsmark, for example those used by bacteria to solubilise Fe(II) under oxidizing conditions: siderophores. Siderophores have been proven to strongly complex uranium and enhance its solubility up to several orders of magnitude under reducing conditions /Frazier et al. 2005/.

Although it would be possible to calculate the saturation index of many different U(IV) and mixed U(IV)/U(VI) solid oxides, the solid used in this work is the one most likely to form under the expected conditions at the site in case of existing a supersaturation of uranium. It is, moreover, the most soluble solid phase if compared with UO_2+x types of solids under the studied conditions. A very important piece of information that would help in the understanding of the three samples showing a certain degree of supersaturation with regard to this solid phase is the type of materials present in the fractures contacting the groundwater samples as well as the possible complexation agents other than the inorganic ones that could be expected to be present at the site.

9 Conclusions

Spatial analysis and 3D visualisation of available representative samples in Forsmark has been performed. It is seen that computed M3 mixing fractions shows a spatial distribution qualitatively correlated with key hydrochemical signatures, such as strontium (for Deep Saline), magnesium (for Littorina), 18-O and 2-H (for Glacial) and tritium (for Modified meteoric). It is worth noting that the most saline waters with the highest Deep signatures are located at deformation zones adjacent to the strongly foliated rocks, which constitute fracture domains FFM04 and FFM05, out of the target area. Maximum glacial signatures are located also out of the target area. In general terms, it is seen that hydrochemical spatial distribution is consistent with the current hydrogeological conceptual model, where the “shallow bedrock aquifer” would be responsible for the observed preservation of Littorina signatures down to a depth of 150–200 m.

SurfaceNet and ChemNet hydrochemical interpretations are consistent in that shallow groundwater near Eckarfjärden contains hydrochemical signatures that can be older/deeper than expected. Particularly, ChemNet observations points towards glacial signatures at that location. On the other hand, the old/deep signatures found by SurfaceNet in the near-surface waters at Northwest and East locations of Forsmark are interpreted as clear Littorina signature in the ChemNet analysis.

Scoping calculations in order to evaluate the magnitude of disturbance that can be allowed for a given groundwater sample at repository depth have been performed. The SKB hydrogeochemical suitability criteria have been used as the reference against which to compare the effect of such disturbances. It can be concluded that suitability criteria related with TDS and pH would be always fulfilled even for complete disturbance of the sample. Ca+Mg criteria could be surpassed in case of dilutions higher than 90 percent of the native groundwater sample. It is seen that cation exchange processes have an effect by lowering the Ca+Mg concentrations in the groundwater, compared with a pure conservative mixing. The oxygen consumption capacity of the granite bedrock has been also evaluated by using reactive transport modelling. It is seen that a hypothetical contamination event by atmospheric oxygen at repository depth would be consumed in a relatively short period of time (about 1 year) if the maximum amounts of reported pyrite are included in the model. However, the model results have been proved to be sensitive with respect to uncertain parameters such as the exact mineralogical composition and the specific reactive surface area of such minerals. An interesting conclusion is that, in the base case considered in the model, the oxygen intrusion in a borehole would only affect a very short distance in the bedrock (of about 1 cm).

Reactive mixing modelling results show that dissolved magnesium in Forsmark groundwater is likely to be affected by cation exchange processes. Therefore, even if it could be a qualitative indicator for Littorina Sea water signature, it should not be used as a quantitative tracer for such an end-member. Computed results show that conservative mixing models using magnesium would underestimate the actual Littorina signature due to the unaccounted effect of cation exchange processes. Then, the calibration of hydrogeological models against either measured magnesium concentrations or M3 computed Littorina mixing fractions, would probably lead to overestimation of the flushing rates in the hydrogeological models, because larger groundwater recharge flows could be required in order to compute smaller amounts of relict Littorina water in the bedrock.

There is a group of groundwater samples in Forsmark that do not have a marine origin according to Bromide/Chloride mass ratios. This group of samples can not be explained by mixing with deep brines similar to those detected in Laxemar or Olkiluoto. Some process and/or a new end-member, able to produce the observed enrichment in the bromide-chloride ratios, must exist. The bromide-chloride ratio of the non-marine waters is highly consistent with the ratios measured in the granite fluid inclusions at the Stripa site. According to all this, a possible Brackish Non-Marine end member is proposed for the Forsmark site. The most likely hypothesis seems to be that such end-member results from water rock interaction processes in the bedrock. It is thought that this issue deserves further investigation in the future. Although the Br/Cl results show good qualitative agreement with the mixing proportions computed by the M3 model, a quantitative exercise shows that the current M3 model could underestimate the amount of Littorina signature in Forsmark, probably due to propagating numerical errors.

Two distinctive evolutions can be identified regarding the chemical evolution of near-surface waters from Forsmark, one involving only surface waters interacting with solid materials from sediments and soils and the other involving the mixing with relict high salinity waters. The evolution of diluted waters is mainly related to the oxidation of organic matter. The redox conditions of the near-surface system appears to be controlled by the Fe(II)/Fe(III) pair, but shifts to the S(-II)/S(VI) pair. The scarcity of Eh data does not allow conclusions to be made on the specific processes controlling the redox of the near-surface system.

The evolution of higher salinity waters in the near-surface system is mainly related to the mixing with ancient Littorina Sea water trapped in the system and equilibrium with a cation exchanger associated with the clay fraction of the materials considered.

The concentrations of uranium in the Forsmark groundwaters are not, in general, anomalously high. The apparently high solubilities under reducing conditions are a consequence of the speciation of uranium in solution, which is mainly in the form of U(VI) tricarbonato species. Most measured data can be explained by the reprecipitation of the uranium released from a primary pitchblende-like source in the form of amorphous UO_2 solid phase, whose solubility is very

close to the one of $UO_2.2H_2O(s)$ in the thermodynamic database used by SKB. This constitutes a further test on the consistency of the dataset used by SKB. According to the representative groundwater samples from cored boreholes, only three locations seem to present a relatively higher uranium concentration than that corresponding to the solubility of a U(IV) solid oxide: KFM02A, KFM03A and KFM08A. No indications of different chemistry of the groundwaters seem to explain these apparent discrepancies, thus the reasons must be sought for in different processes accounting for the enhanced solubilisation of uranium in these areas.

The type of information on the fracture mineralogy provided by /Sandström and Tullborg 2006/ is consistent with the high uranium concentrations measured in KFM03A.

Some of the processes that could account for the enhanced solubilisation of uranium in the few samples presenting anomalous values are: (1) influence of in situ bacterial activity, (2) influence of dissolved organic carbon and, (3) influence of drilling fluid presenting uranium complexing agents such as those resulting from the solubilisation of Fe(III) hydroxides.

Finally, one of the main conclusions extracted is that the concentrations of uranium determined in the area are in general within the range of concentrations expected under the environmental conditions. However, the possibility of enhancing solubility processes (not completely understood yet) can not be discarded at least in 3 available groundwater samples.

10 References

Bruno J, Duro L, Grivé M, 2001. The applicability and limitations of the geochemical models and tools used in simulating radionuclide behaviour in natural waters: lessons learned from the Blind Predictive Modelling exercises performed in conjunction with Natural Analogue studies. SKB TR-01-20, Svensk Kärnbränslehantering AB.

Buckau G, 2006. Analysis of the origin of excessive U concentrations in Forsmark KFM groundwater samples. ChemNet Interim Report.

Casanova J, Négrel Ph, Kloppmann W, Aranyossy J F, 2001. Origin of deep saline groundwaters in the Vienne granitic rocks (France): constrains inferred from boron and strontium isotopes. Geofluids, 1, 91–102.

Davis S N, Fabryka-Martin J, Wolfsberg L E, 2004. Variations of bromide in potable groundwater in the United States. Ground Water 42 (6), 902–909

Drake H, Sandström B, Tullborg E-L, 2006. Mineralogy and geochemistry of rocks and fracture fillings from Forsmark and Oskarshamn: Compilation of data for SR-Can. SKB R-06-109, Svensk Kärnbränslehantering AB. Available at: www.skb.se

Drever J I, 1982. The geochemistry of natural waters. Prentice-Hall, Englewood Cliffs. NJ.

Duro L, Grivé M, Cera E, Domènec C, Bruno J, 2006. Update of a thermodynamic database for radionuclides to assist solubility limits calculation for performance assessment. SKB TR-06-17, Svensk Kärnbränslehantering AB.

Dzombak D A, Morel F M M, 1990. Surface complexation modelling. Whiley Interscience. New York.

Follin S, Johansson P O, Levén J, Hatley L, Holton D, McCarthy R, Roberts D, 2007. Updated strategy and test of new concepts for groundwater flow modelling in Forsmark in preparation of site descriptive modelling stage 2.2. SKB R-07-20, Svensk Kärnbränslehantering AB

Frazier S W, Kretzschmar R Kraemer S M, 2005. Bacterial Siderophores Promote Dissolution of UO_2 under Reducing Conditions. Environ. Sci. Technol., 39 (15), 5709–5715.

Freeman J T, 2007. The use of bromide and chloride mass ratios to differentiate salt-dissolution and formation brines in shallow groundwaters of teh Western Canadian Sedimentary Basin. Hydrogeology Journal, 15, 1377–1385.

Gimeno M J, Auqué L F, Gómez J B, 2006. Chemnet's Issue Report. Forsmark Area version 2.1. UZ/SKB/06/02.

Gimeno M J, Auqué L F, Gómez J B, Acero P, 2008. Water-rock modelling and uncertainties of mixing modelling. SDM-Site Forsmark. SKB R-08-86, Svensk Kärnbränslehantering AB.

Gómez J B, Augué L F, Gimeno M J, 2008. Sensitivity and uncertainty analysis of mixing and mass balance calculations with standard and PCA-based geochemical codes. Appl. Geochem. 23, 1941-1956.

Gustafsson A, Puigdomenech I, 2003. The effect of pH on chlorite dissolution rates at 25°C. Scientific Basis for Nuclear Waste Management XXVI. Materials Research Society Symposium Proceedings Volume 757, pp. 649–655.

Hartley L, Jackson P, Joyce S, Roberts D, Shevelan J, Swift B, Gylling B, 2007. Hydrogeological Pre-Modelling Exercises for Laxemar Site Descriptive Models 2.2. Draft Report. May, 2007.

Haveman S A, Pedersen K, Routsalainen P, 1998. Geomicrobial Investigations of Groundwaters from Olkiluoto, Hństholmen, Kivetty and Romuvaara, Finland. POSIVA Technical Report 89-09.

Hofmann B A, 1999. Geochemistry of natural redox fronts – a review. Nagra Technical Report 99-05, Nagra, Wettingen, Switzerland

King F, Ahonen L, Taxén C, Vuorinen U, Werme L, 2001. Copper corrosion under expected conditions in a deep geologic repository. SKB TR-01-23, Svensk Kärnbränslehantering AB.

Laaksoharju M, Skarman C, Skarman E, 1999. Multivariate mixing and mass balance (M3) calculations, a new tool for decoding hydrogeochemical information. Applied Geochemistry 14, 861-872.

Louvat D, Michelot J L, Aranyossy J F, 1999. Origin and residence time of salinity in the Äspö groundwater system. Applied Geochemistry, 14, 917–925.

Malmström M, Banwart S, 1997. Biotite Dissolution at 25°C: The pH Dependence of Dissolution Rate and Stoichiometry. Geochim. Cosmochim. Acta 1997:61(14):2779–2799.

Nordstrom D K, Lindblom S, Donahoe R J, Barton C C, 1989. Fluid inclusions in the Stripa granite and their possible influence on the groundwater chemistry. Geochimica et Cosmochimica Acta, 53 (8), 1741–1755.

Olofsson I, Simenov A, Stephens M, Follin S, Nilsson A-C, Rshoff K, Lindberg U, Lanaro F, Fredriksson A, Persson L, 2007. A fracture domain concept as a basis for the statistical modelling of fractures and minor deformation zones, and interdisciplinary coordination. Site descriptive modelling Forsmark, stage 2.2. SKB R-07-15, Svensk Kärnbränslehantering AB.

Parkhurst D L, Appelo C A J, 1999. User's Guide to Phreeqc (version 2). A computer program for speciation, batch-reaction, one-dimensional transport and inverse geochemical calculations. USGS Water Resources Investigations Report 99-4259.

Payne T E, 1999. Uranium (VI) interactions with mineral surfaces: controlling factors and surface complexation modelling. Ph.D. Thesis, University of New South Wales.

Rao U, Hollocher K, Sherman J, Eisele I, Frunzi M, Swatkoski S, Hammons A, 2005. The use of 36Cl and chloride/bromide ratios in discerning salinity sources and fluid mixing patterns: A case study at Saratoga Springs. Chemical geology, 222, 94–111.

Sandström B, Tullborg E-L, 2006. Fracture mineralogy. Results from KFM06B, KFM06C, KFM07A, KFM08A, KFM08B. Forsmark site investigation. SKB P-06-226, Svensk Kärnbränslehantering AB.

SKB, 2006. Hydrogeochemical evaluation. Preliminary site description Laxemar subarea – version 2.1. SKB R-06-70, Svensk Kärnbränslehantering AB. Available at: www.skb.se

Strober I, Bucher K, 1999. Origin of salinity of deep groundwater in crystalline rocks. Terra Nova, 11 (4), 181–185.

Stumm W, Morgan J J, 1996. Aquatic Chemistry. John Wiley and Sons.

Tröjbom M, Söderbäck B, 2006. Superficial Indications of Deep/Old Groundwater. Forsmark. Draft Report (Revision 2006-12-08).

Tröjbom M, Söderbäck B, Tullborg E-L, Johansson P O, 2007. Evaluation of the hydrochemistry in the Forsmark area with focus on the surface system. SKB R-07-55, Svensk Kärnbränslehantering AB. Final Version 071010.

USGS, 2007. PHREEQCI – A Graphical User Interface to the Geochemical Model PHREEQC. Version 2.13.2. Available at: http://water.usgs.gov/software

Williamson M A, Rimstidt J D, 1994. The kinetics and electrochemical rate-determining step of aqueous pyrite oxidation. Geochimica et Cosmochimica Acta 58, 5443–5454.

Wolery T J, 1992. EQ3/6, A Software Package for Geochemical Modelling of Aqueous Systems: Package Overview and Installation Guide (version 7.0). UCRL-MA-110662 PT-1. Lawrence Livermore National Laboratory, CA, USA.

Section 3

Application of the Drilling Impact Study (DIS) to Forsmark groundwaters

Mel Gascoyne, GGP Inc.
Ioana Gurban, 3D-Terra

Contents

1 Introduction

Characterisation of a geological formation as a repository for nuclear fuel waste requires deep drilling into the bedrock to gain an understanding of the geological structure, rock types, groundwater flow and the chemical composition of groundwater and the adjacent rock. The methods of characterisation from a hydrogeochemical point of view, might be affected by the various drilling activities and techniques for determining groundwater composition have been employed so that the composition can be corrected for these activities.

SKB has developed and supported the Drilling Impact Study (DIS) project in which a tracer is used as an indicator of contamination to attempt to correct the groundwater composition for dilution or contamination by surface waters. The project began about five years ago /Gurban and Laaksoharju 2002/ with the intention of developing a routine method for determining the extent of contamination of borehole groundwater by drilling water. The main objectives of this work were:

1. Determine the extent of drilling water contamination in permeable zones in a test borehole on the Forsmark site.
2. Correct measured chemical compositions of the groundwaters based on contamination results.
3. Provide a workable methodology for routine correction of groundwater composition.
4. Apply the modified DIS model to suitable borehole zones at the Forsmark site in a systematic fashion
5. Determine uncertainties in DIS modelling.

A memorandum was prepared by /Gascoyne and Gurban 2007/ describing the characteristics of borehole KFM06 and its drilling history. Estimates were made of the amount of drilling water in permeable zones in the borehole and the various approaches to applying results of DIS were described and recommendations made, with an example calculation.

2 Characteristics of drilling and pumping of groundwater

Drilling a borehole in crystalline rock requires a fluid to cool the drill bit and to flush drill cuttings out of the borehole. This fluid is normally water from a nearby lake, stream or shallow borehole and, because it is dilute, and contains species that may not be found in deeper groundwaters (e.g. organics, colloids, ^{3}H, O_2, microorganisms), it would be ideal if these species can be removed before this water is pumped into the borehole. Except for the use of UV light to kill bacteria, this is not practicable in most situations and so efforts are usually made to determine the concentrations of these species so that corrections can be made to the groundwater composition once it has been determined. However, because the exact concentrations of these species are usually not known with sufficient accuracy in the deep groundwaters, correcting for introduction of some species is an imprecise task, at best.

An alternative method to determine how much more pumping is needed and to correct for drilling water contamination is to add a tracer that is not naturally present in either the drilling water or the deep groundwater. Uranine (a soluble di-sodium fluorescein salt) is well-known for its suitability as a groundwater tracer because of its ease of detection at low concentrations and its apparent lack of sorption on rock minerals /Davis 1985/. Uranine is determined using a fluorometer and samples are compared with standard solutions made up in the laboratory. The method of correction requires adding uranine in known amounts to drilling water so that a constant concentration is pumped down the borehole. To induce return of this drilling water to the surface, the standing water in the open borehole can be pumped from near-surface in an oversized section of the borehole (typically within the cased interval of 0–100 m depth). This reduced head limits the amount of drilling water that enters fractures in the rock on its return to the surface.

Two situations typically apply in this situation:

1) the volume of water pumped out at the surface is less than that injected in the borehole, and

2) the volumes of water pumped out at the surface exceeds that injected in the borehole.

The first situation arises when there are fractures or fracture zones of high transmissivity along the length of the borehole (so that drilling water can readily enter the fractures rather than be pumped out). The second situation occurs when transmissivity is low at depth (but may be higher near the surface), in which case drilling water (and surface water) are drawn in by the shallow pump. The pump speed will determine whether more water is withdrawn than injected.

In either situation, some drilling water may be injected into permeable zones during drilling and its return to the surface. By knowledge of the injected and withdrawn volumes and tracer concentrations, it is possible to calculate the proportion of drilling water contamination. Other parameters may complicate this simple system, however, such as variation or imprecise knowledge of injected tracer concentration with time, variations of water pressure along the borehole, and non-conservative behaviour of the tracer (e.g. sorption onto mineral surfaces, interaction with organics, influence of pH, Ca, etc).

3 Drilling water and tracer concentrations used in Forsmark boreholes

A summary of the hydrogeological and pumping/flushing history of Forsmark boreholes and their permeable zones, made during the drilling period is given in Table 3-1 based on information from the site organisation. Indication is given in this table as to whether the permeable zone is suitable for DIS testing, based on the five criteria: a) reliable measurements of uranine in drilling return water, b) stability of uranine injection and satisfactory recording of data, c) adequate drilling water information (times, dates, rates, chemistry), d) adequate records of drilling water pumped in and out from the borehole during drilling, in time and along the boreholes length and e) presence and adequacy of chemical analyses of groundwater.

3.1 Borehole KFM06A

Borehole KFM06A was used as the test case for application of DIS. All data used here were selected from the SKB database SICADA (SKB data base). The record of drilling water injection during the drilling period of KFM06A has been described by /Berg et al. 2005/ and is shown as cumulative plots, against time and length, in Figure 3-1a and 3-1b. The fracture frequency map for KFM06A is shown in Figure 3-2 (the ellipses show the location of the sections 353.5–360.6 and 768–775.1 m borehole length investigated here and their proximity to major deformation zones).

It can be seen that core drilling (100–1,000 m) began in mid-June and terminated at the end of September, 2004 (Figure 3-1a); all activities ceased over the month of July. Over 1,000 m^3 of drilling water were used in core drilling. Figure 3-3 shows that there was a gradual increase in uranine concentration added to drilling water (from about 0.17 to 0.21 mg/L), with depth, probably due to drift in calibration of the metering pump. Uranine concentrations in the return water were consistently lower (~ 0.05 to 0.10 mg/L) than in injected levels, indicating loss of tracer to the fracture system and/or dilution by formation groundwater.

The data for KFM06A is recorded in detail in this report so that a full demonstration can be given of the procedure to evaluate the extent and effects of drilling water contamination in the zone. Other zones to which DIS can be applied include KFM01D, KFM08A and KFM10A (see Table 3-1).

Table 3-1. Details of pumping and flushing information of KFM (Forsmark) boreholes and their suitability for application of DIS (comments from drilling staff were kindly provided by Ann-Chatrin Nilsson).

Idcode	Section (m borehole length)	a	b	c	d	e	Comments
KFM01A	**110.1–120.8** **176.8–183.9**	Y	N	Y	Y	Y	DW source = HFM01. Manual, but stable addition of uranine. Relatively few samples from flushing water and returned water for uranine analyses. **BH could be used for DIS.** However, this was the first borehole and methods have been improved since the early boreholes.
KFM01D	**194.0–195.0*** 263.8–264.8 314.5–319.5 **354.9–355.9*** **369.0–370.0*** **428.5–435.6** **568.0–575.1**	Y	Y/N	Y	Y	Y	DW source = HFM01. A number of the flushing water samples below 560 m borehole length were not collected close to the drilling machine. These samples showed much too low concentrations due to insufficient mixing. Uncertainty about the uranine conc below 560 m may be the reason why the uranine budget does not agree. However, problems with uranine conc. start below the investigated sections. **Therefore, DIS study is recommended.** It could be interesting to include DIS also for one or two low transmissive fractures. The most suitable sections from transmissivity/time to fill reasons are marked.
KFM02A	106.5–126.5 413.5–433.5 509.0–516.1	Y	N	Y	Y	Y	DW source = HFM05. Initial problems with the dosing of uranine. However, the uranine budget agrees very well. **DIS study could be performed, however, the conditions are not ideal.**
KFM03A	386.0–391.0 448.0–453.0 448.5–455.6 639.0–646.1 939.5–946.6 980.0–1,001.2	Y	N	Y	N	Y	DW source = HFM06. Unstable addition of uranine especially from the start. **BH not recommended for DIS.**
KFM04A	230.5–237.6 354.0–361.1	N	N	Y	N	N/Y	DW source = HFM10. Malfunction of the flow meter caused irregular and erroneous dosing of uranine. A faulty flowmeter recorded erroneous drilling water volumes. Some chemistry uncertain in groundwater from the sections due to severe corrosion on the equipment. **BH not recommended for DIS.**
KFM06A	266.0–271.0 **353.5–360.6** **768.0–775.1**	N	N/Y	Y	Y	Y	DW source = HFM05. DW was sampled for chemistry during drilling of KFM06A. Corrected uranine analyses due to systematic error, furthermore there is an increasing trend in the values. **BH recommended for DIS but with a question mark.**
KFM07A	**848.0–1,001.6**	N/Y	Y	Y	Y	Y	DW source = HFM21. DW was sampled for chemistry during drilling of KFM07A. Few DW and return water samples for uranine. **BH recommended for DIS but with a question mark**.
KFM08A	**683.5–690.6**	Y	Y	Y	Y	Y	DW source = HFM22. DW was sampled for chemistry during drilling of KFM08A. **BH recommended for DIS.**
KFM09A	785.1–792.2	Y	N	Y	Y	Y	BH not chemistry prioritised. DW source= drinking water. Sampling of drilling water for uranine was not always performed close to the drilling machine, therefore spread in the results. **BH not recommended for DIS.**
KFM10A	**298.0–305.1** 436.9–437.9 **478.0–487.5**	Y	Y	Y/N	Y	Y	DW source = HFM24. DW was not sampled during drilling of KFM10A but there are earlier analyses. **BH recommended for DIS.**

* Low transmissive section

Sections in bold font are recommended; (BH = borehole; DW = drilling water)

The columns a, b, c, d and e lists Yes or No for the following criteria:

a) Reliable measurements of uranine in drilling return water.

b) Stability of uranine injection and satisfactory recording of data.

c) Adequate drilling water information (times, dates, rates, chemistry).

d) Adequate records of drilling water pumped in and out from the borehole during drilling, in time and along the boreholes length.

e) Presence and adequacy of chemical analyses of groundwater.

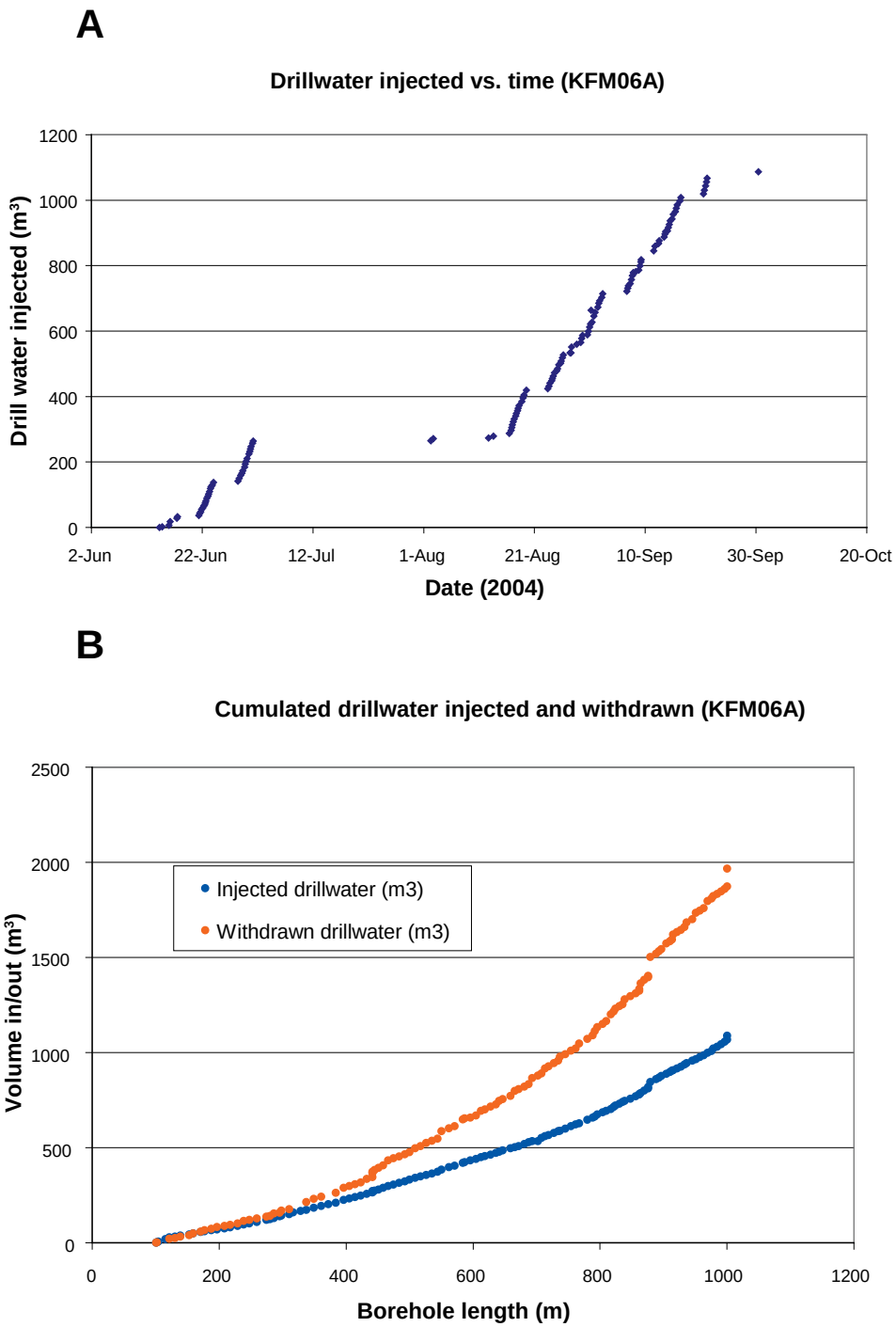

Figure 3-1. *Cumulative plots of a) volume of drilling water injected against time and b) of injected and withdrawn drilling water against length, for borehole KFM06A.*

3.1.1 Calculation of drilling water content

Objectives

The main aim of DIS is to evaluate the extent of contamination of individual fracture-zone groundwaters in borehole KFM06A, due to drilling activities, and then to determine how much groundwater must be pumped from each zone to reduce the uranine content to an acceptable level. The results of this modelling are then compared with the hydrochemical data obtained from each zone.

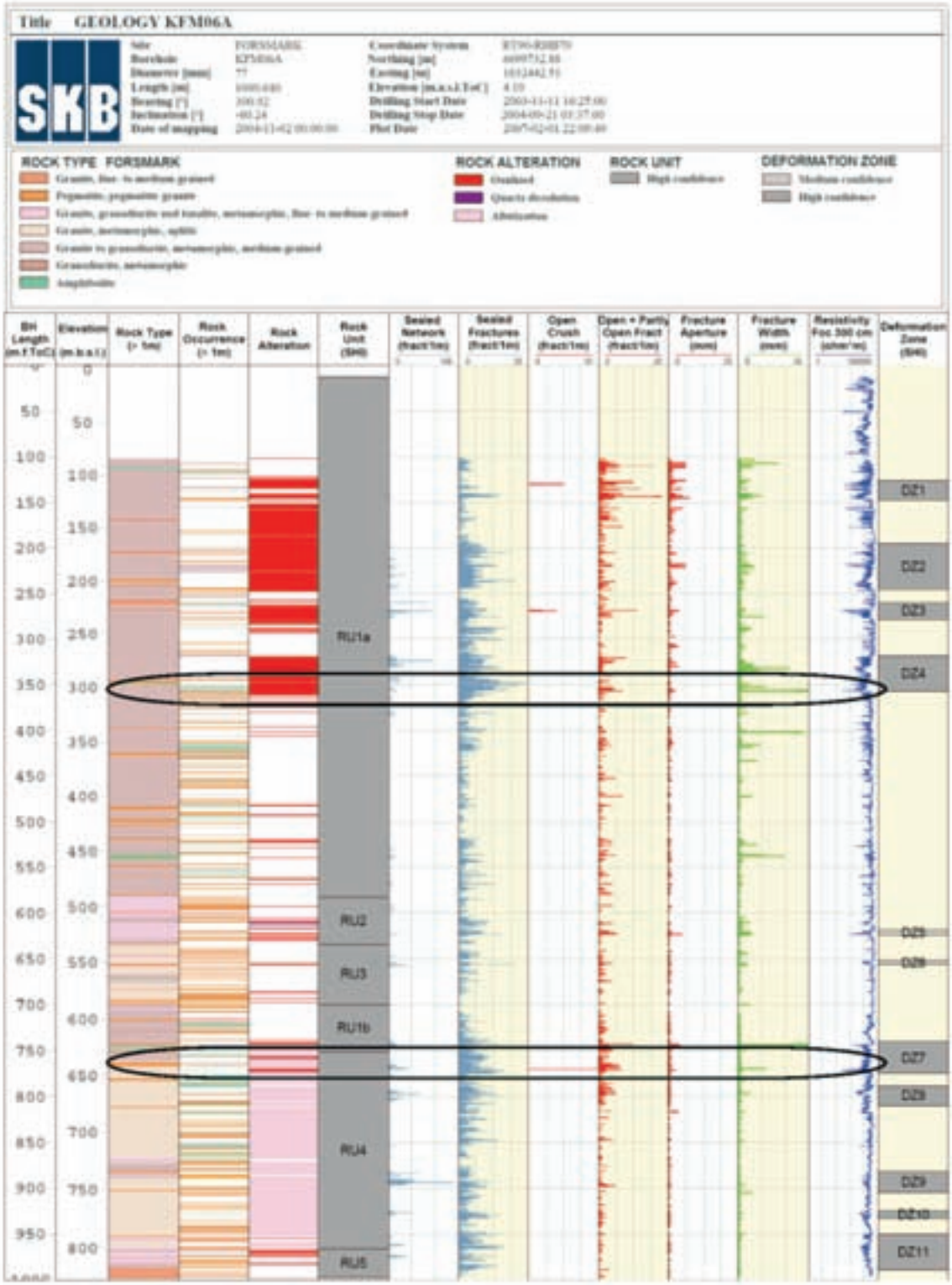

Figure 3-2. *Integrated diagram showing fracture frequency and geophysical parameter profiles with depth (elevation) and length for borehole KFM06. The ellipses show the location of the sections 353.5–360.6 and 768–775.1 m borehole length investigated here and their proximity to major deformation zones.*

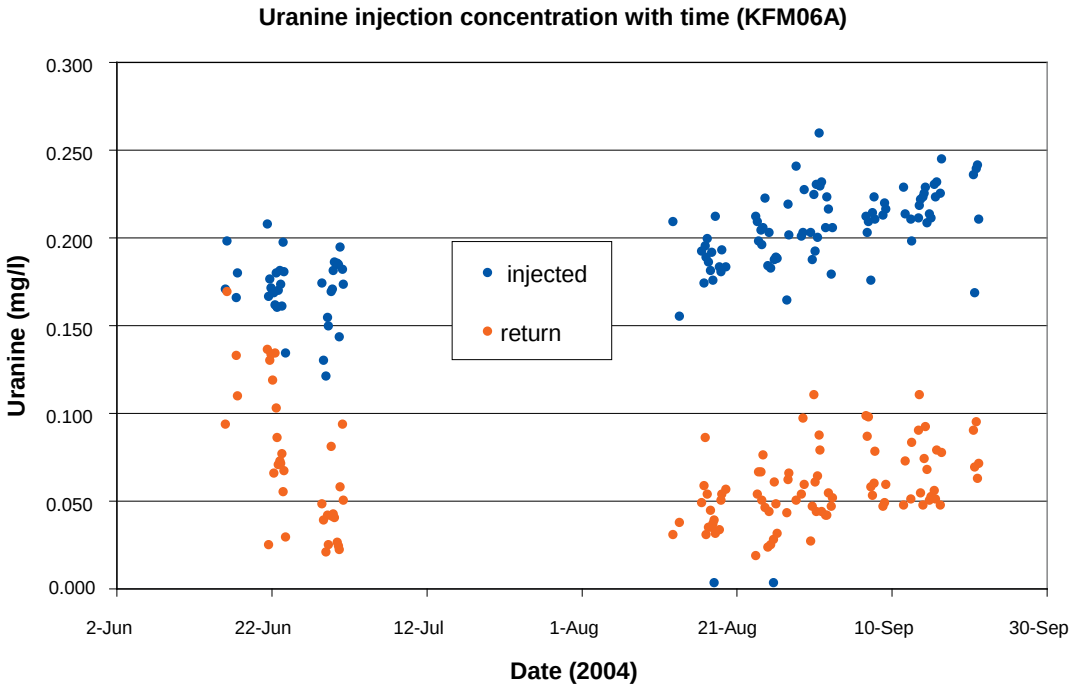

Figure 3-3. *Diagram showing difference in uranine content of injected drilling water and return water, with time for the drilling of borehole KFM06A.*

Basic calculations

The average content of uranine in borehole groundwater at the end of the drilling can be calculated in two ways, as follows after /Berg et al. 2005, Gurban and Laaksoharju 2002/.

1. Gravimetric:

Weight of uranine added to injected drilling water = 200.5 g (from gravimetric measurement).

Weight of uranine returned to surface in withdrawn drilling water = 122 g (from weighted means).

Average content of drilling water in borehole groundwater of KFM06A = (200.5–122) / 200.5 = 39%.

2. Volumetric:

Volume of drilling water injected = 1,087 m^3 (from meter).

Volume of drilling water withdrawn = 1,968 m^3 (from meter; this represents drilling water mixed with formation water and of this volume, as shown above, 60% represents drilling water. The recalculated volume of drilling water withdrawn is 60% of 1,968 m^3, equal to 1,180.8 m^3 (Figure 3-4).

The drilling water pumped out is higher than the volume injected and this makes the calculations more difficult. More return water is due to the use of air-lift pumping from shallow zones. This creates a complex situation with mixing of formation water and ingoing flushing water (it is the general tendency to have more return water in poor rock conditions and a better balance between injected and withdrawn water in tight rock (H. Ask, personal communication). However, if the uranine is correctly monitored, the return water can be calculated based on the percentage of uranine, and a water balance and DIS calculations can be performed.

The gravimetric method is more accurate because uranine weights are more precisely determined than are the water volumes. The first method indicates that borehole water pumped immediately after completion of drilling contains about 40% of drilling water. Therefore, based on a nominal injection concentration of uranine of 0.2 mg/L, approximately 400 m^3 of drilling water has been lost to the borehole and adjacent bedrock. This estimation is uncertain because of the systematic error and the correction to uranine concentrations. Because the uranine concentration of the return

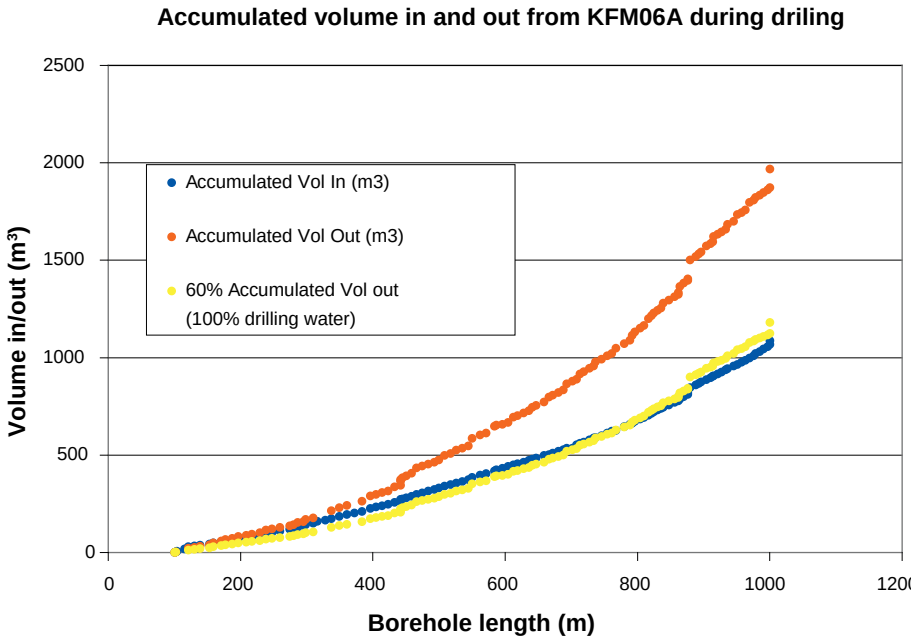

Figure 3-4. *Drilling water pumped in (blue) and out (yellow) from the borehole during drilling. The water pumped out (orange) represents drilling water and formation water as well, based on the measured uranine concentration.*

water is only about half that of the injected concentration, dilution is clearly occurring and, therefore, the volume of uranine-contaminated water will be larger than 400 m^3.

Detailed calculation of drilling water content in fracture groundwater

At the end of the drilling and before pumping began (for flushing and sampling), the sections 353.5–360.6 and 768–775.1 m borehole length contained a maximum of 8% and 24% of drilling water, respectively, (Figure 3-5).

During slow-pumping for sampling purposes, 8.8 and 8.5 m^3, respectively, were removed from the borehole zones. From the drilling records, the accumulated drilling volumes in and out were calculated, as shown in the Figure 3-4, for both sections. The return drilling water was recalculated as explained above (yellow curve in Figure 3-4). Based on these calculations, the maximum amount of drilling water lost in the fractures during drilling was 2.6 m^3 for the upper section and 4.01 m^3 for the lower section. Because a maximum of 8% and 24% of drilling water were found in these sections, this indicates that 32.5 m^3 and 16.7 m^3 should have been pumped from the sections, respectively.

The samples obtained at the end of the pumping/sampling phases show that 7.1% drilling water remained in the first section and 2% drilling water in the second section (Figure 3-5). In order to remove the drilling water, additional amounts of water (23.7 m^3 from the first section and 8.2 m^3 from the second section) would have to be removed. The first section is slightly more permeable than the second; therefore the dilution was higher, as the measurements show.

Alternatively, the amounts of water still to be pumped from the two sections to remove drilling water can be calculated using the measured uranine contents. In the injected drilling water, uranine ranged between 0.17 and 0.26 mg/L and in the return water 0.04 and 0.09 mg/L, indicating about 40% of the return water was drilling water, as noted above. Thus, the maximum amount of drilling water lost to the fracture system was 4.8 and 8.9 m^3, respectively. Therefore, using the 8% and 24% drilling water contents, about 60 and 37 m^3 need to be removed from the system to remove remaining tracer. In fact, only 8.8 and 8.5 m^3 were removed from each section, giving 51 and 28.5 m^3 that remain to be removed.

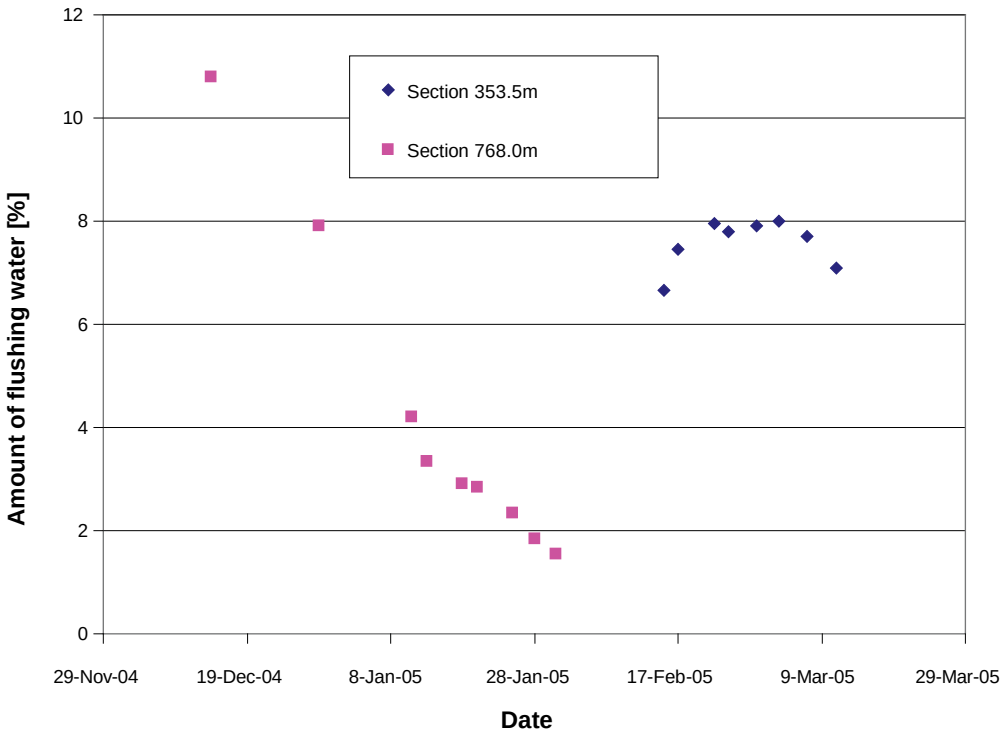

Figure 3-5. *Variation of uranine in flushing and pumped water during hydrogeochemical sampling.*

These data may be influenced, however, by the possible presence of uranine-tagged test water that was used in several Forsmark boreholes (KFM06A was one of these) as part of the Borehole Probe Dilution Test programme. In this programme, uranine (1 mg/L) was injected into packed-off borehole sections and allowed to disperse under natural gradients. Its concentration was followed by monitoring the dispersion into the fractures. This uranine was not pumped out at the end of the programme and so may account for some of the drilling water tracer that was subsequently measured in KFM06A, especially in the shallower section (341–362 m). The relatively stable uranine data for this zone (Figure 3-5) may be due to gradual return of this water to the section during pumping for sampling.

Hydrochemical sampling and analytical results for KFM06A

Drilling of KFM06A was performed using water from the adjacent shallow percussion borehole HFM05 as drilling fluid. This water is brackish in composition and slightly more saline than Baltic seawater (Table 3-2) and is enriched in Ca, Mg and Cl.

Groundwater from borehole KFM06A is defined as a SKB chemical type and so several precautions were taken to minimise contamination by the drilling water /Berg et al. 2005/:

1. The drilling water supply well should also be of a SKB chemical type.
2. Borehole HFM05 was selected to supply drilling and flushing water for KFM06A because of its acceptable concentration of total organic carbon (4.8–6.1 mg/L, target < 5.0 mg/L).
3. Dosing equipment for uranine was used instead of a storage tank (the latter may suffer from biological activity).

Table 3-2. Selected borehole sections from KFM06A for hydrogeochemical characterisation.

Section (m borehole length)	T_D (m^2/s)	T_T (m^2/s)	Pump rate (mL/min)	Pumped vol. (m^3)	Drill fluid at start	Drill fluid at end
266.0–271.0				64		
353.5–360.6	9.1×10^{-7}	3.4×10^{-6}	160–210	8.8	7%	7%
740–747			200	1.9		46%
768.0–775.1			90	8.5	24%	1.6%

There are up to four sections in borehole KFM06A that are permeable and have been pumped and sampled for uranine and chemical composition, as described in Tables 3-2 and 3-3 (data from /Berg et al. 2005/). All hydrogeochemical data were selected from SICADA.

The variations of major and minor ion concentrations in sections 353.5–360.6 and 768.0–775.1 m borehole length are plotted against pumping time in Figures 3-6, 3-7 and 3-8. Only these sections were selected for detailed sampling because zone 266–271 m was used only for simple chemical sampling and zone 740–747 m contained excess uranine (> 5 mg/L).

The data shown in Figure 3-6, for the major ions (Na^+, Ca^{2+}, Cl^-), indicate that there are no detectable changes or trends for any of these ions at either depth interval. This might be expected for the upper section because the uranine stays essentially constant over this period (~ 7%) but the steady change in uranine concentration, from 11% to < 2%, for the lower zone, suggests that some changes and trends might be seen in the major ions. In contrast, however, the minor cations, K^+ and Mg^{2+}, and the other anions, SO_4^{2-} and HCO_3^-, all show distinct decreasing trends as drilling water content is reduced (Figures 3-7 and 3-8). These reductions, however, in all cases exceed the reduction in uranine concentration and range from about 40% to over 500%. It may be significant that several ions (K, Mg, HCO_3, SO_4), at most depths show similar changes (a decline of about 40%).

These characteristics suggests that mixing with other water bodies (e.g. Littorina seawater) might be occurring and rock-water interaction and/or ion exchange may account for some of these changes. The profile of Fe species at both depths (Figure 3-9), however, closely matches the uranine record (i.e. a strong decline in both parameters) suggesting that Fe follows uranine in this borehole. The use of a saline drilling water in this borehole (HFM05, see Table 3-3), would tend to reduce the effect of contamination by drilling water and could account for the apparent stability of the major ion concentrations. In the case of KFM06A both zone waters have a similar Na content as drilling water and Baltic seawater but Ca and Cl are much larger in KFM06A, again suggesting considerably mixing and, possibly, rock-water interaction. The decrease of K, Mg, SO_4^{2-} and HCO_3^- is unlikely to result from mixing because both seawater and HFM05 are significantly more enriched in these ions.

Table 3-3. Groundwater compositions for zones 353-360 m (upper) and 768-775 m (lower) in borehole KFM06A. Drill water (HFM05, sample 4435) and Baltic seawater compositions are shown for reference.

Sampling date	Drill water %	Charge bal %	Na mg/L	K mg/L	Ca mg/L	Mg mg/L	HCO3 mg/L	Cl mg/L	SO4 mg/L	Br mg/l	F mg/L	Si mg/L	Fe[1] mg/L	Fe-tot[2] mg/L	Fell mg/L	Sr mg/L	I mg/L	pH	DOC mg/L
15-Feb-05	6.7	-0.51	1560	19.3	1200	113	67.5	4710	228	46.2	1.22	5.87	0.896	1.17	1.12	12.9	-	7.22	2.4
17-Feb-05	7.5	0.75	1530	16.4	1260	91.4	58.2	4620	188	28	1.24	5.72	1.21	1.59	1.54	13.8	0.101	7.34	1.3
22-Feb-05	8.0	0.84	1490	13.7	1290	77.1	49.8	4580	158	52.9	1.26	5.47	1.10	1.41	1.39	14.5	-	7.34	1.0
24-Feb-05	7.8	-0.13	1440	13.3	1290	73.2	47.8	4600	155	29.5	1.22	5.41	0.92	1.19	1.17	14.7	0.104	7.38	1.1
28-Feb-05	7.9	0.07	1460	12.8	1290	67	45.6	4570	148	53.3	1.25	5.38	0.733	0.967	0.932	14.8	-	7.37	1.0
3-Mar-05	8.0	0.70	1450	13.1	1310	72.3	46.8	4570	155	29.9	1.23	5.43	0.889	1.15	1.12	14.0	0.103	7.37	1.1
7-Mar-05	7.7	0.58	1450	13	1300	71.2	45.7	4560	151	29.5	1.25	5.47	0.90	1.12	1.11	14.9	0.105	7.33	<1
11-Mar-05	7.1	-2.62	1470	13.4	1280	74.1	47.7	4850	157	49.2	1.26	5.5	1.15	-	-	14.9	-	7.41	-
14-Dec-04	10.8	-1.83	1620	10.00	2260	21.7	28.63	6730	72.5	79.6	<0.2	4.19	1.66	2.11	2.12	23.6	-	7.53	1.6
29-Dec-04	7.9	0.85	1790	8.79	2370	16.2	11.20	6830	66.7	59.0	0.8	4.23	1.26	1.51	1.46	25.8	0.224	7.54	1.7
11-Jan-05	4.2	0.78	1810	6.29	2480	8.1	6.91	7040	45.5	89.8	<0.2	4.01	0.298	0.345	0.325	26.8	-	7.74	1.5
13-Jan-05	3.4	0.08	1800	7.55	2430	7.2	6.76	7050	44.5	59.0	<0.2	4.08	0.406	0.425	0.416	27.1	0.239	7.76	1.6
18-Jan-05	2.9	0.72	1780	6.21	2480	5.6	6.50	7000	42.2	90.6	<0.2	3.95	0.241	0.268	0.253	26.7	-	8.04	1.4
20-Jan-05	2.9	-0.02	1800	6.97	2480	5.4	5.97	7150	42.7	58.0	1.0	4.02	0.197	0.211	0.188	27.2	0.240	8.15	1.6
25-Jan-05	2.4	1.00	1790	6.20	2460	4.4	5.78	6940	37.4	93.8	<0.2	3.95	0.110	0.127	0.111	27.0	-	8.11	1.5
28-Jan-05	1.9	1.25	1690	6.46	2500	4.1	5.96	6840	35.1	52.4	<0.2	3.94	0.158	0.077	0.052	26.7	0.237	8.21	1.3
31-Jan-05	1.6	-0.46	1690	6.75	2500	3.9	5.72	7080	35.5	54.0	<0.2	3.90	0.0376	0.077	0.051	26.7	0.232	8.26	1.6
Drill water (HFM05)		-0.9	1740	41	749	199	122	4340	299									TOC:	2.6
Baltic sea water			1960	95	94	234	90	3760	325										

[1] Determined by ICP-AES

[2] Analysed spectrophotometrically

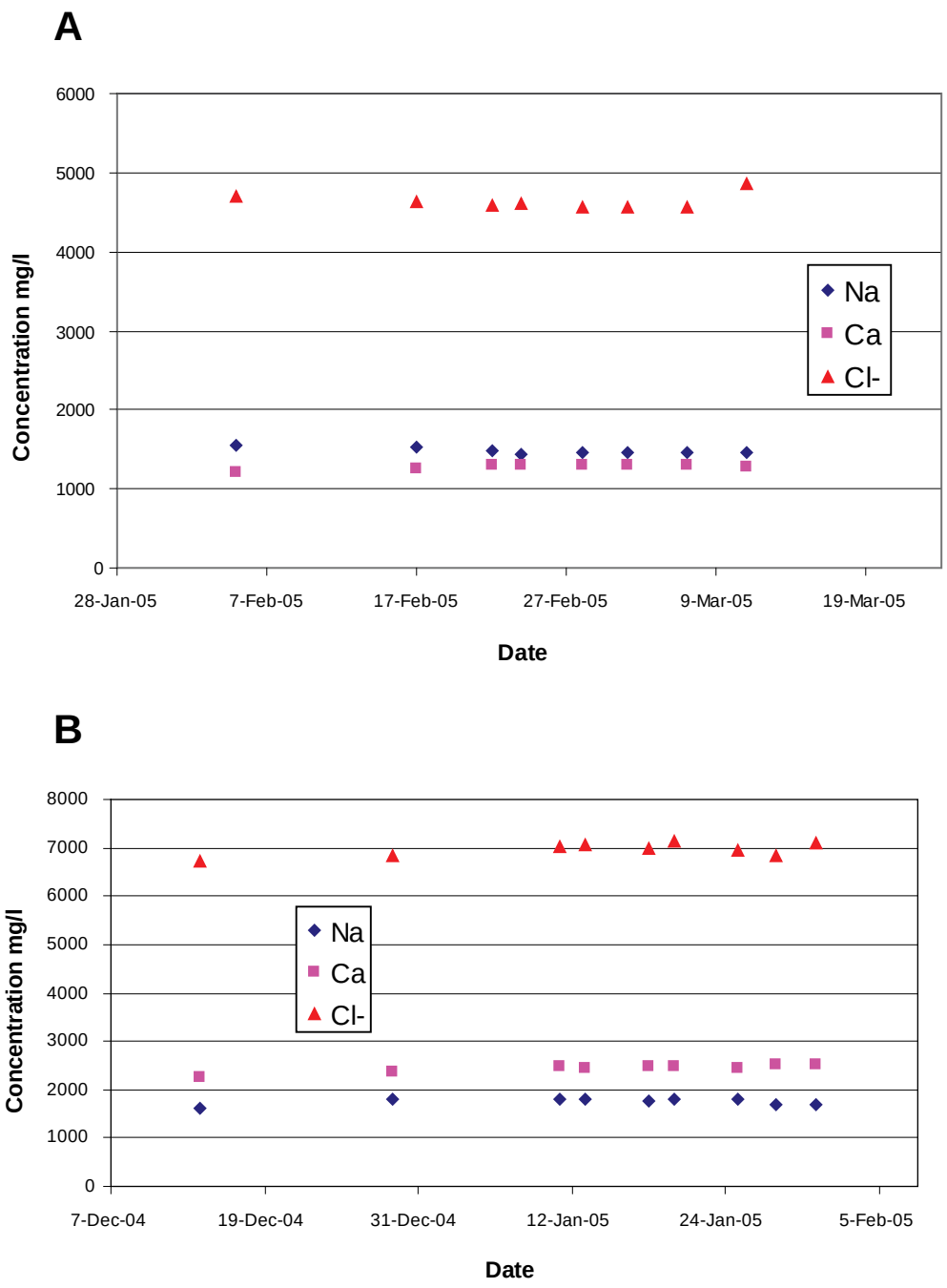

Figure 3-6. *Variation of major ions (Na^+, Ca^{2+}, Cl^-) in sections (a) 353.5–360.6 m and (b) 768.0–775.1 m in groundwater from borehole KFM06A.*

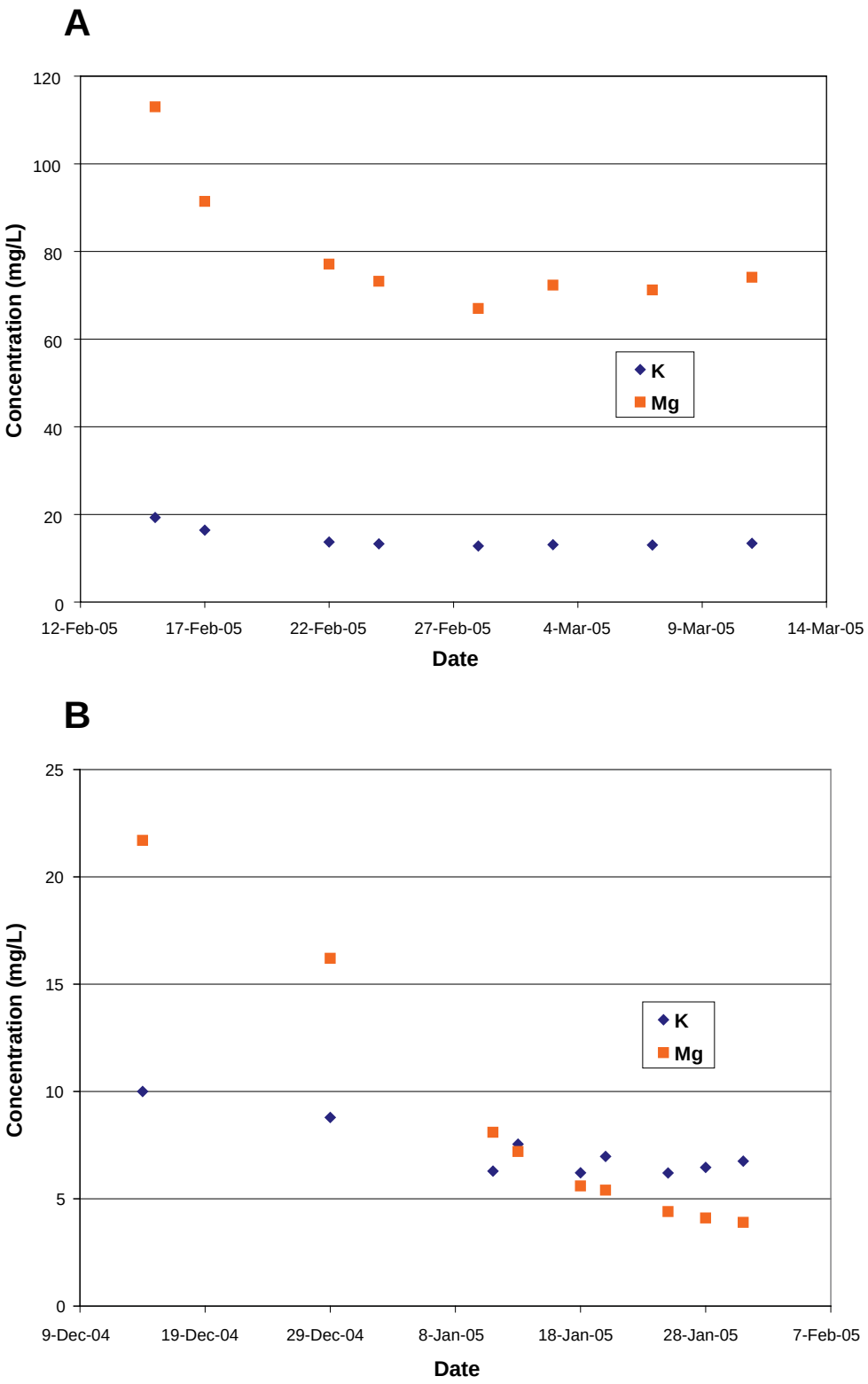

Figure 3-7. *Variation of cations (K^+, Mg^{2+}) in sections (a) 353.5–360.6 m and (b) 768.0–775.1 m in groundwater from borehole KFM06A.*

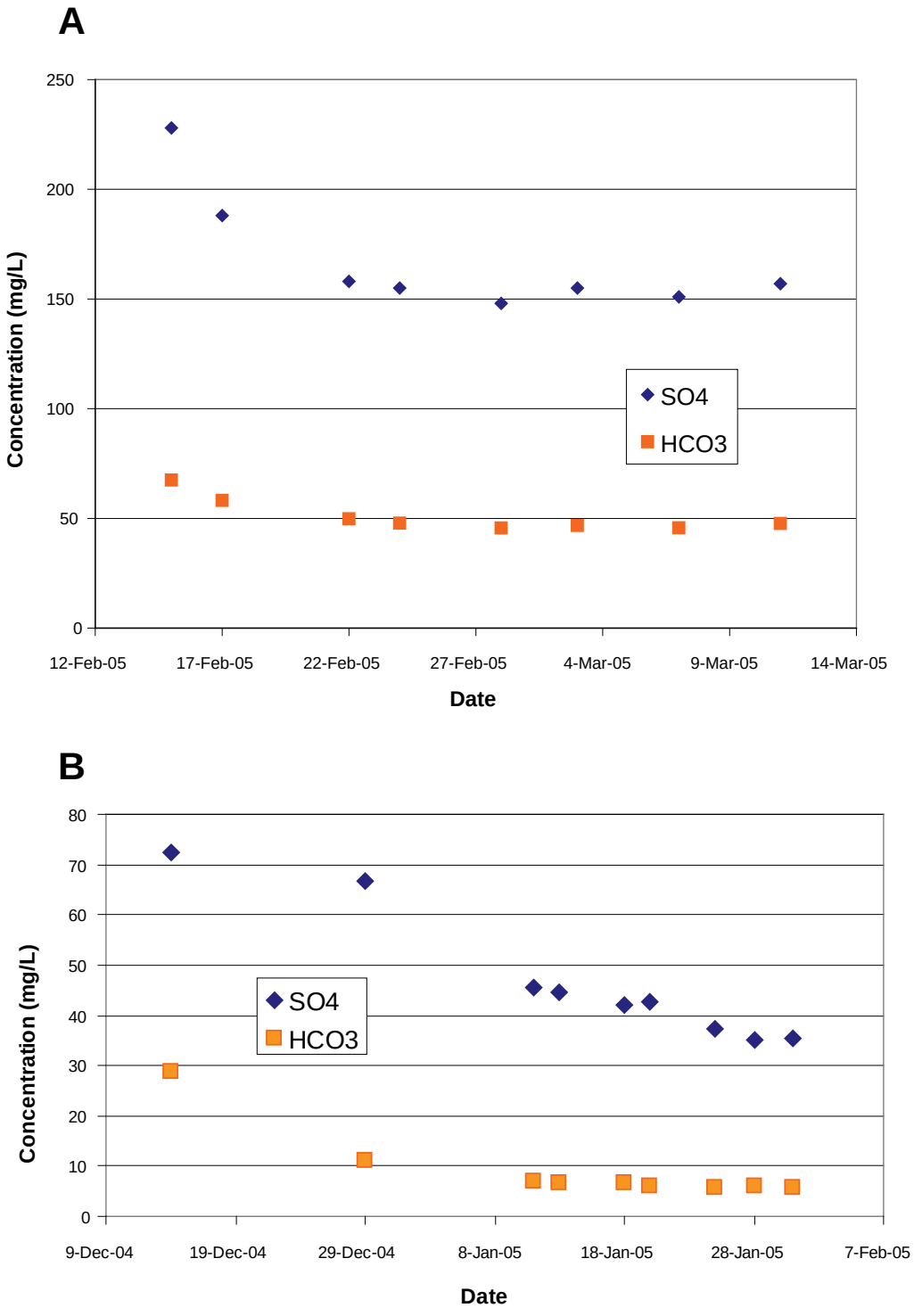

Figure 3-8. *Variation of anions (SO_4^{2-}, HCO_3^-) in sections (a) 353.5–360.6 m and (b) 768.0–775.1 m in groundwater from borehole KFM06A.*

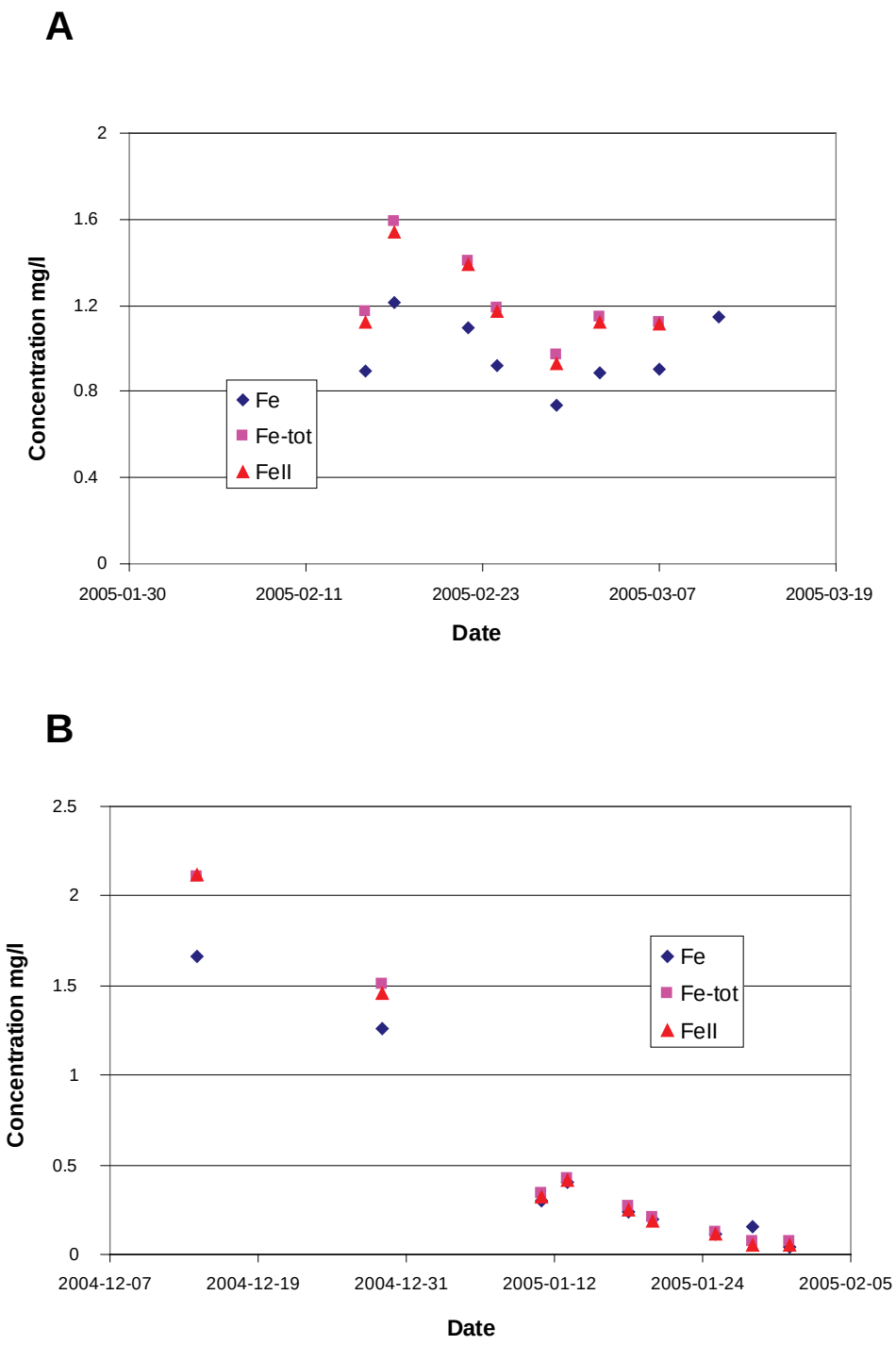

Figure 3-9. *Variation of Fe species in sections (a) 353.5–360.6 m and (b) 768.0–775.1 m in groundwater from borehole KFM06A.*

3.2 Borehole KFM01D

Core drilling of borehole KFM01D (100–800 m) began in mid-June and ended in early August, 2006, (Figure 3-10a). The record of drilling water injection during the drilling period of KFM01D has been described by /Nilsson et al. 2006/ and is shown as cumulative plots, against time and depth, in Figure 3-10a and 3-10b. About 770 m^3 of drilling water were injected in core drilling and 1,080 m^3 were pumped out (Figure 3-10b). This relatively small difference in volumes indicates that fractures in the borehole are of low transmissivity.

The fracture frequency map for KFM01D is shown in Figure 3-11 (the ellipses show the location of the sections 428.50–435.64 and 568.00–575.14 m borehole length investigated here and their proximity to major deformation zones). Figure 3-12 shows that the uranine concentration added to drilling water varied from about 0.20 to 0.25 mg/L, mean = 0.214 mg/L, through most of the borehole depth, except for some low values below 550 m caused by insufficient mixing. Uranine concentrations in the return water were generally similar to or lower than injected levels and ranged from 0.22 to 0.10 mg/L, indicating some loss of tracer to the fracture system and/or dilution by formation groundwater.

The data for KFM01D is recorded in detail in this report so that a demonstration of the procedure to evaluate the extent and effects of drilling water contamination in the zone can be made and compared to data from other boreholes.

3.2.1 Calculation of drilling water content

The extent of contamination, due to drilling, of individual fracture-zone groundwaters in borehole KFM01D is determined by DIS. How much groundwater that must be pumped from each zone to reduce the uranine content to an acceptable level is then determined.

The average content of uranine in borehole groundwater at the end of the drilling is calculated in two ways, as follows (after /Nilsson et al. 2006/):

Weight of uranine added to injected drilling water = 177 g (from gravimetric measurement).

Weight of uranine in drilling water = 165 g (from concentration measurements and volume of injected water).

Weight of uranine returned = 185 g (from average uranine concentration and volume of returned water).

Percentage loss or gain of uranine is determined as

1. (177–185)/177 = –4.5% or
2. (165–185)/165 = –12.1%.

The gravimetric method is more accurate because uranine weights are more precisely determined than are the water volumes. The volume of drilling water pumped out is only slightly greater than the volume injected and, because uranine concentrations are similar or slightly less than in injected water, this leads to the anomalous situation whereby apparently more uranine was recovered than injected. This is most likely due to selecting the appropriate average uranine concentrations and its variance for the injected and return waters (Ann-Chatrin Nilsson, pers. comm. 2007). Analytical error in the measurement of uranine concentration and possible changes in pH or ionic strength may also affect the fluorescence somewhat.

A

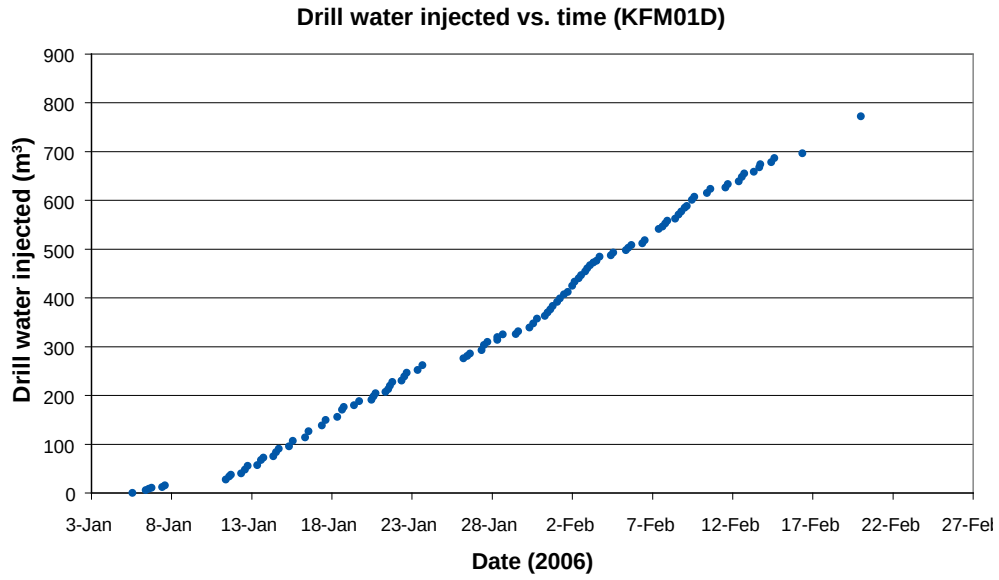

B

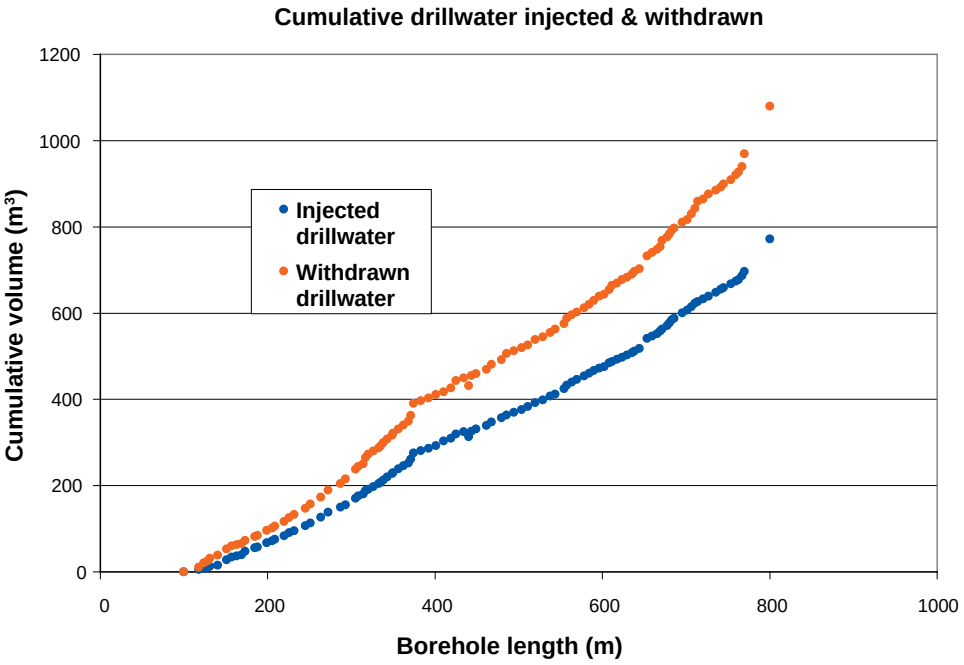

Figure 3-10. *Cumulative plots of a) volume of drilling water injected against time and b) of injected and withdrawn drilling water against length, for borehole KFM01D.*

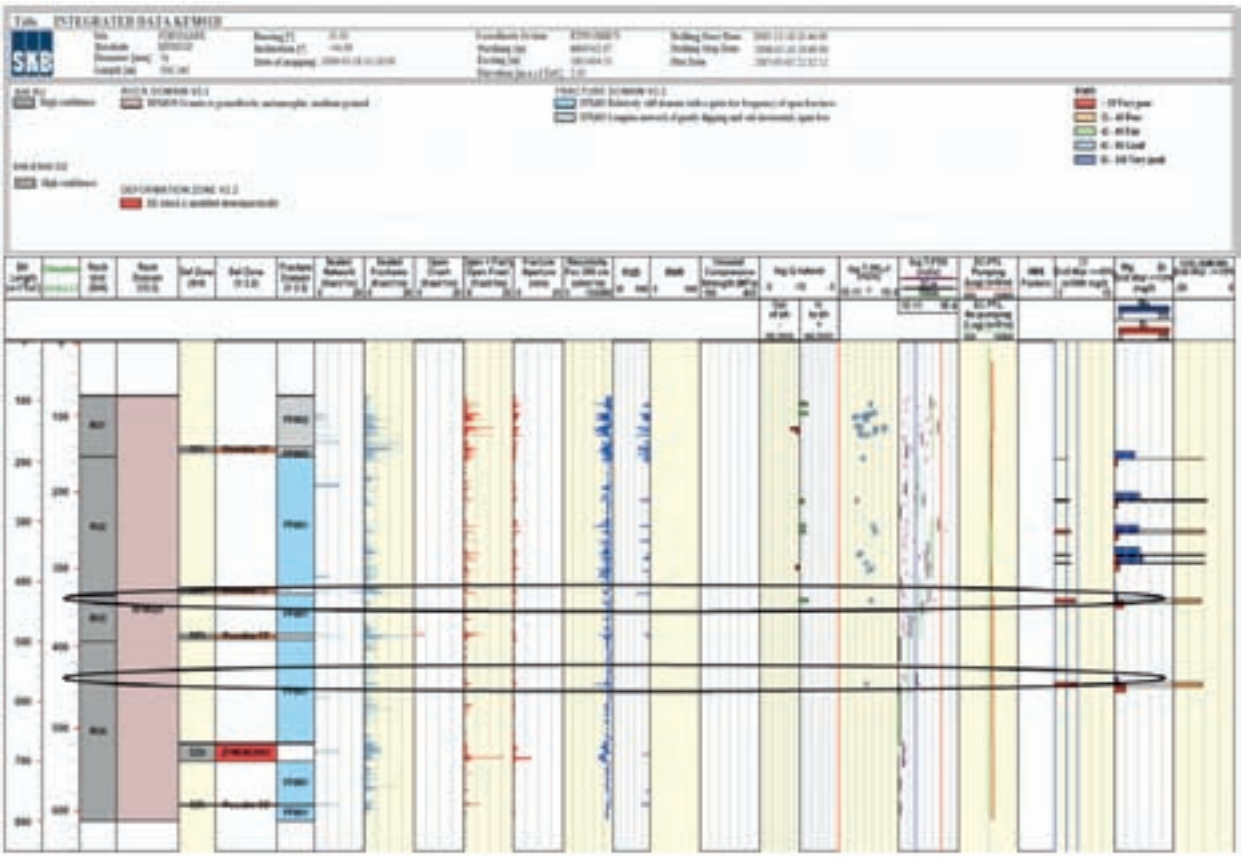

Figure 3-11. *Integrated diagram showing fracture frequency and geophysical parameter profiles with depth (elevation) and length for borehole KFM01D. The ellipses show the location of the sections 428.5–435.64 m and 568.0-575.14 m borehole length investigated here and their proximity to major deformation zones.*

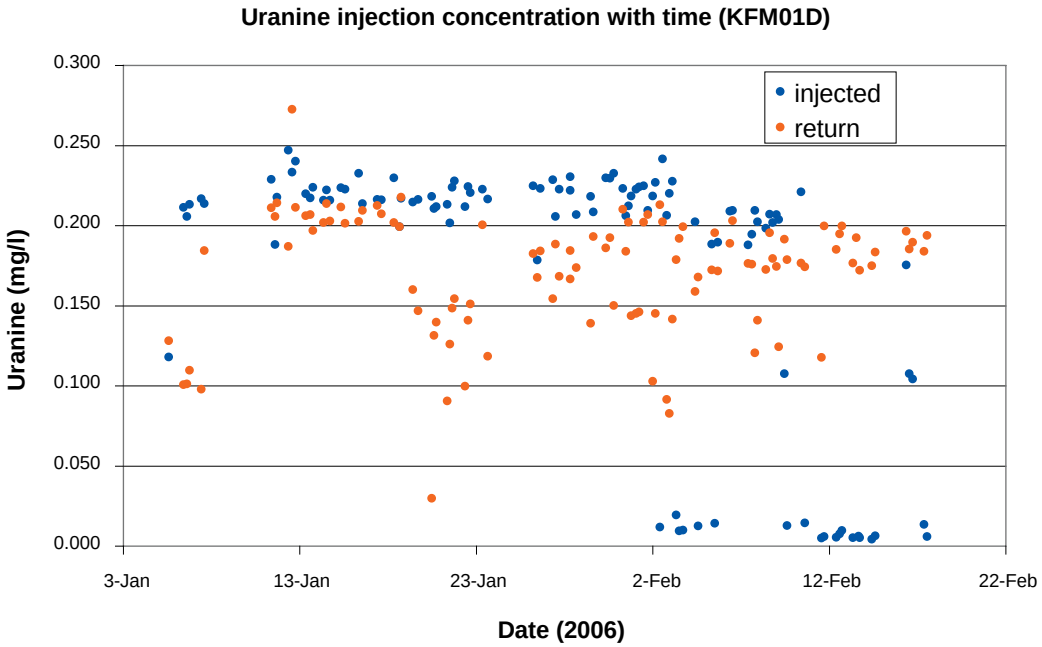

Figure 3-12. *Diagram showing difference in uranine content of injected drilling water and return water, with time, for the drilling of the borehole KFM01D.*

3.2.2 Calculation of drilling water content in fracture groundwater

At the end of the drilling and before pumping began (for flushing and sampling), the sections 428.50–435.64 and 568.00–575.14 m borehole length in borehole KFM01D, contained a maximum of 9.2% and 0.8% of drilling water, respectively, (Table 3-4, Figure 3-13).

During slow-pumping for sampling purposes, 6.8 and 0.54 m^3 (flow rate approx. 200 mL/min and respectively 0–25 mL/min), respectively, were removed from the borehole zones. From the drilling records, the accumulated drilling volumes in and out were calculated, as shown in Figure 3-10, for both sections. The calculated maximum amount of drilling water lost in the fractures during drilling was (–1 m^3) for the upper section and (–1 m^3) for the lower section. As mentioned by /Nilsson et al. 2006/, the uranine budget suggests that only a few cubic meters (corresponding to the error in the budget calculations) of the flushing water might have been lost to the borehole and adiacent host bedrock during drilling. A maximum of 9.2% and 0.8% of drilling water were found in these sections. At the end of the pumping the drilling water content was 6.3% and 0.9%, respectively.

These data may be influenced, however, by the possible presence of uranine-tagged test water that was used in several Forsmark boreholes (the adjacent borehole, KFM01A, was one of these) as part of the Borehole Probe Dilution Test programme. In this programme, uranine (1 mg/L) was injected into packed-off borehole sections and allowed to disperse under natural gradients. Its concentration was followed by monitoring the dispersion into the fractures. This uranine was not pumped out at the end of the programme and so may account for some of the drilling water tracer that was subsequently measured in in KFM01D, especially in the shallower section (428–435 m).

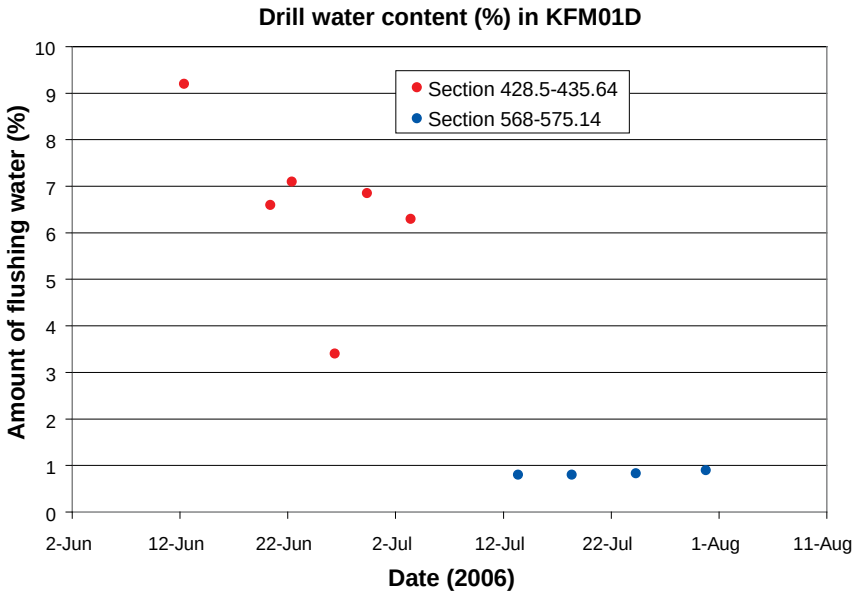

Figure 3-13. *Variation of uranine in flushing and pumping of water for hydrogeochemical sampling of borehole KFM01D.*

Table 3-4. Groundwater compositions for zones 428.50-435.64 (upper) and 568.00-575.14 m (middle) in borehole KFM01D. Drill water (HFM01, sample 4116) and Baltic seawater compositions are shown for reference.

Sampling date	Drill water %	Charge bal %	Na (mg/l)	K (mg/l)	Ca (mg/l)	Mg (mg/l)	HCO3 (mg/l)	Cl (mg/l)	SO4 (mg/l)	Br (mg/l)	F (mg/l)	Si (mg/l)	Fe[1] (mg/l)	Fe-tot[2] (mg/l)	FeII (mg/l)	Sr (mg/l)	I (mg/l)	pH	DOC (mg/l)
3-Jul-06	6.30	-0.66	1550	9.0	1430	19.5	35.8	4940	125.0	34.0	1.22	39.3	1.93	2.08	2.04	17.4	0.163	7.55	3.7
26-Jun-06	3.40	1.71	1630	9.4	1620	13.7	21.5	5160	78.6	37.9	1.41	6.9	1.36	1.35	1.33	18.1	0.175	7.49	2.3
12-Jun-06	9.20	1.03	1650	12.6	1660	21.0	22.7	5370	57.9	39.3	1.35	7.4	0.89	0.92	0.90	17.5		7.43	2.7
22-Jun-06	7.10	0.32	1600	10.0	1660	13.4	18.5	5350	59.2	39.5	1.51	6.7	1.04	1.04	1.04	18.3		7.52	2.5
29-Jun-06	6.85	0.13	1590	9.5	1520	15.0	26.2	5090	101.0	36.3	1.29	47.3	1.53	1.58	1.56	18.8		7.71	2.3
20-Jun-06	6.60	1.47	1670	10.5	1730	14.9	20.3	5460	54.4	42.2	1.47	6.7	1.13	1.13	1.11	19.0	0.195	7.53	3.2
13-Jul-06	0.80	0.14	1770	7.3	1840	10.9	17.1	5960	31.1	46.4	1.16	4.3	0.73	0.76	0.76	20.8	0.321	7.51	11.0
18-Jul-06	0.80	0.74	1770	7.3	1840	10.5	16.2	5890	29.7	44.9	1.21	4.3	0.88	0.89	0.88	20.7	0.319	7.48	6.9
24-Jul-06	0.83	-0.28	1750	7.3	1800	10.7	15.7	5910	29.5	45.6	1.15	4.3	1.09	1.09	1.06	20.4	0.326	7.37	7.7
30-Jul-06	0.90	1.36	1770	7.7	1830	15.2	20.0	5800	38.3	46.2	1.20	4.6	1.25	1.24	1.23	19.8	0.328	7.40	10.0
Drill water (HFM01)		-0.90	489.0	13.8	60.4	16.9	440.0	530.0	202.0									TOC:	10.4
Baltic sea water			1960.0	95.0	94.0	234.0	90.0	3760.0	325.0										

[1] Determined by ICP-AES

[2] Analysed spectrophotometrically

3.2.3 Hydrochemical sampling and analytical results for KFM01D

Groundwater from borehole KFM01D is defined as a SKB chemical type and so several precautions were taken to minimise contamination by the drilling water /Nilsson et al. 2006/:

1. The drilling water supply well should also be of a SKB chemical type.
2. Borehole HFM01 was selected to supply drilling and flushing water for KFM01D even though its TOC was rather large (7.4–7.9 mg/L, target < 5.0 mg/L); however, it had a saline composition.
3. Dosing equipment for uranine was used instead of a storage tank (the latter may suffer from biological activity).
4. The tracer storage tank was purged with N_2 gas to remove O_2 in the flushing water.

The variations of major and minor ion concentrations in sections 428.50–435.64 and 568.00–575.14 m borehole length are plotted against pumping time in Figures 3-14, 3-15 and 3-16.

The data shown in Figures 3-13 and 3-14, for the ions Na^+, Ca^{2+}, Mg^{2+} and Cl^-, indicate that there is a slight *decline* in both uranine and major ion concentrations in the shallower section (428.50–435.64 m) during pumping but there are no detectable changes or trends for these ions in the lower level (568.00–575.14 m) and only a slight increase in uranine concentration. A trend might be expected for the shallower section because the uranine shows an erratic decrease over this period (from about 9 to 4%). The decreasing trend seen in major ions is not what is expected because the concentration of tracer *decreases* rather than increases.

One possible explanation for this is that dilute water from above is entering the pumped zone and causing (untagged) dilute water to mix with the ambient (tagged) saline water. However, this is unlikely because pump rates are very low during the chemical sampling period so that shallow dilute water is less likely to be drawn down and mixed. The fact that Cl also decreases in concert with Na and Ca indicates that the effects seen are not likely to be due to cation exchange with fracture infilling minerals. The drilling water used here (from shallow borehole HFM01) is much more dilute (Table 3-4) than the other drilling waters and pumping of the borehole zones should give a more distinctive, positive trend in major ions than for the other boreholes. However, it does not do this; instead, it shows a negative trend during pumping. The reason for this is not known.

The minor cations, K^+ and Mg^{2+}, and the other anions, SO_4^{2-} and HCO_3^-, (Figures 3-15, 3-16) show different behaviours. Potassium tends to follow the major ions and shows a slight decreasing trend as drilling water is reduced whereas Mg is more variable but still shows distinct trends, probably indicating some mixing and rock-water interaction. These changes, as seen in KFM06A, in all cases exceed the changes in uranine concentrations and range from about 30 to over 100%.

These characteristics again indicate that there are more processes occurring than simple mixing of water types. Rock-water interaction and/or ion exchange may account for part of these changes, especially for the minor ions. The profile of Fe species (Figure 3-17), however, is the exact opposite of that seen in the two zones of KFM06A (Figure 3-9), (i.e. Fe species *increase* in concentration as pumping goes on and uranine decreases).

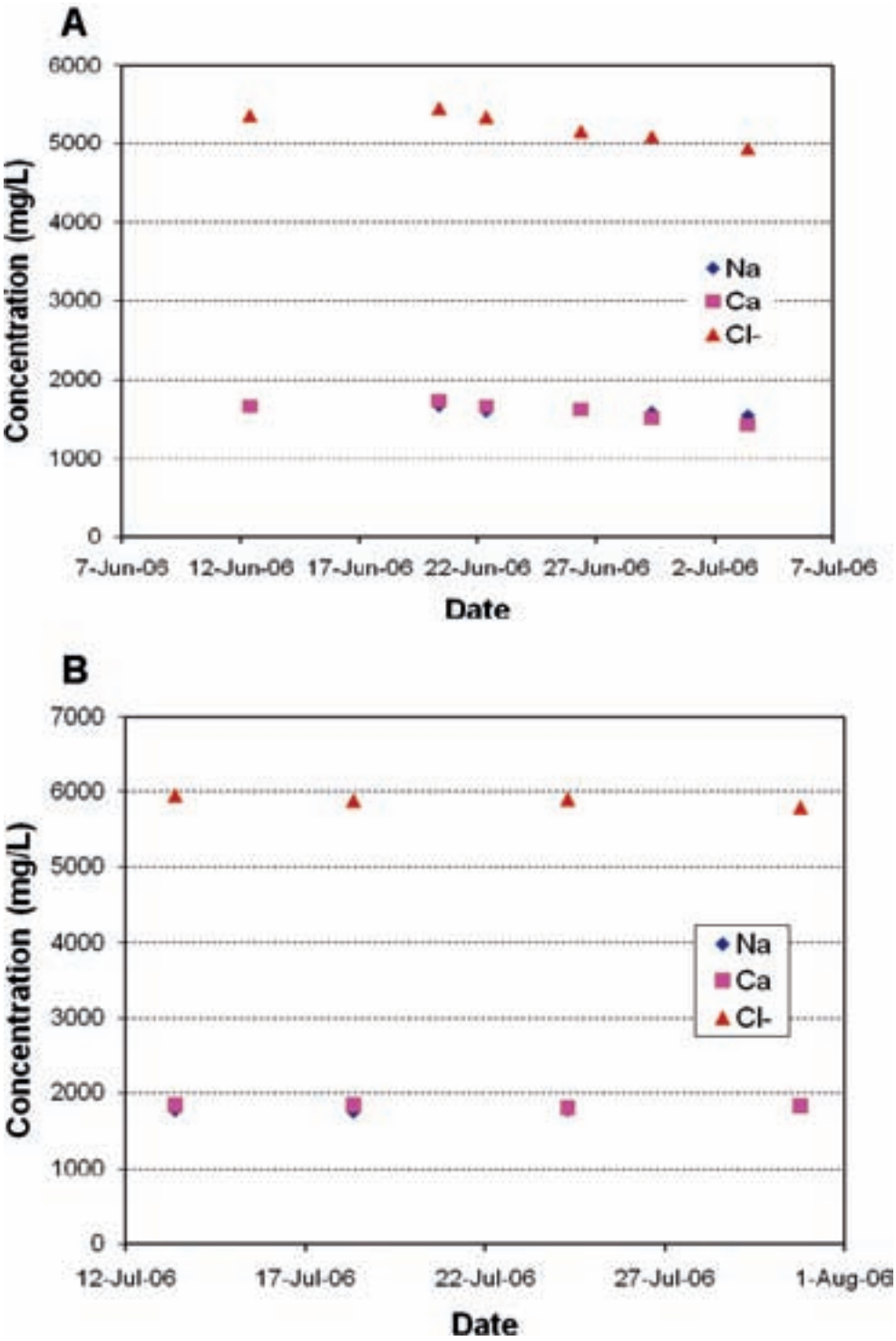

Figure 3-14. *Variation of cations (Na^+, Ca^{2+}, Cl^-) in sections (a) 428.50–435.64 and (b) 568.00–575.14 m boreholes length in groundwater from borehole KFM01D.*

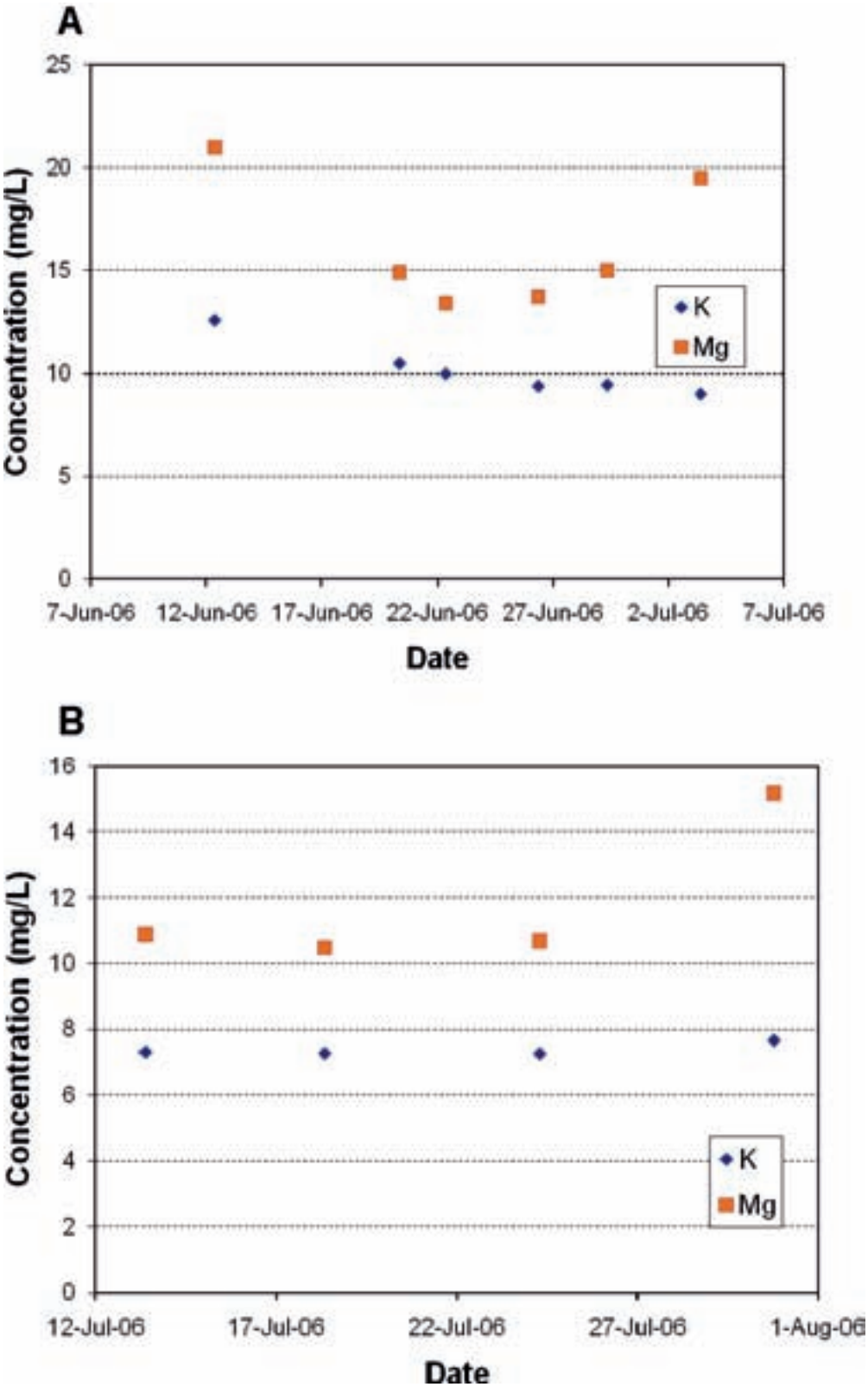

Figure 3-15. *Variation of minor cations (K^+, Mg^{2+}) in sections (a) 428.50–435.64 and (b) 568.00–575.14 m borehole length in groundwater from borehole KFM01D.*

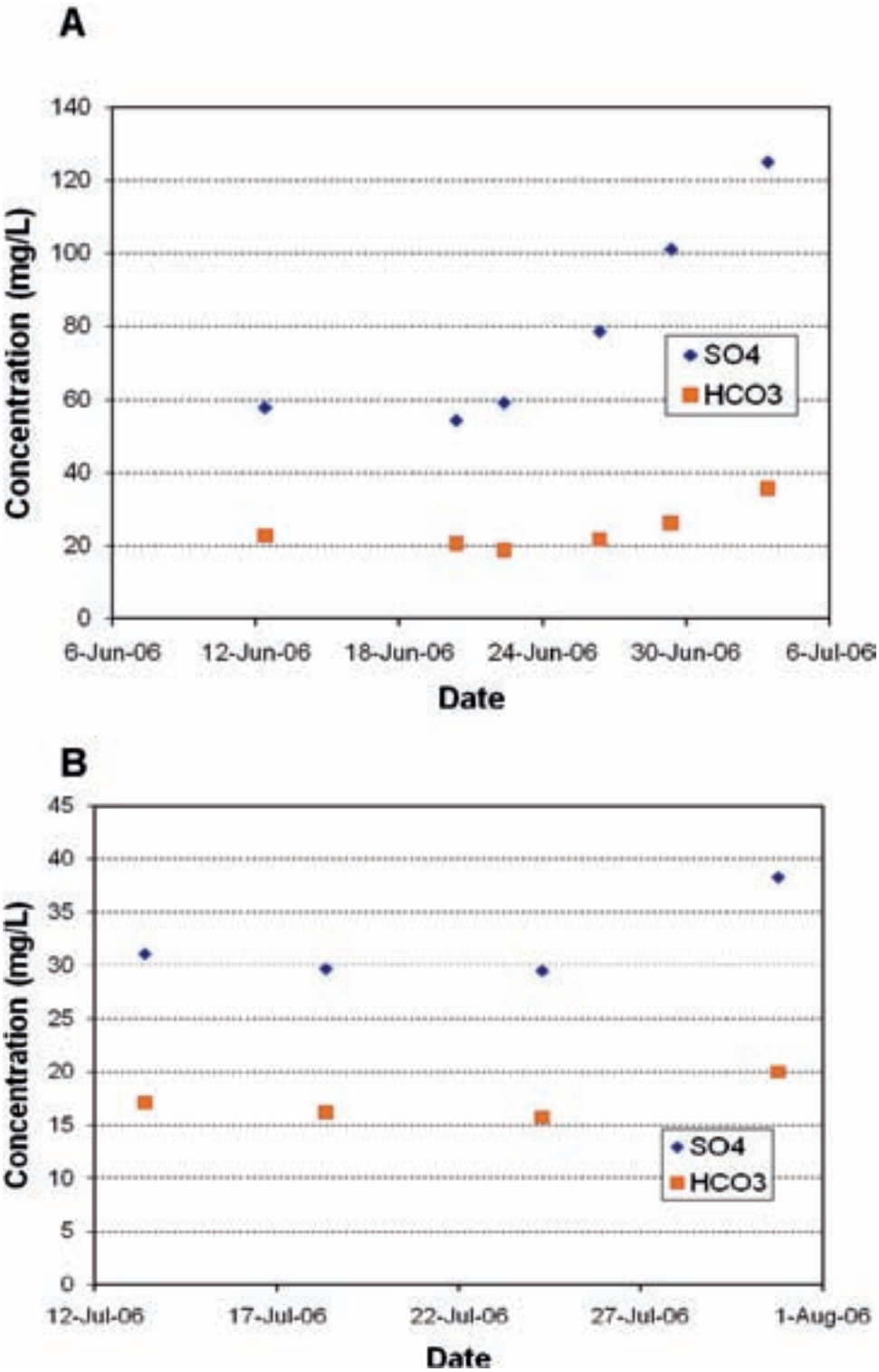

Figure 3-16. *Variation of anions (SO_4^{2-}, HCO_3^-) in sections (a) 428.50–435.64 and (b) 568.00–575.14 m borehole length in groundwater from borehole KFM01D.*

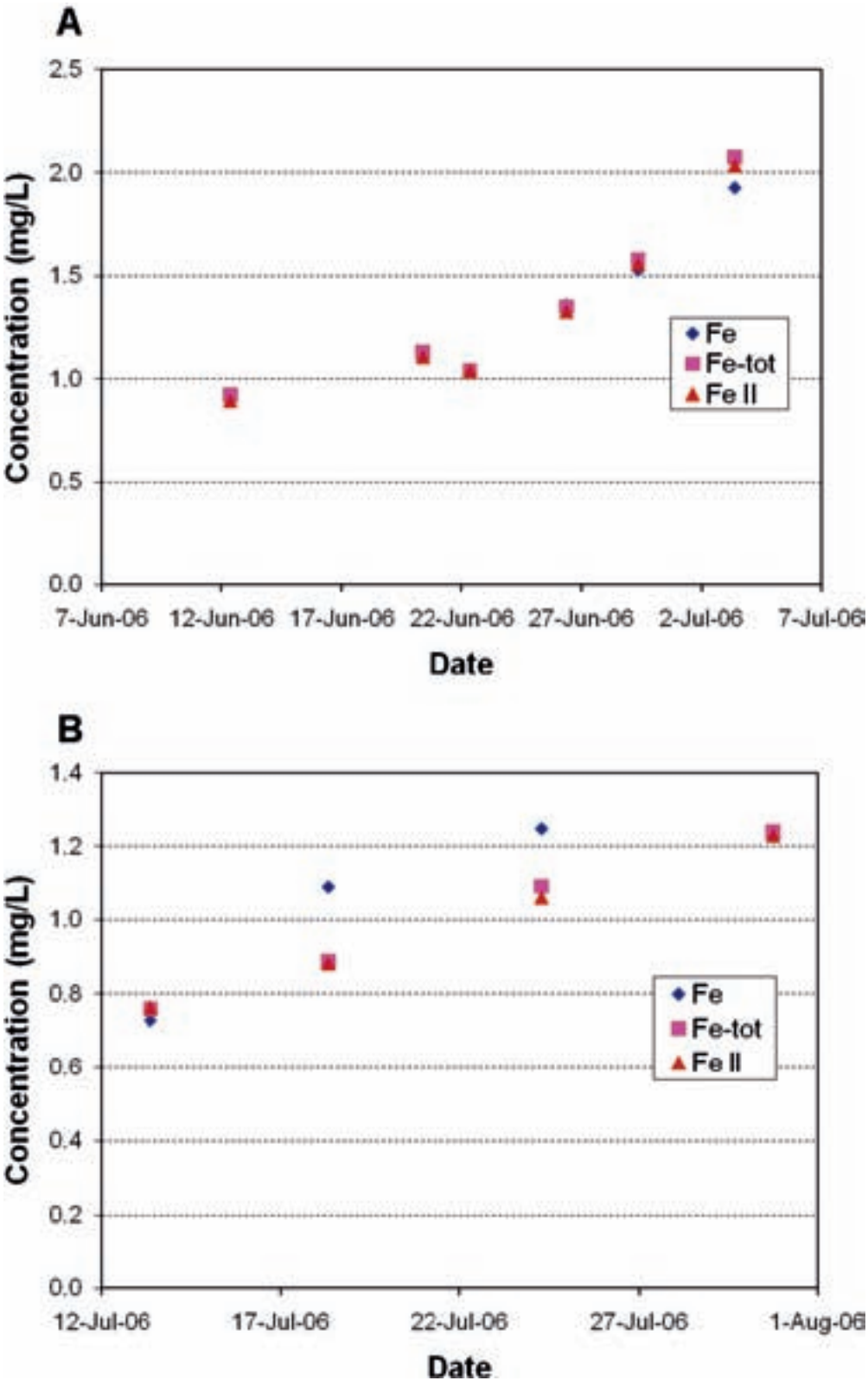

Figure 3-17. *Variation of Fe species in sections (a) 428.50–435.64 and (b) 568.00–575.14 m borehole length, in groundwater from borehole KFM01D.*

3.3 Borehole KFM08A

The record of drilling water injection during the drilling period of KFM08A has been described by /Berg et al. 2006/ and is shown as cumulative plots, against time and depth, in Figure 3-18a and 3-18b. The fracture frequency map for KFM08A is shown in Figure 3-19 (the ellipse shows the location of the section 683.5–690.64 m borehole length investigated here and its proximity to major deformation zones).

It can be seen that core drilling (100–1,000 m) began the 31st January 2005 and terminated at the end of March, 2005. Over 1,196 m^3 of drilling water were used in core drilling and 1,210 m^3 were pumped out.

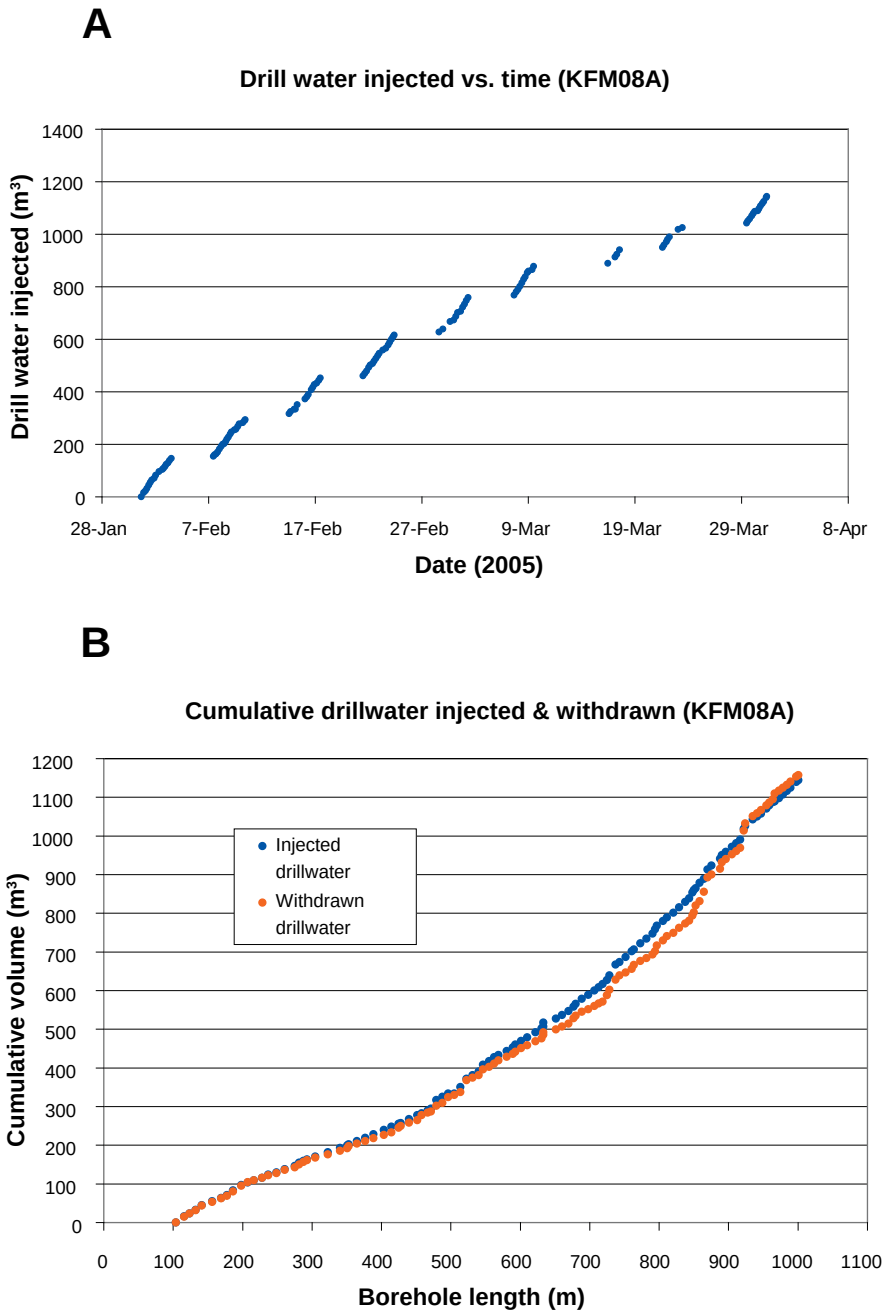

Figure 3-18. *Cumulative plots of a) volume of drilling water injected against time and b) of injected and withdrawn drilling water against length, for borehole KFM08A.*

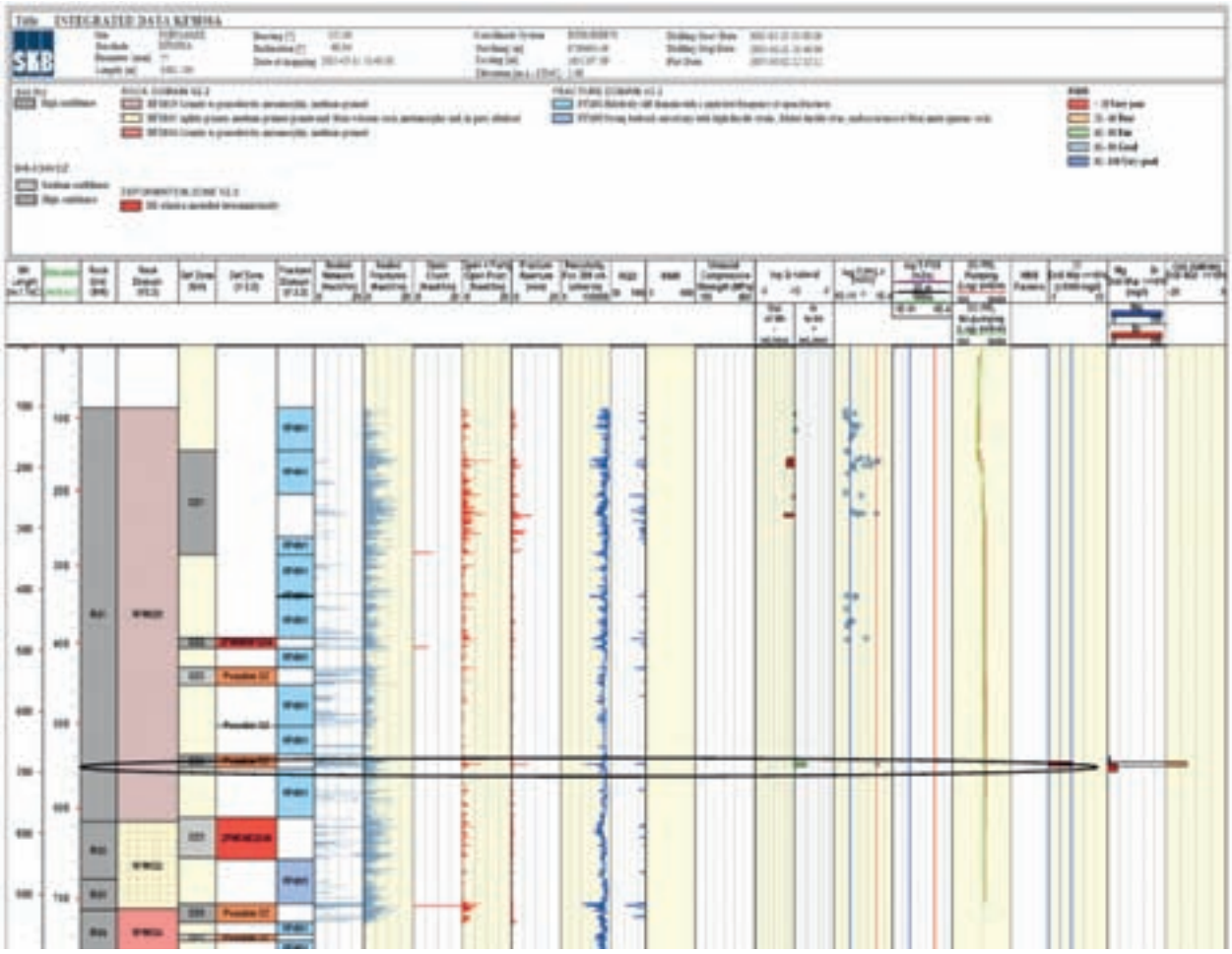

Figure 3-19. *Integrated diagram showing fracture frequency and geophysical parameter profiles with depth (elevation) and length for borehole KFM08A. The ellipse shows the location of the section 683.50–690.64 m borehole length, investigated here and its proximity to major deformation zones.*

Figure 3-20 shows that the average uranine concentration added to drilling water was about 0.2 mg/L. Uranine concentration in the return water averaged 0.173 m/L indicating loss of tracer to the fracture system and/or dilution by formation water.

The data for KFM08A is recorded in detail in this report so that a full demonstration can be given of the procedure to evaluate the extent and effects of drilling water contamination in the zone.

Only one zone (683.5–690.64 m) was suitable for application of DIS in borehole

KFM08A (see Table 3-1 for details). At the end of the drilling and before pumping began (for flushing and sampling), this section contained about 5% of drilling water (Table 3-5, Figure 3-21).

During slow-pumping for sampling purposes, 23.1 m^3 of water (in 4 steps: first 3.2 m^3, 6.8 m^3, then 1.6 m^3 and finally 11.5 m^3), were removed from the borehole zone. Due to the high flushing content during the first pumping period, a clean-up of the borehole was begun. From the drilling records, the accumulated drilling volumes in and out were calculated, as shown in the Figure 3-18. Based on these calculations, the maximum amount of drilling water lost in the fractures during drilling was 3 m^3. A maximum of 5% of drilling water was found in this section in the beginning of the third pumping period.

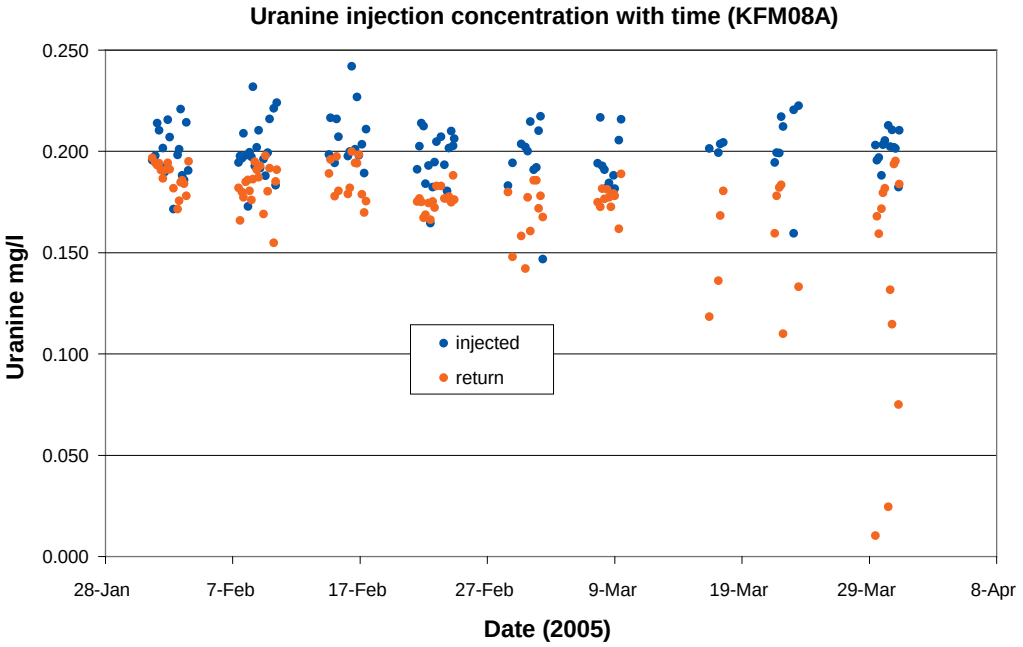

Figure 3-20. *Diagram showing difference in uranine content of injected drilling water and return water, with time, for the drilling of borehole KFM08A.*

3.3.1 Calculation of drilling water content

The extent of contamination of groundwater due to drilling of the single zone in borehole KFM08A can be determined by DIS. The amount of groundwater that must be pumped from each zone to reduce the uranine content to an acceptable level can then be determined.

The average content of uranine in borehole groundwater at the end of the drilling is calculated in two ways, as follows:

Weight of uranine added to injected drilling water = 234 g (from gravimetric measurement).

Weight of uranine in drilling water = 240 g (from concentration measurements and volume of injected water).

Weight of uranine returned = 223 g (from average uranine concentration and volume of returned water).

Percentage loss or gain of uranine is determined as

1) (234–223)/234 = 4.7% or

2) (240–223)/240 = 7.1%.

The volume of drilling water injected in is 1,196 m^3 and pumped out is 1,210 m^3.

The gravimetric method is more accurate because uranine weights are more precisely determined than are the water volumes. As explained by /Berg et al. 2006/, the return water is similar to the flushing water except for the final volume close to the bottom of the borehole where the water-yielding fracture is located. The uranine budget of /Berg et al. 2006/ suggests that only 60–86 m^3 of the flushing water was lost to the borehole and the adjacent host bedrock during drilling.

3.3.2 Calculation of drilling water content in fracture groundwater

At the end of the drilling and before pumping began (for flushing and sampling), groundwater from section 683.5–690.64 m borehole length in KFM08A, contained a maximum of 4.8% of drilling water. At the beginning of the third period of pumping (Table 3-5, Figure 3-21) the drilling water content at the end of the pumping was 5.05%.

From the drilling records, the accumulated drilling volumes in and out were calculated, as shown in the Figure 3-22. Based on these calculations, the maximum amount of drilling water lost in the fractures during drilling was 3 m^3. A maximum of 5.4% of drilling water was found in this section, but 23.1 m^3 were pumped from the section.

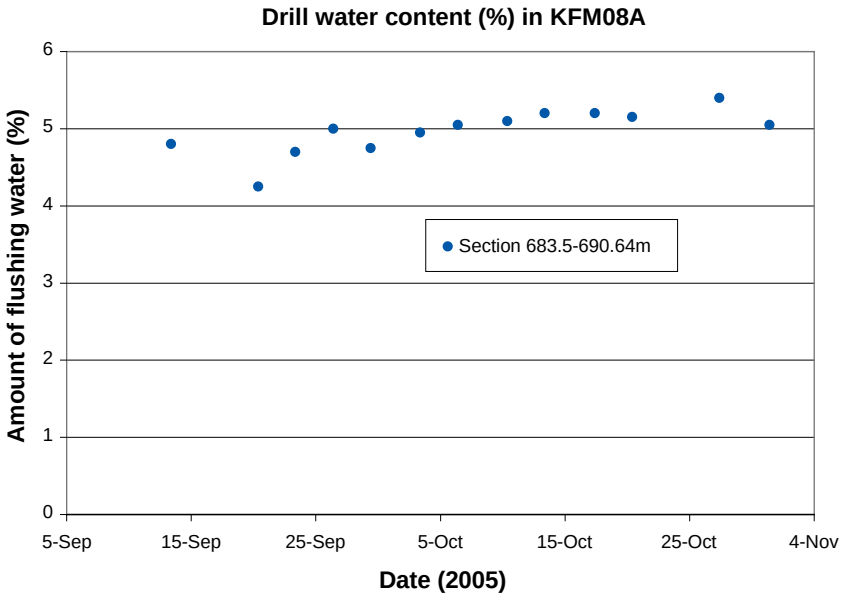

Figure 3-21. *Variation of uranine in flushing and pumping water during hydrogeochemical sampling in borehole KFM08A.*

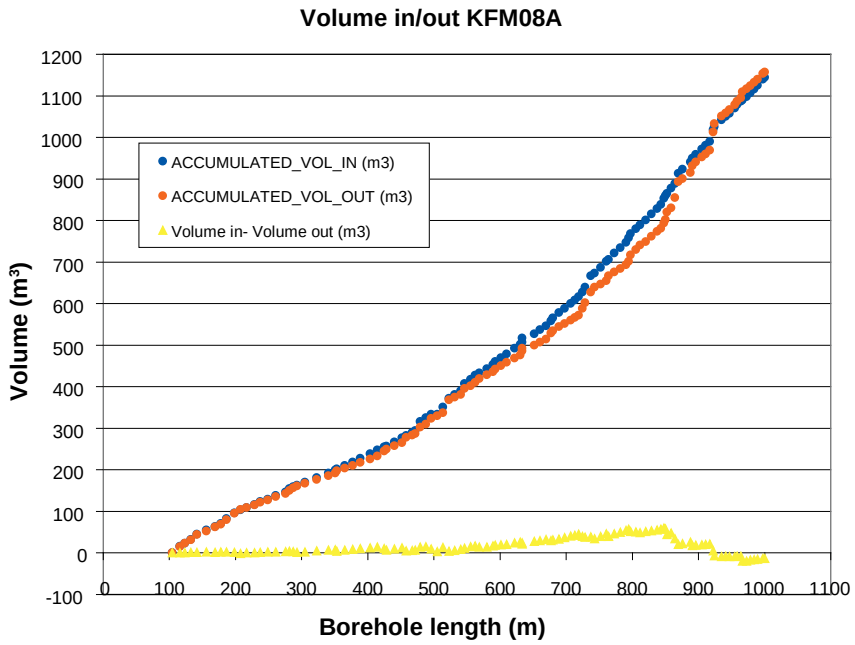

Figure 3-22. *Drilling water pumped in (blue) and out (orange). The water pumped out represents drilling water pumped out plus formation water. The yellow curve represents the difference between the water pumped in and out from the borehole.*

Table 3-5. Groundwater compositions for zone 683.50-690.64 m in borehole KFM08A. Drill water (HFM22, sample 8644) and Baltic seawater compositions are shown for reference.

Sampling date	Drill water %	Charge bal %	Na (mg/l)	K (mg/l)	Ca (mg/l)	Mg (mg/l)	HCO3 (mg/l)	Cl (mg/l)	SO4 (mg/l)	Br (mg/l)	F (mg/l)	Si (mg/l)	Fe[1] (mg/l)	Fe-tot[2] (mg/l)	FeII (mg/l)	Sr (mg/l)	I (mg/l)	pH	DOC (mg/l)
13-Sep-05	5.05	-0.21	1510	9.6	2200	12.5	9.78	6190	91.1	55.4	1.31	4.8	0.371	0.147	0.129	25.3	0.236	6.73	-1.0
20-Sep-05	5.40	-0.26	1510	10.0	2150	12.6	9.47	6180	90.5	49.8	1.33	4.5	0.086	0.022	0.001	25.2	0.235	7.21	2.6
23-Sep-05	5.05	-0.73	1520	10.2	2150	13.2	11.00	6100	88.6	55.0	1.29	4.7	-0.200	0.143	0.140	25.3		7.61	-1.0
26-Sep-05	4.80	-0.04	1500	10.2	2130	13.5	11.80	6010	89.0	46.3	1.32	4.8	0.208	0.127	0.121	24.8		7.67	1.2
29-Sep-05	5.00	0.35	1500	10.4	2160	14.0	12.40	6080	89.8	55.5	1.26	5.0	-0.200	0.199	0.175	24.9	0.230	7.60	-1.0
3-Oct-05	5.20	0.25	1500	10.1	2160	14.0	10.80	6070	92.9	45.2	1.31	5.0	0.214	0.217	0.207	24.4		7.75	-1.0
6-Oct-05	4.70	0.12	1490	10.3	2150	14.3	10.60	6160	93.1	57.3	1.33	5.0	0.210	0.235	0.230	24.4		7.85	-1.0
10-Oct-05	5.10	0.09	1520	10.3	2140	14.3	12.30	6090	91.1	48.3	1.31	5.0	0.289	0.265	0.256	24.6	0.247	7.84	-1.0
13-Oct-05	4.95	0.30	1520	10.5	2170	14.5	11.70	6120	90.1	54.3	1.34	5.1	0.250	0.288	0.270	24.8	0.228	7.46	-1.0
17-Oct-05	4.25	-0.63	1470	10.0	2110	14.4	10.40	6030	94.1	44.6	1.24	4.9	0.506	0.502	0.498	23.7	0.256	7.50	1.0
20-Oct-05	4.75	0.17	1520	10.0	2150	14.6	10.60	6140	92.0	54.0	1.26	5.1	0.355	0.437	0.438	24.7		7.75	-1.0
27-Oct-05	5.20	-0.45	1560	10.6	2130	14.1	13.00	6170	86.2	44.9	1.25	5.0	0.456	0.514	0.509	23.7	0.231	7.22	-1.0
31-Oct-05	5.15	-0.18	1560	10.6	2090	14.1	10.40	6100	91.5	44.5	1.20	5.2	0.676	0.724	0.726	23.3		7.79	-1.0
Drill water (HFM22)		-2.70	1500	40.3	575	153.0	173.00	3660	422.0									TOC:	3.1
Baltic sea water			1960.0	95	94	234	90	3760.0	325.0										

[1] Determined by ICP-AES

[2] Analysed spectrophotometrically

3.3.3 Hydrogeochemical sampling and analytical results for KFM08A

Groundwater from borehole KFM08A is defined as a SKB chemical type and so several precautions were taken to minimise contamination by the drilling water /Nilsson et al. 2006/:

1. The drilling water supply well was also of a SKB chemical type.
2. Borehole HFM22 was selected to supply drilling and flushing water for KFM08A because its TOC was low (3.1–3.3 mg/L, target < 5.0 mg/L); however, it had a saline composition.
3. Dosing equipment for uranine was used instead of a storage tank (the latter may suffer from biological activity).
4. The tracer storage tank was purged with N_2 gas to remove O_2 in the flushing water.

The variations of major and minor ion concentrations in groundwater in section 683.50–690.64 m borehole lenght are plotted against pumping time in Figures 3-23, 3-24, 3-25 and 3-26.

The small amount of drilling water that enters the host rock at KFM08A, as determined by tracer recovery, is also indicated here from an examination of the hydrogeochemistry. The major ions (Na^+, Ca^{2+}, Cl^-) maintain constant concentrations over the entire 2+ months of pumping and sampling, probably because the drilling water from HFM22 is about as saline as the groundwater being sampled. The minor ions (K^+, Mg^{2+}, SO_4^{2-}, HCO_3^-) also remain fairly constant but the Fe species describe an increasing trend, similar to that of KFM01D (Figure 3-17).

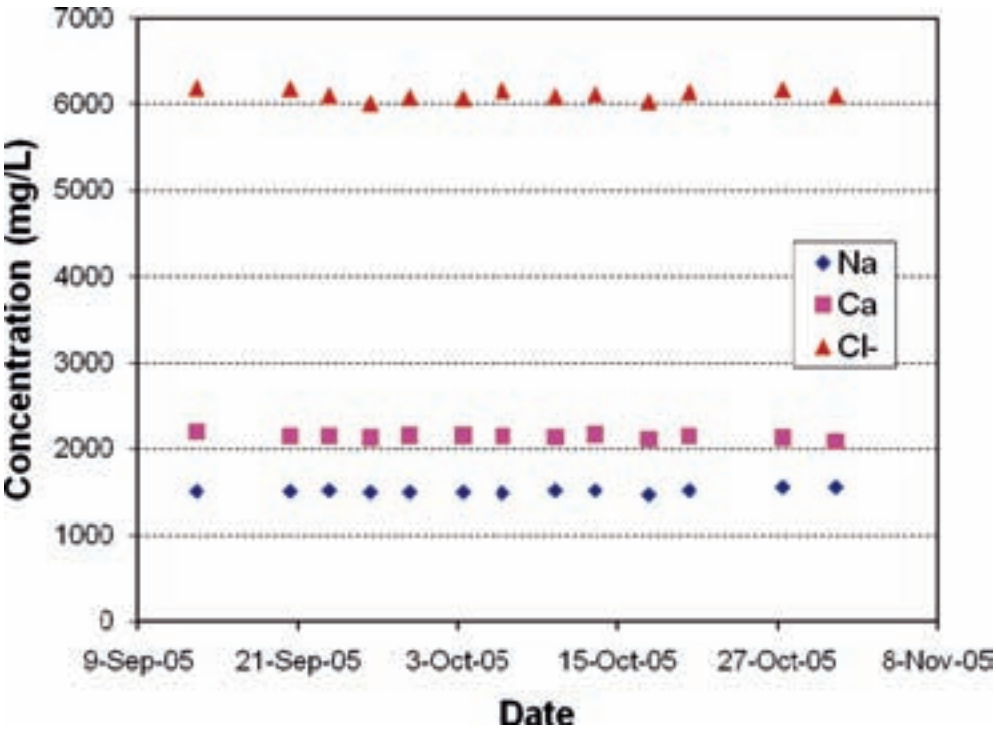

Figure 3-23. *Variation of major ions in groundwater from the section 683.50–690.64 m borehole length in KFM08A.*

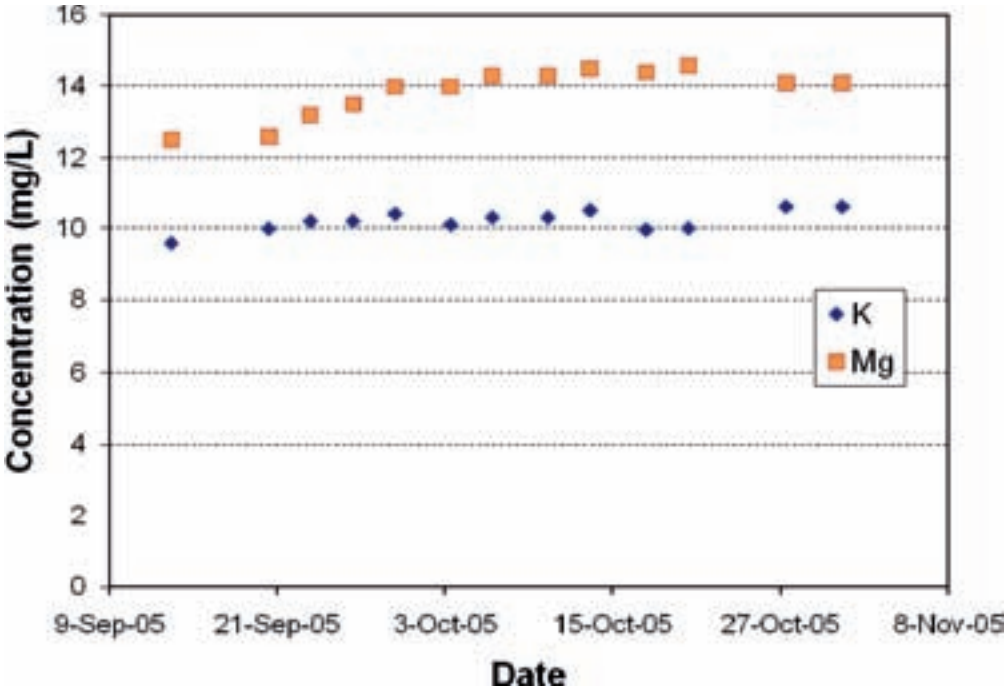

Figure 3-24. *Variation of minor cations in groundwater from the section 683.50–690.64 m, borehole length in KFM08A.*

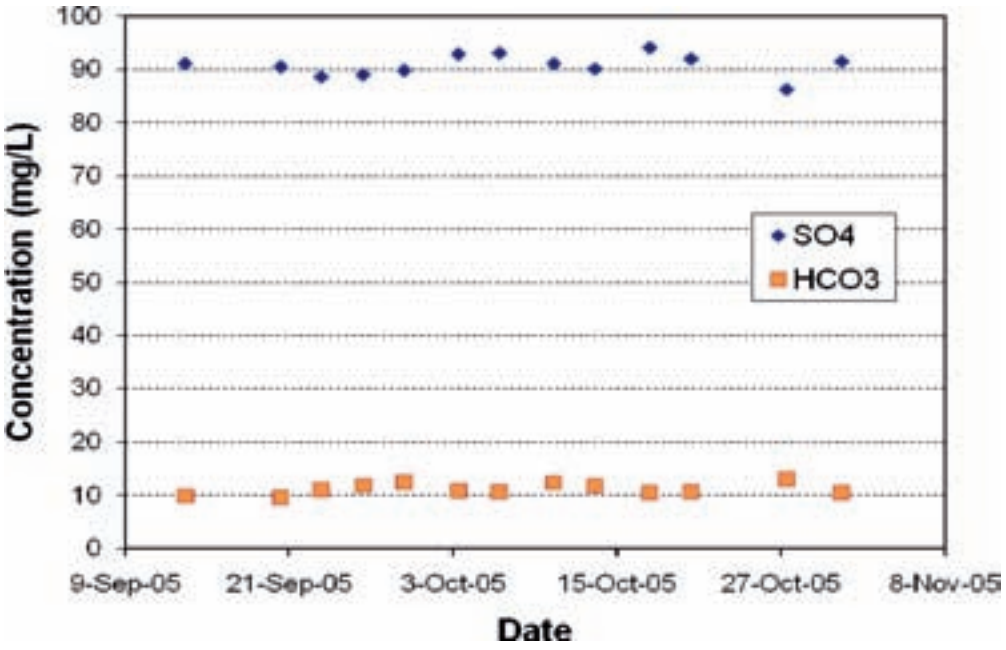

Figure 3-25. *Variation of minor anions in groundwater from the section 683.50–690.64 m, borehole length in KFM08A.*

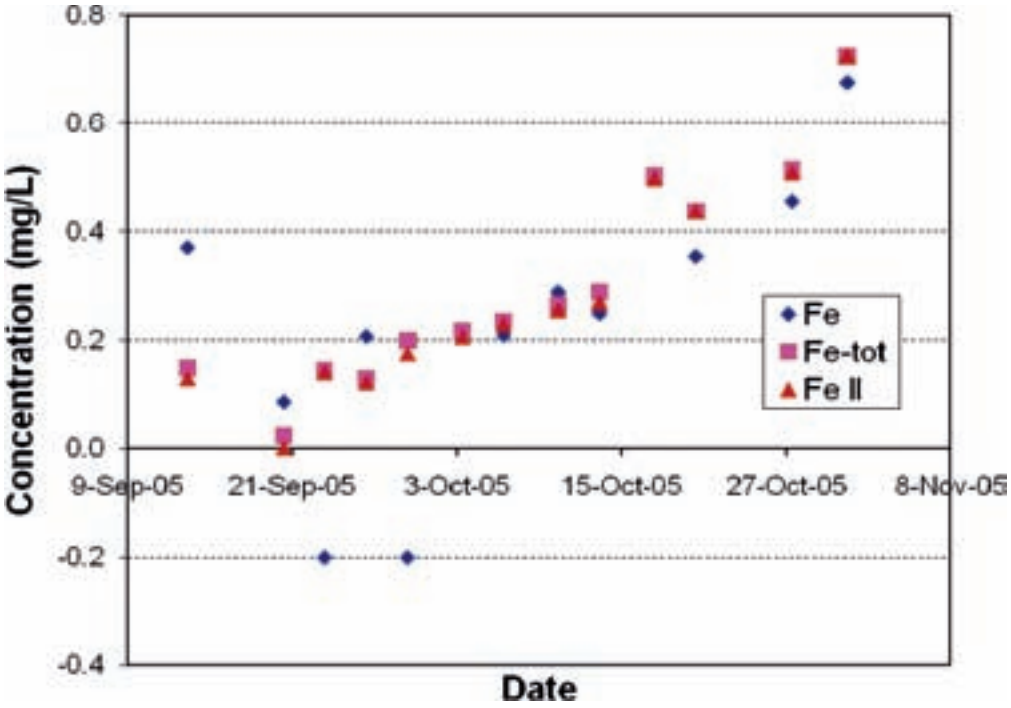

Figure 3-26. *Variation of Fe species in groundwater from the section 683.50–690.64 m borehole length KFM08A.*

3.4 Borehole KFM10A

Core drilling of borehole KFM10A (60–500 m) began in March and ended in early June, 2006, (Figure 3-27a). The record of drilling water injection during the drilling period of KFM10A has been described by /Bergelin et al. 2007/ and is shown as cumulative plots, against time and borehole length, in Figure 3-27a and 3-27b. About 479 m^3 of drilling water were injected in core drilling and 926 m^3 were pumped out (Figure 3-27b).

The fracture frequency map for KFM10A is shown in Figure 3-28 (the ellipses show the location of the sections 298.0–305.5 m and 478–487.5 m borehole length investigated here and their proximity to major deformation zones). Figure 3-29 shows that the uranine concentration added to drilling water varied between 0.003 and 0.322 mg/L (average = 0.174 mg/L), through most of the borehole depth. Uranine concentrations in the return water were generally similar or to or lower than injected levels and ranged from 0.202 to 0.046 mg/L (average = 0.125 mg/L), indicating some loss of tracer to the fracture system and/or dilution by formation groundwater

The data for KFM10A is recorded in detail in this report so that a demonstration of the procedure to evaluate the extent and effects of drilling water contamination in the zone can be made and compared to data from other boreholes.

3.4.1 Calculation of drilling water content

Objectives

The main aim of DIS is to evaluate the extent of contamination of individual fracture-zone groundwaters in borehole KFM10A, due to drilling activities, and then to determine how much groundwater must be pumped from each zone to reduce the uranine content to an acceptable level. The results of this modelling are then compared with the hydrochemical data obtained from each zone.

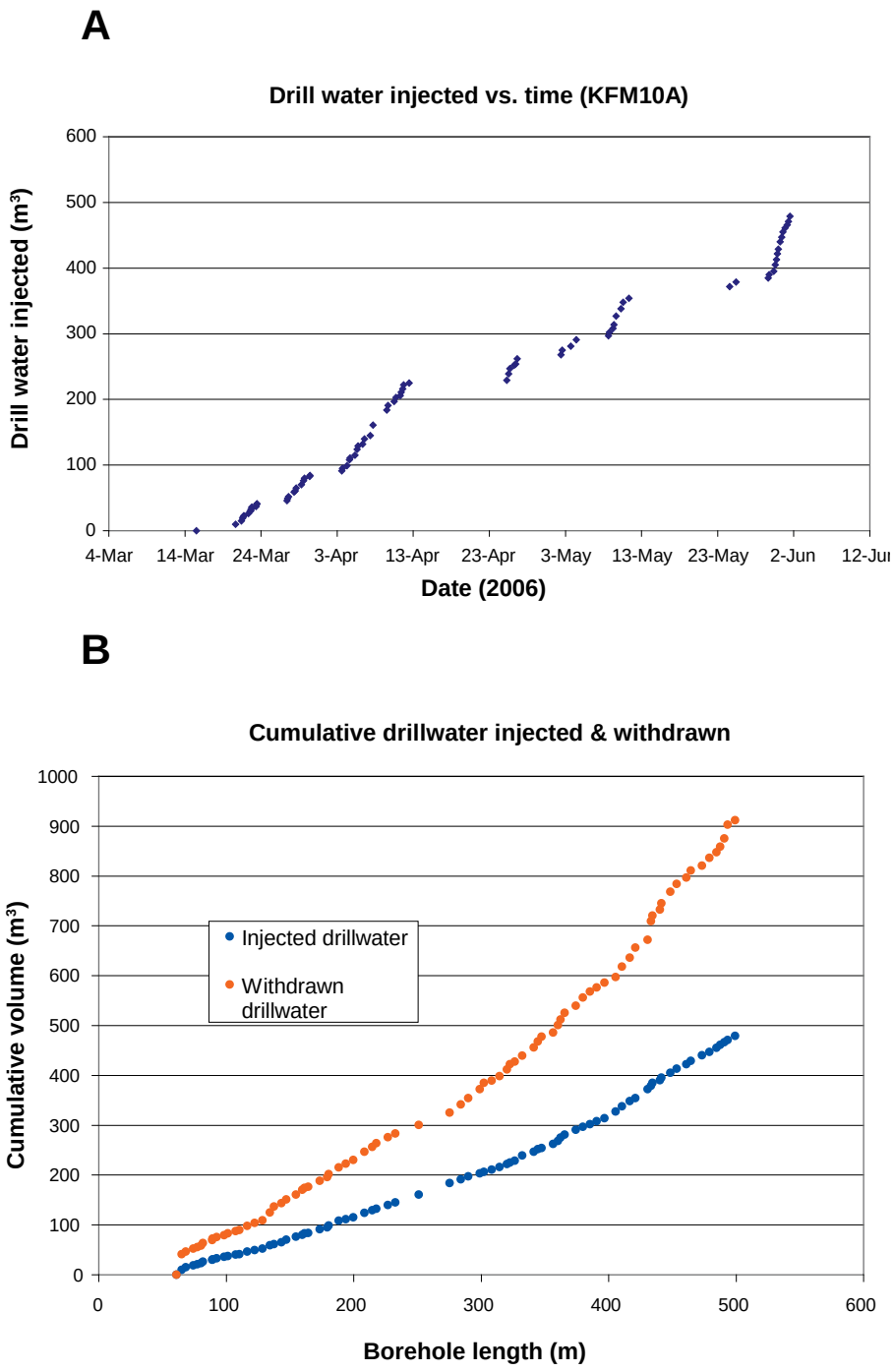

Figure 3-27. *Cumulative plots of a) volume of drilling water injected against time and b) of injected and withdrawn drilling water against length, for borehole KFM10A.*

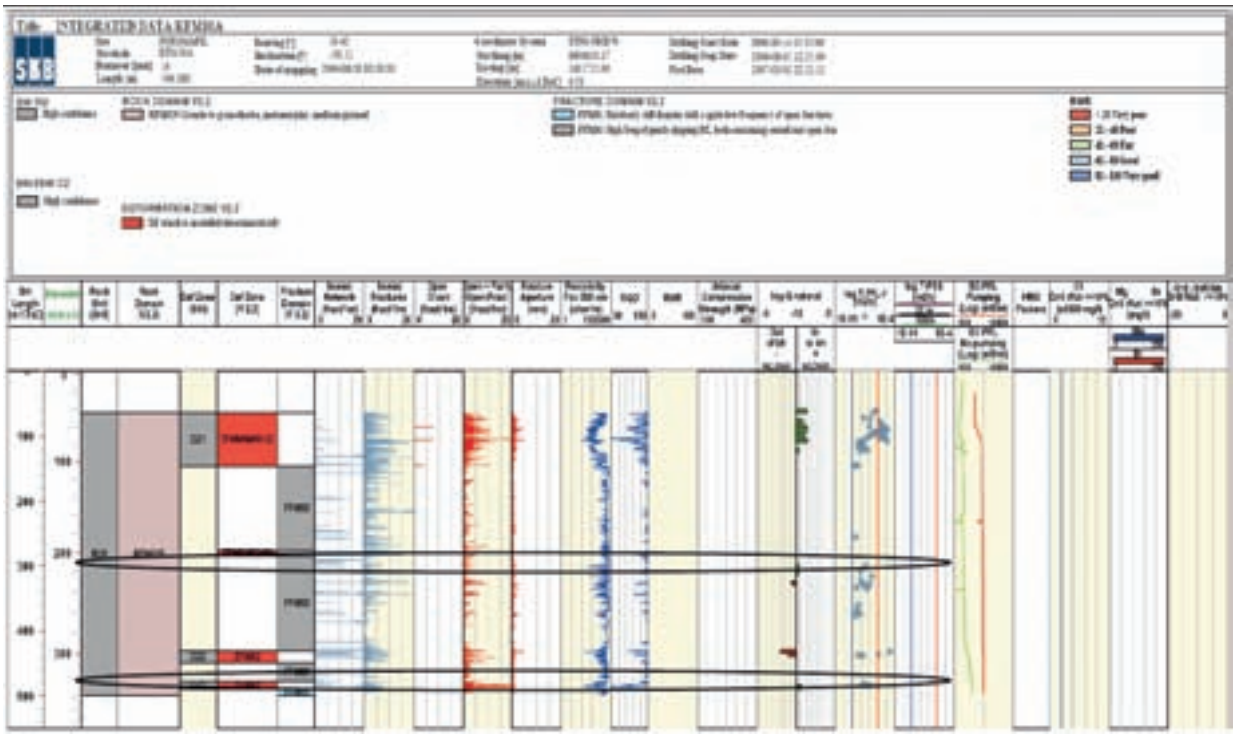

Figure 3-28. *Integrated diagram showing fracture frequency and geophysical parameter profiles with depth (elevation) and length for borehole KFM10A. The ellipses show the location of the sections 298.0–305.5 m and 478.0–487.5 m borehole length investigated here and their proximity to major deformation zones.*

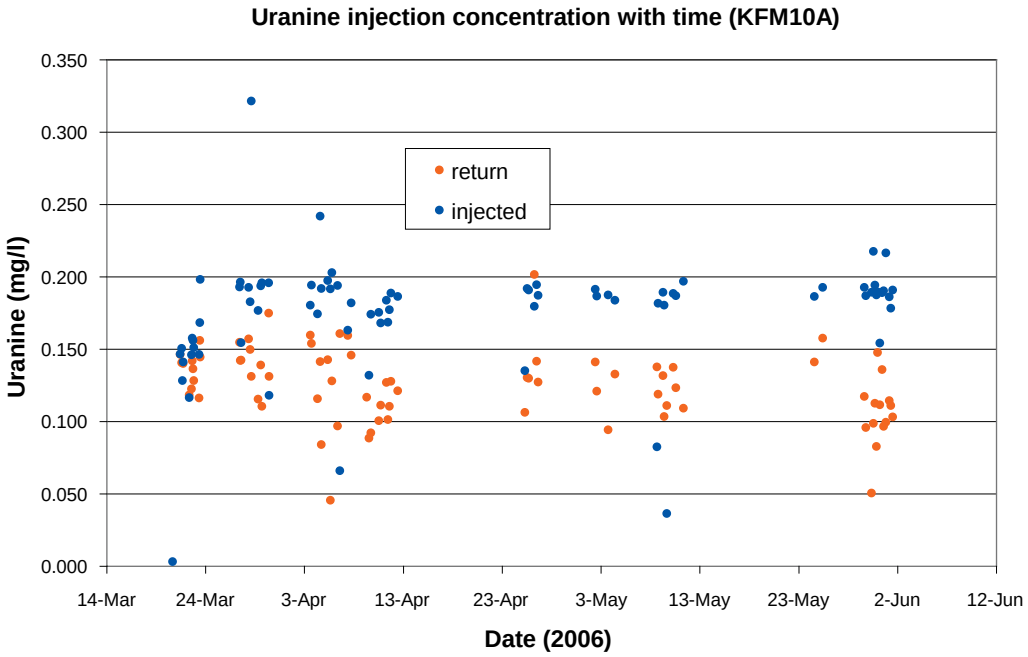

Figure 3-29. *Diagram showing difference in uranine content of injected drilling water and return water, with time, for the drilling of borehole KFM10A.*

Basic calculations

The average content of uranine in borehole groundwater at the end of the drilling can be calculated in two ways, as follows (after /Bergelin et al. 2007/):

1. Gravimetric:

Weight of uranine added to injected drilling water = 95 g (from gravimetric measurement).

Weight of uranine in drilling water = 84 g (from concentration measurements and volume of injected water).

Weight of uranine returned to surface in withdrawn drilling water = 116 g (from weighted means).

Percentage loss or gain of uranine is determined as:

1) (95–116)/95 = –22%

2) (84–116)/84 = –38%

This is an anomalous situation whereby considerably more uranine appears to have been recovered than injected.

2. Volumetric:

Volume of drilling water injected = 479 m^3 (from meter).

Volume of drilling water withdrawn = 926 m^3 (from meter; this represents drilling water mixed with formation water).

The gravimetric method is more accurate because uranine weights are more precisely determined than are the water volumes. The volume of drilling water pumped out is higher than that injected and this makes the calculations more difficult. More return water is due to the use of air-lift pumping from shallow zones. This creates a complex situation with mixing of formation water and ingoing flushing water (it is the general tendency to have more return water in poor rock conditions and a better balance between injected and withdrawn water in tight rock). However, if the uranine is correctly monitored, the return water can be calculated based on the percentage of uranine, and a water balance and DIS calculations can be performed.

The gravimetric method is more accurate because weights are more precisely determined than the origin of the volumes measured.

Detailed calculation of drilling water content in fracture groundwater

At the end of the drilling and before pumping began (for flushing and sampling), the sections 298.0–305.5 m and 478.0—487.5 m borehole length contained a maximum of 12.9% and 0.5% of drilling water, respectively, (Figure 3-30).

During slow-pumping for sampling purposes, 1.7 m^3 and 4.9 m^3, respectively, were removed from the borehole zones. From the drilling records, the accumulated drilling volumes in and out were calculated, as shown in the Figure 3-27, for both sections. Based on these calculations, the maximum amount of drilling water lost in the fractures during drilling was 6 m^3 for the upper section and 14 m^3 for the lower section. The water pumped out during the drilling of these sections was 14.6 m^3 for the first section and 22 m^3 for the second section. These volumes represent flushing water mixed with formation water. Because of the high values of the water pumped out from the borehole it is difficult to calculate the flushing water lost in the fractures. That could be done by a uranine budget calculations, but as shown above, the uranine recovered was apparently higher than the uranine injected due to various possible causes, making the calculations impossible.

The samples obtained at the end of the pumping/sampling phases show that 4.5% drilling water remained in the first section and 3.6% drilling water in the second section (Figure 3-30).

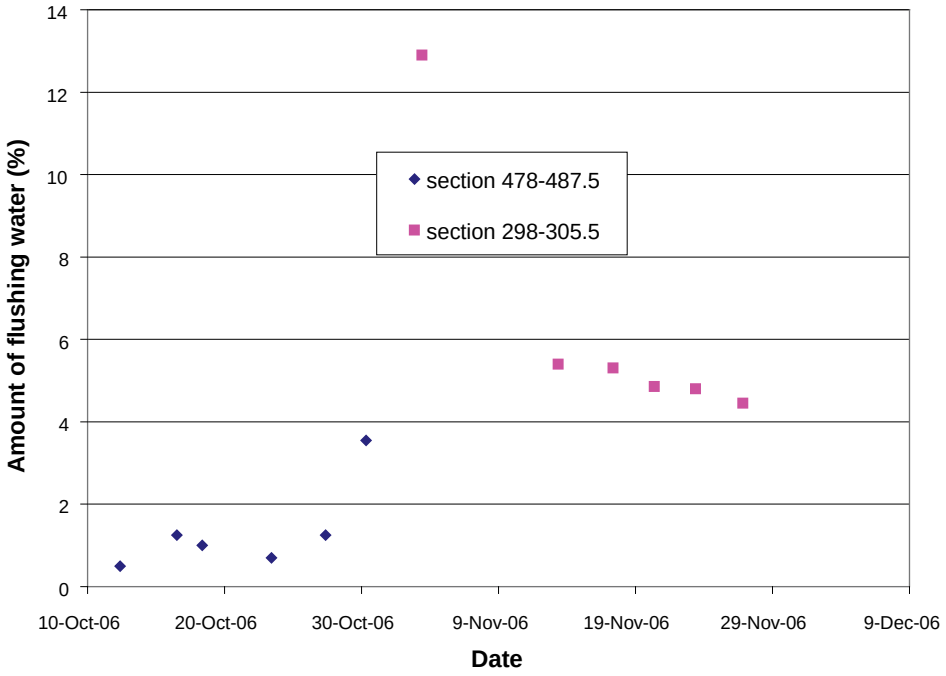

Figure 3-30. *Variation of uranine in flushing and pumping water during hydrogeochemical sampling.*

These data may be influenced, however, by the possible presence of uranine-tagged test water that was used in several Forsmark boreholes (although not included in the test, KFM10A was close to the other test boreholes) as part of the Borehole Probe Dilution Test programme. In this programme, uranine (1 mg/L) was injected into packed-off borehole sections and allowed to disperse under natural gradients. Its concentration was followed by monitoring the dispersion into the fractures. This uranine was not pumped out at the end of the programme and so may account for some of the drilling water tracer that was subsequently measured in KFM10A, especially in the shallower section (298–305 m).

3.5 Hydrogeochemical sampling and analytical results for KFM10A

Groundwater from borehole KFM10A is defined as a SKB chemical type and so several precautions were taken to minimise contamination by the drilling water /Nilsson et al. 2006/:

1. The drilling water supply well was also of a SKB chemical type.
2. Borehole HFM24 was selected to supply drilling and flushing water for KFM10A.
3. Dosing equipment for uranine was used instead of a storage tank (the latter may suffer from biological activity).
4. The tracer storage tank was purged with N_2 gas to remove O_2 in the flushing water.

The variations of major and minor ion concentrations in groundwater in section 290–305.5 and 478–487.5 m are plotted against pumping time in Figures 3-31, 3-32, 3-33 and 3-34.

Table 3-6. Groundwater compositions for zones 290.0-305.5 and 478.0-487.5 m in borehole KFM10A. Drill water (HFM24, sample 12222) and Baltic seawater compositions are shown for reference.

Sampling date	Drill water %	Charge bal %	Na (mg/L)	K (mg/L)	Ca (mg/L)	Mg (mg/L)	HCO3 (mg/L)	Cl (mg/L)	SO4 (mg/L)	Br (mg/L)	F (mg/L)	Si (mg/L)	Fe[1] (mg/L)	Fe-tot[2] (mg/L)	Fell (mg/L)	Sr (mg/L)	I (mg/L)	pH	DOC (mg/L)
30-Oct-06	3.55	-1.8	1410	29.1	731	151.0	169	3690	400	14.0	1.38	6.37	14.70	15.30	15.40	6.61	0.028	7.13	15.0
23-Oct-06	0.70	-0.8	1850	31.1	953	189.0	156	4730	494	18.0	1.31	6.71	6.88	7.26	7.24	8.80	0.030	7.34	3.5
12-Oct-06	0.50						148	4530										7.16	
18-Oct-06	1.00	-0.8	1680	31.4	931	185.0	160	4420	479	17.8	1.31	6.57	10.10	9.17	8.97	8.61	0.032	7.35	4.7
27-Oct-06	1.25	-1.7	1650	30.1	872	173.0	157	4340	462	16.2	1.35	6.33	11.70	12.50	12.40	8.25		7.31	4.3
16-Oct-06	1.25	-0.4	1630	32.5	969	193.0	155	4370	469	16.5	1.32	6.90	9.18	7.58	7.46	8.88		7.34	5.2
3-Nov-06	12.90						136	2960										7.50	
13-Nov-06	5.40	-1.6	1260	7.7	1070	21.5	19	3900	160	17.7	1.49	5.28	2.19	2.37	2.35	10.40	0.077	6.95	8.0
17-Nov-06	5.30	-1.3	1280	9.4	1050	32.0	32	3880	183	17.8	1.43	5.38	3.81	4.15	4.11	10.20	0.069	7.08	4.0
20-Nov-06	4.85	-0.7	1330	6.9	1110	24.7	19	3990	189	19.8	1.43	5.46	1.91	2.00	1.97	11.00	0.070	7.19	2.8
23-Nov-06	4.80	-0.9	1340	6.3	1110	23.9	21	4020	196	17.9	1.43	5.30	1.24	1.43	1.46	10.80		7.39	1.5
26-Nov-06	4.45	-0.7	1350	6.6	1130	29.6	21	4050	215	18.8	1.47	5.64	1.01	1.45	1.43	11.00	0.074	6.89	2.0
Drill water (HFM24)		-1.35	340	14.3	102	23.4	391	501	103										
Baltic sea water			1960	95	94	234	90	3760	325										

[1] Determined by ICP-AES

[2] Analysed spectrophotometrically

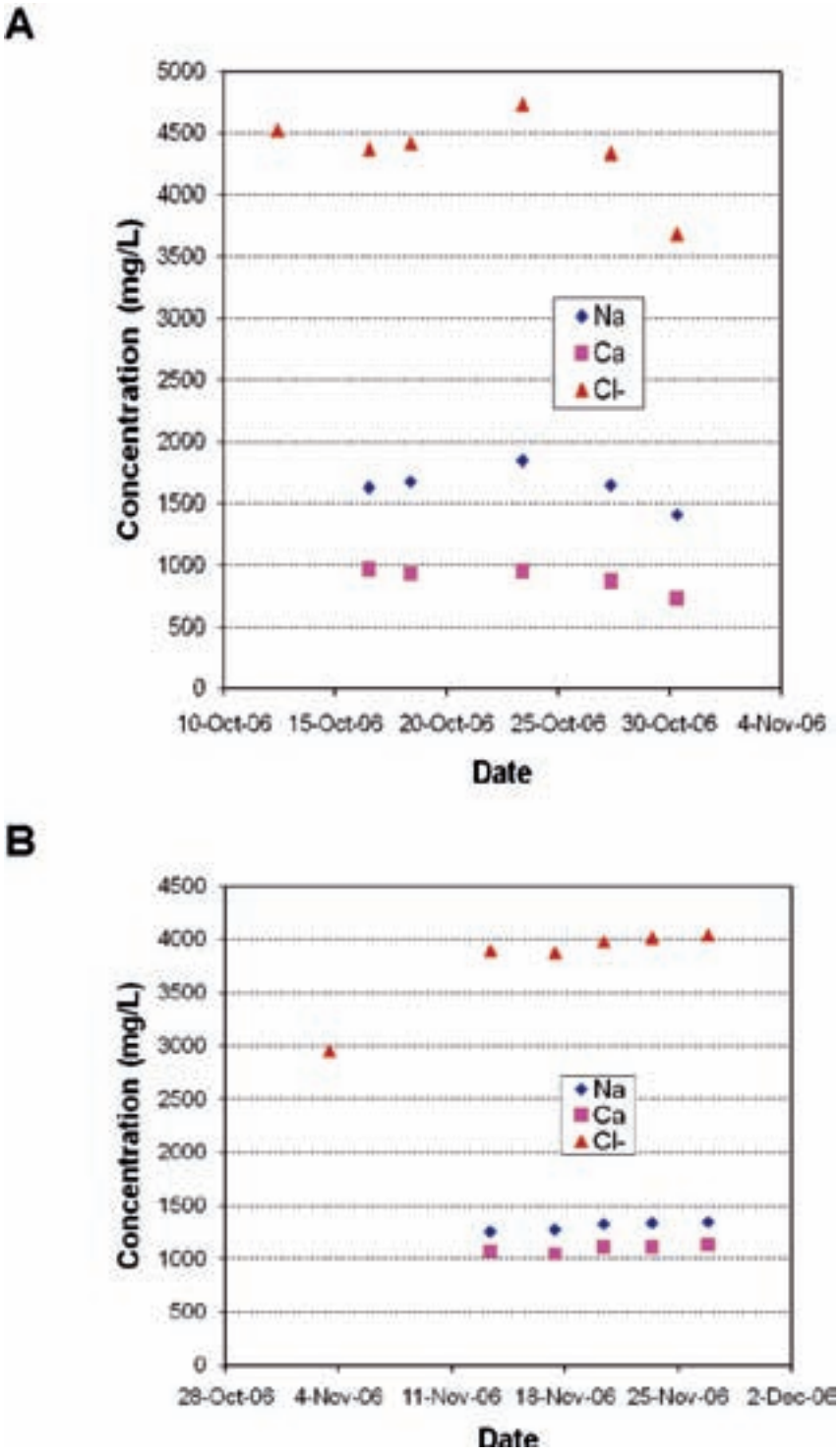

Figure 3-31. *Variation of major ions in groundwater from sections a) zone 290.0–305.5 and b) 478.0–487.5 m borehole length, borehole KFM10A*

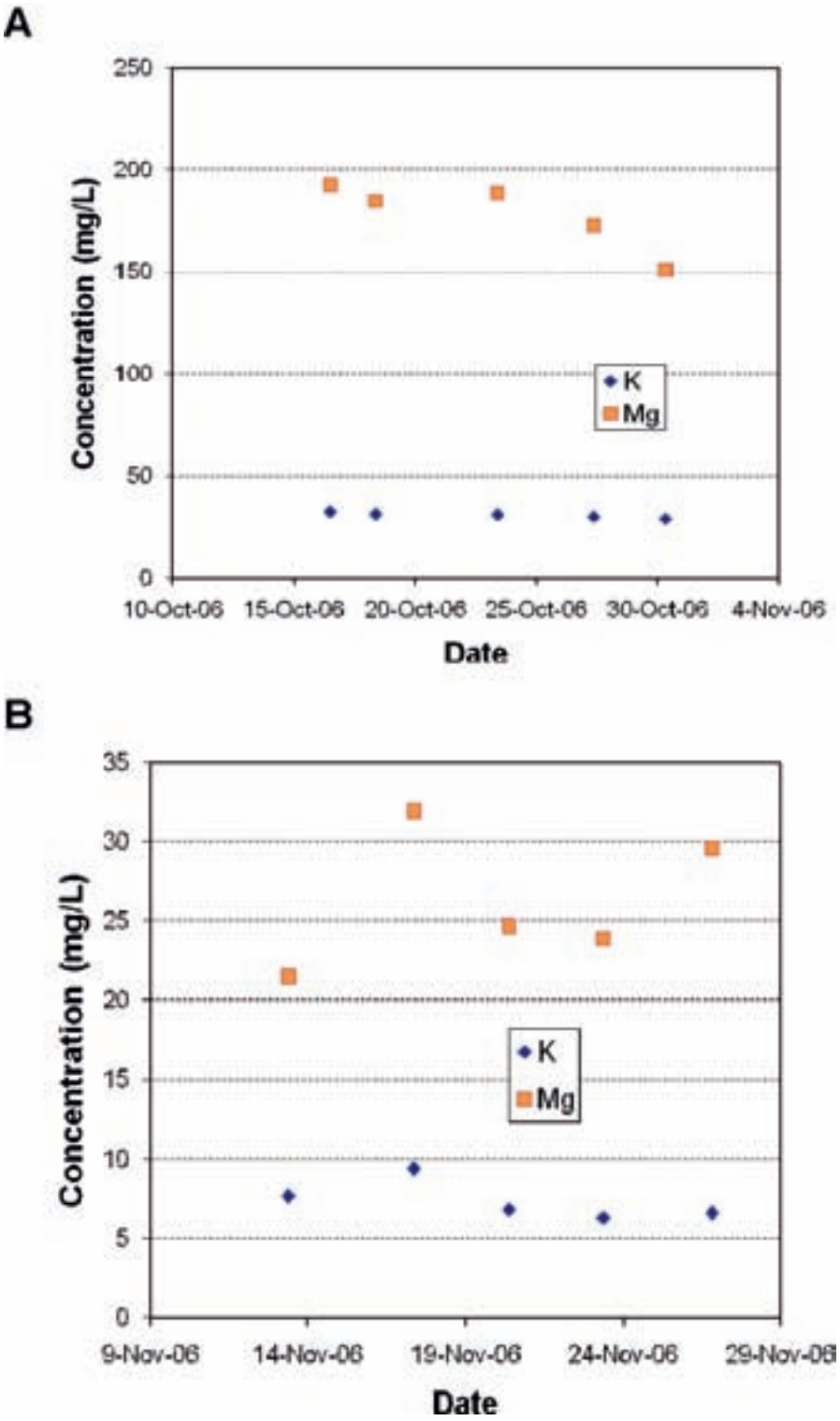

Figure 3-32. *Variation of minor cations in groundwater from sections a) zone 290.0–305.5 and b) 478.0–487.5 m borehole length, borehole KFM10A*

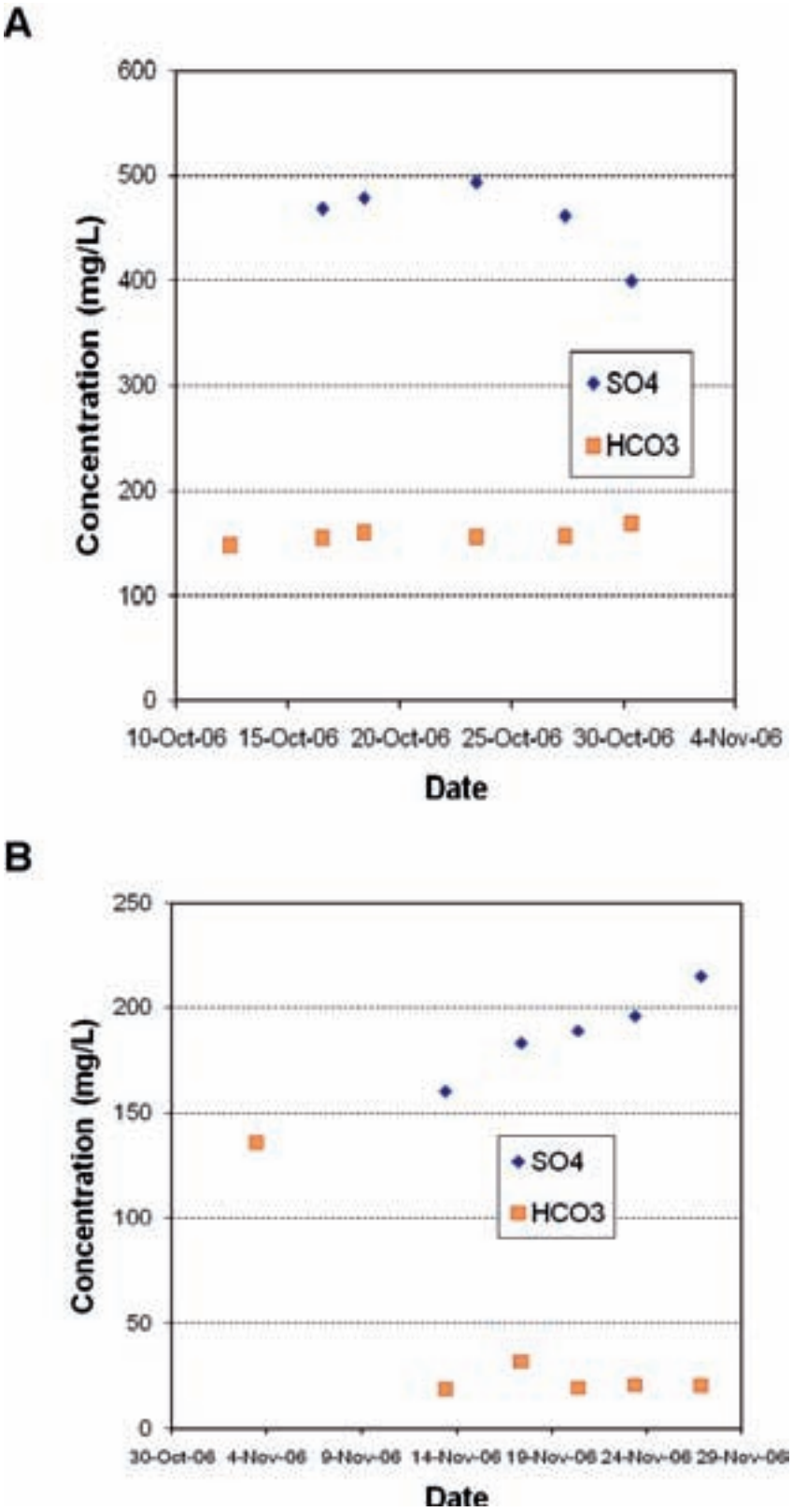

Figure 3-33. *Variation of minor anions in groundwater from sections a) zone 290.0–305.5 and b) 478.0–487.5 m borehole length, borehole KFM10A .*

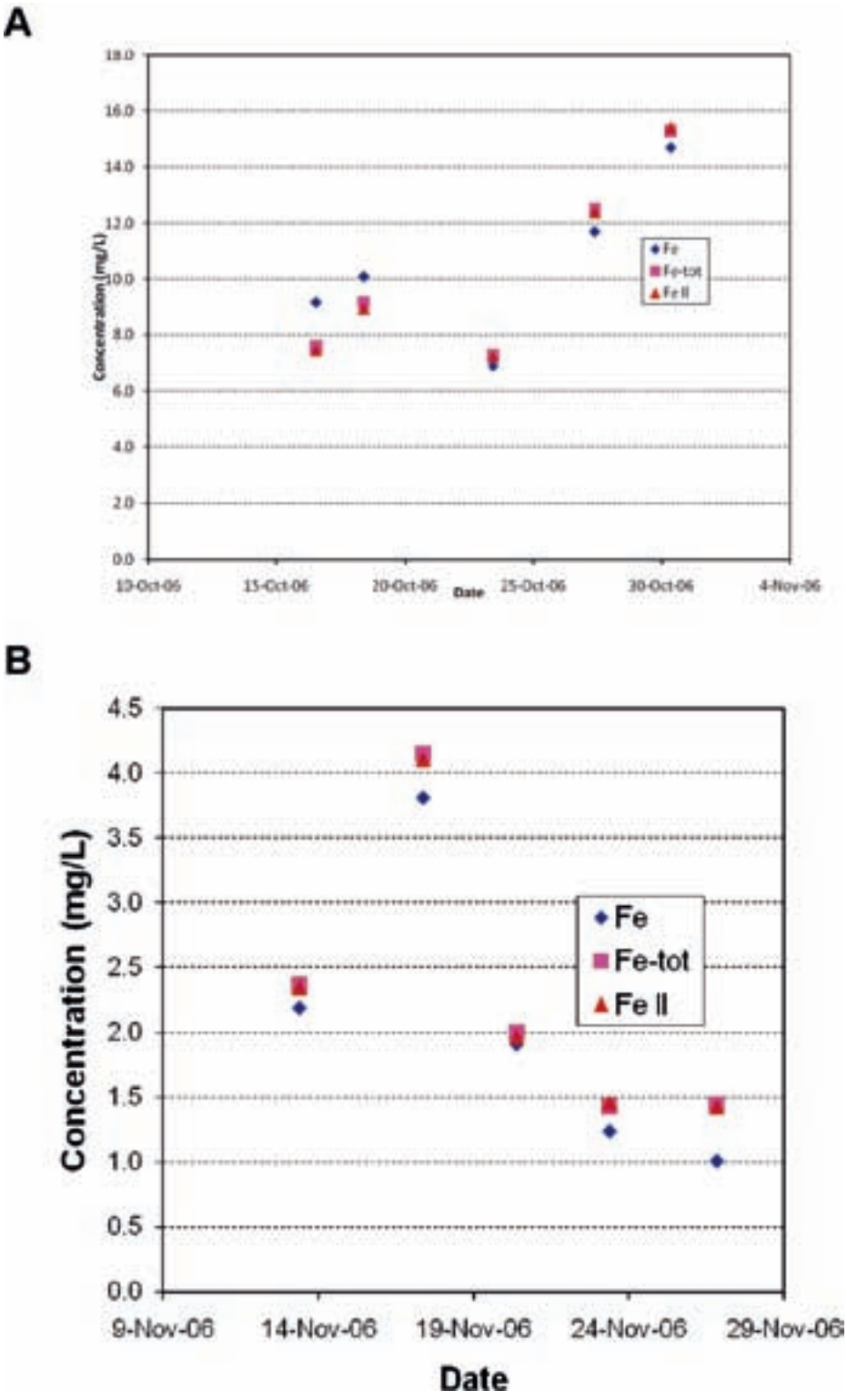

Figure 3-34. *Variation of Fe species in groundwater from sections a) zone 290.0–305.5 and b) 478.0–487.5 m borehole length, borehole KFM10A .*

4 Interpretation of DIS results

4.1 General aspects of tracing drilling water

The simple calculations performed above for uranine in drilling water and flushing water apply to the entire borehole, irrespective of the number, location and transmissivity of fractures intersected. When drilling has ended, it is important that a system of packers is installed as soon as possible to prevent cross-flow between permeable fractures at different depths. When first pumped for groundwater sampling, fractures that took drilling water will initially yield groundwater that has a composition similar to drilling water and most of the ambient groundwater will have been pushed back into the fracture system, driven by the pressure in the drill stem).

Depending on how much drilling water was ingested and other hydraulic characteristics of the fracture, the composition will change gradually, or rapidly, to that of a groundwater mixed with drilling water. From then on, further pumping should lower the concentration of tracer but the rate of lowering is not only dependent on the quantity that was injected but also on the extent of dilution by mixing. For instance, the injected water that has entered as an unbroken slug of water as it pushes the ambient groundwater ahead of it should, therefore, should return as the same. Alternatively, the injected water may have immediately split into several pathways in the bedrock and mixed with ambient groundwater before returning. Furthermore, the injected water may been subject to local hydraulic gradients and migrated away from the borehole, only returning under high pumping and drawdown conditions.

4.2 Determination of drilling water content and uncertainties

In the drilling performed at borehole KFM06, the loss of uranine tracer and the excess of return water over that injected into the borehole clearly shows that the water does not move as an unbroken slug into the permeable fracture. Instead, the dilution of tracer and the excess of return water show that the injected water is being diluted and approximately only 60% of the return water is made up of drilling water. This value can be obtained by gravimetric methods (i.e. measuring the *weights* of uranine injected and recovered). It is important to have a stable tracer concentration in the injected drilling water. The typical uncertainty in uranine concentrations is less than 5% for a single analysis but over the course of a drilling campaign (several months), may drift to 25% (see Figure 3-3, for example).

In the drilling of borehole KFM06, a constant uranine injection rate could not be maintained and the borehole was left open for one month during drilling. While the uranine concentration declined in almost a linear fashion from 24% to less than 2% in the deeper section (768–775 m), the upper section (353.5–360.6 m) showed an almost constant uranine concentration (~ 7%) and calculations showed that, despite its lower uranine content, a much larger volume of water (25–50 m^3 versus 8–28 m^3) still needs to be pumped from that section in order to reduce the uranine (and, hence, drilling water content) to acceptable levels.

An apparently similar profile of uranine concentrations was observed in KFM01D, in which uranine appeared to be lost to the fracture network but could be accounted for when the higher volume of discharged water was allowed for. However, in this case, the amount of return water closely matched injected volumes giving the anomalous result that more uranine was recovered than injected (approximately 5 to 10% more). Pumping during sampling caused a reduction in uranine from 9 to 6% in the shallow zone but there was no change in the deeper zone.

The results of pumping borehole KFM08A were similar to those of KFM01D in that volumes returned were comparable to those injected and concentrations of uranine in both cases were also similar. Only a ~ 5% loss of uranine to the fractures was calculated.

Anomalies were also found in the pumping and sampling of KFM10A in which considerably more uranine appeared to be withdrawn than was injected (the apparent gain was about 20 to 40%). These observations showed that rarely was uranine concentration ever reduced to zero by pumping during sampling but, instead, its concentrations might be variable with no obvious trend.

The calculations made in this report are based mainly on uranine measurements, which may be erroneous as reported by /Berg et al. 2005/. These calculations are also based on the volume of water injected at the time of drilling. During and after drilling, and during all the operations that occur in the borehole before sampling, waters of different sections can mix. These may make the DIS calculations very difficult. An estimate of contamination due to drilling can be made based only on the drilling data, as shown above. This should be regarded more as guidance for the sampling that follows.

As described in section 3.2.1, the variance in the uncertainty associated with the calculations is most likely due to selecting the appropriate average uranine concentrations and their variance, for the injected and return waters. Analytical error in the measurement of uranine concentration and possible changes in pH or ionic strength may also affect the fluorescence somewhat.

To improve the understanding of the hydrogeological system, it would be worthwhile monitoring the uranine concentration in return water during flushing (i.e. when injection due to drilling has ended and before pumping for sampling begins). This would indicate how much dilution of drilling water has occurred, how easily it can be removed and how extensively it has penetrated the fracture network.

4.3 Interpretation of hydrogeochemical data

The uranine data appear to show that there is no clear correlation of trend in uranine with trend in major ion concentration, except possibly for KFM01D (in which a decrease in uranine appears to follow a slightly decreasing trend of major ion). However, as noted above, this is the inverse to what might be expected (i.e. removal of uranine should cause major ions to increase if drilling water is dilute). Saline drilling water induced less changes in the groundwater chemistry simply because it is nearer the chemistry of the groundwater than are low salinity surface waters.

Most graphs of major ion concentrations (Na^+, Ca^{2+}, Cl^-) versus time showed remarkably constant concentrations during pumping for sampling, irrespective of uranine concentration or trend during pumping. Relative stability might be expected if a saline groundwater is used as a drilling water tracer rather than a fresh water (from rivers, lakes, etc). In two out of the four boreholes considered here (KFM06A, KFM08A), saline groundwaters, taken from nearby large diameter, shallow (0–100 m) boreholes, were used as drilling fluids. These fluids typically had the composition of Baltic seawater with some modifications in Ca^{2+}, Mg^{2+} and Cl^-. However, in Figures 3-6, 3-14, 3-23 and 3-31b, no zones showed an increased in major ion concentration (Na^+, Ca^{2+}, K^+ and Cl^-) as uranine was pumped out of the borehole zone during sampling. Only in Figure 3-31a is there a pronounced *decrease* in ion concentration, which may indicate removal of late-arriving groundwater.

The ions Mg^{2+}, HCO_3^- and SO_4^{2-} are more variable, showing clear trends of increase or decrease during pumping. These changes may be due to mixing with residual Littorina seawater and/or drilling water and, may result from changes in redox conditions as seen in the clear trends of Fe species.

One further variable that may affect uranine recovery is the presence of dissolved organic carbon in the drilling water (see DOC data in Tables 3-3, 3-4, 3-5 and 3-6). Because shallow waters used in drilling tend to be enriched in DOC (measured here as total organic carbon, TOC), it is possible that these organics mask some of the uranine by interfering with its fluorescence. To attempt to minimize this effect when drilling, the injection water is passed through a UV light irradiator before entering the drill string. However, it is likely that this does not completely oxidise the organics because of the large volume to be treated and the high flow rate (Ann-Chatrin Nilsson, pers. comm.). The possibility that the organics may have their own natural fluorescence which would augment the fluorescence of uranine (thus accounting for > 100% recovery of uranine in two of the tested zones) has also been examined (Ann-Chatrin Nilsson, pers. comm.) but DOC was not found to contribute any significant amount of fluorescence.

5 Conclusions

The Drilling water Impact Study has shown the following:

- by calculating the drilling water volume lost in the fractures during drilling, it is possible to determine how much water should be pumped out from the section before sampling. This type of water balance could help and guide the sampling,
- when the uranine measurements are correct and reliable (for example when the metering system works correctly), the uranine dilution can be calculated, allowing a better estimation of the volume to be removed from the fractures. This also can guide and help the sampling,
- the content of drilling water if higher than 5% may sometimes disqualify a sample. By checking the variability of the chemical parameters, additional information may be gained. For example, if the chemistry is stable, a sample with 7% drilling water could be considered representative,
- the EC from the DIFF measurements will be used in order to check the variability in the sections.

Pumping for groundwater sampling, after drilling and flushing is complete, has not always shown a decline in uranine concentration, as might be expected. Three out of the seven zones tested in this study showed that uranine levels decreased as water was removed but the remaining four zones either remained fairly stable or actually *increased in uranine concentration* as water was pumped. There appears to be no relationship with depth of zone (plotted here as length along the borehole). It might be expected that the lower permeablity sections, which are typically found at depth, would show clearer trends, but this is not the case.

The correlation of trends in uranine content of drilling water with expected trends in ionic species has also not been clearly and reproducibly seen in this study, Instead, the tendency has been for major ion (Na^+, Ca^{2+}, Cl^-) concentrations to remain constant or only slightly changing (sometimes in the wrong direction) as uranine content changes in response to pumping. Minor ions (in particular, Mg^{2+} and SO_4^{2-}) are more prone to vary and this may be due to various extents of mixing with residual Littorina seawater that is postulated to exist in the upper ~ 500 m in the Forsmark area.

The unpredictable nature of uranine recovery and the expected declining trend when pumping during chemical sampling, have not been consistently seen in this study of seven zones in Forsmark boreholes. Part of the lack of coincident trends may be due to the use of saline water as a drilling fluid (in two out of the four boreholes). Saline drilling fluids would tend to suppress the range over which any correlation is seen. However, examination of the zones in boreholes drilled with dilute waters (KFM01D and KFM10A) shows no improvement in the extent of agreement between trends in the uranine and chemical profiles.

It might be concluded from this study that the use of uranine as a drilling water tracer and chemical indicator will not give consistent results. However, the following factors may impede the success of uranine as a drilling water tracer:

1. Use of a drilling water that has a composition close to saline water at ~ 500 m depth.
2. Problems inherent in monitoring tracer injection and withdrawal.
3. The practice of leaving borehole zones open to each other between testing periods.
4. The possibility of non-conservative behaviour of uranine (interaction with clays, dissolved organics, etc).

Despite the above problems, the use of uranine as a conservative drilling water tracer should be continued so that a more extensive database of its behaviour can be assembled. Correlation of uranine trends with those seen in hydrochemical data may help to resolve some of these difficulties, especially if dilute drilling fluids can be used. It is clear though, that uranine concentration

is not an ideal parameter on which to base acceptance or rejection of a suite of chemical analyses in groundwater, for use in calibrating hydrochemical and hydrogeological models. Stability of dissolved ion concentration is at least equally important as a guide and this approach is used for determining representative groundwater samples (John Smellie, pers. comm.).

6 References

Berg C, Wacker P, Nilsson A-C, 2005. Forsmark Site Investigation: Chemical characterisation in borehole KFM06A. SKB P-05-178, Svensk Kärnbränslehantering AB.

Berg C, Bergelin A, Wacker P, Nilsson A-C, 2006. Forsmark Site Investigation: Chemical characterisation in borehole KFM08A. SKB P-06-63, Svensk Kärnbränslehantering AB.

Bergelin A, Lindquist A, Nilsson K, Nilsson A-C, 2007. Forsmark Site Investigation: Hydrochemical characterisation in borehole KFM10A. SKB P-07-42, Svensk Kärnbränslehantering AB.

Davis S N, 1985. Ground Water Tracers, NWWA, Worthington, Ohio.

Gascoyne M, Gurban I, 2007. Memorandum on the Drilling Impact Study, Techn. Memo. Unpublished report to ChemNet, March 2007.

Gurban I, Laaksoharju M, 2002. Drilling Impact Study (DIS); Evaluation of the influences of drilling, in special on the changes on groundwater parameters. SKB report PIR-03-02, Svensk Kärnbränslehantering AB.

Nilsson K, Bergelin A, Lindquist A, 2006. Forsmark Site Investigation: Hydrochemical characterisation in borehole KFM01D. SKB P-06-227, Svensk Kärnbränslehantering AB.

Section 4

Analytical uncertainties

Ann-Chatrin Nilsson, Geosigma AB

Contents

1 Introduction

The hydrochemical data generated from the site investigation programme in Forsmark constitute the following four types:

1. Data from chemical analyses.
2. Data from long term on-line measurements in flow through cells (Chemmac measurements).
3. Data from field measurements in surface waters and near surface groundwaters.
4. Special studies or experiments

This quality evaluation assesses the chemical analyses performed by SKB laboratories (Äspö chemical laboratory and the mobile field laboratory at the Forsmark site) and by contracted external laboratories. Analytical methods and reported measurement uncertainties are presented in Chapter 2. A detailed general description concerning sampling methods, sample preparation and analytical methods is given in /Nilsson A-C 2005/.

The discussions in this document focus on some selected constituents of special importance for hydrochemical interpretations and modelling as well as on methods/constituents that have been questioned or are known, from experience, to be somewhat unreliable.

Of first concern, when interpreting the hydrogeochemical data, is contamination by drilling water in the groundwater samples. Not only the reliability of the uranine analyses (the dye used to trace the drilling water) and the size of the analytical errors, but also other conditions affect the confidence in the drilling water budget calculations as well as in drilling water contents in water samples and indirectly the judgement of sample quality/representativity /see Smellie et al. 2008/.

Second, there is a need to establish a consistent set of major constituents (mainly Na, Ca, Cl, SO_4 and possibly Mg and HCO_3) for each sample.

Of fundamental importance are also the reliability of data for constituents and parameters that are indicators of groundwater origin (especially magnesium, bromide and oxygen-18) or constituents and parameters that are of importance in order to understand redox conditions (such as iron and sulphide). The sulphide concentration is also a critical parameter for safety assessment evaluations /SKB 2006/.

2 Measurement uncertainties, detection limits and reporting limits

An updated list of analytical methods, reporting limits and general measurement uncertainties as reported from the contracted laboratories at present are displayed in Table 2-1. The uncertainties are included as error bars in the diagrams displayed in the following chapters.

Measurement uncertainties were reported as general estimates as well as separate values stated for each reported concentration value. General advance estimates of measurement uncertainties for different components were reported from the contracted laboratories at the start of the site investigations in 2002. Only a few changes/modifications of methods or changes of laboratories have occurred during the site characterisation period. However, despite this, reported general measurement uncertainties have varied from time to time for several constituents. Generally, the uncertainties have increased due to a more critical approach and change of estimation method according to more recently established and internationally accepted methods.

For example, the general measurement uncertainties for different ICP analyses reported after 2005 were generally about twice as high as the initially reported ones. These extended measurement uncertainties were reported for concentrations ten times and one hundred times the reporting limits and sometimes also for three different salinity ranges (ICP SFMS). The

values in Table 2-1 are selected to represent the most relevant bedrock groundwater conditions. However, the major concentrations in groundwaters were often much higher than one hundred times the reporting limit.

For evaluation and modelling purposes, the separate/individual measurement uncertainties as reported for each concentration value were difficult to handle. The data volume is very large and to work with separate uncertainty values would be very time consuming. Furthermore, the SICADA database does not support storage of these separate uncertainties yet and many data software for modelling and evaluation purposes lacks the possibility to include them. General estimates for each component were more suitable to use. However, the laboratories use somewhat different methods for their estimation and some of the uncertainties seem overestimated compared to the observations from trend plots and other consistency checks. The uncertainties might be valid in the case of only one sample but with a large number of samples at hand the reliability increases.

The concentration values were, most often, reported down to the limit of quantification (10×std). However, some anion analyses performed by SKB were reported down to the detection limit (3×std) in order to facilitate further interpretations.

Table 2-1. Methods, reporting limits and measurement uncertainties (updated 2008).

Component	Method[1]	Reporting limits (RL), detection limits (DL) or range[2]	Unit	Measurement uncertainty[3]
pH	Potentiometric	3–10	pH unit	±0.1
EC	Electrical Conductivity meas.	1–150 150–10,000	mS/m	5% 3%
HCO_3	Alkalinity titration	1	mg/L	4%
Cl^- Cl^-	Mohr-titration IC	≥ 70 0.5–70	mg/L	5% 8%
SO_4	IC	0.5	mg/L	12%
Br^-	IC	DL 0.2, RL 0.5	mg/L	15%
Br	ICP SFMS	0.001, 0.004, 0.010[4]	mg/L	25%[5]
F^- F^-	IC Potentiometric	DL 0.2, RL 0.5 DL 0.1, RL 0.2	mg/L	13% 12%
I^-	ICP SFMS	0.001, 0.004, 0.010[4]	mg/L	25%[5]
Na	ICP AES	0.1	mg/L	13%
K	ICP AES	0.4	mg/L	12%
Ca	ICP AES	0.1	mg/L	12%
Mg	ICP AES	0.09	mg/L	12%
S(tot)	ICP AES	0.16	mg/L	12%
Si(tot)	ICP AES	0.03	mg/L	14%
Sr	ICP AES	0.002	mg/L	12%
Li	ICP AES	0.004	mg/L	12.2%
Fe	ICP AES	0.02	mg/L	13.3%[6]
Fe	ICP SFMS	0.0004, 0.002, 0.004[4]	mg/L	20%[6]
Mn	ICP AES	0.003	mg/L	12.1%[5]
Mn	ICP SFMS	0.00003, 0.00004, 0.0001[4]	mg/L	53%[6]
Fe(II), Fe(tot)	Spectrophotometry	DL 0.006, RL 0.02	mg/L	0.005 (0.02–0.05 mg/L) 9% (0.05–1 mg/L) 7% (1–3 mg/L)
HS^-	Spectrophotometry, SKB	SKB DL 0.006, RL 0.02	mg/L	25%

Component	Method[1]	Reporting limits (RL), detection limits (DL) or range[2]	Unit	Measurement uncertainty[3]
HS^-	Spectrophotometry, external laboratory	0.01	mg/L	0.02 (0.01–0.2 mg/L) 12% (> 0.2 mg/L)
NO_2 as N	Spectrophotometry	0.1	µg/L	2%
NO_3 as N	Spectrophotometry	0.2	µg/L	5%
NO_2+NO_3 as N	Spectrophotometry	0.2	µg/L	0.2 (0.2–20 µg/L) 2% (> 20 µg/L)
NH_4 as N	Spectrophotometry, SKB	11	µg/L	30% (11–20 µg/L) 25% (20–50 µg/L) 12% (50–1,200 µg/L)
NH_4 as N	Spectrophotometry external laboratory	0.8	µg/L	0.8 (0.8–20 µg/L) 5% (> 20 µg/L)
PO_4 as P	Spectrophotometry	0.7	µg/L	0.7 (0.7–20 µg/L) 3% (> 20 µg/L)
SiO_4	Spectrophotometry	1	µg/L	2.5% (> 100 µg/L)
O_2	Iodometric titration	0.2–20	mg/L	5%
Chlorophyll a, c pheopigment[7]	/1/	0.5	µg/L	5%
PON[7]	/1/	0.5	µg/L	5%
POP[7]	/1/	0.1	µg/L	5%
POC[7]	/1/	1	µg/L	4%
Tot–N[7]	/1/	10	µg/L	4%
Tot–P[7]	/1/	0.5	µg/L	6%
Al,	ICP SFMS	0.2, 0.3, 0.7[4]	µg/L	17.6%[6]
Zn	ICP SFMS	0.2, 0.8, 2[4]	µg/L	15.5, 17.7, 25.5%[6]
Ba, Cr, Mo,	ICP SFMS	0.01, 0.04, 0.1[4]	µg/L	Ba 15%[4], Cr 22%[5] Mo 39%[6]
Pb	ICP SFMS	0.01, 0.1, 0.3[4]	µg/L	15%[6]
Cd	ICP SFMS	0.002, 0.02, 0.5[4]	µg/L	15.5%[6]
Hg	ICP AFS	0.002	µg/L	10.7%[6]
Co	ICP SFMS	0.005, 0.02, 0.05[4]	µg/L	25.9%[6]
V	ICP SFMS	0.005, 0.03, 0.05[4]	µg/L	18.1%[6]
Cu	ICP SFMS	0.1, 0.2, 0.5[4]	µg/L	14.4%[6]
Ni	ICP SFMS	0.05, 0.2, 0.5[4]	µg/L	15.8%[6]
P	ICP SFMS	1, 5, 40[4]	µg/L	16.3%[6]
As	ICP SFMS	0.01 (520 mS/m)	µg/L	59.2%[6]
La, Ce, Pr, Nd, Sm, Eu, Gd, Tb, Dy, Ho, Er, Tm, Yb, Lu	ICP SFMS	0.005, 0.02, 0.05[4]	µg/L	20%, 20%, 25%[6]
Sc, In, Th	ICP SFMS	0.05, 0.2, 0.5[4]	µg/L	25%[6]
Rb, Zr, Sb, Cs	ICP SFMS	0.025, 0.1, 0.25[4]	µg/L	15%, 20%, 20%[5] 25%[6]
Tl	ICP SFMS	0.025, 0.1, 0.25[4]	µg/L	14.3%[5 and 6]
Y, Hf	ICP SFMS	0.005, 0.02, 0.05[4]	µg/L	15%, 20%, 20%[5] 25%[6]
U	ICP SFMS	0.001, 0.005, 0.01[4]	µg/L	13.5%, 14.3%, 15.9%[5] 19.1%, 17.9%, 20.9%[6]
DOC	UV oxidation, IR Carbon analysator	0.5	mg/L	8%
TOC	UV oxidation, IR Carbon analysator	0.5	mg/L	10%
δ^2H	MS	2	‰ SMOW[8]	0.9 (one standard deviation)

Component	Method[1]	Reporting limits (RL), detection limits (DL) or range[2]	Unit	Measurement uncertainty[3]
$\delta^{18}O$	MS	0.1	‰ SMOW[8]	0.1 (one standard dev.)
^{3}H	LSC	0.8	TU[9]	0.8
$\delta^{37}Cl$	A (MS)	0.2	‰ SMOC[10]	0.2[17]
$\delta^{13}C$	A (MS)	–	‰ PDB[11]	0.3[17]
^{14}C pmc	A (MS)	–	PMC[12]	0.4[17]
$\delta^{34}S$	MS	0.2	‰ CDT[13]	0.4 (one standard dev.)
$^{87}Sr/^{86}Sr$	TIMS	–	No unit (ratio)[14]	0.00002
$^{10}B/^{11}B$	ICP SFMS	–	No unit (ratio)[14]	–
^{234}U, ^{235}U, ^{238}U, ^{232}Th[2], ^{30}Th	Alfa spectr.	0.0001	Bq/L[15]	≤ 5% (Counting statistics uncertainty)
^{222}Rn, ^{226}Ra	LSS	0.015	Bq/L	≤ 5% (Count. stat. uncert.)

1. Many elements may be determined by more than one ICP technique depending on concentration range. The most relevant technique and measurement uncertainty for the concentrations normally encountered in groundwater are presented. In cases where two techniques were frequently used, both are displayed.

2. Reporting limits (RL), generally 10×standard deviation, if nothing else is stated. Measured values below RL or DL are stored as negative values in SICADA (i.e. –RL value and –DL value).

3. Measurement uncertainty reported by the laboratory, generally as ± percent of measured value in question at 95% confidence interval.

4. Reporting limits at electrical cond. 520 mS/m, 1,440 mS/m and 3,810 mS/m respectively.

5. Measurement uncertainty at concentrations 100×RL.

6. Measurement uncertainty at concentrations 10×RL.

7. Determined only in surface waters. PON, POP and POC refers to Particulate Organic Nitrogen, Phosphorous and Carbon, respectively.

8. Per mille deviation[16] from SMOW (Standard Mean Oceanic Water).

9. TU=Tritium Units, where one TU corresponds to a tritium/hydrogen ratio of 10^{-18} (1 Bq/L Tritium = 8.45 TU).

10. Per mille deviation[16] from SMOC (Standard Mean Oceanic Chloride).

11. Per mille deviation[16] from PDB (the standard PeeDee Belemnite).

12. The following relation is valid between pmC (percent modern carbon) and Carbon-14 age: $pmC = 100 \times e^{((1,950-y-1.03t)/8,274)}$ where y = the year of the C-14 measurement and t = C-14 age.

13. Per mille deviation[16] from CDT (the standard Canyon Diablo Troilite).

14. Isotope ratio without unit.

15. The following expressions are applicable to convert activity to concentration, for uranium-238 and thorium-232: 1 ppm U = 12.4 Bq/kg^{238}U, 1 ppm Th = 3.93 Bq/kg^{232}Th.

16. Isotopes are often reported as per mill deviation from a standard. The deviation is calculated as: $\delta^{y}I = 1,000\times(K_{sample}-K_{standard})/K_{standard}$, where K= the isotope ratio and $^{y}I = {}^{2}H$, ^{18}O, ^{37}Cl, ^{13}C or ^{34}S etc.

17. SKB estimation from duplicate analyses by the contracted laboratory.

3 Reliability of drilling water contents

The determination of drilling water contents in water samples was based on analyses of the dye uranine which was used to trace the drilling water (nominal concentration 0.2 mg/L) during drilling of the cored boreholes. Samples for uranine analyses were collected at different occasions and for the following purposes:

1. To check the stability of the automatic dosing of uranine to the drilling water used during drilling and to determine the drilling water content in the return water in order to calculate a drilling water budget from drilling the borehole, see Table 3-1.

2. To monitor changes in the drilling water content during borehole clean up pumping and nitrogen flushing (N_2 class 2 quality) conducted in order to decrease the drilling water content in the boreholes prior to hydrogeochemical investigations.
3. To determine the drilling water content in the water samples collected during the subsequent hydrogeochemical investigations.

The fluorescence method used to determine the uranine concentration is straightforward and quite reliable down to about 0.3 μg/L, corresponding to 0.15% drilling water. However, factors other then analytical errors may obstruct the different interpretations.

Additional fluorescence from organic constituents in the groundwater has been reported as a source of errors. Two tests were conducted in order to check the effect of groundwater organics on the measured uranine concentration;

- Fluorescence measurements in several blanks consisting of near surface groundwater samples with varying and high contents of TOC (Total Organic Carbon) see Table 3-2.
- Uranine was added at a concentration of 10 μg/L to different waters with TOC concentrations in the range usually encountered in the sampled groundwaters. The fluorescence was measured before and after the additions and the corresponding uranine concentrations were recorded, see Table 3-3. The observed interference from TOC was not linear. The reason may be that organic constituents in the different samples do not have the same fluorescent properties.

Table 3-1. Uranine additions to drilling water, uranine recovery from return water and drilling water budget from core drilling.

Borehole ID code	Weighed amount of uranine added to drilling water (g)	Average* uranine conc. and standard deviation in drilling water (mg/L)	Estimated amount of uranine in drilling water** (g)	Estimated amount of uranine recovered in return water** (g)	Estimated volume of drilling water remaining in the bore-hole after drilling (m^3)
KFM01A	–	0.194±0.014	186 (64 samples)	142 (63 samples)	220***
KFM01D	177	0.214±0.017	165 (108 samples)	185 (80 samples)	~ 0
KFM02A	250	0.223±0.111	252 (61 samples)	230 (61 samples)	100
KFM03A	139	0.147±0.070	106 (63 samples)	91.1 (64 samples)	240
KFM04A	165	0.089±0.093	88 (74 samples)	145 (151 samples)	100
KFM05A	170	0.171±0.075	185 (125 samples)	175 (125 samples)	~ 0
KFM06A	200	0.193±0.036	210 (125 samples)	122 (125 samples)	400
KFM07A	255	0.213±0.016	239 (116 samples)	181(120 samples)	370
KFM08A	234	0.200±0.014	240 (114 samples)	223 (114 samples)	55
KFM08D	197	0.203±0.023	179 (126 samples)	121 (126 samples)	380
KFM09A	138	0.161±0.039	138 (92 samples)	0.15 (92 samples, no air lift pumping)	860
KFM10A	95	0.174±0.041	84 (80 samples)	116 (80 samples)	~ 0
KFM11A	195	0.165±0.023	160 (121 samples)	244 (121 samples)	~ 0
KFM12A	98	0.163±0.029	80 (58 samples)	61 (58 samples)	185

* Average and std. as calculated from the number of samples given in next column.
** The amount of uranine is calculated using total volumes of drilling water and return water together with the average uranine concentrations from the number of samples given within parentheses.
*** The resulting volume is not realistic since the yield of water from the borehole itself is extremely small and the volume of return water pumped out is somewhat larger than the volume introduced. The conclusion was drawn from the uranine budget that more frequent sampling was needed in order to obtain more precise information.

Table 3-2. Fluorescence measurements – analyses of near surface groundwater samples with uranine concentration=zero at high and varying TOC concentrations (Total Organic Carbon).

Idcode	Water type	TOC (mg/L)	Corresponding uranine concentration (µg/L) from blank fluorescence
SFM0087	Near surface groundwater	19.7	0.7
SFM0095	Near surface groundwater	20.0	1.2
SFM0032	Near surface groundwater	20.9	1.0
SFM0037	Near surface groundwater	22.9	1.3
SFM0049	Near surface groundwater	23.3	0.7
SFM0001	Near surface groundwater	24.6	1.0
SFM0102	Near surface groundwater	125	3.5

Table 3-3. Analyses of uranine standard solutions (10 µg/L) prepared from waters with different TOC concentrations.

Idcode	Water type	TOC (mg/L)	Corresponding uranine (µg/L) from blank fluorescence	Recovery, 10 µg/L uranine
–	Deionised water	0–0.5	0 (adjusted to zero)	9.9
HFM27	Groundwater	5	0.7	9.7
HFM01	Groundwater	10	0.6	10.9
HFM16	Groundwater	13	1.0	10.6
PFM000074	Lake water	20	0.3	9.8

From the tests it was concluded that the effect from TOC is relatively small and most often negligible. Factors that are more likely to interfere with drilling water interpretations are;

- Unstable/inhomogeneous uranine concentration in drilling water injected into the borehole. The average uranine concentrations and standard deviations in the drilling water samples collected during drilling are given for each borehole in Table 3-1.
- Inadequate mixing prior to sampling of drilling water for uranine analyses and therefore inhomogeneous uranine concentration. The uranine concentration in the drilling water injected into the borehole will seem to vary more than is really the case.
- Too few samples or bias in the sampling (i.e. all samples collected at the same drilling situation - for example just after core retrieval) may result in unrepresentative average uranine concentrations for the drilling water injected into the borehole and for the return water withdrawn from the borehole. Sampling of return water with a highly varying content of drilling water is especially critical in order to obtain a consistent drilling water budget.

The weighed total amount of uranine added to each borehole is known from borehole logs. These values, together with the calculated/estimated amount of uranine added and withdrawn from each borehole, are given in Table 3-1. The comparison reveals the large uncertainties in the estimated values (calculated from average uranine concentrations and accumulated water volumes).

4 Quality of basic water analyses

Major constituents

In order to establish a consistent set of major constituent concentrations (mainly Na, Ca, Cl, SO_4 and possibly Mg and HCO_3) for each sample, the first step was to compare chloride concentrations and electrical conductivity values in x–y diagrams. The diagram in Figure 4-1 includes chloride concentrations and EC values (field-EC or lab-EC) as reported in SKB database SIMON. The diagram shows that the main part of the 1,790 data points follow the trend line and indicate that the EC and chloride data sets are quite consistent.

The relative charge balance gives an indication of the quality and uncertainty of the analyses of the major ions and, together with the chloride – EC correlation; they were used to verify that the concentrations of the most dominating ions were consistent. The errors, as calculated for each one of the 1,790 samples in SKB database SIMON, very seldom exceeded the acceptable limits ± 5% (8 samples) and ± 10% (11 samples) for groundwater and dilute surface waters, respectively.

Magnesium

Magnesium was determined by ICP-AES (Inductively Coupled Plasma Atomic Emission Spectrometry) and doublet analyses were conducted for a minor part of the samples (85 samples) by a second laboratory. The agreement between the reported concentrations from the two laboratories was not always satisfactory, see Figure 4-2. Despite of this, the selected magnesium concentrations (exclusively lab 1) were regarded as fully reliable and of good quality. Generally, lab 2 was less familiar with the type of saline groundwater samples addressed. Also in the cases of iron and sulphur analyses, see below, the results from lab 2 deviated and here the results from lab 1 were confirmed by a second method.

Sulphate

Sulphate and elemental sulphur were determined regularly in every sample by Ion Chromatography (IC) and ICP-AES, respectively. Doublet ICP analyses of elemental sulphur were performed by a second laboratory (lab 2) for a minor part of the samples, see Figure 4-3. Generally, the agreement between the IC and the ICP-AES results by the regular laboratories was quite good but the reported results from the checking laboratory show more deviation.

The ICP-AES analyses of sulphur were severely affected by the presence of sulphide at high concentrations in a few samples and those results were rejected. The effect is due to hydrogen sulphide gas entering the plasma.

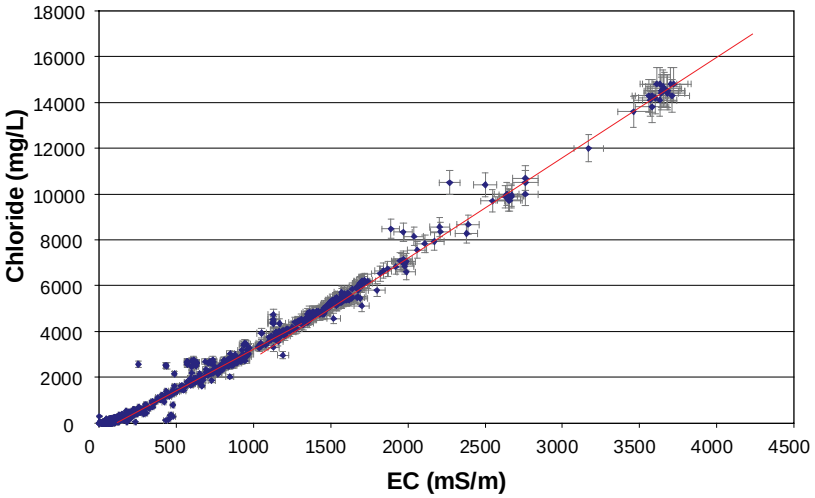

Figure 4-1. *Chloride concentrations plotted versus EC values (SKB database SIMON).*

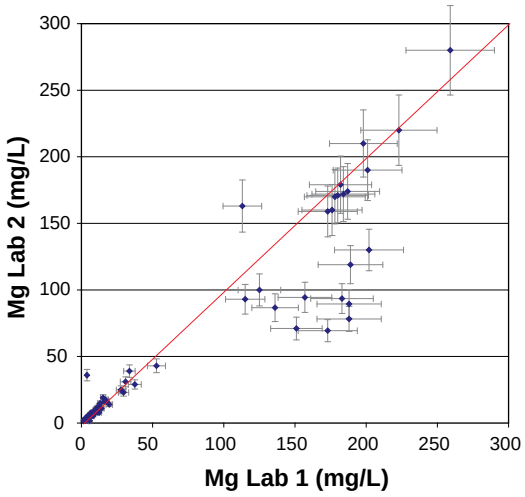

Figure 4-2. *Comparison of magnesium concentrations (ICP) reported by the regular laboratory (lab 1) and the checking laboratory (lab 2). 85 doublet analyses.*

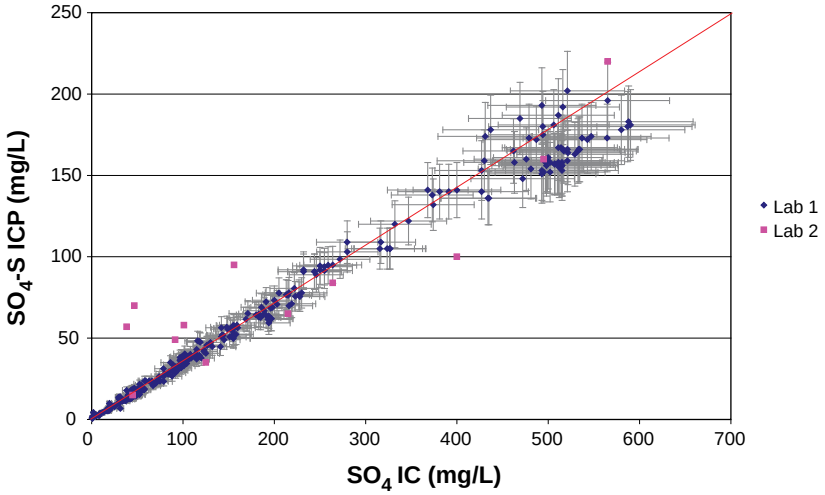

Figure 4-3. *Comparison of sulphur by the ICP-AES technique (two laboratories) and sulphate by IC. Without significant contribution of other sulphur species, 3×SO_4-S by ICP should correspond to SO_4 by IC.*

Bromide

The bromide concentrations obtained by IC were often and systematically too high at high chloride concentrations due to a contribution from the chloride peak. Another drawback with the method is the relatively high detection limit (0.2 mg/L). The bromide concentrations in many surface waters measured below or close to the detection limit. For these reasons, complementary analyses of bromine by the ICP-SFMS technique were performed rather frequently in order to check and verify the bromide results. Some obviously erroneous results have been reported also from the ICP-SFMS method.

A comparison of the analytical results by ion chromatography (IC) and by ICP-SFMS is presented in Figure 4-4. As demonstrated, the IC analyses of bromide were often higher, especially at high concentrations and the spread is considerable. Selected bromide/bromine values (often the ICP-SFMS results) for each sample are plotted versus the corresponding chloride concentrations in Figure 4-5 as a rough consistency check. The data points form two clear trends (mixing lines) and most points do not differ too much from these trend lines. The two different trends correspond to marine and non-marine origin, respectively. The bromide analyses, whatever analytical method used, were impaired by larger uncertainty than most other major constituents.

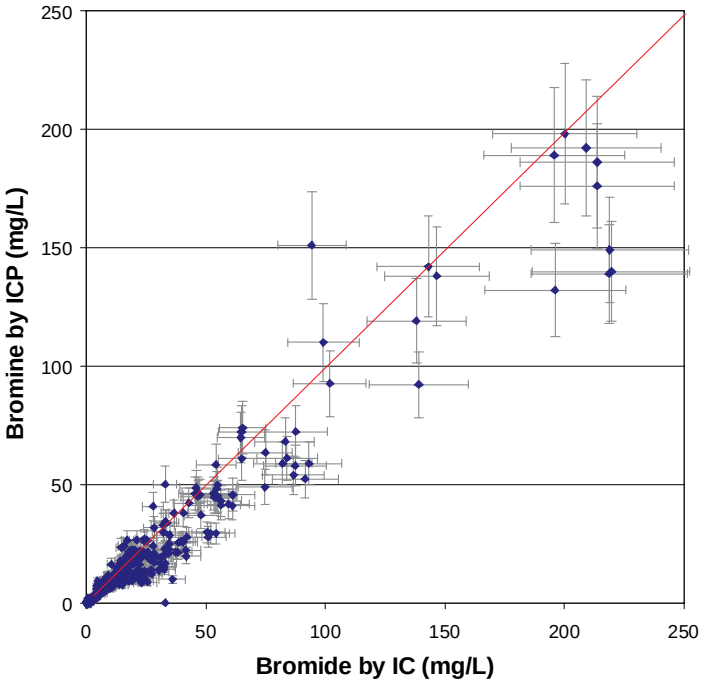

Figure 4-4. *Comparison of bromine by ICP technique and bromide by ion chromatography. The error bars correspond to 15% (IC and ICP).*

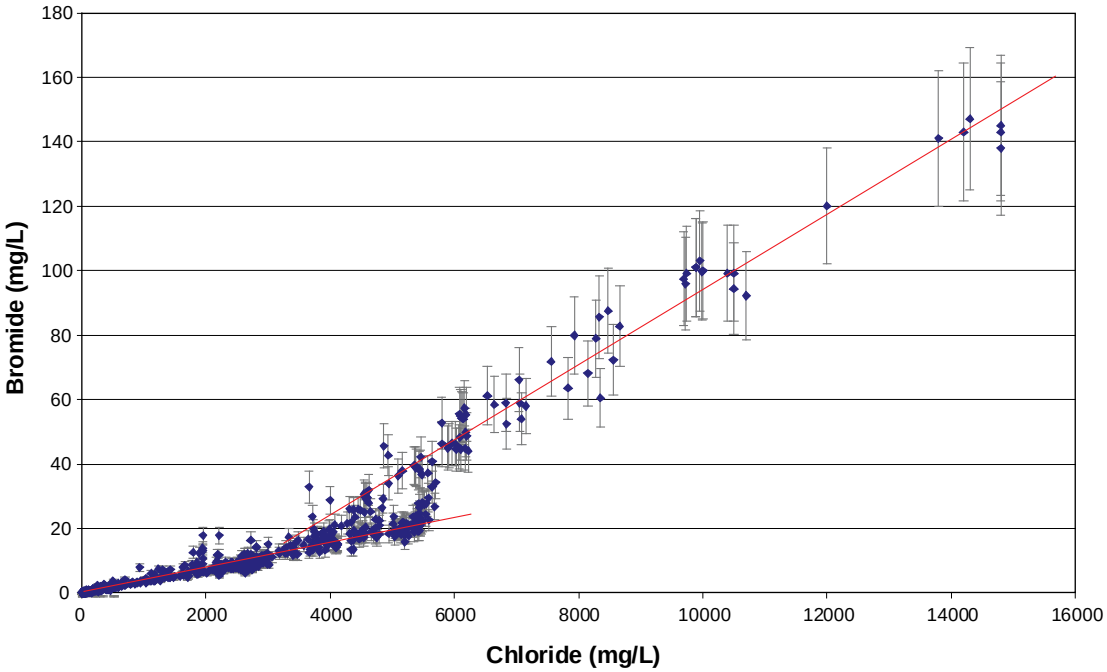

Figure 4-5. *Bromide/bromine values as selected in SKB database SIMON plotted versus chloride concentrations. The error bars correspond to ±15%.*

However, the frequent possibility to compare results from two different methods and the careful selection of data improved the final bromide data set. Generally, if values from both methods were available and they agreed within 15%, ICP values were selected. If the two methods disagreed or if only IC results were available, a judgement of plausibility was made. This was based on comparison with other samples from the same object, evaluation of water type and bromide versus chloride plots. Marine waters should have a bromide/chloride ratio of approximately 0.0035 whereas ratios around 0.01 are more typical of water/rock interaction.

Iron

The risk for impacts from pumping flow rate changes and/or processes like sorption/ desorption on/from long tubing, filters or other equipment can not be disregarded for deep groundwaters. However, comparisons between concentrations by ICP AES and by the spectrophotometric method indicated if short time variations occurred. Furthermore, reproducible and repeatable results from different sampling methods and/or sampling occasions may also strengthen the credibility.

Total/ferrous iron and elemental iron were determined regularly by a spectrophotometric method and by ICP-AES, respectively. Doublet ICP analyses of elemental iron were performed by a checking laboratory (lab 2) on a minor part of the samples, see Figure 4-6. Generally, the agreement between the spectrophotometric – and the ICP results by the regular laboratories were very good, but the reported results from the checking laboratory show more deviation.

The iron concentrations obtained by the spectrophotometric method and by ICP may differ due to the presence of a colloidal phase. The spectrophotometric method do not include, or only partly include, eventual bounded iron that passes a 0.40 µm filter but the ICP method make no distinction between different iron containing species. This is obvious from Figure 4-6 which displays a diverging trend at about 4 mg/L spectrophotometrically determined iron. The samples giving this trend were from the same two boreholes/borehole sections.

Sulphide

Sulphide was determined by a spectrophotometric method and doublet analyses by a second laboratory were conducted for a minor part of the samples (12 class 5 samples). The agreement between the reported concentrations from the two laboratories was satisfactory with a few exceptions, see Table 4-1. Hydrogen sulphide concentrations had a tendency to vary with time during the pumping and sampling periods and more so in certain borehole sections. Not only analytical errors but also varying concentrations in the pumped sample water may be the explanation for deviating doublet analyses. Due to the preservation procedure, each sample bottle/ aliquot was filled directly from the pumped water.

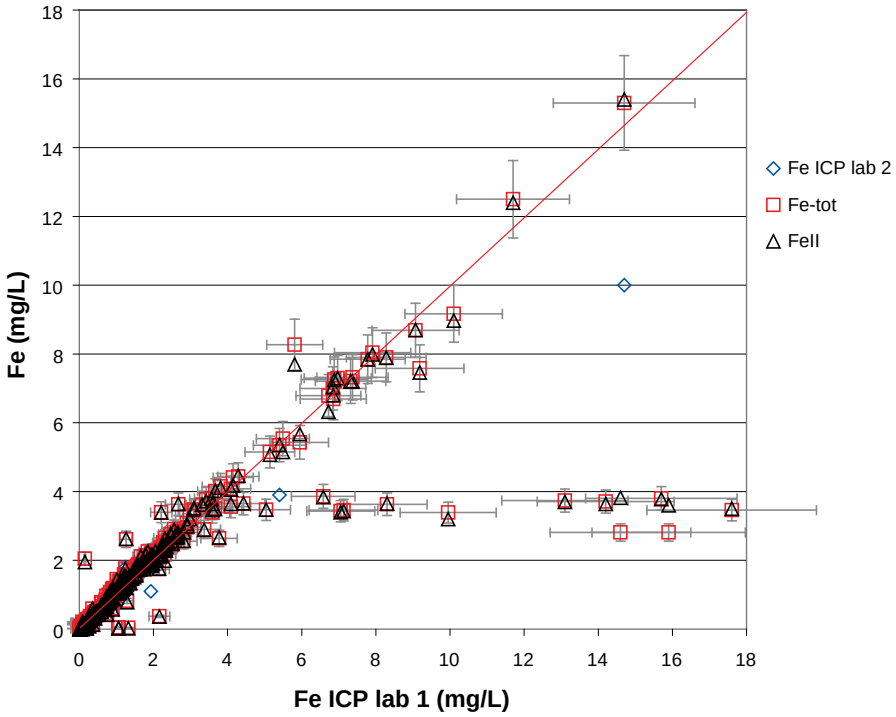

Figure 4-6. *Comparison of iron concentrations. Total and ferrous iron by a spectrometric method and elemental iron by the ICP-AES technique at a second laboratory (16 analyses by lab 2) are plotted versus iron determined by ICP-AES at the regular laboratory (1,790 samples).*

Table 4-1. Comparison of doublet hydrogen sulphide analyses by two laboratories.

Idcode	Secup	Seclow	Sample No.	HS^- (mg/L) lab 1	HS^- (mg/L) lab 2	Support from other samples
HFM04	58.0	66.0	12519	0.055	0.040	Agreement in sample series Earlier sample = 0.047 mg/L
KFM01D	428.5	435.6	12326	0.006	< 0.015	Agreement in sample series
KFM01D	568.0	575.0	12354	0.005	0.030	Agreement in sample series
KFM01D	311.0	321.0	12771	0.287	0.220	Large variation in sample series
KFM03A	448.5	455.6	8284	0.047	0.039	Agreement in sample series
KFM04A	354.0	361.1	8287	0.005	< 0.015	Agreement in sample series
KFM07A	828.0	835.5	8879	0.134	< 0.015	Large variation in sample series, subsequent sample = 0.116 mg/L
KFM08D	828.4	835.5	12776	0.068	< 0.010	Large variation in sample series
KFM08D	669.7	676.8	12818	0.006	< 0.010	Agreement in sample series
KFM10A	478.0	487.5	12517	0.065	0.030	Other samples in series agree with lab 2
KFM10A	298.0	305.1	12552	0.027	0.040	Large variation in sample series
KFM11A	447.5	454.6	12727	0.012	< 0.010	Agreement in sample series

5 Quality of isotopic analyses

Uranium-238 activity and uranium concentration

In total, 127 samples of surface and groundwaters were analysed for both uranium concentration by ICP MS and for uranium-238 by alfa spectroscopy. The two different uranium determinations are compared in Figures 5-1a and b. The initial laboratory for U-238 determinations was changed due to unacceptably high detection limit (50 mBq/kg corresponding to 4.03 µg/L). A few samples have activity results only from this first laboratory (lab a) and as shown in the diagram the agreement is less good for those samples. Generally, the determinations of uranium element concentrations and uranium-238 activities agree surprisingly well considering the different analytical techniques and the often very low concentrations.

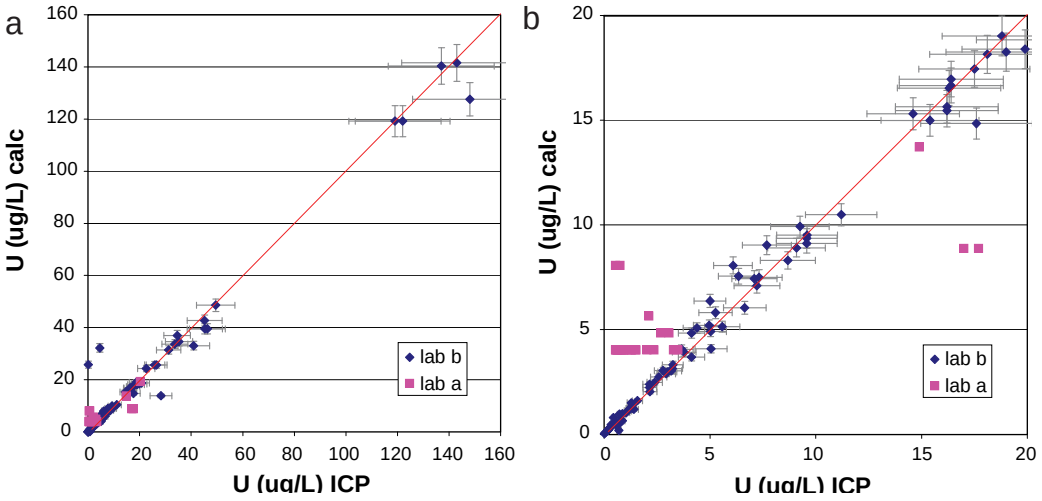

Figure 5-1. *a) Comparison of uranium concentrations (µg/L) by ICP-MS and calculated from uranium-238 activities for a total of 127 samples. 1 ppm U = 12.4 Bq/kg ^{238}U. b) Comparison of uranium concentrations (µg/L) by ICP-MS and calculated from uranium-238 activities in the limited concentration range 0–20 µg/L.*

Deuterium and oxygen-18 isotopes

Doublet analyses of deuterium and oxygen-18 were conducted by routine on the last sample in each sample series from packed-off sections in core drilled boreholes. The isotope results from two independent laboratories, the regular laboratory (lab 1) and the checking laboratory (lab 2), are compared in Figures 5-2 and 5-3. The isotope values are gathered close to the equality line in both cases and show good agreement. The average standard deviations were similar to the reported measurement uncertainties from the contracted laboratories and amounted to 1.1‰ SMOW and 0.2‰ SMOW for deuterium and oxygen-18, respectively.

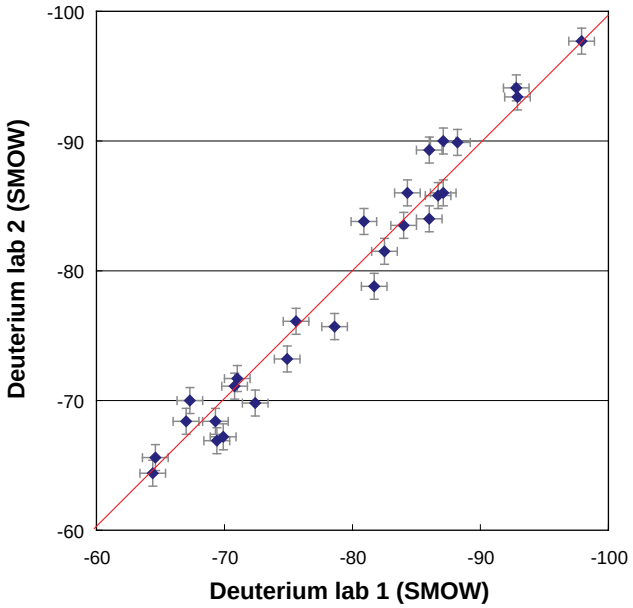

Figure 5-2. *Comparison of doublet deuterium analyses. Deuterium (δ^2H‰ SMOW) was determined by a regular laboratory (lab 1) and a checking laboratory (lab 2) for 27 samples from Forsmark.*

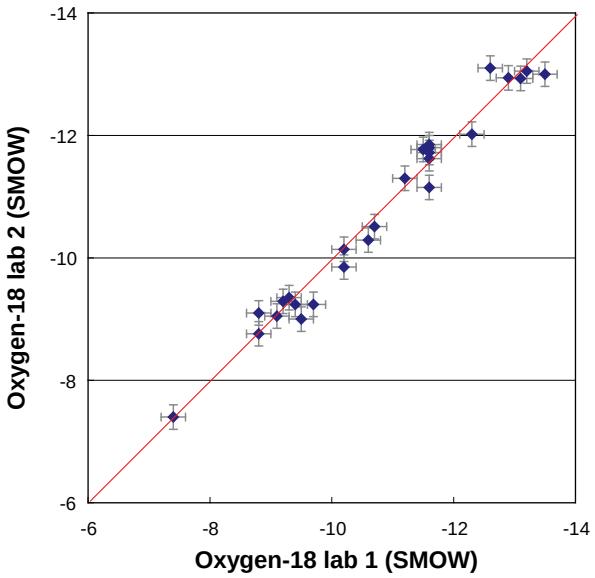

Figure 5-3. *Comparison of doublet oxygen-18 analyses. Oxygen-18 ($\delta^{18}O$‰ SMOW) was determined by a regular laboratory (lab 1) and a checking laboratory (lab 2) for 27 samples from Forsmark.*

Carbon isotopes

Doublet analyses of carbon isotopes (in TIC) were conducted on the last sample in each sample series from packed of sections in core drilled boreholes. However, due to low hydrogen carbonate concentrations in many groundwaters, only 11 doublet results are available, see Figures 5-4 and 5-5. Generally, the agreement between the two laboratories was satisfactory, but some discrepancies exist.

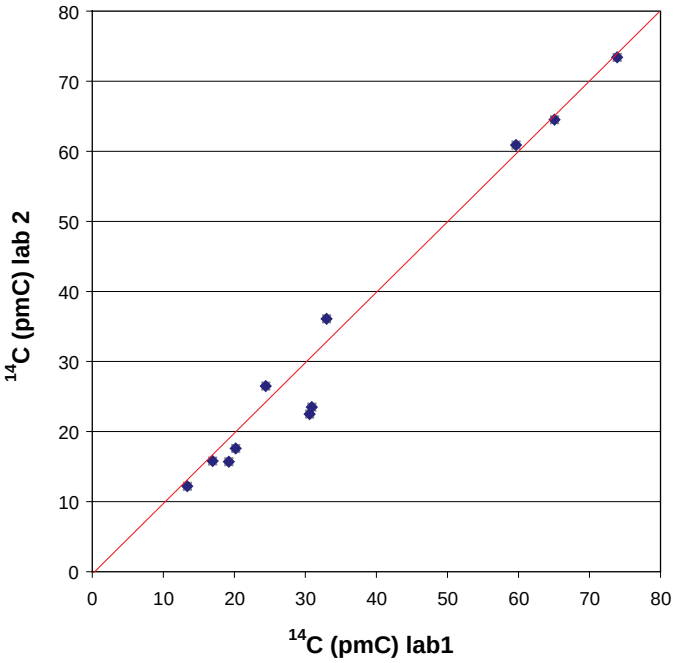

Figure 5-4. *Comparison of doublet pmC determinations. Determinations of pmC (TIC) were performed by a regular laboratory (lab 1) and a checking laboratory (lab 2) for 11 samples from Forsmark.*

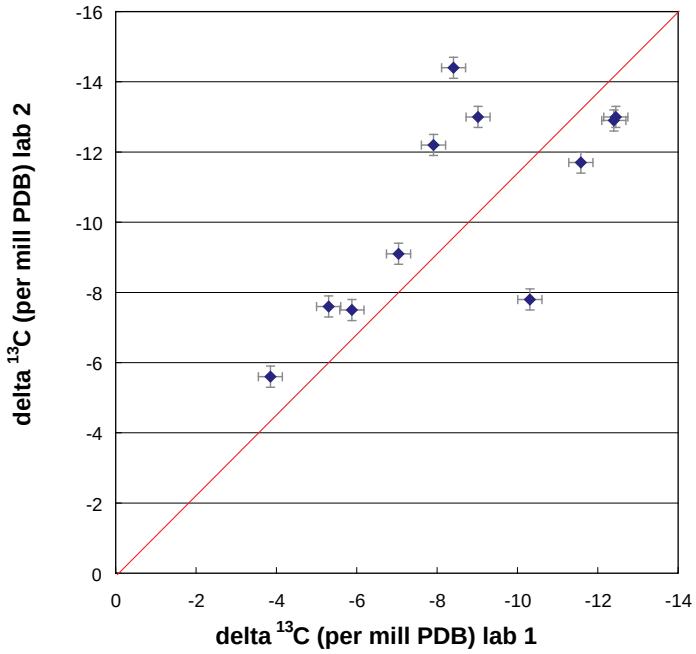

Figure 5-5. *Comparison of doublet $\delta^{13}C$ determinations. $\delta^{13}C$ was determined by a regular laboratory (lab 1) and a checking laboratory (lab 2) for11 samples from Forsmark.*

6 Conclusions

- Factors such as unstable additions or inhomogeneous mixing of the uranine dye to the drilling water used for drilling caused errors in the determination of drilling water contents. The impact from these shortcomings in the large scale drilling water treatment in the field was most probably larger than from the errors in the analyses of the uranine. The stability of the uranine concentration in the drilling water injected into the each core drilled borehole is an indication to the reliability of the drilling water determinations. The errors caused by additional fluorescence from TOC were relatively small and negligible.
- The reported general measurement uncertainties from the contracted laboratories often seem to be somewhat large when compared to the impression from trend plots and other consistency checks. Especially, the measurement uncertainties for the analyses of major ions seem to be overestimated.
- There is high confidence in the set of major constituents for each sample. Independent methods were used to check the consistency of the major ions and to confirm the concentrations of chloride, sulphate, bromide and iron.
- The bromide analyses were found to be more uncertain than most other major ions. However, the frequent use of two different methods (IC and ICP-SFMS) and comparison of the two results and check of Br/Cl ratios, improved the final bromide data set.
- Two commercial laboratories conducted ICP-AES and ICP-MS analyses. All samples were analysed by the regular laboratory (long cooperation with SKB and with universities) and doublet analyses were carried out for a minor part of the samples by a checking laboratory (general routine laboratory). The performance of the two laboratories was not comparable and results from the regular laboratory were reported exclusively.
- Apart from analytical errors and contamination problems, the analytical results may be biased by sampling equipment, sampling methods or sampling conditions. Factors such as sorption on long tubing or effects from varying pumping flow rates may affect, for example, the concentrations of iron and other trace metals and probably also microbial activity and indirectly the hydrogen sulphide concentrations. The reproducibility and stability of the water compositions on different occasions and conditions indicated if this was a problem or not.
- Relatively large variations in sulphide concentrations were observed for doublet samples and sample series. This may be due to analytical error, but varying concentrations in the sample water as an effect of pumped volume and pumping flow rate is also likely, especially at intermediate and high concentrations.
- Doublet isotope determinations by two laboratories generally showed good agreement and the uranium-238 data were verified by ICP-SFMS determinations of the element.

7 References

SKB, 2006. Long-term safety for KBS-3 repositories at Forsmark and Laxemar – a first evaluation. Main report of the SR-Can project. SKB TR-06-09, Svensk Kärnbränslehantering AB.

Nilsson A-C, 2005. Platsundersökningar i Forsmark och Oskarshamn. Översikt över provhanterings- och analysrutiner för vattenprov. SKB P-05-198, Svensk Kärnbränslehantering AB.

Smellie J, Tullborg ELT, Nilsson A–C, 2008. Explorative analysis and expert judgement of major components and isotopes. SKB R-08-84, Svensk Kärnbränslehantering AB.